

Cover Page



Universiteit Leiden



The handle <http://hdl.handle.net/1887/20120> holds various files of this Leiden University dissertation.

Author: Bogaard, Simon Johannes Adrianus van den

Title: Huntington's disease : quantifying structural brain changes

Date: 2012-11-14

HUNTINGTON'S DISEASE

QUANTIFYING STRUCTURAL BRAIN CHANGES

SIMON J.A. VAN DEN BOGAARD

Financial support for the TRACK-HD research was provided the CHDI/High Q Foundation, Inc., a not-for-profit organization dedicated to finding treatments for Huntington's disease.

Financial support for the publication of this thesis was kindly provided by: the Dutch Huntington Association, Guerbet Nederland B.V., Philips Medical Systems Nederland B.V., Sectra Benelux B.V., Lundbeck B.V. and Novartis Pharma B.V.

PhD Thesis, Leiden University Medical Center, Leiden 2012

ISBN: 978-90-9026978-8

Design & layout: Eve Dumas, Seven Design

Printed by Drukkerij Wilco B.V.

© 2012 S.J.A van den Bogaard, Leiden

Copyright of the published chapters is held by the publisher of the journal in which the work appeared. All rights reserved. No part of this book may be reproduced or transmitted in any form or by any means with permission of the copyright owner.

HUNTINGTON'S DISEASE

QUANTIFYING STRUCTURAL BRAIN CHANGES

Proefschrift

ter verkrijging van

de graad van Doctor aan de Universiteit Leiden,
op gezag van Rector Magnificus prof.mr. P.F. van der Heijden,
volgens besluit van het College voor Promoties
te verdedigen op woensdag 14 november 2012
klokke 15.00 uur

door

Simon Johannes Adrianus van den Bogaard

geboren te Woerden
in 1979

Promotiecommissie

Promotores

Prof. Dr. R.A.C. Roos

Prof. Dr. M.A. van Buchem

Co-promotor

Dr. J. van der Grond

Overige leden

Prof. Dr. H.P.H. Kremer

Prof. Dr. C.B.L.M. Majoie

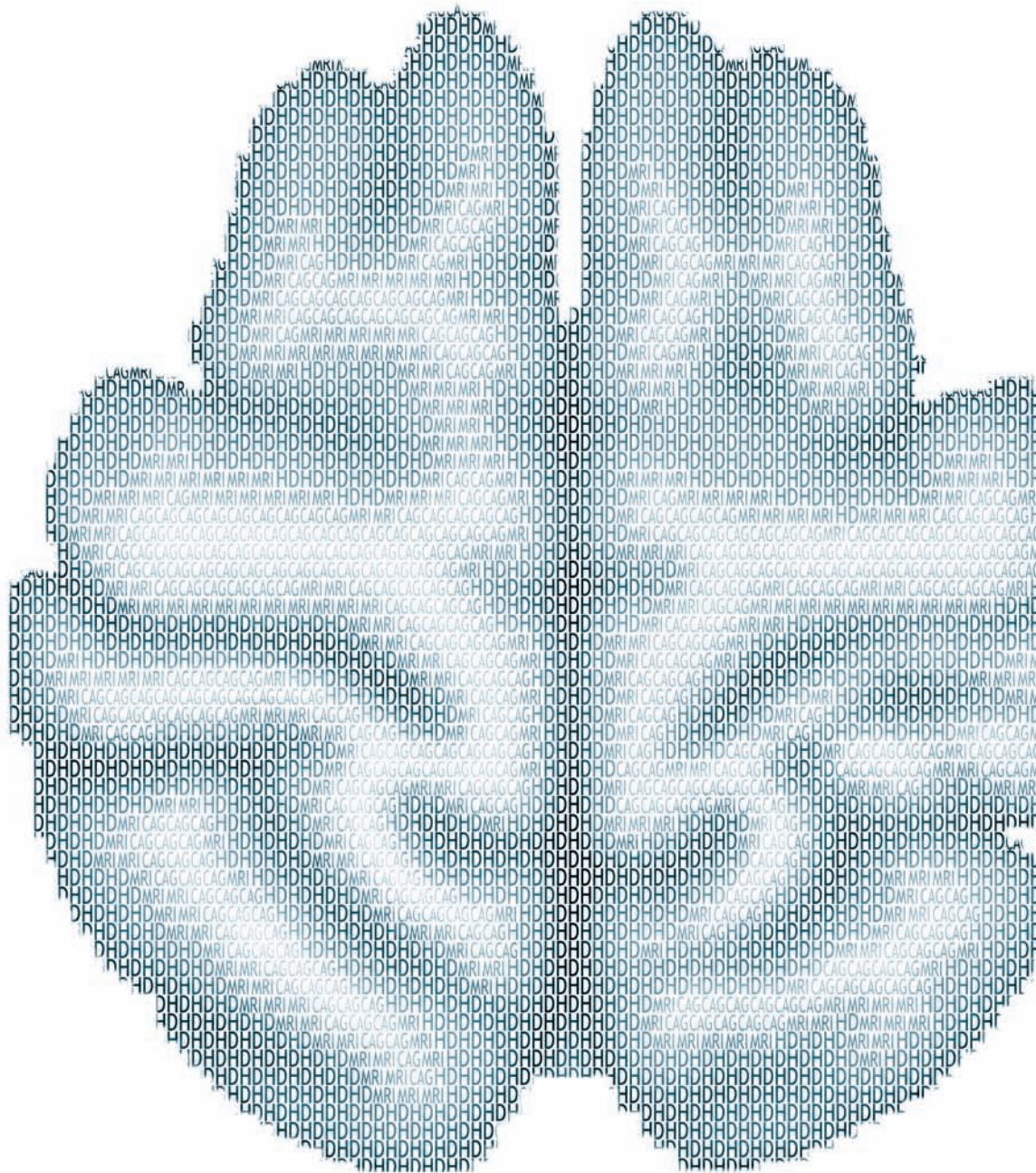
Prof. Dr. S.A.R.B. Rombouts

voor Eve & Emily

Contents

Chapter 1	9
General Introduction	
Chapter 2	19
MRI biomarkers in Huntington's disease	
SJA van den Bogaard, EM Dumas, J van der Grond, MA van Buchem, RAC Roos	
<i>Frontiers in Bioscience (Elite Ed). January 2012; 1;4: 1910-25</i>	
Chapter 3	47
Early atrophy of pallidum and accumbens nucleus in Huntington's disease	
SJA van den Bogaard, EM Dumas, TP Acharya, H Johnson, DR Langbehn, RI Scahill, SJ Tabrizi, MA van Buchem, J van der Grond, RAC Roos; TRACK-HD Investigator Group	
<i>Journal of Neurology. March 2011; 258(3): 412-20</i>	
Chapter 4	69
Shape analysis of subcortical nuclei in Huntington's disease, global versus local atrophy - Results from the TRACK-HD study	
SJA van den Bogaard, EM Dumas, L Ferrarini, J Milles, MA van Buchem, J van der Grond, RAC Roos	
<i>Journal of the Neurological Sciences. August 2011; 15; 307(1-2): 60-8</i>	
Chapter 5	91
Magnetization Transfer Imaging in premanifest and manifest Huntington's disease - Results from the TRACK-HD study	
SJA van den Bogaard, EM Dumas, J Milles J, R Reilmann, JC Stout, D Craufurd, MA van Buchem, J van der Grond, RAC Roos	
<i>American Journal of Neuroradiology. May 2012; 33(5): 884-889</i>	
Chapter 6	109
Early changes in white matter pathways of the sensorimotor cortex in premanifest Huntington's Disease	
EM Dumas, SJA van den Bogaard, ME Ruber, R Reilmann RR, Stout JC, D Craufurd, SL Hicks, C Kennard, SJ Tabrizi, MA van Buchem, J van der Grond, RAC Roos	
<i>Human Brain Mapping. January 2012; 33(1): 203-12</i>	

Chapter 7	129
Exploratory 7 Tesla Magnetic Resonance Spectroscopy in Huntington's disease provides in vivo evidence for impaired energy metabolism	
SJA van den Bogaard, EM Dumas, WM Teeuwisse, HE Kan, A Webb, RAC Roos, J van der Grond	
<i>Journal of Neurology. December 2011; 258(12): 2230-9</i>	
Chapter 8	147
Magnetization Transfer Imaging in premanifest and manifest Huntington's disease: a 2 year follow up	
SJA van den Bogaard, EM Dumas, EP Hart, J Milles, R Reilmann, JC Stout, D Craufurd, SJ Tabrizi, MA van Buchem, J van der Grond, RAC Roos	
<i>American Journal of Neuroradiology. 2012, in press</i>	
Chapter 9	167
From premanifest to manifest Huntington's disease: a two year follow up study with Magnetic Resonance Spectroscopy at 7 Tesla	
SJA van den Bogaard, EM Dumas, WM Teeuwisse, HE Kan, A Webb, RAC Roos, J van der Grond	
<i>Submitted</i>	
Chapter 10	183
Discussion, concluding remarks and future perspectives	
Summary	193
Dutch summary	197
List of publications	202
Dankwoord	206
CV	208





CHAPTER 1

GENERAL INTRODUCTION

Huntington's disease

Huntington's disease (HD) is a progressive neurodegenerative disorder first described by George Huntington in his paper *On Chorea*¹ in 1872. He described a form of chorea he called *hereditary chorea*, evident in some families living on Long Island, USA, which seemed different to the chorea occurring in children. As an acknowledgment of his accurate description, the disease was later named after him.

The observations by George Huntington still hold true to this day. Besides giving a detailed description of chorea, he also described the hereditary nature of the disease, a tendency towards insanity and suicide, and onset in adult life¹. More recent clinical descriptions elaborate on the symptoms and signs describing motor-, cognitive-, and psychiatric disturbances, and also autonomic nervous system impairment, weight loss and sleep disturbances^{2,3}.

Motor symptoms are the most visibly explicit symptoms and consist of chorea, dystonia, loss of postural reflexes, bradykinesia and rigidity². Cognitive decline is also evident with impairment in memory, psychomotor speed, negative emotion recognition and executive functioning⁴. Among the psychiatric symptoms a high risk of depression, suicide, obsessive compulsive disorders, irritability and aggression exists^{2,5}. Symptoms originating from the autonomic nervous system are gastrointestinal, urinary, cardiovascular, temperature regulation, and sexual problems³. Also weight loss and sleep disturbances are important features of the disease^{2,6,7}. Notably the most overt physical signs, such as chorea, do not necessarily have the most impact on quality of life of both patients and family members. Patients report that psychosocial factors influence quality of life more than physical factors⁸. The mean age of disease onset is between 35-44 years of age, with a wide range from early infancy to 90 years of age⁹. The duration of illness, from clinical diagnosis until death ranges from 15-30 years¹⁰. The initial symptom varies between individuals and can start with problems in any of the above described domains. Chorea and balance impairments are easily noticed by patients. However, family members may notice psychiatric or cognitive symptoms many years prior to diagnosis¹⁰.

Genetics and pathophysiology

The genetic defect responsible for HD was discovered in 1993¹¹. The gene defect is located on the short arm of chromosome 4 and consists of an expanded Cytosine-

Adenosine-Guanine (CAG) repeat in the *HTT*-gene. The normal gene produces *huntingtin* (*HTT*) protein. A normal repeat length is up to 26 repeats; extended CAG-repeat lengths of 27-35 do not lead to disease but have a potential to expand >35 within one or more generations. CAG-repeat lengths above 36 will eventually lead to the development of the disease, with repeat lengths of 36-39 with reduced penetrance and ≥ 40 with full penetrance¹². Sixty to seventy percent of the variability in the age of onset can be explained by the length of the CAG repeat, leaving a reasonable amount of unknown factors⁹. Expected age of onset can be reasonably predicted by the formula devised by Langbehn *et al.* (2004,2010)^{13,14}. However, due to various limitations, this formula is usually only used for research purposes and not in clinical practice.

The exact pathophysiological mechanism responsible for the neurodegeneration is still not understood. The following five neurodegenerative mechanisms have been described. First, direct neurotoxic effects of mutant *HTT*-protein. Second, impaired energy metabolism due to mitochondrial disturbances. Third, transcriptional dysregulation of multiple genes, encoding for neurotransmitter receptors, enzymes and proteins involved in neuronal structure, stress responses and axonal transport. Fourth, disrupted dynamic intracellular processes, including trafficking of vesicles from the Golgi apparatus and within the cytoskeleton, transport along microtubules in axons, and synaptic disruptions. Fifth, excitotoxicity based on increased sensitivity to neurotransmitter mediated stimulation, causing overstimulation and cell death^{9,15-17}. In recent reports, substantial evidence has been found for a role of these mechanisms in the neurodegeneration observed in HD. It is not likely that any of these mechanisms are solely responsible. Rather, a combination of mechanisms could be responsible with interactions between these different pathogenic pathways. This interaction theory is highlighted when reviewing the evidence for N-methyl d-aspartate receptor (NMDAR) involvement⁹. Evidence exists for the transcriptional dysregulation of genes involved with the NMDAR. Also selectively activated NMDARs in animal models resulted in a HD neurodegenerative pattern. Finally, mitochondrial dysfunction has been shown to sensitize cells to NMDAR mediated cell death⁹. Hence, these theories describe the complex interaction between multiple pathways in the pathogenesis of HD.

Neuropathology

George Huntington stated in his opening sentence “chorea is essentially a disease of the nervous system”, which of course, as we know now, is certainly the case. However, he hypothesized that the cerebellum was responsible for disease

symptoms. Later neuropathological findings pointed towards the striatum being the most affected brain regions. Jelgersma was the first to correlate atrophy of the caudate nucleus with HD in 1908 and since then many other reports emerged on pathologic findings in HD¹⁸. In 1985 a grading system was proposed by Vonsattel et al, describing the amount of striatal involvement in relationship to clinical disability¹⁹. The pathologic spectrum however extends greatly beyond the striatum¹⁸.

On gross examination, atrophy of the striatum and whole brain is apparent, with the frontal lobe being more affected than others¹⁸. Microscopic findings include neuronal nuclear inclusions of mutant *HTT*, which occur in the striatal, neocortex and allocortex neurons^{20;21}. In the striatum reactive fibrillary astrocytosis, increased density of oligodendrocytes and reactive microgliaocytes can be detected. Mild to marked neuronal loss is also seen in globus pallidus, thalamus, subthalamic nucleus, substantia nigra, white matter and cortex, usually without reactive gliosis. This widespread atrophy is especially evident in grades 3 and 4 of the Vonsattel grading^{18;19}. Overall, striatal abnormalities are most evident with other brain regions becoming affected at a later stage. Interestingly, involvement of the cerebellum, as first thought of by George Huntington, is the one region still heavily debated¹⁸.

The neuropathologic findings are generally limited to end-stage HD patients. It does not tell us when, how and where changes begin in premanifest HD gene carriers. Nor is a neuropathological outcome suitable for making statements regarding the success of a therapeutic strategy. These findings do point out the regions most interesting for further study.

Biomarkers

As our understanding of the pathophysiology of the disease increases, the development of therapeutic strategies becomes possible. For therapeutic strategies the point of application within the pathogenic pathway from mutant gene to neuronal loss is vast. Possibilities include gene therapy, post-transcriptional alterations, metabolic alterations, neuroprotective agents and more¹⁶. Many promising strategies are being examined, however no successful compound has been found to date. To measure possible effects of such compounds, biological markers (biomarkers) are used. A biomarker is defined as “a characteristic that is objectively measured and evaluated as an indicator of normal biological processes, pathogenic processes, or pharmacologic responses to a therapeutic intervention”²². The application of biomarkers is diverse; they can be used in early efficacy and

safety evaluations and “proof of concept” applications, mostly for in vitro or in vivo studies. Furthermore biomarkers can be used as either a diagnostic tool, for disease staging, as indicators of disease progression or prediction and monitoring of clinical response to an intervention. The term surrogate endpoint is a specific application of biomarker but is often used interchangeably. A surrogate endpoint is defined as: “a biomarker that is intended to substitute for a clinical endpoint”. A surrogate endpoint is expected to predict clinical benefit (or harm or lack of benefit or harm) based on epidemiologic, therapeutic, pathophysiologic, or other scientific evidence²².

The need for robust and sensitive biomarkers in HD is highlighted by the fact that several problems are present in measuring effectiveness in HD. First of all HD has a very heterogenic clinical profile. We can roughly predict the age of onset, however it is not exactly known when or with what set of symptoms the disease will start. Motor symptoms are most overt and usually lead individuals to seek medical attention. Cognitive decline can develop slowly and even go unnoticed for many years. Psychiatric illness can appear as a first symptom of HD or are not related to HD at all. A second challenge is the slow rate of disease progression, taking up more than a decade from diagnosis to death². This makes medication trials long lasting and very expensive. Thirdly, it is difficult to measure any clinical effect in the premanifest stage of the disease, as no symptoms are present. Conversely, this group is most likely to benefit from any potential therapeutic strategy when the neuronal loss is still limited.

For manifest HD many potential biomarkers could be appropriate, such as the quantification of motor or cognitive symptoms. To grade clinical severity the Unified Huntington’s Disease Rating Scale (UHDRS) is the most widely applied measure²³. Premanifest HD-gene carriers can display *subtle* motor, cognitive or psychiatric abnormalities that are not captured by this scale. Therefore this scale is unsuitable as a biomarker in the premanifest phase.

Alternative biomarkers to clinical outcome measures are sought whereby the most obvious candidates are magnetic resonance imaging (MRI) parameters. These could serve as biomarkers individually or in combination with other measures such as chemical markers (blood, urine or cerebral spinal fluid) or other imaging techniques such as positron emission tomography. The choice for imaging techniques such as MRI seems logical as they allow for direct examination of the damaged structure, namely the brain. Furthermore MRI can be applied fairly easily and objectively and the biggest advantage is that it can be used in the premanifest stage of the disease. Indeed, early MRI studies already showed striatal abnormalities in at risk HD gene carriers^{24;25}.

In this thesis the term MRI biomarkers refers to indicators of disease progression with the purpose of disease monitoring. Ultimately, these measures can serve as surrogate endpoints in clinical trials. As a first step, prior to use in clinical trials, it is absolutely vital to determine the 'natural history' of disease changes as measured by MRI biomarkers.

Magnetic Resonance Imaging

MRI can give *in vivo* insight in HD pathology. Conventional MRI sequences, such as T1- and T2-weighted sequences, are based on protons bound to water molecules. Relaxation properties of these protons in different tissues provide contrast between grey and white matter. A more recently introduced sequence of diffusion weighted imaging (DWI) makes use of the displacement or diffusion properties of protons. This technique can be extended to diffusion tensor imaging (DTI), creating a 3 dimensional image per voxel of the principal movement direction of protons. This is especially useful for visualizing white matter tracts, using a technique commonly referred to as tractography.

Protons bound to other molecules than water, have different resonance characteristics, creating possibilities to quantify these molecules. Magnetic resonance spectroscopy (MRS) is a technique for quantifying concentrations of certain metabolites in the brain. An example is N-acetylaspartate (NAA), a metabolite considered a marker of neuronal integrity. Magnetization transfer imaging (MTI) is based on the exchange of protons between a pool of protons bound to macromolecules and a pool of free protons water.

Functional MRI makes use of the magnetic properties of oxygen-rich and oxygen-depleted blood in the brain. Oxygen is carried by the molecule hemoglobin, and deoxygenated hemoglobin is more magnetic than oxygenated hemoglobin, which is virtually nonmagnetic. Utilizing these properties it is possible to map neuronal activity.

These different MRI techniques show the many possibilities MRI has to offer to the field of biomarker research. MRI techniques are subject to fast development and are still further developing. Techniques such as T2*-weighted imaging, susceptibility weighed imaging, asymmetric spin echo and other techniques are of importance, however will not be discussed in this thesis.

Aims and outline of the thesis

The primary aim of this thesis is to search for MRI biomarkers for HD. The value of different techniques as biomarkers will be explored for the different stages of HD. Neuropathologic findings and previous MRI studies are starting points for the study of potential biomarkers. Known genetic and clinical factors will be taken into consideration. Finally, based on our observations, a recommendation will be given regarding MRI as potential biomarker in HD.

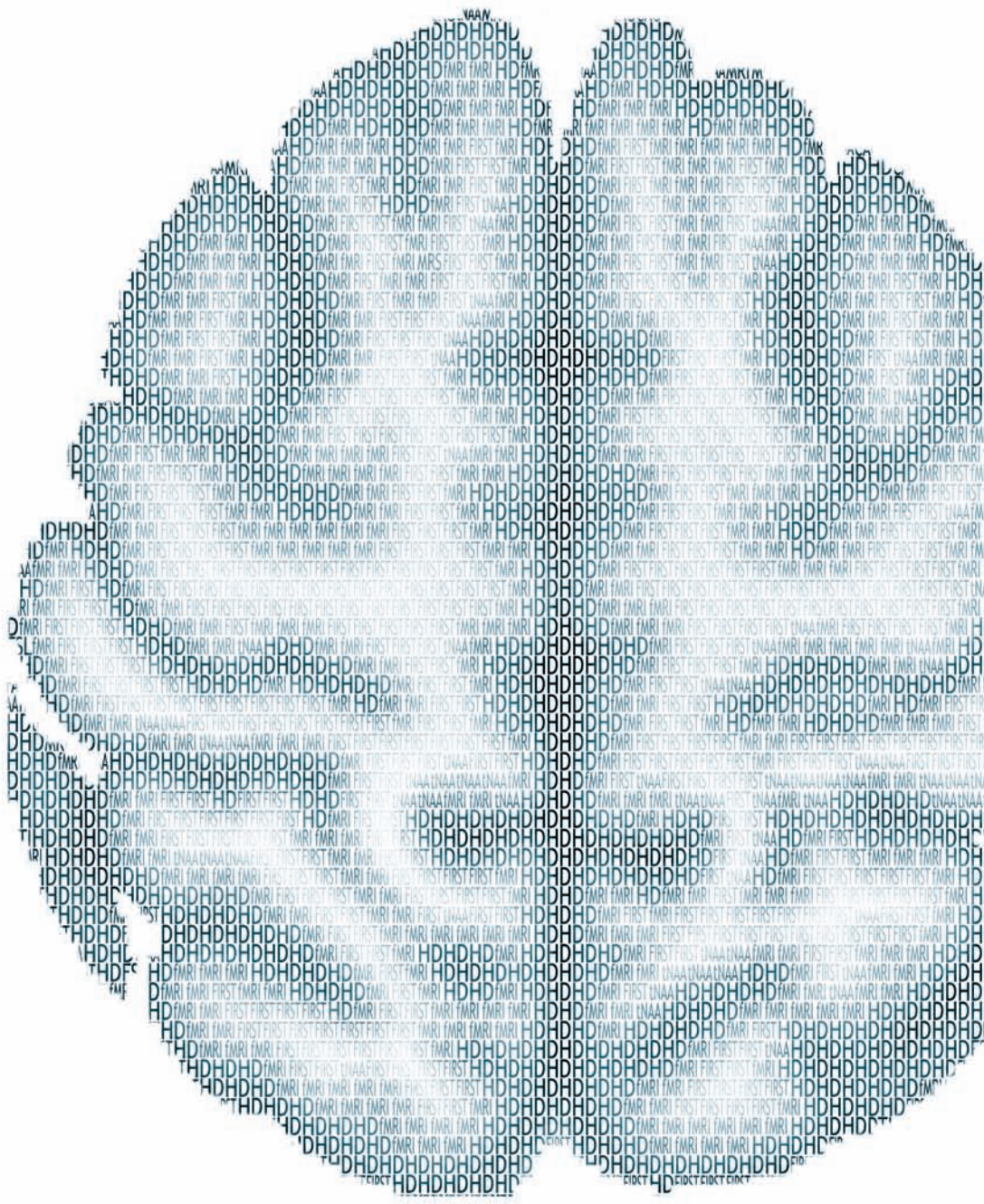
An overview of all current literature on MRI research in HD is given in chapter 2. An extensive volumetric MRI analysis of the main structures of the HD brain is described in chapter 3. More structures than striatum alone will be addressed providing an overview of the atrophy of subcortical grey matter. To gain insight into the localized changes in these nuclei, shape analysis has been performed on these subcortical structures and is discussed in chapter 4. The more recent MRI techniques of MTI, DTI and MRS are discussed in chapters 5, 6 and 7 respectively. The technique of MRS diverts somewhat from structural MRI scanning as it measures metabolites which can be both markers of neuronal integrity as well as part of dynamic processes. How structural integrity changes occur over time as measured by MTI is outlined in chapter 8 and how metabolites change over time using MRS is discussed in chapter 9. A general discussion of findings, final conclusions and future perspectives are outlined in chapter 10.

References

1. Huntington G. On chorea. *Med.Surg.Rep* 26, 317-321. 1872.
2. Novak MJ, Tabrizi SJ. Huntington's disease. *BMJ* 2010;340:c3109
3. Aziz NA, Anguelova GV, Marinus J, et al. Autonomic symptoms in patients and pre-manifest mutation carriers of Huntington's disease. *Eur J Neurol* 2010;17(8):1068-74
4. Dumas EM, van den Bogaard SJ, Middelkoop HAM, Roos RAC, a review of cognition in Huntington's disease. *Front in Biosci.* 2012 in press
5. van Duijn E, Kingma EM, van der Mast RC. Psychopathology in verified Huntington's disease gene carriers. *J Neuropsychiatry Clin Neurosci* 2007;19(4):441-48
6. Aziz NA, Anguelova GV, Marinus J, et al. Sleep and circadian rhythm alterations correlate with depression and cognitive impairment in Huntington's disease. *Parkinsonism Relat Disord* 2010;16(5):345-50
7. Aziz NA, van der Burg JM, Landwehrmeyer GB, et al. Weight loss in Huntington disease increases with higher CAG repeat number. *Neurology* 2008;71(19):1506-13
8. Helder DI, Kaptein AA, van Kempen GM, et al. Impact of Huntington's disease on quality of life. *Mov Disord* 2001;16(2):325-30
9. Sturrock A, Leavitt BR. The clinical and genetic features of Huntington disease. *J Geriatr Psychiatry Neurol* 2010;23:243-59
10. Novak MJ, Tabrizi SJ. Huntington's disease: clinical presentation and treatment. *Int Rev Neurobiol* 2011;98:297-323
11. A novel gene containing a trinucleotide repeat that is expanded and unstable on Huntington's disease chromosomes. The Huntington's Disease Collaborative Research Group. *Cell* 1993;72(6):971-83
12. Semaka A, Creighton S, Warby S, et al. Predictive testing for Huntington disease: interpretation and significance of intermediate alleles. *Clin Genet* 2006;70(4):283-94
13. Langbehn DR, Brinkman RR, Falush D, et al. A new model for prediction of the age of onset and penetrance for Huntington's disease based on CAG length. *Clin Genet* 2004;65:267-77
14. Langbehn DR, Hayden MR, Paulsen JS. CAG-repeat length and the age of onset in Huntington disease (HD): A review and validation study of statistical approaches. *Am J Med Genet B Neuropsychiatr Genet* 2010; 153B(2):397-408
15. Roze E, Saudou F, Caboche J. Pathophysiology of Huntington's disease: from huntingtin functions to potential treatments. *Curr Opin Neurol* 2008;21:497-503
16. Ross CA, Tabrizi SJ. Huntington's disease: from molecular pathogenesis to clinical treatment. *Lancet Neurol* 2011;10(1):83-98
17. Estrada Sanchez AM, Mejia-Toiber J, Massieu L. Excitotoxic neuronal death and the pathogenesis of Huntington's disease. *Arch Med Res* 2008;39:265-76
18. Vonsattel JP, Keller C, Cortes Ramirez EP. Huntington's disease - neuropathology. *Handb Clin Neurol* 2011;100:83-100
19. Vonsattel JP, Myers RH, Stevens TJ, et al. Neuropathological classification of Huntington's disease. *J Neuropathol Exp Neurol* 1985;44:559-77
20. Maat-Schieman ML, Dorsman JC, Smoor MA, et al. Distribution of inclusions in neuronal nuclei and dystrophic neurites in Huntington disease brain. *J Neuropathol Exp Neurol* 1999;58(2):129-37
21. Gourfinkel-An I, Cancel G, Duyckaerts C, et al. Neuronal distribution of intranuclear inclusions in Huntington's disease with adult onset. *Neuroreport* 1998;9(8):1823-26
22. Biomarkers and surrogate endpoints: preferred definitions and conceptual framework. *Clin Pharmacol Ther* 2001;69(3):89-95
23. Unified Huntington's Disease Rating Scale: reliability and consistency. Huntington Study Group. *Mov Disord* 1996;11:136-42
24. Aylward EH, Brandt J, Codori AM, et al. Reduced basal ganglia volume associated with the gene

for Huntington's disease in asymptomatic at-risk persons. *Neurology* 44(5)(pp 823-828), 1994
Date of Publication: May 1994 1994;823-28

25. Aylward EH, Codori AM, Barta PE, et al. Basal ganglia volume and proximity to onset in presymptomatic Huntington disease. *Arch Neurol* 1996;53:1293-96



CHAPTER 2

MRI BIOMARKERS IN HUNTINGTON'S DISEASE

SIMON J.A. VAN DEN BOGAARD¹, EVE M. DUMAS¹,
JEROEN VAN DER GROND²,
MARK A. VAN BUCHEM², RAYMUND A.C. ROOS¹

1. DEPARTMENT OF NEUROLOGY, LEIDEN UNIVERSITY MEDICAL CENTER, LEIDEN, THE NETHERLANDS
2. DEPARTMENT OF RADIOLOGY, LEIDEN UNIVERSITY MEDICAL CENTER, LEIDEN, THE NETHERLANDS

Abstract

Huntington's disease (HD) is a devastating neurodegenerative disease affecting the brain resulting in neuronal dysfunction and neuronal loss. Since the identification of the gene responsible for HD, genetic testing has become widely available, allowing for genetic status of persons at risk for HD to be determined. For the effective evaluation of future therapeutic trials a great need exists for sensitive biomarkers. In (premanifest) HD, MRI of the brain is one of the most logical candidates as a biomarker, as opposed to clinical measures, since brain neurons are the main target of the disease. These biomarkers can facilitate early detection of disease related changes, but are also needed to monitor disease progression from the premanifest phase of HD onwards. MRI derived parameters have this biomarker potential as they have been shown to identify brain abnormalities before symptom onset. In this review the available MRI techniques of conventional MRI, Diffusion Tensor Imaging, Magnetization Transfer Imaging, Magnetic Resonance Spectroscopy and Functional MRI will be discussed and the findings will be placed into context of different HD stages.

Introduction

Huntington's disease (HD) is a devastating neurodegenerative disease affecting the brain through neuronal dysfunction and loss. The disease is caused by a Cytosine-Adenine-Guanine (CAG)-repeat on chromosome four in the *HTT* gene, resulting in a mutant huntingtin protein. The disease is clinically characterized by a triad of progressive symptoms that occur with varying severity amongst patients. First and foremost HD is regarded as a movement disorder with chorea, dystonia, rigidity, bradykinesia and gait impairments. Besides motor disturbances cognitive decline is apparent with disturbances in psychomotor speed, executive functioning and memory with relative preservation of language and speech tasks. Lastly, behavioural abnormalities are characterised by depression, anxiety, disinhibition, aggressive behaviour and a tendency to suicide^{1,2}. Besides the classical triad, reports also show symptoms of weight loss, sleep disorders and autonomic nervous system disturbances³⁻⁵.

The onset of Huntington's disease typically occurs in the third or fourth decade of life, with a large range in disease onset, for 60-70% explained by the length of the CAG mutation⁶. Since genetic testing became available in 1993 it is possible to determine the genetic status of those at risk of HD. The symptom free period of gene carriers prior to inevitable disease onset is typically referred to as the preclinical or premanifest phase of the disease and historically has always been defined by the absence of motor disturbances. However, it is been recognised for some time now that the disease can begin with cognitive or behavioural problems^{7,8}.

The pathologic hallmark has always been atrophy of the striatum, with further histological findings of nuclear inclusions in neurons and atrophy both globally as well as specific brain areas^{9,10}. The disadvantage of the available histological data is that it is typically only available from end-stage HD patients. For characterisation of the brain changes in the premanifest phase and early stages of HD we must rely on *in vivo* imaging techniques.

Since the early nineties reports of *in vivo* atrophy using MRI appear in the literature. These reports followed initial findings using Computerized Tomography, showing a decreased bicaudate ratio¹¹. Initially, MRI studies only discussed the manifest disease stages, but after the widespread introduction of genetic testing, reports have also documented the premanifest phase of HD. MRI is a non-invasive tool for imaging the brain in high resolution yielding good contrast between grey and white matter. Currently, MRI has progressed from just detecting contrast differences to the

development of techniques such as Diffusion Tensor Imaging (DTI), Magnetization Transfer Imaging (MTI), Magnetic Resonance Spectroscopy (MRS), functional MRI (fMRI) and more. However, given the multitude of possibilities, it is pertinent to ask what it is we are measuring with these applications. Atrophy for instance, is the consequence or end product of the disease as this is the measurement of tissue loss. Newer techniques such as MRS can measure metabolic levels, delving further into the pathophysiological processes than atrophy alone. DTI was developed to investigate the integrity of brain tissue by quantifying the properties of tissues and their boundaries, in terms of the water molecule displacement across or alongside these boundaries. Therefore DTI is perhaps able to give insight into both deterioration itself as well as the processes underlying such deterioration. Therefore it is always important to specify the goal of an MRI study in terms of understanding of pathophysiological processes or measuring and quantifying change.

In this review we will focus on measurements and quantification of the different MRI-studies in HD as our main interest is biomarker research. The MRI approaches of conventional or volumetric MRI, DTI, MTI, MRS and fMRI will be discussed and the findings will be placed into context of the different HD stages.

Biomarkers

To measure and quantify brain changes by means of MRI is to enter the field of the biomarker research. A biomarker is defined as “a characteristic that is objectively measured and evaluated as an indicator of normal biological processes, pathogenic processes, or pharmacological responses to interventions”¹². In the context of HD research many different measurements could potentially qualify as a biomarker, physically (motor, cognitive and psychiatric measures), chemically, or by imaging. However, the question remains, what makes a good biomarker and furthermore, why is one needed for HD? To start with the latter it is relevant to note that currently no cure exists for HD, however there are many potential agents currently under investigation¹³. Given that the symptoms of HD arise as a consequence of underlying brain changes, the search for an effective cure should embrace the premanifest period in which brain changes have started but have not yet resulted in symptom manifestation. In this phase of disease development neuroprotective therapies could be at their most effective. Currently, testing new agents in manifest HD is difficult as it is a slowly progressive disease taking up to 15 to 20 years from disease onset until death. As clinical trials are not deemed

effective when a long follow up is required, a shorter set-up is preferential. To measure the effect of an agent over a short time an effective biomarker in HD must be able to detect change over this relatively short period. Subsequently once an agent is found to be effective, the next pertinent question will be when to start with the intervention? Is it most effective when applied in the period that symptoms are not noticed by gene carriers, but when brain changes have already started? If so, another issue arises, when no clinical symptoms can be measured, we must rely on other biologically based markers, hence returning to the term biomarker as a so called surrogate marker or end-point. In (premanifest) HD, MRI of the brain is one of the most logical candidates as a biomarker, as opposed to clinical measures, as brain neurons are the main target of the disease, and show the earliest disruption.

Currently the search for biomarkers in HD has focussed on medical imaging in an attempt to provide an *in vivo* overview of pathological changes in the natural course of HD. In essence, what happens to which part of the brain in progressing disease states? Aylward *et al.* (2007) discussed three criteria for a biomarker in the context of MRI and striatal volume: first it must be objectively measurable, secondly it must be able to predict known endpoints and thirdly it must be associated to known mechanisms of pathology of the disease¹⁴. The application of these criteria can be extended, from the striatal region only, to all brain regions and other MRI techniques.

In summary, the ideal biomarker in HD would measure pathologic change over a relatively short period, these changes would be disease specific and reflect specific disease stages. Furthermore it would detect brain changes before symptoms are present and could therefore be deployed in the premanifest phase.

Methods

In reviewing the literature on MRI in HD, a search was performed for all relevant articles on HD in the PubMed and Medline databases published up to December 2010. The following search terms were used for HD: “huntington”, “huntington’s disease” or “HD” whether or not in combination with “Neurodegenerative Diseases”. Furthermore, the terms for MRI specifically were: “mri”, “magnetic resonance imaging”, “mr imaging”, “mrs”, “magnetic resonance spectroscopy”, “mrsi”, “fmri”, “dti”, “diffusion tensor”, “mti” and “magnetization transfer imaging” in combination with any of the above described HD search criteria. All papers that reported on HD with MRI outcome measures were initially included. We then

categorized the papers based on the type of MRI research and only those who reported on the topics described in the introduction were included. For the section on MRS it is noteworthy we only included 1H-MRS studies as opposed to carbon or phosphor MRS. Furthermore, we limited our review to reports that included only genetically confirmed Huntington's disease patients or premanifest gene carriers.

This review will not describe the various techniques with their advantages and disadvantages, but rather focus on the outcome of these studies in terms of changing brain structures in HD.

Structural Imaging

Structural or volumetric MRI was the first *in vivo* imaging application to be described in HD¹⁵. Since the start of the MRI era the analysis or post-processing techniques of these T1-weighted and T2-weighted scans has evolved significantly. Various manual segmentation techniques have been described as well as the more recent application of semi- to fully-automated techniques such as Voxel Based Morphometry (VBM), Boundary Shift Integral (BSI) and FMRIB's Integrated Registration and Segmentation Technique (FIRST)¹⁶⁻¹⁸.

The hallmark of HD has always been atrophy of the caudate nucleus and putamen, which together form the striatum. MRI studies from the early nineties report atrophy of these structures in manifest HD¹⁹⁻²³ and every study since has confirmed this finding^{16-18,24-33}. It has also become clear that atrophy is already present well before disease onset in premanifest gene carriers^{16,17,34-42}. Earlier reports only make the distinction between manifest and premanifest HD, but later reports also include a distinction within premanifest gene carriers of "far from predicted disease onset" and "close to predicted disease onset"^{16,17,40,43}. These predictions of disease onset, or sometimes disease burden, are most regularly based on Langbehn's formula of predicted age of onset^{6,44,45}. Also many studies include correlation analysis of predicted disease onset with the amount of atrophy of the striatum in premanifest gene carriers^{37,41,43,46}. Exactly when in the disease stages this reported atrophy of caudate nucleus and putamen shows significant difference to control subjects varies per study, but the reports suggest as early as 11-15 years before disease onset^{43,46,47}. Longitudinal analyses of atrophy of the striatum are available and demonstrate a relative stable or linear rate of decline from premanifest to moderate severe HD onwards^{26,47}. Such changes in premanifest HD could not be demonstrated in a cohort "very far from disease onset" of 18.1 years⁴⁸. The most

recent longitudinal publication of the large TRACK-HD study reports atrophy rates in the premanifest group of 1.37% higher than controls and 2.86% in manifest HD of the caudate nucleus over 12 months follow up⁴⁹. Cross sectional analysis from studies examining more than just two disease phases, but rather making subgroups within (pre)manifest HD, suggest that the striatal decline seems to slow down the further the disease progresses with little or no differences than is seen in the early HD stages^{16,17}. A pilot study from Aylward *et al.*(2003) rated caudate atrophy in a clinical trial investigating remacemide and co-enzyme Q10 and state that these atrophy measures show great potential as an outcome measure⁵⁰. To summarize, striatal atrophy seems to begin more than a decade before disease onset, displays a rate of decline disproportionate to whole brain atrophy and volume seems to decrease substantially until at least the early HD stages.

Extra-striatal subcortical grey matter structures have been less studied than the striatum, yet there is convincing evidence that almost all other subcortical grey matter structures are affected to some degree at various disease stages. In manifest HD reports exist on atrophy of the thalamus^{17,19,22,31,33,51}, pallidum^{17,25,30,31,36}, accumbens nucleus^{17,25,31,33}, amygdala and hippocampus^{17,25,31}. For the premanifest phase some controversy exists for the thalamus as some studies report atrophy in this stage^{35,40,43} and others do not⁴² or report that atrophy is consistent with whole brain atrophy¹⁷. The report which does not report atrophy is a study with a relatively small number of participants and did not discriminate between far and close to disease onset. The largest studies, e.g. the PREDICT-HD and TRACK-HD studies do report thalamic atrophy in the premanifest phase of HD. When combining the evidence it is apparent that although not as significant as in the striatum, the thalamus does show reduced volume in the premanifest phase.

Atrophy of the pallidum is also under some dispute in the premanifest phase as two reports did not demonstrate atrophy^{34,35}, however more reports found support for atrophy in the premanifest phase^{17,38,39,42}. Furthermore, the reports in favour of pallidum atrophy are again the larger and more recent trials. Therefore the same conclusion applies for the pallidum as for the thalamus. In a large sample of premanifest gene carriers also the accumbens nucleus and hippocampus were shown to show signs of atrophy¹⁷.

Longitudinal analysis of extra-striatal structures is underreported, especially in the premanifest phase. One report found a significant decrease in accumbens nucleus and thalamus over a two year follow up in manifest HD, but not in premanifest HD⁴⁸. The pallidum has been found to show progressive atrophy in manifest HD

by Ruocco *et al.* (2008)⁵², although this was not found in an earlier study²⁷. The two studies on pallidum atrophy in manifest HD were comparable in terms of duration of symptoms and mean CAG repeat length of the participants as well as scan interval. However the study by Ruocco *et al.* (2008) included slightly more participants and used VBM as opposed to manual segmentation. On the basis of these two studies the rate of atrophy is difficult to assess.

Cortical grey matter has repeatedly been shown to be affected in manifest HD, as measured by VBM^{18,31,52,53}, cortical thickness measurements^{16,54-56} or other volumetric measures^{19,33}. In the premanifest phase of HD one report exists of an enlargement of cortical grey matter volume⁴⁰, however the same group did not replicate this in subsequent studies with larger populations⁴³. It seems apparent that cortical grey matter is affected already far (>15 years)⁴³ or midway (9-15 years)^{16,57} from predicted disease onset. The cortical areas reported to be affected in the earliest premanifest stage are the posterior frontal¹⁶, parietal and occipital regions⁵⁷. Other studies who did not specify the number of predicted years to onset of their group, report atrophy of insular regions³⁸, superior temporal, precuneus, middle and pre-central frontal regions⁵⁵ and prefrontal cortex⁵⁸. Longitudinal analysis of cortical disturbances has not been reported to a great extent. Ruocco *et al.* (2008) observed in manifest HD progressive volume loss in the insula, cingulate, prefrontal, medial temporal and frontal cortex over a follow up period of 1 year⁵². Hobbs *et al.* (2010) reported progressive frontal, occipital and parietal cortex loss over a 2 year period in manifest HD, but not in premanifest HD⁴⁸. When summarizing the findings it appears that regionally specific cortical atrophy appears in premanifest HD around a decade before disease onset, and spreads over almost the entire cortex in early HD stages.

Besides grey matter, also white matter demonstrates volume reductions in both manifest^{19,25,33,59,60} and premanifest^{38,40,43} HD. The earliest report of white matter volume loss is in a “far from predicted disease onset” premanifest HD group (<15 years) and the authors report this as a good predictor of disease onset⁴³. Longitudinal analysis demonstrated severe progressive white matter loss in early HD^{48,49}, and the TRACK-HD study showed this progressive white matter loss already in the premanifest phase far from disease onset⁴⁹.

With reports on cortical grey, subcortical grey and white matter loss, whole brain atrophy is a logical consequence in premanifest and manifest HD^{16,43}. This measure demonstrated significant difference from controls in “far from”⁴³ and “close to”¹⁶ predicted disease onset groups. Longitudinal analysis seems to indicate this is a

fairly stable and easy measure in manifest HD only, as this change is relatively severe in early HD and can be demonstrated with just a six month follow up period⁶¹⁻⁶³. The most recent study found a 0.20% higher atrophy rate in premanifest HD and 0.60% in manifest HD in one year follow up⁴⁹.

To capture all the literature into one overview we have constructed hypothetical models. These models are our own interpretation of the combined evidence and are therefore not to be taken as proven fact, rather as a way of providing a guide towards temporal changes in the brain of HD. Figure 1 graphically displays the hypothetical model for atrophy of different brain regions and their relation to disease stage.

Atrophy of cerebral structures depicted by percentage of atrophy

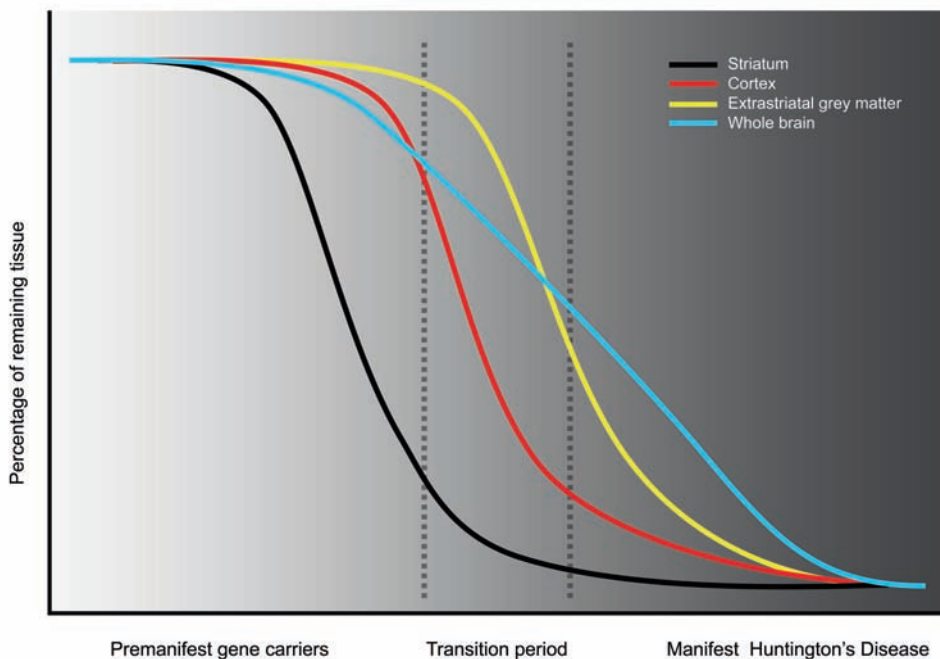


Figure 1. Atrophy of cerebral structures depicted by percentage of atrophy. The x-axis displays time, the y-axis displays percentage of remaining tissue of the different brain structures. GM = grey matter.

Diffusion tensor Imaging

Diffusion Tensor Imaging (DTI) is based upon the diffusion properties of protons in the intra- and extracellular space, and was developed to investigate the integrity of tissue matter. During a DTI scan the preferential orientation of the diffusion as well as the strength or directionality of the diffusion of water molecules is measured throughout the brain. In highly organised tissue, such as the white matter comprising of dense axon bundles, the diffusion properties are dramatically influenced because of the ‘boundaries’. In essence the axons in white matter provide a pathway for diffusion along the axonal axis, whereas diffusion is frustrated by cellular barriers perpendicular to axis of axons. DTI is not restricted for use in white matter only, but can be applied in grey matter as well. The two most widely derived measures from DTI scans are fractional anisotropy (FA) representing the strength of the main direction of diffusion, and mean diffusivity (MD) portraying the speed of the diffusion, although Apparent Diffusion Coefficient (ADC) is also used in this regard. Sometimes TraceD is used, which is the total diffusivity, meaning the sum instead of the mean of the three eigenvalues. An FA value close to 0 is representative of equal diffusion in all directions, as is seen in cerebral spinal fluid. In contrast an FA value close to or equal to one represents highly directional diffusion. High MD values represent unrestricted diffusion (for example in CSF) and low MD values suggest restricted diffusion. The post-processing techniques used for DTI consisted of either a (manual) region of interest (ROI) segmentation technique (combined with computed tracts between ROI’s) or a voxel wise statistical approach such as tract based spatial statistics (TBSS).

In manifest HD disturbances in either FA or ADC in white matter have been reported in the corpus callosum⁶⁴⁻⁶⁷, fornix⁶⁶, internal capsula⁶⁵, external capsula⁶⁶, capsula extrema⁶⁶, frontal subcortical white matter^{65,67}, sensorimotor white matter pathway⁶⁷, inferior fronto-occipital fasciculus⁶⁶, inferior longitudinal fasciculus⁶⁶ and total white matter²⁸. The grey matter is also reported to show disturbances in the putamen^{28,65,68-70}, caudate nucleus^{28,67-70}, pallidum^{65,69,70} and thalamus⁷⁰. It is important to note that these studies report increased FA in the grey matter, whereas in white matter a decrease in this measure is apparent. Douaud *et al.* (2009) explains this as a decrease of dispersion of the fibre orientation, characterising a loss of connections from these structures⁷⁰.

In premanifest HD the findings seem comparable to the findings in manifest HD, only not as extensive. General widespread white matter⁷¹ is reported to display

disturbed DTI properties, as well as specific areas such as the corpus callosum^{64,65}, external capsula⁷², putamen⁷² and different areas of frontal white matter⁷³. Furthermore specific pathways to the sensorimotor cortex⁶⁷ and the fronto-striatal connections⁷⁴ have been found to be affected. The integrity of the corpus callosum has been reported affected in a far from predicted disease onset group (>11 years)⁶⁴. The disturbances were found to correlate well to predicted time to disease onset^{67,71,72}.

Longitudinal findings from Weaver *et al.* (2009) show FA reduction in white matter throughout the brain, which increased during a one year follow up in manifest HD, and not in controls⁷⁵. Sritharan *et al.* (2010) examined the subcortical grey matter structures over a one year period using the MD instead of FA and found higher values in the putamen and caudate nucleus at both time points, however no longitudinal change was observed⁷⁶. Similarly, Vandenberghe *et al.* (2009) did not demonstrate a longitudinal change over two years in the striatum in a manifest population and even suggests that volumetric change is more sensitive as a longitudinal marker. When considering this conclusion it must be noted that this report only examined TraceD in the striatum and not diffusion properties in the rest of the brain⁶⁸. When combining the information from these three longitudinal studies it is evident that these studies all included relatively small samples, ranging from 7 gene carriers (mixed premanifest and manifest) in the study by Weaver *et al.* (2009)⁷⁵ to 8 manifest HD by Vandenberghe *et al.* (2009)⁶⁸ up to a maximum of 18 manifest HD by Sritharan *et al.* (2010)⁷⁶. On examination of the data it can be seen that all the measures used change over time in the expected direction in each study, yet none but the study by Weaver *et al.* (2009) demonstrates significant results⁷⁵. It is likely that the results of these studies were influenced by power issues which hindered demonstration of significant change over time.

In summary, widespread diffusion abnormalities have been demonstrated in both manifest and premanifest HD, most notably the white matter, but also in subcortical grey matter. Measuring longitudinal change of the diffusion properties of white matter seems more promising than those in grey matter. It remains the question whether FA, MD or TraceD (or some combination) is the best single measure. Furthermore the choice of post-processing technique can affect the outcome. A priori a voxelwise approach may have a greater sensitivity for detecting change as opposed to a region/tractography based method, yet how sensitive this is over time remains unclear. Noteworthy is also the introduction of radial and axial diffusivity, making use of more than only the principal diffusion direction^{70,75}, as this may provide not only be a more sensitive measure, but could also shed light on

pathophysiological processes. Weaver *et al.* (2009) reported larger decreases of axial diffusivity (a marker of the stability of axons), than radial diffusivity (a marker for demyelination), and concluded that axonal injury plays a larger role than myelination disturbances⁷⁵.

Also for DTI we have constructed the same type of hypothetical model as with the volumetric MRI data. Figure 2 graphically displays the hypothetical model for DTI changes in different brain regions and their relation to disease stage.

Diffusion tensor imaging values in relation to time.

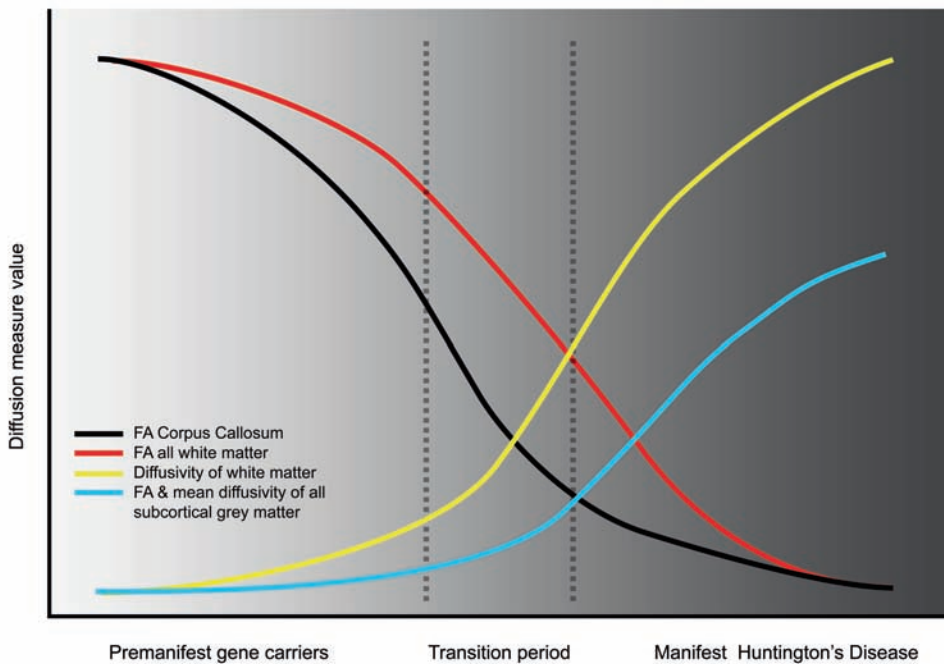


Figure 2: Diffusion tensor imaging values in relation to time. The x-axis displays time, the y-axis displays percentage of diffusion measure value. FA = fractional anisotropy.

Magnetization Transfer Imaging

Magnetization Transfer Imaging (MTI) offers a way of examining tissue structure and structural components in a different way than conventional MRI. The technique of MTI relies on interaction between protons in free fluid and protons bound to macromolecules. The magnetization saturation and relaxation within macromolecules affect the observable signal. The magnetization transfer ratio

(MTR), representing the percentage of variation in the MR signal between the saturated and unsaturated acquisitions, is a measure used in clinical studies⁷⁷. MTI differs from other techniques such as DTI in the sense that it measures properties of macromolecules found in cells as opposed to the properties of water molecules. Two main outcome measures are reported, the mean MTR and the MTR peak height from histogram analysis.

In manifest HD, Mascalchi *et al.* (2004) reported no differences between a group of 21 gene carriers (of which 19 manifest HD) and 21 controls examining the mean MTR²⁸. In contrast Ginestroni *et al.* (2010) found a statistically significant decrease of the MT ratio in all subcortical grey matter structures (except putamen) and in the cerebral cortex diffusely. The whole brain white matter was not significantly decreased⁷⁸. There was a close correlation found to clinical measures of motor and neuropsychological testing and disease duration⁷⁸. The difference between these studies are only obvious in post-processing methodology, Ginestroni *et al.* (2010) used the automated segmentation tools provided by FSL and Mascalchi *et al.* (2004) used manual segmentation. In terms of the patient characteristics we cannot determine if any differences exist in clinical severity due to the fact that mainly by Mascalchi *et al.* (2004) this is not described in detail, only by a gross measure, namely the TFC²⁸. Based on these two studies it is not possible to draw any definite conclusions.

In premanifest HD only one study has published results examining not only the mean MTR, but also the MTR histogram peak height. There were no group differences, however there was a good correlation between this measure and subtle motor disturbances and CAG repeat length⁷⁹. Unpublished results from our own study group confirm the findings by both Jurgens *et al.* (2010) and Ginestroni *et al.* (2010) whereby group differences exist in the manifest stage of the disease only and that there is a relation to clinical^{78,79}.

In summary, there is a lack of sufficient data, but the data at hand suggests that MTI is only potentially useful as a biomarker in the manifest stages of the disease. More studies, particularly longitudinal studies, should be performed to examine MTI measures in HD.

Magnetic Resonance Spectroscopy

Whereas conventional MRI uses hydrogen protons to characterize different tissues, MRS uses these hydrogen protons to measure metabolite concentrations. This technique therefore does not give direct structural information, rather this enables interpretation of changes in physiologically related processes. This is based on quantifications of a number of different metabolite compounds which reflect underlying processes. The most common metabolites examined are: N-acetylaspartate (NAA), which is seen as a marker for neuronal and axonal integrity, creatine which is regarded a marker for brain energy metabolism, choline reflecting membrane turnover, myo-inositol (MI) is seen as an osmolyte and astrocyte marker, lactate which is regarded as representing interruption of oxidative processes and beginning of anaerobic glycolysis, and glutamate, with its precursor glutamine, is a neurotransmitter⁸⁰.

In manifest HD lower NAA and creatine has been demonstrated in putamen and/or caudate nucleus⁸¹⁻⁸⁵ and thalamus⁸⁶. Furthermore an increase in glutamate has been demonstrated⁸⁷⁻⁸⁹ however, this is under some dispute as this is not a consistent finding in all studies^{81,82}, and has even been reported to be lower than in controls⁸¹. A consideration with the reports on increased glutamate may be the fact that glutamate was reported as a ratio to creatine, however, creatine itself does not appear to be a stable metabolite in HD. Furthermore, the reports on increased glutamate were performed in the early nineties, use different methodology, have lower field strength and have a smaller sample size. This is all in contrast to recent reports. Therefore we are of the opinion that based on the reports, it is more likely that glutamate is lowered rather than increased in HD.

Increased MI in manifest HD has been reported in the putamen and therefore a ratio between MI and NAA could be a useful marker for tracking disease pathology⁸¹. Energy metabolism disturbances can be demonstrated with creatine measurements, but also lactate is important in this respect. Increased lactate (or ratio of lactate to either NAA or creatine) has been found in basal ganglia, cerebellum, occipital, parietal and frontal cortex^{83,84,90,91}. It must be noted, that although quite some studies suggest impaired energy metabolism, not all studies concur, as Hoang *et al.* (1998) conclude that no evidence can be found for impaired energy metabolism using a combination on 1H-MRS and 31P-MRS⁹², and furthermore Reynolds *et al.* (2005) stress the issue of heterogeneity in MRS findings in HD, stating that there is no pathognomic alteration of any metabolite for HD⁹³. There is substantial evidence from non-clinical studies that energy

metabolism is impaired in HD⁹⁴, also the number of positive results from in vivo MRI-studies described above is quite substantial, therefore we feel that it is not really a question if energy metabolism is impaired, but rather how it can be measured accurately. Finally, only one report found an alteration of choline, with a decreased NAA/choline ratio in the frontal cortex⁹⁰.

Conflicting results exist for the premanifest stage of HD with regards to alterations of metabolites. As in manifest HD, lower creatine and NAA are reported in putamen and caudate nucleus^{81,85}, although other studies did not find these differences^{95,96}. Of the other metabolites, only choline is reported to be decreased in the frontal cortex⁹⁶. There are important differences between the studies in favour and those in dispute of NAA or creatine changes in the premanifest stage, Sturrock *et al.* (2010) used a higher magnetic field (3 Tesla as opposed to 1.5 Tesla) and had the largest sample size as well the benefit of occurring as part of the methodologically well set up TRACK-HD study⁸¹. The higher magnetic field has a definite theoretical advantage to obtain good quality spectra. In light of the above described findings the evidence in favour of premanifest changes in the concentrations of these metabolites weighs more heavily than against the presence of such changes.

There appears to be a relationship between alterations in metabolites and measures of motor performance^{81,85}, disease severity⁹⁰, neuropsychological assessment⁹⁶ and disease burden⁸¹. Another interesting feature of MRS has been demonstrated by using MRS in the evaluation of high dose oral creatine as a treatment of HD. The brain concentrations were shown to be elevated by this therapy and even had an effect on the glutamate concentration, however no clinical improvement was shown, nevertheless it does show a potential application of this technique^{97,98}.

A great lack of longitudinal MRS studies exists. Sturrock *et al.* (2010) is the only available longitudinal study as it is part of the TRACK-HD study¹⁶. Preliminary data presented at the European Huntington's Disease Network congress did not show any longitudinal change over a one year follow-up period⁹⁹.

Overall, creatine and NAA are reported to be lowered in different brain regions and lactate possibly increased. Choline has not been reported as widely and it remains unclear whether or not glutamate is different in HD. The alterations of metabolites is likely to occur already in the premanifest stage, not only based on the above described studies, but also from a hypothetical point of view, where structural changes normally would occur simultaneously or be preceded by metabolic

changes. Figure 3 graphically displays the hypothetical model for metabolite concentration changes and their relation to disease stage.

Magnetic Resonance Spectroscopy in Huntington's Disease in relation to disease stage

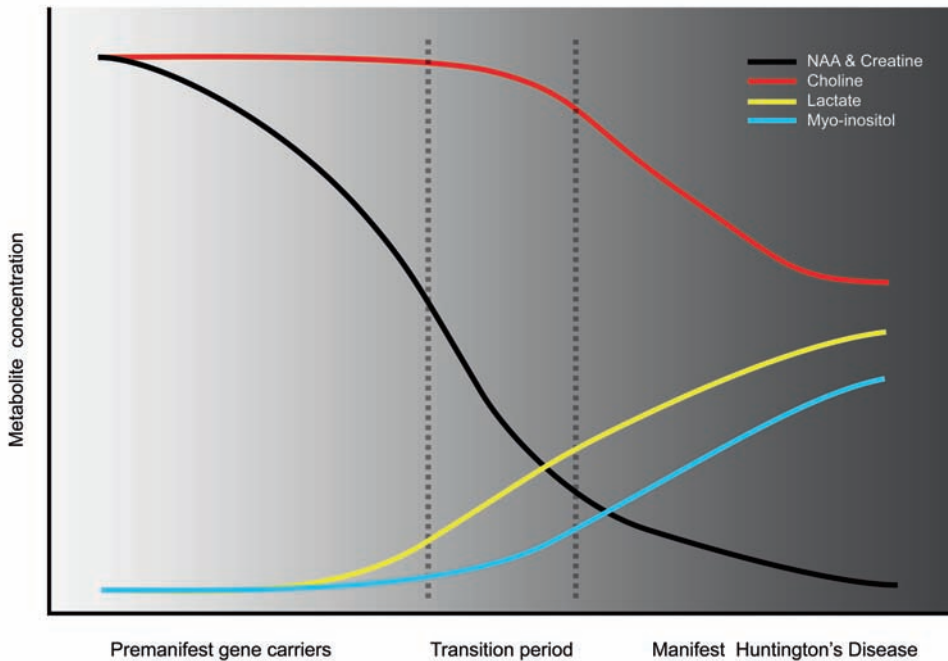


Figure 3: Magnetic Resonance Spectroscopy in Huntington's Disease in relation to disease stage. The x-axis displays time, the y-axis displays percentage concentration of metabolite. NAA = N-acetylaspartate. Glutamate is not depicted due to conflicting data in the literature.

Functional MRI

Event related functional MRI (fMRI) uses the blood-oxygen-level-dependent (BOLD) signal to discriminate brain regions with altered activation. Simply put, this means that when a brain region is activated it will require an increase in energy resulting in blood demand, which is measurable with this method. Different functional tasks can be employed during fMRI scanning to measure activation in different brain regions or networks.

In HD research several studies are available with reports in both premanifest and manifest HD of aberrant connectivity or activation patterns. In manifest HD one

case report and five studies are available. The first fMRI report is a case study with a clock reading task whereby increased parietal activation suggested a higher neuronal effort was required to perform the task¹⁰⁰. Subsequently several case control studies were performed: using a verbal working memory task lower activation of parietal cortex, putamen and cerebellum were shown in HD¹⁰¹. Using a porteus maze task a reduced signal in occipital, parietal and somato-motor cortex and the caudate nucleus, and furthermore an increased signal in the postcentral cortex and right middle frontal gyri was demonstrated¹⁰². Using a Simon task, which activates the lateral prefrontal and anterior cingulate cortex, reduced functional connectivity of this region was found¹⁰³. In a mixed premanifest and manifest population, using a serial reaction time task a reduced activation of middle frontal, occipital, and precuneus regions was demonstrated¹⁰⁴. In slight contrast to these reports increased activation of the anterior cingulate-frontal-motor-parietal circuit was found using a Simon task¹⁰⁵. The two studies using the Simon task are from the same research group, whereby they differ as one examines functional connectivity¹⁰³ and the other activation patterns¹⁰⁵, both using fMRI. Although measuring different parameters the two studies seem at conflict with each other. However one might argue that when there is reduced connectivity the cortical recruitment of these regions can (or must) be enhanced. Currently definite conclusions on activation cannot be drawn as many different tasks have been utilised and therefore also different cortical regions have been examined. Although both increased and decreased activation have been reported, it seems that predominantly reduced activation patterns are found in manifest HD.

In premanifest HD a pattern of increased activation of several regions was demonstrated in premanifest gene carriers 'far from predicted disease onset' whereas premanifest gene carriers 'close to onset' show a reduction of activation^{106,107}. Reductions in activation in premanifest HD were specifically reported in areas such as left anterior cingulate cortex, lateral prefrontal cortex, parietal cortex, putamen¹⁰⁸⁻¹¹¹. An interesting finding by the authors is that the change in activation pattern from far from onset to close to onset is related to the presence of atrophy in the striatum^{106,107}.

The use of different methodology and tasks applied during scanning complicates summarizing the results from the fMRI studies. Overall, the regions and networks shown to be affected in fMRI studies appear to be widespread, confirming that HD is more than just a basal ganglia disorder, even in the premanifest stages of the disease. There appears to be mainly decreased activation in manifest HD and premanifest close to disease onset, although the study by Georgiou *et al.* (2007)

contradicts this¹⁰⁵. The interesting finding of increased activation in premanifest gene carriers far from onset HD is hypothesized to be the result of cortical recruitment, in essence HD gene carriers need activation of more neurons and/or higher activity of these neurons in order to achieve the same task performance as controls. The pro's and con's of fMRI are discussed in a review by Paulsen *et al.* (2009) with commentary in Georgiou-Karistianis *et al.* (2009)^{112,113}.

Discussion

Temporal relationships of MRI measures with HD have been extensively examined making use of the many and diverse capabilities of MRI. However, drawing decisive conclusions from all these studies together is challenged by a number of issues. Firstly, when a particular MRI technique is applied, many options in terms of acquisition and post-processing remain undecided, resulting in different methodology across studies. Secondly, when comparing studies, it is evident that differences in definition exist for even the most basic principles which can lead to different inclusion criteria, the most pertinent being the definition of premanifest and manifest HD. Although many studies use some form of motor examination, even when the same standard (e.g. the UHDRS motor score) is applied, different cut-off points are used for determining disease manifestation. Thirdly, MRI is ever evolving, using evermore sophisticated techniques, therefore the validity of comparing a study from 1991 versus one from 2010 can be questioned. Finally, the comparison of a study with more than 300 participants, to a study of 6 controls versus 6 manifest HD is also challenging. This is not to say that the validity of smaller studies is less than larger studies. One might in fact argue the opposite, when something can be demonstrated using only 12 participants, this can be a much stronger argument when needing 300 participants to prove a point. Despite the difficulties posed in providing an overview, this review has discussed many different studies using various techniques in an attempt to combine their findings into a hypothetical temporal model of brain changes (figure 4). This hypothetical model is constructed based on all the literature available and is our own interpretation of the data available. When conflicts in literature exist, we have weighed the different studies as described in the specific MRI subsections. Figure 4 depicts the temporal MRI changes in relation to disease stage and to each other.

When summarising the literature it seems apparent that striatal atrophy is the first measurable brain change, starting between 10 to 20 years before disease onset^{16,17,40,46}. DTI measures reflect signs of abnormal structure, especially in the white matter, at the same time or shortly afterwards the striatal atrophy, with

reports of change in the corpus callosum being the most consistent^{64,65,67,75}. With the combination of subcortical grey matter, cortical grey matter and white matter disturbances, whole brain atrophy is no more than a logical consequence^{16,62}. The longitudinal change of whole brain atrophy seems especially apparent in the early manifest stage^{49,61,62}. MTI seems to be sensitive only in the early manifest stage onwards^{78,79}. MRS demonstrates changes in metabolites before disease onset with changes in NAA and creatine^{81,85}. Functional MRI seems to start with a form of enhanced activation in the premanifest stage^{106,107}, which is depicted by the negative curve in figure 4, and shows reduced activation in later disease stages^{101,102}.

MRI changes in HD brains depicted as a function of time

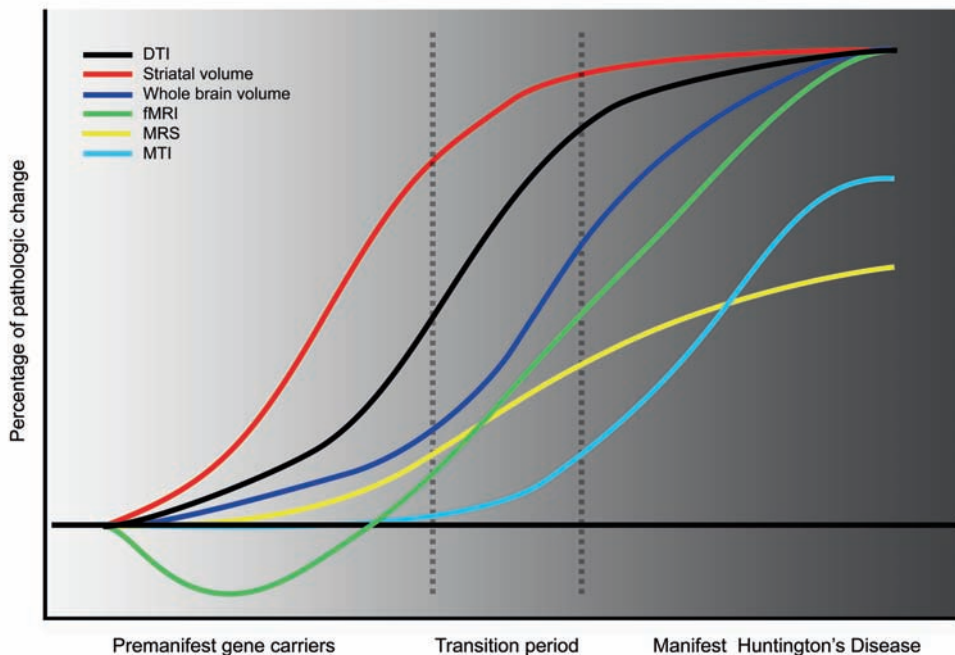


Figure 4. MRI changes in HD brains depicted as a function of time. Functional MRI displays a negative curve in the premanifest 'far from onset phase' as literature suggests increased activation. This is in fact also a pathologic change, however this is displayed as opposite of reduced activation patterns in later stages. The x-axis displays time, the y-axis displays amount of pathologic change. DTI= diffusion tensor imaging, MTI = magnetization transfer imaging, MRS = magnetic resonance spectroscopy, fMRI = functional MRI.

This model, however is not at all without its limitations. The s-shaped curves are assumptions made on available data. The curves are, from a pathophysiological point of view, a common form, where some minor changes occur, a certain

threshold is subsequently reached and there is some form of exacerbation which slows down eventually. The use of such temporal models for biomarkers has been reported on in Alzheimer's disease¹¹⁴ and seems plausible for more neurodegenerative diseases. For understanding temporal changes, longitudinal assessments are the most relevant, however cross-sectional analysis of multiple disease stages are also very relevant and also more abundant. The literature is however too limited to make very firm claims. These models should therefore not be taken as proven fact, but rather be used to test further research on and provide a framework for future clinical trials. Furthermore this model is deficient in the sense that it is limited to the most commonly used techniques and therefore not all MRI-techniques available are included and we appreciate the fact that possibly more sensitive techniques exist.

The most abundantly researched candidate biomarker technique is volumetric MRI. It seems to be quite robust and fairly easy to use. The use of T1-weighted MRI is part of routine MRI and therefore easily implemented in any type of study. However, volumetric measurements can be performed in a many different ways from simple hand-drawn measurements to newer techniques such as VBM, which also has its pitfalls¹¹⁵. Nonetheless, this technique is claimed to be robust and suitable to use in a clinical trial by many studies such as the large cohort studies PREDICT-HD and TRACK-HD^{14,16,49,116}.

DTI has been applied extensively the last decade and has the advantage that it can detect abnormalities in integrity in multiple ways, with different outcome values such as FA and MD, but also more recently applied measures such as radial or axial diffusivity, all with different proposed pathological meaning⁷⁰. The potential use of DTI measures as a biomarker in HD has been suggested by many authors^{67,69,71,72,75}. There is also a downside of DTI as the options available of examining DTI are plentiful in terms of not only outcome measure, but also software programme used for analysis and the choice of the examined structure, e.g. ROI-based, voxel-based or specific pathway based analysis. The most sensitive DTI marker is difficult to identify from all these studies. However, taking this into account, the number of studies combined with the rapid expansion and standard clinical use of DWI/DTI makes this technique very promising and in our view can rival with volumetric outcome measures in terms of early detection, robustness and rate of decline. More so, it has the added bonus of detecting a more pathophysiological process i.e. structural integrity, rather than only the outcome of neuronal loss, namely atrophy.

For MTI the s-shaped curve and the model itself is the one being least supported by literature, with the obvious reason of the absence of large numbers of studies. This technique has been used in many other diseases including neurodegenerative diseases⁷⁷, however the use in HD is limited. The evidence suggests that this technique is only sensitive at later stages than volumetric or DTI measures^{28,78,79}.

MRS has some clear advantages over the other techniques described because it can be used for biomarker research, but also inevitably adds to our pathophysiological understanding of the disease as the measured metabolites represent changes in more functional processes. Every metabolite has a different substrate in the physiological processes in the brain⁸⁰, and therefore informs us about different pathologic processes. The downside of MRS lies in the fact that measuring techniques can influence the outcome severely, with the field strength used being the most apparent one. Also, the use of metabolite ratios versus absolute quantification is another important issue. For example using a ratio to creatine when creatine is reported to be lowered in HD^{81,85} is a serious issue. The absence of longitudinal reports of MRS, makes it difficult to make any firm claim regarding its use for biomarker research, although the cross sectional results are promising^{81,85}.

Finally, fMRI is a technique where the use as a biomarker is clouded by the many studies using different paradigms, besides the, again, many analysis options. However, fMRI does give us a great insight into which functional deficits occur, or in case of premanifest HD, compensation strategies in brains activation patterns^{106,107}. The temporal changes described are all based on cross-sectional results, rather than longitudinal changes. However the potential of this technique is clear and can provide possible markers for early diagnosis and possibly disease monitoring^{107,112}. Also, fMRI showed us that brain changes do not limit themselves to the frontostriatal circuitry but were more widespread^{110,111} and will provide more understanding of the brain networks in both disease and healthy states.

In general, when considering the use of MRI derived measures as biomarkers it is worth noting that scanning is non-invasive, generally well tolerated by participants and easily applied in the daily clinic as many techniques are available in a standardized form for hospital care. Claustrophobia and metal implants, however, are always of some concern and can cause patient drop out in studies. Furthermore costs can be quite high as a single MRI scanning session usually costs several hundred dollars/euro's. However, high costs are also associated with many potential biomarkers such as any biochemical or DNA marker. As MRI becomes

more and more the standard, the costs will be limited and in our opinion does not outweigh the potential gain for HD patients. Furthermore, we envision MRI will not be used for diagnostic purposes but only for evaluating therapeutic interventions.

Conclusion

MRI could be used as outcome measure for clinical trials in HD. Overall a combination of MRI techniques is most appropriate with different modalities being the most suitable biomarker at different disease stages. For large multicenter trials an automated set up with standardized scanning protocols and post-processing is essential. However for many volumetric and DTI measures the exact analysis method chosen for the specific techniques is relatively unimportant as studies consistently report the same changes. In our opinion striatal volumetric measures and white matter (DTI) integrity measures are most appropriate for the premanifest stage of HD. These measures are the best described and deemed to be robust with consistent results throughout studies. In the transition phase to early manifest HD more measures become suitable, such as whole brain atrophy, MTI and possibly MRS. The role for fMRI lays more in the understanding of brain network functioning in neurodegeneration, although early diagnosis seems plausible as well. Therefore, we recommend constructing multimodal MRI approaches and choosing the technique, or combination of techniques, depending on the disease stage being examined in order for MRI to fulfil its role as a biomarker.

References

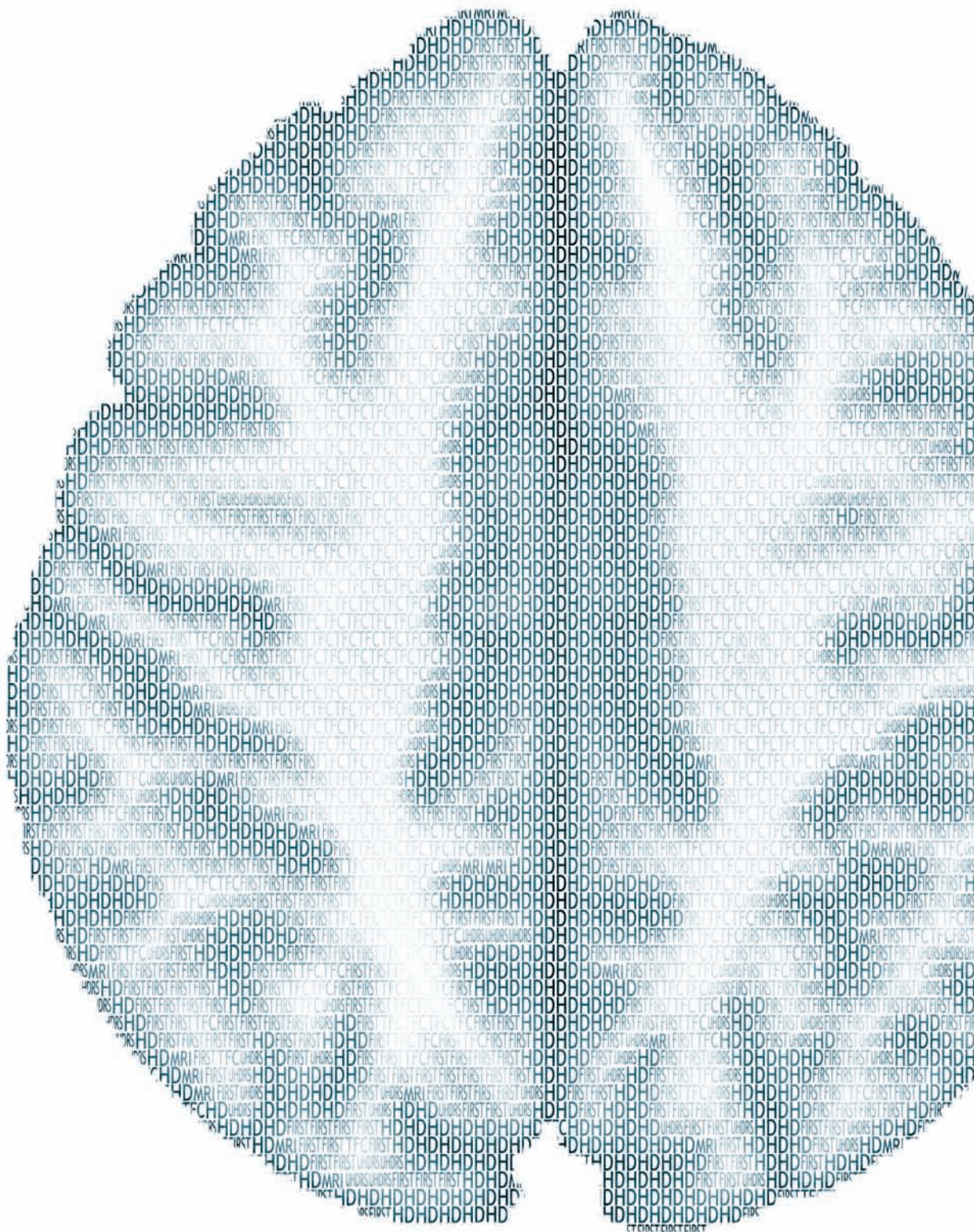
1. Phillips W, Shannon KM, Barker RA. The current clinical management of Huntington's disease. *Mov Disord* 2008;23(11):1491-504
2. Novak MJ, Tabrizi SJ. Huntington's disease. *BMJ* 2010;340:c3109
3. Aziz NA, Anguelova GV, Marinus J, et al. Autonomic symptoms in patients and pre-manifest mutation carriers of Huntington's disease. *Eur J Neurol* 2010;17(8):1068-74
4. Aziz NA, Anguelova GV, Marinus J, et al. Sleep and circadian rhythm alterations correlate with depression and cognitive impairment in Huntington's disease. *Parkinsonism Relat Disord* 2010;16(5):345-50
5. Aziz NA, van der Burg JM, Landwehrmeyer GB, et al. Weight loss in Huntington disease increases with higher CAG repeat number. *Neurology* 2008;71(19):1506-13
6. Langbehn DR, Brinkman RR, Falush D, et al. A new model for prediction of the age of onset and penetrance for Huntington's disease based on CAG length. *Clin Genet* 2004;65:267-77
7. Lemiere J, Decruyenaere M, Evers-Kiebooms G, et al. Cognitive changes in patients with Huntington's disease (HD) and asymptomatic carriers of the HD mutation--a longitudinal follow-up study. *J Neurol* 2004;251(8):935-42
8. van Duin E, Kingma EM, van der Mast RC. Psychopathology in verified Huntington's disease gene carriers. *J Neuropsychiatry Clin Neurosci* 2007;19(4):441-48
9. Roos RAC. Neuropathology of Huntington's chorea. Vinken, P. J., Bruyn, G. W, and Klawans, H. L. *Handbook of Clinical Neurology; Extrapyramidal Disorders*. 5. 1986. Elsevier Science Publishers.
10. Vonsattel JP, Myers RH, Stevens TJ, et al. Neuropathological classification of Huntington's disease. *J Neuropathol Exp Neurol* 1985;44:559-77
11. Terrence CF, Delaney JF, Alberts MC. Computed tomography for Huntington's disease. *Neuroradiology* 1977;13(4):173-75
12. Biomarkers and surrogate endpoints: preferred definitions and conceptual framework. *Clin Pharmacol Ther* 2001;69(3):89-95
13. Hersch SM, Rosas HD. Neuroprotection for Huntington's disease: ready, set, slow. *Neurotherapeutics* 2008;5(2):226-36
14. Aylward EH. Change in MRI striatal volumes as a biomarker in preclinical Huntington's disease. *Brain Res Bull* 2007;72:152-58
15. Bydder GM, Steiner RE, Young IR, et al. Clinical NMR imaging of the brain: 140 cases. *AJR Am J Roentgenol* 1982;139(2):215-36
16. Tabrizi SJ, Langbehn DR, Leavitt BR, et al. Biological and clinical manifestations of Huntington's disease in the longitudinal TRACK-HD study: cross-sectional analysis of baseline data. *Lancet Neurol*. 2009 Sep;8(9):791-801
17. van den Bogaard SJ, Dumas EM, Acharya TP, et al. Early atrophy of pallidum and accumbens nucleus in Huntington's disease. *J Neurol* 2011; 258(3): 412-20
18. Kassubek J, Juengling FD, Kioschies T, et al. Topography of cerebral atrophy in early Huntington's disease: a voxel based morphometric MRI study. *J Neurol Neurosurg Psychiatry* 2004;75:213-20
19. Jernigan TL, Salmon DP, Butters N, et al. Cerebral structure on MRI, Part II: Specific changes in Alzheimer's and Huntington's diseases. *Biol Psychiatry* 1991;29:68-81
20. Harris GJ, Pearlson GD, Peyser CE, et al. Putamen volume reduction on magnetic resonance imaging exceeds caudate changes in mild Huntington's disease. *Ann Neurol* 1992;31:69-75
21. Starkstein SE, Brandt J, Bylsma F, et al. Neuropsychological correlates of brain atrophy in Huntington's disease: a magnetic resonance imaging study. *Neuroradiology* 1992;34:487-89
22. Backman L, Robins-Wahlin TB, Lundin A, et al. Cognitive deficits in Huntington's disease are predicted by dopaminergic PET markers and brain volumes. *Brain* 1997;120 (Pt 12):2207-17
23. Brandt J, Bylsma FW, Aylward EH, et al. Impaired source memory in Huntington's disease and its relation to basal ganglia atrophy. *J Clin Exp Neuropsychol* 1995;17:868-77

24. Rosas HD, Goodman J, Chen YI, et al. Striatal volume loss in HD as measured by MRI and the influence of CAG repeat. *Neurology* 2001;57:1025-28
25. Rosas HD, Koroshetz WJ, Chen YI, et al. Evidence for more widespread cerebral pathology in early HD: an MRI-based morphometric analysis. *Neurology* 2003;60:1615-20
26. Aylward EH, Codori AM, Rosenblatt A, et al. Rate of caudate atrophy in presymptomatic and symptomatic stages of Huntington's disease. *Mov Disord* 2000;15:552-60
27. Aylward EH, Li Q, Stine OC, et al. Longitudinal change in basal ganglia volume in patients with Huntington's disease. *Neurology* 1997;48:394-99
28. Mascalchi M, Lolli F, Della NR, et al. Huntington disease: volumetric, diffusion-weighted, and magnetization transfer MR imaging of brain. *Radiology* 2004;232:867-73
29. Peinemann A, Schuller S, Pohl C, et al. Executive dysfunction in early stages of Huntington's disease is associated with striatal and insular atrophy: a neuropsychological and voxel-based morphometric study. *J Neurol Sci* 2005;239:11-19
30. Ruocco HH, Lopes-Cendes I, Li LM, et al. Striatal and extrastriatal atrophy in Huntington's disease and its relationship with length of the CAG repeat. *Braz J Med Biol Res* 2006;39:1129-36
31. Douaud G, Gaura V, Ribeiro MJ, et al. Distribution of grey matter atrophy in Huntington's disease patients: a combined ROI-based and voxel-based morphometric study. *Neuroimage* 2006;32:1562-75
32. Muhlau M, Gaser C, Wohlschlagel AM, et al. Striatal gray matter loss in Huntington's disease is leftward biased. *Mov Disord* 2007;22:1169-73
33. Fennema-Notestine C, Archibald SL, Jacobson MW, et al. In vivo evidence of cerebellar atrophy and cerebral white matter loss in Huntington disease. *Neurology* 2004;63:989-95
34. Campodonico JR, Aylward E, Codori AM, et al. When does Huntington's disease begin? *J Int Neuropsychol Soc* 1998;4:467-73
35. Harris GJ, Codori AM, Lewis RF, et al. Reduced basal ganglia blood flow and volume in pre-symptomatic, gene-tested persons at-risk for Huntington's disease. *Brain* 1999;122 (Pt 9):1667-78
36. Aylward EH, Brandt J, Codori AM, et al. Reduced basal ganglia volume associated with the gene for Huntington's disease in asymptomatic at-risk persons. *Neurology* 1994; 44(5) 823-828
37. Aylward EH, Codori AM, Barta PE, et al. Basal ganglia volume and proximity to onset in presymptomatic Huntington disease. *Arch Neurol* 1996;53:1293-96
38. Thieben MJ, Duggins AJ, Good CD, et al. The distribution of structural neuropathology in pre-clinical Huntington's disease. *Brain* 2002;125:1815-28
39. Kipps CM, Duggins AJ, Mahant N, et al. Progression of structural neuropathology in preclinical Huntington's disease: a tensor based morphometry study. *J Neurol Neurosurg Psychiatry* 2005;76:650-55
40. Paulsen JS, Magnotta VA, Mikos AE, et al. Brain structure in preclinical Huntington's disease. *Biol Psychiatry* 2006;59:57-63
41. Paulsen JS, Langbehn DR, Stout JC, et al. Detection of Huntington's disease decades before diagnosis: the Predict-HD study. *J Neurol Neurosurg Psychiatry* 2008;79:874-80
42. Jurgens CK, van de WL, van Es AC, et al. Basal ganglia volume and clinical correlates in 'preclinical' Huntington's disease. *J Neurol* 2008;255:1785-91
43. Paulsen JS, Nopoulos PC, Aylward E, et al. Striatal and white matter predictors of estimated diagnosis for Huntington disease. *Brain Res Bull* 2010;82(3-4):201-07
44. Langbehn DR, Hayden MR, Paulsen JS. CAG-repeat length and the age of onset in Huntington disease (HD): A review and validation study of statistical approaches. *Am J Med Genet B Neuropsychiatr Genet* 2010; Mar 5;153B(2):397-408.
45. Penney JB, Jr., Vonsattel JP, MacDonald ME, et al. CAG repeat number governs the development rate of pathology in Huntington's disease. *Ann Neurol* 1997;41(5):689-92
46. Aylward EH, Sparks BF, Field KM, et al. Onset and rate of striatal atrophy in preclinical Huntington disease. *Neurology* 2004;63:66-72

47. Hobbs NZ, Barnes J, Frost C, et al. Onset and progression of pathologic atrophy in Huntington disease: a longitudinal MR imaging study. *AJNR Am J Neuroradiol* 2010;31(6):1036-41
48. Hobbs NZ, Henley SM, Ridgway GR, et al. The progression of regional atrophy in premanifest and early Huntington's disease: a longitudinal voxel-based morphometry study. *J Neurol Neurosurg Psychiatry* 2010;81(7):756-63
49. Tabrizi SJ, Scahill RI, Durr A, et al. Biological and clinical changes in premanifest and early stage Huntington's disease in the TRACK-HD study: the 12-month longitudinal analysis. *Lancet Neurol*. 2011 Jan;10(1):31-42.
50. Aylward EH, Rosenblatt A, Field K, et al. Caudate volume as an outcome measure in clinical trials for Huntington's disease: a pilot study. *Brain Res Bull* 2003;62:137-41
51. Kassubek J, Juengling FD, Ecker D, et al. Thalamic atrophy in Huntington's disease co-varies with cognitive performance: a morphometric MRI analysis. *Cereb Cortex* 2005;15:846-53
52. Ruocco HH, Bonilha L, Li LM, et al. Longitudinal analysis of regional grey matter loss in Huntington disease: effects of the length of the expanded CAG repeat. *J Neurol Neurosurg Psychiatry* 2008;79:130-35
53. Henley SM, Wild EJ, Hobbs NZ, et al. Relationship between CAG repeat length and brain volume in premanifest and early Huntington's disease. *J Neurol* 2009;256:203-12
54. Rosas HD, Liu AK, Hersch S, et al. Regional and progressive thinning of the cortical ribbon in Huntington's disease. *Neurology* 2002;58:695-701
55. Rosas HD, Hevelone ND, Zaleta AK, et al. Regional cortical thinning in preclinical Huntington disease and its relationship to cognition. *Neurology* 2005;65:745-47
56. Rosas HD, Salat DH, Lee SY, et al. Cerebral cortex and the clinical expression of Huntington's disease: complexity and heterogeneity. *Brain* 2008;131:1057-68
57. Nopoulos PC, Aylward EH, Ross CA, et al. Cerebral cortex structure in prodromal Huntington disease. *Neurobiol Dis* 2010;40(3):544-54
58. Gomez-Anson B, Alegret M, Munoz E, et al. Prefrontal cortex volume reduction on MRI in preclinical Huntington's disease relates to visuomotor performance and CAG number. *Parkinsonism Relat Disord* 2009;15(3):213-19
59. Aylward EH, Anderson NB, Bylsma FW, et al. Frontal lobe volume in patients with Huntington's disease. *Neurology* 1998;50:252-58
60. Beglinger LJ, Nopoulos PC, Jorge RE, et al. White matter volume and cognitive dysfunction in early Huntington's disease. *Cogn Behav Neurol* 2005;18:102-07
61. Wild EJ, Henley SM, Hobbs NZ, et al. Rate and acceleration of whole-brain atrophy in premanifest and early Huntington's disease. *Mov Disord* 2010;25(7):888-95
62. Henley SM, Frost C, Macmanus DG, et al. Increased rate of whole-brain atrophy over 6 months in early Huntington disease. *Neurology* 2006;67:694-96
63. Henley SM, Wild EJ, Hobbs NZ, et al. Whole-brain atrophy as a measure of progression in premanifest and early Huntington's disease. *Mov Disord* 2009;24:932-36
64. Rosas HD, Lee SY, Bender AC, et al. Altered white matter microstructure in the corpus callosum in Huntington's disease: implications for cortical "disconnection". *Neuroimage* 2010;49(4):2995-3004
65. Rosas HD, Tuch DS, Hevelone ND, et al. Diffusion tensor imaging in presymptomatic and early Huntington's disease: Selective white matter pathology and its relationship to clinical measures. *Mov Disord* 2006;21:1317-25
66. Della NR, Ginestroni A, Tessa C, et al. Regional distribution and clinical correlates of white matter structural damage in Huntington disease: a tract-based spatial statistics study. *AJNR Am J Neuroradiol* 2010;31(9):1675-81
67. Dumas EM, van den Bogaard SJ, Ruber ME, et al. Early changes in white matter pathways of the sensorimotor cortex in premanifest Huntington's disease. *Hum Brain Mapp*. 2012 Jan;33(1):203-12.
68. Vandenberghe W, Demaerel P, Dom R, et al. Diffusion-weighted versus volumetric imaging of the striatum in early symptomatic Huntington disease. *J Neurol* 2009;256:109-14

69. Seppi K, Schocke MF, Mair KJ, et al. Diffusion-weighted imaging in Huntington's disease. *Mov Disord* 2006;21:1043-47
70. Douaud G, Behrens TE, Poupon C, et al. In vivo evidence for the selective subcortical degeneration in Huntington's disease. *Neuroimage* 2009;46:958-66
71. Stoffers D, Sheldon S, Kuperman JM, et al. Contrasting gray and white matter changes in preclinical Huntington disease: an MRI study. *Neurology* 2010;74(15):1208-16
72. Magnotta VA, Kim J, Kosciak T, et al. Diffusion tensor imaging in preclinical Huntington's disease. *Brain Imaging and Behavior* 2009;3:77-84
73. Reading SA, Yassa MA, Bakker A, et al. Regional white matter change in pre-symptomatic Huntington's disease: a diffusion tensor imaging study. *Psychiatry Res* 2005;140:55-62
74. Kloppel S, Draganski B, Golding CV, et al. White matter connections reflect changes in voluntary-guided saccades in pre-symptomatic Huntington's disease. *Brain* 2008;131:196-204
75. Weaver KE, Richards TL, Liang O, et al. Longitudinal diffusion tensor imaging in Huntington's Disease. *Exp Neurol* 2009;216(2):525-29
76. Sriharan A, Egan GF, Johnston L, et al. A longitudinal diffusion tensor imaging study in symptomatic Huntington's disease. *J Neurol Neurosurg Psychiatry* 2010;81:257-62
77. Filippi M, Rocca MA. Magnetization transfer magnetic resonance imaging of the brain, spinal cord, and optic nerve. *Neurotherapeutics* 2007;4(3):401-13
78. Ginestroni A, Battaglini M, Diciotti S, et al. Magnetization Transfer MR Imaging Demonstrates Degeneration of the Subcortical and Cortical Gray Matter in Huntington Disease. *AJNR Am J Neuroradiol.* 2010 Nov;31(10):1807-12.
79. Jurgens CK, Bos R, Luyendijk J, et al. Magnetization transfer imaging in 'premanifest' Huntington's disease. *J Neurol* 2010;257(3):426-32
80. Gujar SK, Maheshwari S, Bjorkman-Burtscher I, et al. Magnetic resonance spectroscopy. *J Neuroophthalmol* 2005;25:217-26
81. Sturrock A, Laule C, Decolongon J, et al. Magnetic resonance spectroscopy biomarkers in premanifest and early Huntington disease. *Neurology* 2010;75(19):1702-10
82. Clarke CE, Lowry M, Quarrell OWJ. No change in striatal glutamate in Huntington's disease measured by proton magnetic resonance spectroscopy. *Parkinsonism and Related Disorders* 1998; 4 (3) 125-27
83. Jenkins BG, Koroshetz WJ, Beal MF, et al. Evidence for impairment of energy metabolism in vivo in Huntington's disease using localized ¹H NMR spectroscopy. *Neurology* 1993;43:2689-95
84. Jenkins BG, Rosas HD, Chen YC, et al. ¹H NMR spectroscopy studies of Huntington's disease: correlations with CAG repeat numbers. *Neurology* 1998;50:1357-65
85. Sanchez-Pernaute R, Garcia-Segura JM, del Barrio AA, et al. Clinical correlation of striatal ¹H MRS changes in Huntington's disease. *Neurology* 1999;53:806-12
86. Ruocco HH, Lopes-Cendes I, Li LM, et al. Evidence of thalamic dysfunction in Huntington disease by proton magnetic resonance spectroscopy. *Mov Disord* 2007;22:2052-56
87. Taylor-Robinson SD, Weeks RA, Bryant DJ, et al. Proton magnetic resonance spectroscopy in Huntington's disease: evidence in favour of the glutamate excitotoxic theory. *Mov Disord* 1996;11:167-73
88. Taylor-Robinson SD, Weeks RA, Sargentoni J, et al. Evidence for glutamate excitotoxicity in Huntington's disease with proton magnetic resonance spectroscopy. *Lancet* 1994;343:1170
89. Davie CA, Barker GJ, Quinn N, et al. Proton MRS in Huntington's disease. *Lancet* 1994;343:1580
90. Harms L, Meierkord H, Timm G, et al. Decreased N-acetyl-aspartate/choline ratio and increased lactate in the frontal lobe of patients with Huntington's disease: a proton magnetic resonance spectroscopy study. *J Neurol Neurosurg Psychiatry* 1997;62:27-30
91. Martin WR, Wieler M, Hanstock CC. Is brain lactate increased in Huntington's disease? *J Neurol Sci* 2007;263:70-74
92. Hoang TQ, Bluml S, Dubowitz DJ, et al. Quantitative proton-decoupled ³¹P MRS and ¹H MRS in

- the evaluation of Huntington's and Parkinson's diseases. *Neurology* 1998;50:1033-40
93. Reynolds NC, Jr., Prost RW, Mark LP. Heterogeneity in 1H-MRS profiles of presymptomatic and early manifest Huntington's disease. *Brain Res* 2005;1031:82-89
 94. Roze E, Saudou F, Caboche J. Pathophysiology of Huntington's disease: from huntingtin functions to potential treatments. *Curr Opin Neurol* 2008;21:497-503
 95. van Oostrom JC, Sijens PE, Roos RA, et al. 1H magnetic resonance spectroscopy in preclinical Huntington disease. *Brain Res* 2007;1168:67-71
 96. Gomez-Anson B, Alegret M, Munoz E, et al. Decreased frontal choline and neuropsychological performance in preclinical Huntington disease. *Neurology* 2007;68:906-10
 97. Bender A, Auer DP, Merl T, et al. Creatine supplementation lowers brain glutamate levels in Huntington's disease. *J Neurol* 2005;252:36-41
 98. Tabrizi SJ, Blamire AM, Rajagopalan B, et al. High dose creatine therapy for Huntington's disease: Clinical and 31 phosphorous magnetic resonance spectroscopy ((31P) MRS) findings in a 2-year study. *Movement Disorders* 2004;19:S51
 99. Sturrock A, Laule C, Decolongon J, et al. H06: Cross sectional and longitudinal 3T magnetic resonance spectroscopy in a TRACK-HD cohort of individuals with premanifest and early Huntington's disease. *Journal of Neurology, Neurosurgery & Psychiatry* 2010;81:A35
 100. Dierks T, Linden DE, Hertel A, et al. Multimodal imaging of residual function and compensatory resource allocation in cortical atrophy: a case study of parietal lobe function in a patient with Huntington's disease. *Psychiatry Res* 1999;90:67-75
 101. Wolf RC, Vasic N, Schonfeldt-Lecuona C, et al. Cortical dysfunction in patients with Huntington's disease during working memory performance. *Brain Mapp.* 2009 Jan;30(1):327-39
 102. Clark VP, Lai S, Deckel AW. Altered functional MRI responses in Huntington's disease. *Neuroreport* 2002;13:703-06
 103. Thiruvady DR, Georgiou-Karistianis N, Egan GF, et al. Functional connectivity of the prefrontal cortex in Huntington's disease. *J Neurol Neurosurg Psychiatry* 2007;78:127-33
 104. Kim JS, Reading SA, Brashers-Krug T, et al. Functional MRI study of a serial reaction time task in Huntington's disease. *Psychiatry Res* 2004;131:23-30
 105. Georgiou-Karistianis N, Sriharan A, Farrow M, et al. Increased cortical recruitment in Huntington's disease using a Simon task. *Neuropsychologia* 2007;45:1791-800
 106. Zimbelman JL, Paulsen JS, Mikos A, et al. fMRI detection of early neural dysfunction in preclinical Huntington's disease. *J Int Neuropsychol Soc* 2007;13:758-69
 107. Paulsen JS, Zimbelman JL, Hinton SC, et al. fMRI biomarker of early neuronal dysfunction in presymptomatic Huntington's Disease. *AJNR Am J Neuroradiol* 2004;25:1715-21
 108. Reading SA, Dziorny AC, Peroutka LA, et al. Functional brain changes in presymptomatic Huntington's disease. *Ann Neurol* 2004;55:879-83
 109. Wolf RC, Vasic N, Schonfeldt-Lecuona C, et al. Dorsolateral prefrontal cortex dysfunction in presymptomatic Huntington's disease: evidence from event-related fMRI. *Brain* 2007;130:2845-57
 110. Wolf RC, Vasic N, Schonfeldt-Lecuona C, et al. Functional imaging of cognitive processes in Huntington's disease and its presymptomatic mutation carriers. *Nervenarzt* 2008; 79(4) 408-20
 111. Wolf RC, Sambataro F, Vasic N, et al. Aberrant connectivity of lateral prefrontal networks in presymptomatic Huntington's disease. *Exp Neurol* 2008;213:137-44
 112. Paulsen JS. Functional imaging in Huntington's disease. *Exp Neurol* 2009;216:272-77
 113. Georgiou-Karistianis N. A peek inside the Huntington's brain: will functional imaging take us one step closer in solving the puzzle? *Exp Neurol* 2009;220:5-8
 114. Jack CR, Jr., Knopman DS, Jagust WJ, et al. Hypothetical model of dynamic biomarkers of the Alzheimer's pathological cascade. *Lancet Neurol* 2010;9:119-28
 115. Henley SM, Ridgway GR, Scahill RI, et al. Pitfalls in the use of voxel-based morphometry as a biomarker: examples from huntington disease. *AJNR Am J Neuroradiol* 2010;31:711-19
 116. Paulsen JS, Hayden M, Stout JC, et al. Preparing for preventive clinical trials: the Predict-HD study. *Arch Neurol* 2006;63:883-90



Abstract

In Huntington's disease (HD) atrophy of the caudate nucleus and putamen has been described many years before clinical manifestation. Volume changes of the pallidum, thalamus, brainstem, accumbens nucleus, hippocampus, and amygdala are less well investigated, or reported with contradicting results. The aim of our study is to provide a more precise view of the specific atrophy of the subcortical grey matter structures in different stages of Huntington's disease, and secondly to investigate how this influences the clinical manifestations. All TRACK-HD subjects underwent standardised T1-weighted 3T MRI scans encompassing 123 manifest HD (stage 1, $n = 77$; stage 2, $n = 46$), 120 premanifest HD (close to onset $n = 58$, far from onset $n = 62$) and 123 controls. Using FMRIB's FIRST and SIENAX tools the accumbens nucleus, amygdala, brainstem, caudate nucleus, hippocampus, pallidum, putamen, thalamus and whole brain volume were extracted. Results showed that volumes of the caudate nucleus and putamen were reduced in premanifest HD far from predicted onset (> 10.8 years). Atrophy of accumbens nucleus and pallidum was apparent in premanifest HD in the close to onset group (0–10.8 years). All other structures were affected to some degree in the manifest group, although brainstem, thalamus and amygdala were relatively spared. The accumbens nucleus, putamen, pallidum and hippocampus had a strong significant correlation with functional and motor scores. We conclude that volume changes may be a sensitive and reliable measure for early disease detection and in this way serve as a biomarker for Huntington's disease. Besides the caudate nucleus and putamen, the pallidum and the accumbens nucleus show great potential in this respect.

Introduction

Huntington's disease (HD) is an autosomal dominantly inherited, slowly progressive, neurodegenerative disease localised on chromosome four. The pathophysiological mechanism is complex and although impaired energy metabolism and neuronal excitotoxicity are named as major contributors^{1,2}, it is still not fully understood, but the main result is neuronal dysfunction and loss in the brain. The disease is characterised by clinical symptoms in the motor, cognitive, and psychiatric domains.

Loss of brain cells and their connections, referred to as atrophy, can be visualised with Magnetic Resonance Imaging (MRI) techniques and has been the focus of many studies in search of objective biomarkers for tracking disease progression. The striatum has been the primary region of interest, due to previous findings in pathological studies that demonstrated the most severe loss of neurons in this region³. In manifest HD, the evidence for widespread atrophy is extensive, whereby several MRI studies showed striatal⁴⁻¹² and cortical atrophy^{13,14}. The striatal atrophy occurs in the premanifest stages of HD, with atrophy of the caudate nucleus and putamen present up to a decade or more before clinical manifestation¹⁵⁻²⁰.

Other subcortical grey matter structures have been examined to a lesser degree. Thalamic^{4,5,9,21} and pallidum^{9,10,22,23} atrophy is apparent in the manifest stages of HD; however, findings are controversial in the premanifest stage, as not all studies are in agreement^{16-19,22,24}. Atrophy of the hippocampus, amygdala, accumbens nucleus, and brainstem has only been reported in the manifest stage in a very limited number of studies^{9,22}. Whole brain atrophy has been demonstrated in HD^{25,26}. However, the rate of volume reduction of the subcortical structures as compared to whole brain atrophy has not been reported in any of the above mentioned studies and is of importance as this regional atrophy may very well only be a reflection of whole brain atrophy. Correlation studies have been performed for volume reductions and global clinical measures in manifest HD^{8,9,22}. However, reports on the relationship of atrophy with clinical measures of all these structures in different disease stages in one large cohort has not been previously reported.

With the possibilities of new therapies for HD, there has been increasing interest in the development of robust, reproducible biomarkers to assess the efficacy of potential treatments. The TRACK-HD study is an international multi-centre study investigating candidate biomarkers for HD and encompasses a large, well defined, sample of HD gene carriers²⁶. Application of a fully automated MRI-analysis tool to

this study sample provides the opportunity to study brain atrophy in detail within a very large HD cohort. The aim of this study is to provide a more precise overview of the specific atrophy of the subcortical grey matter structures in different disease stages, whilst taking into account whole brain atrophy and provide better targets for biomarker research. Secondly, we aim to examine the relationship of all subcortical grey matter structure volumes to clinical measures for HD.

Methods

Subjects

The TRACK-HD study recruited 366 participants from four centres (the National Hospital for Neurology and Neurosurgery in London, the Department of Medical Genetics at University of British Columbia in Vancouver, the Department of Genetics and Cytogenetics at the Hôpital de la Salpêtrière-Université Pierre and Marie Curie in Paris and the Department of Neurology at Leiden University Medical Center in Leiden) totalling 123 early manifest HD, 120 premanifest HD and 123 control subjects. Inclusion criteria for the early manifest HD group consisted of genetic confirmation of an expanded CAG repeat of ≥ 40 , presence of motor disturbances on the Unified Huntington's Disease Rating Scale (UHDRS), defined as a diagnostic motor confidence score of 4 and a total motor score (TMS) of > 5 , and a Total Functional Capacity (TFC) of ≥ 7 . Inclusion criteria for the premanifest group consisted of genetic confirmation of an expanded CAG repeat of ≥ 40 , absence of motor disturbances on the UHDRS, defined as a TMS of ≤ 5 . Furthermore, premanifest gene carriers required a burden of pathology score >250 , based on CAG length and age²⁷, to ensure a premanifest HD sample close to onset. Spouses or partners of premanifest and affected subjects or gene-negative siblings were recruited as healthy control subjects. The control group was age- and gender-matched to the combined premanifest and manifest HD group. Further subdivision of the premanifest group was performed on the basis of predicted years to diagnosis into preHD-A (10.8 or more years to disease onset) and preHD-B (closer than 10.8 years to disease onset) based on Langbehn's *et al.* (2004) survival analysis formula^{28,29}. The early manifest HD subjects were also divided into two groups based on disease stage by means of TFC score, the HD1 group (TFC score: 11-13) and the HD2 group (TFC score: 7-10)³⁰. The study was approved by the local ethical committees and written informed consent was obtained from each subject. For full details on study design see Tabrizi *et al.* (2009)²⁶.

Clinical measures

From the total TRACK-HD assessment battery, the UHDRS motor scale and TFC were used for this study. The UHDRS TMS is a representation of the severity of motor disturbances, scores potentially range from 0-124, with higher scores indicating more severe motor abnormalities. The TFC is a scale used for assessment of global impairments within daily activities, ranging from 0-13, with lower scores indicating impaired global functioning.

MRI acquisition

All participants underwent 3Tesla MRI scanning. T1-weighted image volumes were acquired using a 3D MPRAGE acquisition sequence on a 3.0T Siemens or a 3.0T Phillips whole body scanner with the following imaging parameters: TR = 2200ms (Siemens) / 7.7ms (Philips), TE=2.2ms (Siemens) / 3.5ms (Philips), FA=10° (Siemens) / 8° (Philips), FOV= 28cm (Siemens) / 24cm (Philips), matrix size 256x256 (Siemens) / 224x224 (Philips), 208 (Siemens) / 164 (Philips), sagittal slices to cover the entire brain with a slice thickness of 1.0 mm with no gap between slices.

Post-processing

All T1-weighted scans were analysed using software provided by FMRIB's Software Library (FSL)³¹. Eight subcortical regions were assessed using FMRIB's integrated registration and segmentation tool (FIRST)³²⁻³⁴, namely the accumbens nucleus, amygdala, brainstem, caudate nucleus, hippocampus, pallidum, putamen, and the thalamus. Total brain tissue volume was estimated with SIENAX^{35;35;36;36}. For details on MRI post-processing please see the Supplementary Material. The whole brain volume was used to calculate ratios of atrophy of the subcortical structures to whole brain atrophy. The obtained ratio was divided by the control group value in order to obtain an easily interpretable ratio whereby 1.00 is the control (normal) value ratio. The following formula was used:

[volume structure / (whole brain volume - volume structure)] / control group value

A value below 1.00 demonstrates that the structure displays more atrophy than the overall whole brain atrophy. A value greater than 1.00 demonstrates that the overall whole brain atrophy is greater than the atrophy of the structure at hand.

Statistics

Analysis of variance for group comparison was performed for volumes and ratios of the eight different subcortical structures, whilst correcting for intracranial volume, study site, age and gender. (Note that each site used a different MRI Scanner model, and thus potential scanner effects can not be differentiated from site

effects.) Comparisons of each structure were made for each disease group as compared to the control group, and as compared to the previous disease stage group, e.g. the preHD-B group was, besides comparison to the control group, also compared to the preHD-A group. We calculated partial correlations between the various subcortical structures and total motor score (TMS) and total functional capacity (TFC) from the UHDRS battery. These correlations used volumes corrected for intracranial volume and were further controlled for age, site, and gender by “partialing” these covariates out during the correlation calculations. The UHDRS TMS and TFC analyses were performed on the basis of a two-way group division, namely the premanifest gene carriers and the manifest HD group in order to keep sufficient power to perform this analysis. The significance level was set at p value < 0.05 .

Results

Characteristics

The clinical characteristics of the five study groups are shown (Table 1). The progressive nature of HD inherently leads to a higher age of the manifest HD groups. Except for the HD2 group, which displayed lower levels of education, there were no significant differences in education level between the disease groups and the controls. For full details on group characteristics we refer to the recent baseline TRACK-HD paper²⁶.

Table 1: Group characteristics

	Control	PreHD-A	PreHD-B	HD1	HD2
N	123	62	58	75	46
Leiden	30	16	14	76	14
London	30	14	16	19	11
Paris	30	14	16	25	4
Vancouver	33	18	12	15	17
Age (SD) (range; years)	46.1 (10.2) (23.0–65.7)	41.1 (8.6) (18.6–59.4)	40.6 (9.2) (22.3–64.1)	46.9 (10.2) (22.8–64.1)	51.4 (8.6) (33.3–63.3)
Women (%)	68 (55%)	33 (53%)	33 (57%)	45 (60%)	21 (46%)
Education (SD) levels 1-6	4.0 (1.3)	4.1 (1.1)	3.8 (1.3)	3.8 (1.3)	3.2 (1.4)
Disease-burden score (SD)	n.a.	259.1 (30.1)	333.1 (30.0)	364.1 (75.0)	397.6 (67.5)

Descriptive statistics of the five different groups. Data are mean (SD, range) or number (%).

Volumes

Examples of a typical output from the segmentation by the FIRST and SIENAX tools are depicted (Figure 1), for the FIRST examples only the left hemisphere segmentations are shown, however both sides were segmented for the analysis.

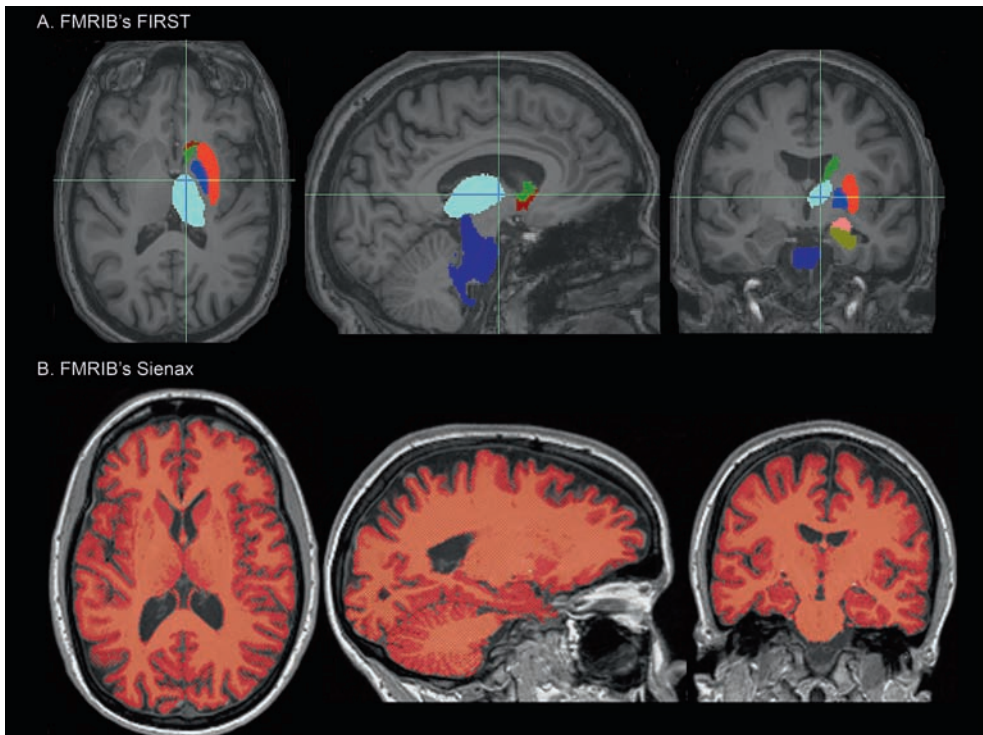


Figure 1: FSL-FIRST and SIENAX. A. Example segmentations by FSL FIRST. Dark blue = brainstem, blue = pallidum, light blue = thalamus, green = caudate nucleus, dark red = accumbens nucleus, red = putamen, copper = hippocampus, pink = amygdala. B. Example output from the FSL SIENAX tool. Red depicts the final sienax segmentation results.

Volume comparisons for eight subcortical structures in five groups are shown (Table 2). Furthermore, figure 2 shows the amount of volume reduction in terms of percentage of the control value. The putamen and the caudate nucleus show a similar pattern of a smaller volume in the preHD-A group and in every subsequent disease stage group with a continuous decline in volume. The accumbens nucleus and pallidum show a decreased volume in the preHD-B group and from every following disease stage group as compared to the controls as well as to the previous disease stage group except for the accumbens nucleus between HD1 and HD2.

Table 2: Volumetric analysis of eight structures

	Control		PreHD-A		PreHD-B		HD1		HD2	
	Mean volume	SD	Mean Volume	SD	Mean volume	SD	Mean Volume	SD	Mean volume	SD
Accumbens	1.202	0.251	1.170	0.258	1.038**††	0.245	0.873**†††	0.239	0.752**	0.239
Amygdala	3.345	0.825	3.331	0.939	3.346	0.869	3.246	0.757	2.914	0.851
Brainstem	24.043	2.672	23.828	3.001	23.011*	2.947	22.204*	2.592	21.098**††	3.063
Caudate	6.915	0.989	6.325**	1.067	5.722**††	0.923	5.057**†††	0.756	4.830**	0.816
Hippocampus	8.417	1.271	8.391	1.319	8.115*†	1.290	7.668**	1.233	6.617**†††	1.351
Pallidum	3.593	0.505	3.526	0.562	3.099**†††	0.510	2.718**†††	0.615	2.238**†††	0.679
Putamen	10.277	1.383	9.610**	1.442	8.644**†††	1.220	7.548**†††	0.987	6.935**†††	1.203
Thalamus	16.112	1.707	16.152	1.718	15.620**	1.656	14.525**††	1.524	13.681**	1.448

Means are the observed unadjusted measured values (mm³). Significance is after correction for ICV, site, gender and age. preHD = premanifest Huntington's disease, HD = manifest Huntington's disease.

* significant difference from controls $p < 0.05$

** significant difference from controls $p < 0.001$

† significant difference from previous group $p < 0.05$

†† significant difference from previous group $p < 0.01$

The brainstem and thalamus show signs of reduced volume in preHD-B, HD1 and HD2 as compared to the control group.

The amygdala showed no reduced volume as compared to the control group. The hippocampus showed volume reduction in stages preHD-B, HD1 and HD2 as compared to controls. In terms of percentages of volume reduction as compared to the control group value it is apparent that the pallidum and accumbens nucleus show marked atrophy with only 62% and 60% of the normal volume remaining in the HD2 group, respectively. These structures are closely followed by the putamen and the caudate nucleus with 67% and 70% remaining volume, respectively. Percentages for all structures in the four disease stages are also available in the supplementary material.

Ratios

Comparisons for volume ratio of eight structures as compared to whole brain atrophy are shown (Table 3). A smaller ratio indicates that the volume of this specific structure declines faster than the overall brain atrophy. The putamen atrophy ratio showed a continuous smaller value across subsequent disease stage groups. The caudate nucleus atrophy ratio showed a similar pattern, except within the manifest stage this ratio did not show a significant difference across HD1 and HD2. The accumbens nucleus and the pallidum atrophy ratio showed a decrease over disease stages from the preHD-B group onwards.

The ratio of whole brain atrophy to amygdala atrophy is comparable or slightly higher to the control group ratio. The atrophy ratio for the brainstem and thalamus shows no or slightly higher ratios as compared to the control group, stating that atrophy of these structures is comparable or slower to whole brain atrophy. Finally, the hippocampus atrophy ratio shows a drop in value in HD2 as compared to control and HD1.

Clinical measures

The UHDRS total motor score in the premanifest stage is most strongly correlated to the atrophy of the caudate nucleus ($R=-0.272$, $p=0.003$) and putamen ($R=-0.240$, $p=0.009$), but also to the atrophy of accumbens nucleus, pallidum and thalamus. The TFC demonstrates a strong ceiling effect in the premanifest stage and no significant correlations are to be found. In the manifest stage of the disease the UHDRS total motor score is most strongly related to the putamen ($R=-0.530$, $p<0.0001$), pallidum ($R=-0.390$, $p<0.0001$) and accumbens nucleus ($R=-0.380$, $p<0.0001$), but also to the hippocampus, thalamus, and brainstem.

Table 3: Ratio analysis of volumes for eight structures

	PreHD-A		PreHD-B		HD1		HD2	
	Ratio	SD	Ratio	SD	Ratio	SD	Ratio	SD
Accumbens Nucleus	1.00	0.18	0.91 ^{†††}	0.18	0.82 ^{†††}	0.18	0.73 ^{†††}	0.18
Amygdala	0.97	0.26	1.03	0.23	1.06*	0.23	1.00*	0.29
Brainstem	0.99	0.07	0.99	0.08	1.04 [†]	0.10	1.00 [†]	0.11
Caudate Nucleus	0.92 ^{**}	0.13	0.87 ^{†††}	0.11	0.83 ^{†††}	0.13	0.81 ^{**}	0.14
Hippocampus	1.00	0.13	1.01	0.13	1.03	0.16	0.91 ^{†††}	0.18
Pallidum	0.97	0.12	0.91 ^{†††}	0.12	0.85 ^{††}	0.21	0.70 ^{†††}	0.21
Putamen	0.93 ^{**}	0.11	0.87 ^{†††}	0.08	0.82 ^{†††}	0.08	0.77 ^{†††}	0.09
Thalamus	1.00	0.73	1.01	0.73	1.01	0.86	0.97	0.08

Ratios are the observed unadjusted measured values. Significance is after correction for ICV, site, gender and age. preHD = premanifest Huntington's disease, HD = manifest Huntington's disease.

* = $p < 0.05$ from control group

** = $p < 0.001$ from control group

† = $p < 0.05$ from previous group

†† = $p < 0.001$ from previous group

Table 4: Volume Correlations with Motor Score and Functional Capacity

	UDHRS Total Motor Score			Total Functional Capacity				
	PreHD		HD	PreHD		HD		
	Partial R	ρ	Partial R	ρ	Partial R	ρ		
Accumbens Nucleus	-0.24	0.01	-0.38	<0.0001	-0.025	0.79	0.21	0.03
Amygdala	-0.121	0.21	-0.11	0.23	-0.14	0.13	0.10	0.29
Brainstem	-0.12	0.23	-0.22	0.02	0.00	>0.99	0.20	0.03
Caudate Nucleus	-0.272	0.003	-0.14	0.12	-0.15	0.10	0.02	0.82
Hippocampus	0.03	0.78	-0.31	0.0008	0.03	0.73	0.24	0.01
Pallidum	-0.20	0.03	-0.39	<0.0001	0.03	0.75	0.23	0.01
Putamen	-0.24	0.009	-0.53	<0.0001	0.00	0.99	0.27	0.004
Thalamus	-0.23	0.015	-0.29	0.002	0.05	0.59	0.13	0.17

Statistic is partial correlation of volumes corrected for intracranial volume with statistical (partial) correction for site, gender and age.
 UHDRS = Unified Huntington's Disease Rating Scale, preHD = premanifest Huntington's disease, HD = manifest Huntington's disease.

The TFC is most strongly correlated to atrophy of the putamen ($R=0.270$, $p=0.004$), hippocampus ($R=0.240$, $p=0.01$) and pallidum ($R=0.230$, $p=0.01$) and a weak correlation to accumbens nucleus and brainstem.

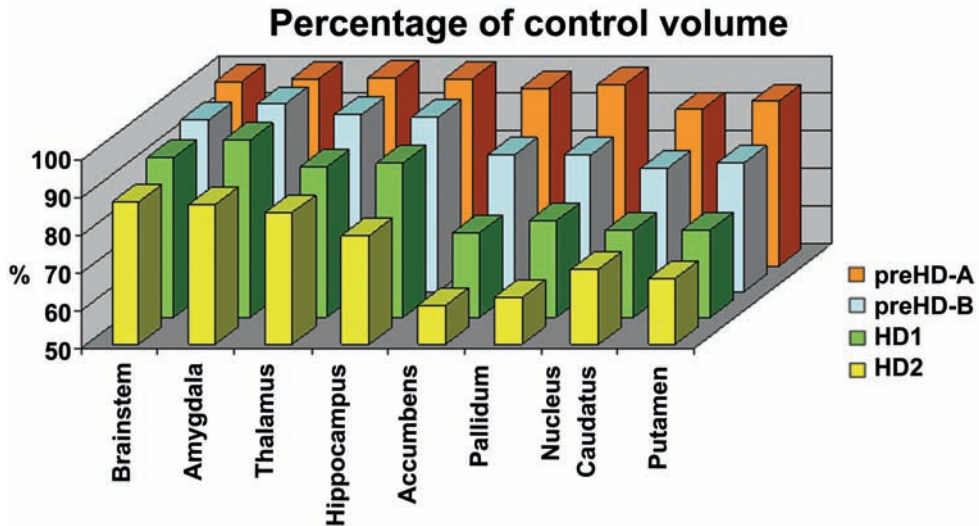


Figure 2: Percentage of volume for eight structures as compared to the control value. PreHD-A = premanifest gene carriers far from expected disease onset, preHD-B = premanifest gene carriers close to disease onset, HD1 = manifest HD stage 1, HD2 = manifest HD stage 2.

Discussion

The aim of this study was to provide a comprehensive overview of the atrophy of subcortical structures, with respect to disease stage while taking into account whole brain atrophy. The main findings show that all subcortical grey matter structures at some point have a reduced absolute volume. However, the accumbens nucleus, the caudate nucleus, the pallidum and the putamen display a true progressive decline in volume reduction which is disproportionate to overall whole brain atrophy and this is already visible in the premanifest stages of HD. Conversely, the amygdala, brainstem and thalamus do show reduced volumes, but this merely reflects the overall whole brain atrophy rate. The hippocampus is exceptional in the fact that only in the manifest stage a true rapid decline in this structure is observed. Furthermore, the volume reductions of the accumbens nucleus, putamen, pallidum and hippocampus have a severe impact on clinical measures in manifest HD.

The atrophy of the caudate nucleus and putamen in the premanifest stages confirms earlier studies. The fact that this happens a decade or more before estimated time to onset is in accordance with the findings of Aylward *et al.* (1996)³⁷, the findings of the PREDICT-HD study^{20;20} and with the results reported in TRACK-HD baseline paper²⁶.

Atrophy of the pallidum and thalamus in the premanifest stages of HD is controversial. Campodonico *et al.* (1998) and Harris *et al.* (1999) report no significant reduction in volume of the pallidum^{18;24}, while others do report this finding^{16;17;19}. With regard to the thalamus in the premanifest stage, reports of reduced volume are available in favor^{16;24} and in dispute^{19;38} of thalamic involvement. Our findings, using 3T MRI and in the largest cohort reported thus far, confirms that atrophy in the pallidum is apparent in the premanifest stage closer to predicted disease onset, but not in the further from predicted onset stage. Although thalamic atrophy is also apparent in the premanifest close to onset stage, this merely reflects the whole brain atrophy.

The brainstem, thalamus, and amygdala follow the normal atrophy rate of the whole brain in the manifest stages of the disease. In fact, in HD stage 1 the brainstem and the amygdala show signs of being relatively spared. The hippocampus shows a different pattern of atrophy as it starts to show signs of atrophy in preHD-B stage, but really becomes significant in terms of volume loss in HD stage 2. To some degree the above described findings have been reported by Rosas *et al.* (2003) and Douaud *et al.* (2006)^{9;22}. The added value of our study lies not only in the large sample size facilitating the further specification of the premanifest and manifest groups, but particularly in the fact that the atrophy described takes into account whole brain atrophy. It should be noted that some caution is appropriate when interpreting the ratio to whole brain atrophy, as this method does not necessarily imply that the volume reduction of a certain structure has to be greater than the whole brain atrophy to be of significance in terms of clinical symptoms.

The clinical impact of atrophy of subcortical grey matter is difficult to assess as many brain structures are involved in complex functionality. We have demonstrated that of the subcortical grey matter structures, specifically volume reductions of the accumbens nucleus, putamen and pallidum have the greatest influence on predicting the motor disturbances in manifest HD, and perhaps surprisingly, the impact of the caudate nucleus is minimal. The role of the pallidum in motor function is underestimated and surpasses the caudate nucleus and the thalamus. However,

the putamen is the most important structure for this clinical symptom. Our study shows that decreased global functioning of manifest HD was mainly related to volume loss of the hippocampus, putamen and pallidum. Cognitive and motor deficiencies have been shown in a number of separate studies, all examining only part of the deep grey matter structures, to relate to volume reductions of the basal ganglia, thalamus and frontal lobe^{4;6;11;18;19;24;39;40}. Within one small cohort examination of clinical measures with the TFC was carried out by Rosas *et al.* (2003) who provided evidence for an association between each separate structure and the TFC in the manifest stage²², which, apart from some differences between studies, is largely confirmed by our study. All these studies show that there is an association between volumes and clinical measures; however, we hope by examining all structures within one large, well defined cohort we can provide evidence for which structure has the most contribution (or at least the strongest correlation) to global functioning and motor disturbances.

TRACK-HD is a longitudinal observational biomarker study aimed at providing essential methodology for the assessment of therapeutic interventions. In respect to this goal we can add that the accumbens nucleus and pallidum show similar biomarker potential in addition to the well recognised structures putamen and caudate nucleus. The hippocampus is also of importance as it has a high correlation with clinical symptoms. The important role of the caudate nucleus in the premanifest stage of the disease seems to diminish after manifestation, as was also suggested by the TRACK-HD baseline paper²⁶. It is possibly fair to say that at different disease stages different structures play a role. A biomarker would ideally show sensitivity across all disease stages and would reflect the underlying pathologic processes. From this cross-sectional analysis it is not possible to draw any definitive conclusions, however, the putamen possibly shows the greatest potential. Longitudinal evaluation has to be performed to confirm the putamen's true potential. Furthermore we would like to stress how taking whole brain atrophy into account aids our interpretation of regional atrophy rates and in this way their potential as biomarkers can be assessed more effectively.

A limitation of our study could be the use of a relatively new software package from FSL used for segmentation, which hasn't specifically been validated in HD. Visual inspection, however, did not reveal any significant mismatches. The method applied gives structure segmentation on an individual basis and can therefore be used to compare groups. In contrast to this limitation several clear reasons exist in favor of using FIRST; first of all, compared to manual segmentation the automated segmentation uses voxel intensity in contrast to the sometimes difficult visual contrast differences, reducing a rater dependent bias. Secondly this automated

technique is suitable for implantation on large datasets, whereas manual segmentation is labour intensive and prone to human error.

In conclusion, we have demonstrated that atrophy of the pallidum and the accumbens nucleus exists in the premanifest stages of the disease and confirmed the well known atrophy of the caudate nucleus and putamen. Furthermore, we have shown the important correlation of the accumbens nucleus, putamen, pallidum and hippocampus with clinical symptoms. The importance of the remaining subcortical structures should be regarded when taking into account that they show similar amounts of atrophy as the brain as a whole. These findings have implications for biomarker research, as several subcortical structures now show great potential for use as a disease progression measure.

Acknowledgment

The authors wish to thank the TRACK-HD study participants, the Cure for Huntington's Disease Initiative (CHDI)/High Q Foundation, a not-for-profit organisation dedicated to finding treatments for HD, Beth Borowsky, Allan Tobin, Sherry Lifer, Saiqah Munir, Azra Hassanali, Daniel van Kammen, Ethan Signer, Michael Hayden, Susan Creighton, 2mt Software GmbH, Anne Rosser, Andrea Nemeth, Emma Hobson, the Huntington's disease clinic at Guy's hospital, Centre d'Investigation Clinique Hospital de la Salpêtrière Paris, National Hospital for Neurology London, Leiden University Medical Centre, Katja Vitkin, Felix Mudoh Tita, Irina Vainer, Theresia Kelm, Biorep Technologies, Arthur Toga, Laboratory of Neuro Imaging UCLA (LONI) and IXICO for all their help in enabling all aspects of TRACK-HD to move forward. Some of this work was undertaken at University College London Hospital/University College London, which received funding from the Department of Health NIHR Biomedical Research Centres funding scheme.

TRACK-HD study group

Canada—A Coleman, R Dar Santos, J Decolongon, A Sturrock, B Leavitt (University of British Columbia, Vancouver). *France*—E Bardinet, C Jauffret, D Justo, S Lehericy, C Marelli, K Nigaud, R Valabrègue, A. Durr (APHP, Hôpital Salpêtrière, Paris). *Germany*—N Bechtel, R. Reilmann (University of Münster, Münster); A Hoffman, P Kraus (University of Bochum, Bochum), B Landwehrmeyer (University Ulm, Ulm). *Netherlands*—J van der Grond, EP t'Hart, C Jurgens, M-N Witjes-Ane (Leiden University Medical Centre, Leiden). *UK*—N Arran, J Callaghan, D Craufurd (St Mary's Hospital, Manchester); C Frost, R Jones (London School of Hygiene and Tropical Medicine, London); N Hobbs, N Lahiri, R Ordidge, G Owen, T Pepple, J Read, M Say, E Wild, N. Fox (University College London, London); S Keenan (Imperial College London, London); D M Cash (IXICO, London) C Kennard, S Hicks (Oxford, UK). *USA*—E Axelson, C Wang (University of Iowa, Iowa City, IA); S Lee, W Monaco, D. Rosas (Massachusetts General Hospital, Harvard, MA); C Campbell, S Queller, K Whitlock (Indiana University, IN). *Australia*—C Campbell, M Campbell, E Frajman, C Milchman, A O'Regan, J. Stout (Monash University, Victoria).

References

1. Estrada Sanchez AM, Mejia-Toiber J, Massieu L. Excitotoxic neuronal death and the pathogenesis of Huntington's disease. *Arch Med Res* 2008;39:265-76
2. Roze E, Saudou F, Caboche J. Pathophysiology of Huntington's disease: from huntingtin functions to potential treatments. *Curr Opin Neurol* 2008;21:497-503
3. Roos RAC. Neuropathology of Huntington's chorea. Vinken, P. J., Bruyn, G. W, and Klawans, H. L. *Handbook of Clinical Neurology; Extrapyramidal Disorders*. 5. 1986. Elsevier Science Publishers.
4. Backman L, Robins-Wahlin TB, Lundin A, et al. Cognitive deficits in Huntington's disease are predicted by dopaminergic PET markers and brain volumes. *Brain* 1997;120 (Pt 12):2207-17
5. Jernigan TL, Salmon DP, Butters N, et al. Cerebral structure on MRI, Part II: Specific changes in Alzheimer's and Huntington's diseases. *Biol Psychiatry* 1991;29:68-81
6. Aylward EH, Codori AM, Rosenblatt A, et al. Rate of caudate atrophy in presymptomatic and symptomatic stages of Huntington's disease. *Mov Disord* 2000;15:552-60
7. Kassubek J, Juengling FD, Kioschies T, et al. Topography of cerebral atrophy in early Huntington's disease: a voxel based morphometric MRI study. *J Neurol Neurosurg Psychiatry* 2004;75:213-20
8. Muhlau M, Gaser C, Wohlschlaeger AM, et al. Striatal gray matter loss in Huntington's disease is leftward biased. *Mov Disord* 2007;22:1169-73
9. Douaud G, Gaura V, Ribeiro MJ, et al. Distribution of grey matter atrophy in Huntington's disease patients: a combined ROI-based and voxel-based morphometric study. *Neuroimage* 2006;32:1562-75
10. Ruocco HH, Lopes-Cendes I, Li LM, et al. Striatal and extrastriatal atrophy in Huntington's disease and its relationship with length of the CAG repeat. *Braz J Med Biol Res* 2006;39:1129-36
11. Peinemann A, Schuller S, Pohl C, et al. Executive dysfunction in early stages of Huntington's disease is associated with striatal and insular atrophy: a neuropsychological and voxel-based morphometric study. *J Neurol Sci* 2005;239:11-19
12. Harris GJ, Pearlson GD, Peyser CE, et al. Putamen volume reduction on magnetic resonance imaging exceeds caudate changes in mild Huntington's disease. *Ann Neurol* 1992;31:69-75
13. Rosas HD, Liu AK, Hersch S, et al. Regional and progressive thinning of the cortical ribbon in Huntington's disease. *Neurology* 2002;58:695-701
14. Rosas HD, Hevelone ND, Zaleta AK, et al. Regional cortical thinning in preclinical Huntington disease and its relationship to cognition. *Neurology* 2005;65:745-47
15. Aylward EH, Sparks BF, Field KM, et al. Onset and rate of striatal atrophy in preclinical Huntington disease. *Neurology* 2004;63:66-72
16. Thieben MJ, Duggins AJ, Good CD, et al. The distribution of structural neuropathology in pre-clinical Huntington's disease. *Brain* 2002;125:1815-28
17. Kipps CM, Duggins AJ, Mahant N, et al. Progression of structural neuropathology in preclinical Huntington's disease: a tensor based morphometry study. *J Neurol Neurosurg Psychiatry* 2005;76:650-55
18. Campodónico JR, Aylward E, Codori AM, et al. When does Huntington's disease begin? *J Int Neuropsychol Soc* 1998;4:467-73
19. Jurgens CK, van de WL, van Es AC, et al. Basal ganglia volume and clinical correlates in 'preclinical' Huntington's disease. *J Neurol* 2008;255:1785-91
20. Paulsen JS, Langbehn DR, Stout JC, et al. Detection of Huntington's disease decades before diagnosis: the Predict-HD study. *J Neurol Neurosurg Psychiatry* 2008;79:874-80
21. Kassubek J, Juengling FD, Ecker D, et al. Thalamic atrophy in Huntington's disease co-varies with cognitive performance: a morphometric MRI analysis. *Cereb Cortex* 2005;15:846-53
22. Rosas HD, Koroshetz WJ, Chen YI, et al. Evidence for more widespread cerebral pathology in early HD: an MRI-based morphometric analysis. *Neurology* 2003;60:1615-20
23. Aylward EH, Brandt J, Codori AM, et al. Reduced basal ganglia volume associated with the gene for Huntington's disease in asymptomatic at-risk persons. *Neurology* 1994; 44(5) 823-828

24. Harris GJ, Codori AM, Lewis RF, et al. Reduced basal ganglia blood flow and volume in pre-symptomatic, gene-tested persons at-risk for Huntington's disease. *Brain* 1999;122 (Pt 9):1667-78
25. Henley SM, Frost C, Macmanus DG, et al. Increased rate of whole-brain atrophy over 6 months in early Huntington disease. *Neurology* 2006;67:694-96
26. Tabrizi SJ, Langbehn DR, Leavitt BR, et al. Biological and clinical manifestations of Huntington's disease in the longitudinal TRACK-HD study: cross-sectional analysis of baseline data. *Lancet Neurol.* 2009 Sep;8(9):791-801
27. Penney JB, Jr., Vonsattel JP, MacDonald ME, et al. CAG repeat number governs the development rate of pathology in Huntington's disease. *Ann Neurol* 1997;41:689-92
28. Langbehn DR, Brinkman RR, Falush D, et al. A new model for prediction of the age of onset and penetrance for Huntington's disease based on CAG length. *Clin Genet* 2004;65:267-77
29. Langbehn DR, Hayden MR, Paulsen JS. CAG-repeat length and the age of onset in Huntington disease (HD): A review and validation study of statistical approaches. *Am J Med Genet B Neuropsychiatr Genet.* 2010 Mar 5;153B(2):397-408.
30. Shoulson I, Fahn S. Huntington disease: clinical care and evaluation. *Neurology* 1979;29:1-3
31. Smith SM, Jenkinson M, Woolrich MW, et al. Advances in functional and structural MR image analysis and implementation as FSL. *Neuroimage* 2004;23 Suppl 1:S208-S219
32. Patenaude B. Bayesian Statistical Models of Shape and Appearance for Subcortical Brain Segmentation. 2007. Thesis. D.Phil.
33. Patenaude B, Smith S, Kennedy D, et al. FIRST - FMRIB's integrated registration and segmentation tool. 2007. In Human Brain Mapping Conference.
34. Patenaude B, Smith S, Kennedy D, et al. Improved Surface Models for FIRST. 2008. In Human Brain Mapping Conference.
35. Smith SM, De Stefano N, Jenkinson M, et al. Normalized accurate measurement of longitudinal brain change. *J Comput Assist Tomogr* 2001;25:466-75
36. Smith SM, Zhang Y, Jenkinson M, et al. Accurate, robust, and automated longitudinal and cross-sectional brain change analysis. *Neuroimage* 2002;17:479-89
37. Aylward EH, Codori AM, Barta PE, et al. Basal ganglia volume and proximity to onset in presymptomatic Huntington disease. *Arch Neurol* 1996;53:1293-96
38. Paulsen JS, Hayden M, Stout JC, et al. Preparing for preventive clinical trials: the Predict-HD study. *Arch Neurol* 2006;63:883-90
39. Aylward EH. Change in MRI striatal volumes as a biomarker in preclinical Huntington's disease. *Brain Res Bull* 2007;72:152-58
40. Ruocco HH, Bonilha L, Li LM, et al. Longitudinal analysis of regional grey matter loss in Huntington disease: effects of the length of the expanded CAG repeat. *J Neurol Neurosurg Psychiatry* 2008;79:130-35

Supplementary Material

Table 1: Percentage of the volume as compared to the control group value for eight separate structures.

	PreHD-A	PreHD-B	HD1	HD2
Accumbens Nucleus	97.4 %	86.4 %	72.6 %	60.3 %
Amygdala	99.6 %	100.0 %	97.0 %	87.1 %
Brainstem	99.1 %	95.7 %	92.4 %	87.7 %
Caudate Nucleus	91.5 %	82.8 %	73.1 %	69.8 %
Hippocampus	99.7 %	96.4 %	91.1 %	78.6 %
Pallidum	98.1 %	86.2 %	75.6 %	62.3 %
Putamen	93.5 %	84.1 %	73.4 %	67.5 %
Thalamus	100.3 %	97.0 %	90.2 %	84.9 %

Values represent percentage of the volume as compared to the control group value for eight separate subcortical structures. PreHD-A = premanifest gene carriers far from expected disease onset, preHD-B = premanifest gene carriers close to disease onset, HD1 = manifest HD stage 1, HD2 = manifest HD stage 2.

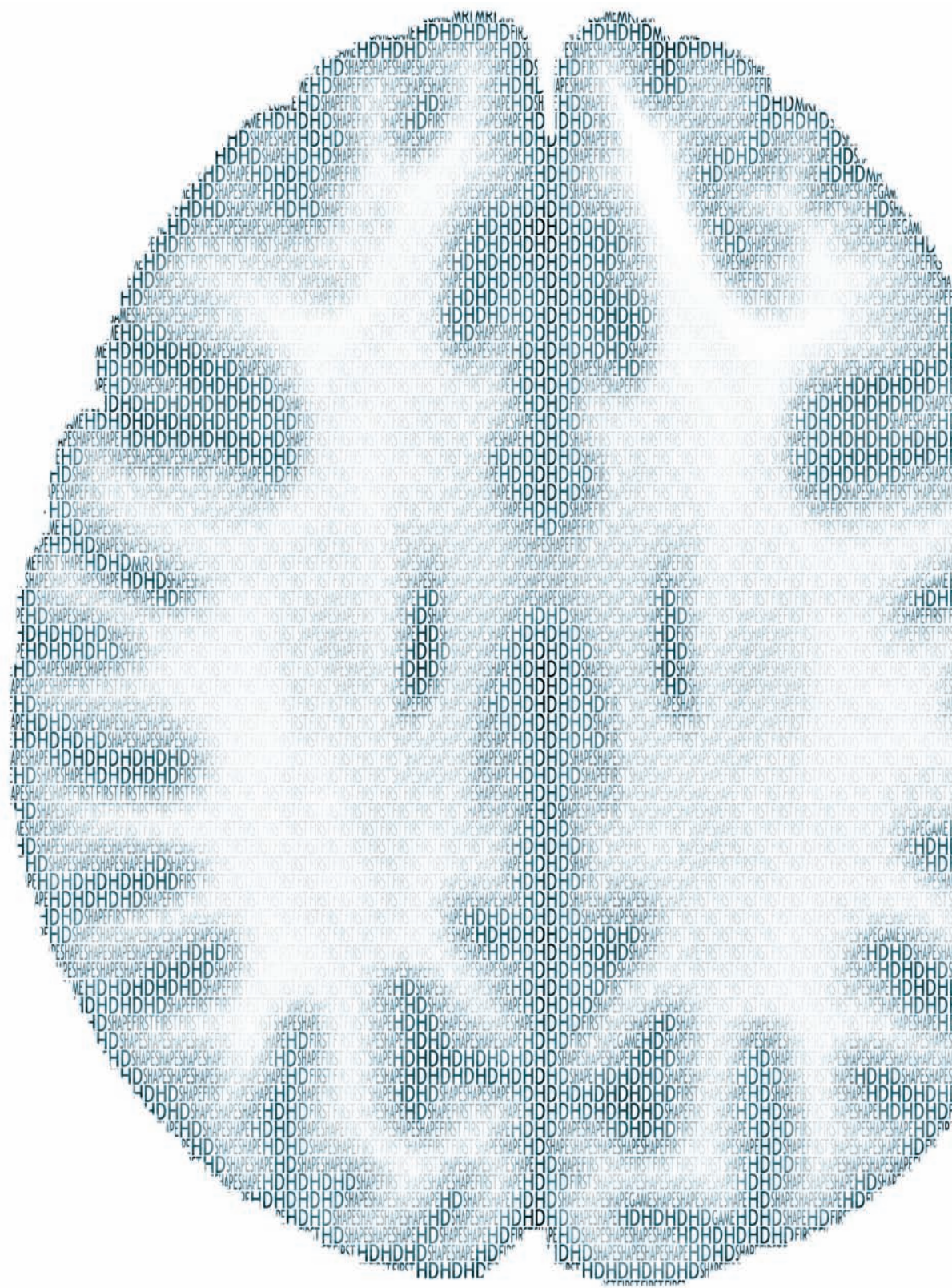
Methods: MRI Postprocessing

All T1-weighted scans were analysed using software provided by FMRIB's Software Library (FSL)¹. Eight subcortical regions were assessed using FMRIB's Integrated Registration and Segmentation Tool (FIRST)²⁻⁴, namely the accumbens nucleus, amygdala, brainstem, caudate nucleus, hippocampus, pallidum, putamen, and the thalamus. Using FIRST, the T1 weighted images were first registered to MNI (Montreal Neurological Institute) 152 standard space, using linear registration with 12 degrees of freedom⁵⁻⁶. FIRST draws upon a vast library of manually segmented images, which were transformed into deformable surface meshes. These meshes were applied to our dataset to be used as subcortical masks to locate the specific structures. Subsequently, segmentation was carried out using the voxel intensities and mesh models. Finally a boundary correction was applied to prevent overlap with adjacent structures. After registration and segmentation the absolute volume was calculated having taken into account the obtained information from previous steps. A visual inspection of all registrations was performed and of the final segmentations 20% were selected at random and visually inspected for accuracy. Total brain tissue volume was estimated with SIENAX⁷⁻⁸. This program extracts brain and skull images from the single whole-head input data⁹. The brain images were then affine-registered to MNI152 space, using the skull images to determine

the registration scaling. Next, tissue-type segmentation with partial volume estimation was carried out¹⁰.

References

1. Smith SM, Jenkinson M, Woolrich MW, et al. Advances in functional and structural MR image analysis and implementation as FSL. *Neuroimage* 2004;23 Suppl 1:S208-S219
2. Patenaude, B. Bayesian Statistical Models of Shape and Appearance for Subcortical Brain Segmentation. 2007. Thesis. D.Phil
3. Patenaude, B, Smith, S, Kennedy, D, et al. FIRST - FMRI's integrated registration and segmentation tool. 2007. In Human Brain Mapping Conference.
4. Patenaude, B, Smith, S, Kennedy, D, et al. Improved Surface Models for FIRST. 2008. In Human Brain Mapping Conference
5. Jenkinson M, Smith S. A global optimisation method for robust affine registration of brain images. *Med Image Anal* 2001;5:143-56.
6. Jenkinson M, Bannister P, Brady M, et al. Improved optimization for the robust and accurate linear registration and motion correction of brain images. *Neuroimage* 2002;17:825-41.
7. Smith SM, De Stefano N, Jenkinson M, et al. Normalized accurate measurement of longitudinal brain change. *J Comput Assist Tomogr* 2001;25:466-75
8. Smith SM, Zhang Y, Jenkinson M, et al. Accurate, robust, and automated longitudinal and cross-sectional brain change analysis. *Neuroimage* 2002;17:479-89.
9. Smith SM. Fast robust automated brain extraction. *Hum Brain Mapp* 2002;17:143-55.
10. Zhang Y, Brady M, Smith S. Segmentation of brain MR images through a hidden Markov random field model and the expectation-maximization algorithm. *IEEE Trans Med Imaging* 2001;20:45-57.





CHAPTER 4

SHAPE ANALYSIS OF SUBCORTICAL NUCLEI IN HUNTINGTON'S DISEASE, GLOBAL VERSUS LOCAL ATROPHY - RESULTS FROM THE TRACK-HD STUDY

SIMON J.A. VAN DEN BOGAARD¹, EVE M. DUMAS¹, LUCA FERRARINI²,
JULIEN MILLES², MARK A. VAN BUCHEM³,
JEROEN VAN DER GROND³, RAYMUND A.C. ROOS¹

1. DEPARTMENT OF NEUROLOGY, LEIDEN UNIVERSITY MEDICAL CENTER, LEIDEN, THE NETHERLANDS
2. DIVISION OF IMAGE PROCESSING (LKEB), DEPARTMENT OF RADIOLOGY,
LEIDEN UNIVERSITY MEDICAL CENTER, LEIDEN, THE NETHERLANDS
3. DEPARTMENT OF RADIOLOGY, LEIDEN UNIVERSITY MEDICAL CENTER, LEIDEN, THE NETHERLANDS

Abstract

Huntington's disease (HD) is characterized by brain atrophy. Localized atrophy of a specific structure could potentially be a more sensitive biomarker reflecting neuropathologic changes rather than global volume variation. We examined 90 TRACK-HD participants of which 30 were premanifest HD, 30 were manifest HD and 30 were controls. Using FMRIB's Integrated Registration and Segmentation Tool, segmentations were obtained for the pallidum, caudate nucleus, putamen, thalamus, accumbens nucleus, amygdala, and hippocampus and overall volumes were calculated. A point distribution model of each structure was obtained using Growing and Adaptive Meshes. Permutation testing between groups was performed to detect local displacement in shape between groups. In premanifest HD overall volume loss occurred in the putamen, accumbens and caudate nucleus. Overall volume reductions in manifest HD were found in all subcortical structures, except the amygdala, as compared to controls. In premanifest HD shape analysis showed small areas of displacement in the putamen, pallidum, accumbens and caudate nucleus. When the premanifest group was split into two groups according to predicted disease onset, the premanifest HD group close to expected disease onset showed more pronounced displacements in caudate nucleus and putamen compared to premanifest HD far from disease onset or the total premanifest group. Analysis of shape in manifest HD showed widespread shape differences, most prominently in the caudal part of the accumbens nucleus, body of the caudate nucleus, putamen and dorsal part of the pallidum. We conclude that shape analysis provides new insights in localized intrastructural atrophy patterns in HD, but can also potentially serve as specific target areas for disease tracking.

Introduction

Huntington's disease (HD) is a slowly progressive neurodegenerative genetic disease that affects the brain. Disease onset occurs typically between the age of 35 and 45 years, with clinical symptoms in motor, cognitive and behavior domains. Since the discovery of the genetic defect on chromosome 4, the gene status of at-risk individuals can be determined, making identification of premanifest gene carriers possible. This makes examination of brain structures possible in this symptom free period, and can provide insight into pathophysiological changes underlying the disease.

Currently, many studies focus on finding reliable markers to monitor disease progression^{1,2}. MRI measures show great potential of becoming sensitive biomarkers for HD, as they are objective and have been applied to demonstrate abnormalities of both gray and white matter structures³. Changes in basal ganglia are of special interest as these structures display overall volume reduction in the premanifest stages of HD. The caudate nucleus and putamen are reported to be atrophied up to a decade before disease onset^{1,2,4}.

Two pathologic studies report on localized loss of neurons within a structure, namely within the medial paraventricular portions of the caudate nucleus, in the tail of the caudate nucleus, and in the dorsal part of the putamen in a dorsal ventral manner^{5,6}. Currently, in vivo measures of atrophy have predominantly reported overall volumetric change of a structure, representing a generalized loss of neurons and axons. Unrepresented in this approach is localized loss of neurons, or any other remodeling effects, which go unnoticed if these local changes do not significantly affect the total volume of the structure.

To examine how subcortical nuclei change locally, we have chosen an automated MRI analysis set-up using FMRIB's Integrated Registration and Segmentation Tool (FIRST) and the Growing and Adaptive Meshes (GAMEs) tools. This approach is chosen because in this way we obtain a per participant individual segmentation and outer surface of several subcortical structures. This approach is fundamentally different from Voxel Based Morphometry (VBM) where a voxel wise comparison is made between groups, also in this way we avoid some known methodological issues associated with VBM^{7,8}.

The TRACK-HD study is a biomarker study¹, dedicated to finding objective and sensitive measures for disease progression. This study allows examination of a

well defined cohort of premanifest gene carriers, manifest HD and controls. The aim of our study is to determine how the subcortical nuclei locally change in shape in the premanifest and the manifest stage of HD in relation to global volumetric changes.

Methods

Subjects

The multicentre Track-HD cohort consists in total of 366 participants. All of the 90 participants enrolled at the Leiden University Medical Centre from the TRACK-HD cohort were included for this analysis (premanifest HD n=30, manifest HD n=30, control n=30). Inclusion criteria for the premanifest group consisted of a CAG repeat length ≥ 40 , absence of motor disturbances on the Unified Huntington's Disease Rating Scale (UHDRS) defined as a total motor score (TMS) ≤ 5 . The UHDRS TMS is a clinical rating of the amount of motor disturbances, grading several distinct motor features separately such as chorea, dystonia, rigidity, bradykinesia and eye movements, resulting in a sum score ranging from 0 to 124. Additionally a disease burden score of ≥ 250 was mandatory to ensure that the premanifest group was within 16 years of the predicted age of onset^{9;10}. For an additional analysis within the premanifest group, a further subdivision of the group was performed on the basis of the median predicted years to diagnosis into premanifest A (10.8 or more years to disease onset, N = 16) and premanifest B (closer than 10.8 years to disease onset, N = 14) based on Langbehn's *et al.* (2004, 2010) survival analysis formula^{10;11} identical to previous reports from the TRACK-HD study^{1;12}. Inclusion criteria for the manifest HD group consisted of a CAG repeat ≥ 40 , a TMS > 5 and a Total Functional Capacity (TFC) ≥ 7 . The TFC is a clinical scale assessing the activities in daily life (range 0-13) such as job capability, finances, daily chores and self care. Healthy gene negative family members or partners/spouses were included as controls. Exclusion criteria consisted of any significant (neurological) comorbidity, history of severe head trauma, a major psychiatric diagnosis and MRI incompatibility. The medical ethical committee approved the study, and written informed consent was obtained from all participants. Detailed description of recruitment and inclusion criteria is given in the TRACK-HD baseline paper¹.

MRI acquisition

In accordance with the TRACK-HD protocol, all participants underwent MRI scanning on a 3 Tesla Philips whole body scanner (Philips Medical Systems, Best, The Netherlands) with an eight channel receive and transmit coil array. T1-

weighted image volumes were acquired using a 3D MPRAGE acquisition sequence with the following imaging parameters: TR = 7.7ms, TE= 3.5ms, FA= 8°, FOV= 24cm, matrix size 224x224x164 with sagittal slices to cover the entire brain with a slice thickness of 1.0 mm with no gap between slices, total acquisition time was ~9 minutes.

Post-Processing and Statistics

The analysis pipeline is depicted in figure 1.

Analysis processing pipeline

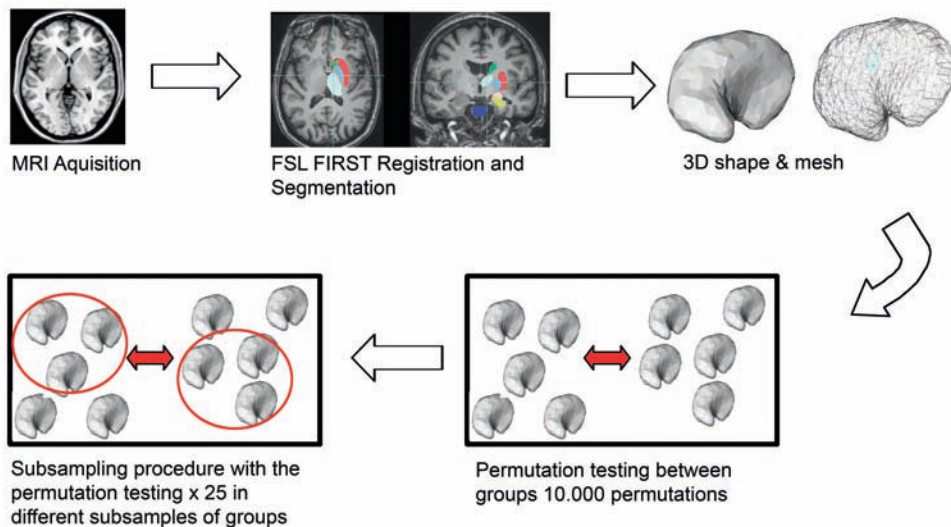


Figure 1: Analysis processing pipeline from MRI acquisition to Hotelling's T2 statistics

Overall volume analysis

Using FMRIB's Integrated Registration and Segmentation Tool (FIRST), subcortical nuclei were affine registered to MNI152 standard space using linear registration and subsequently automatically segmented^{13,14}. Volumes for pallidum, caudate nucleus, putamen, thalamus, accumbens nucleus, amygdala, and the hippocampus were calculated. Analysis of variance was performed, correcting for age, gender and intracranial volume (ICV).

The rationale to use FSL FIRST as our registration and segmentation tool was the fact that the tool has an automated set-up and is therefore an unbiased approach.

The validity of the tool to register and segment with great accuracy is described by Patenaude *et al.* (2007, 2008)¹³⁻¹⁵. Furthermore the automated set-up makes it relatively easy to use in large cohorts. A previous study showed the reliable use of this tool in HD for volumetric analysis in HD¹². This tool has been and is currently being used in many other studies regarding different neurological disorders, among others in Alzheimer's Disease¹⁶. FSL FIRST has been compared to another automated segmentation tool, namely Freesurfer, with comparison to manual segmentation. It was concluded that Freesurfer provided better results for the hippocampus and FIRST for the amygdala in terms of segmentation and shape analysis. However, also relevant is the comparison they made to expert manual segmentation, where no significant difference was found for the amygdala volume manual versus FIRST segmentation¹⁷. FIRST performed better in the smaller subcortical structures in a scan-rescan study¹⁸, and since TRACK-HD is set-up as a longitudinal study this is the logical choice considering all of the above arguments. However, it must be noted that all these methodological studies make use of a healthy control group, and to our knowledge no study comparing expert manual tracing versus automated segmentation in diseased/atrophied states exists.

Additional quality control was performed via a visual inspection of all the segmentations using the original T1-weighted scans and projecting the individual segmentations on top of these images. Special attention was given to the outliers in terms of volume. Several registration errors resulted in erroneous segmentations and subsequently these scans were re-run until satisfactory segmentations were acquired. No significant mismatches were visually seen after these steps.

Shape Analysis

To perform shape analysis, comparative meshes for each structure were built. For this purpose the Growing and Adaptive Meshes (GAMEs) algorithm was utilized¹⁹, making use of the segmentations acquired from FIRST. GAMEs has been previously successfully applied for analyzing shape variations in Alzheimer's disease^{20,21}. This algorithm builds a deformable surface mesh model based on an average of the 30 control group segmentations. This general mesh model consists of numerous nodes which are equal in number for all meshes used for the comparative analysis across groups. Using these meshes, local shape analysis was performed by repeated permutation tests via a Hotelling's T2 statistical test. The following procedure was applied: a subsampling process was performed, with random samples taken from the control and the HD group; subsequently, permutation test (based on 10.000 iterations, in order to allow for p -values as low as 10^{-4}) were performed to detect significant different location between groups, at a

confidence level of 99%. In total 25 sub-sampling iterations were performed, each sub-sample containing a minimum of 60% of the entire group population. For each node the significance level was assessed for all structures analyzed. The latter step is to ensure that the findings are not due to outliers in either the control or the HD group. True findings appear in the majority of the subsample analyses, which can be defined as either 80 or 95% of the subsamples depending on the desired statistical scrutiny. Graphical display does not only show the area of the surface affected in 80-95% of the sub-sampling, but also the amount of displacement in millimeters. We have chosen to use the most conservative option, namely the 95% level; thus the significant locations are at an $\alpha=0.01$, 95% of the times in which the sub-sampling was performed. Three groups were included in the analysis, and the comparisons are displayed for the premanifest group versus the control group and secondly the manifest HD group versus the control group. An additional analysis was performed in an identical manner with the premanifest A and premanifest B groups both compared to the control group. The rationale to perform this additional analysis lies in the fact that there were only limited findings in the premanifest group, which could be due to the fact of a heterogenous premanifest group in terms of predicted years to disease onset. This was addressed by the subdivision of the premanifest group according to predicted disease onset as described above; however noted was the potential disadvantage of loss of statistical power.

Results

Demographic characteristics of the study groups

The clinical features of the three groups are shown in table 1. There were no statistically significant differences between the control and premanifest group. The UHDRS total motor score and total functional capacity were different between the manifest and control or premanifest group.

Table 1: Group characteristics

	Control (Mean ± SD)	Premanifest HD (Mean ± SD)	Manifest HD (Mean ± SD)
Age	48.6 ± 8.3	43.3 ± 8.0	47.6 ± 10.3
CAG	n.e.	42.5 ± 2.4	43.6 ± 2.6
Years to onset	n.a.	11.6 ± 4.3	n.a.
UHDRS TMS	2.6 ± 2.4	2.5 ± 1.4	21.9 ± 11.1 *
TFC	13.0 ± 0.2	12.6 ± 0.8	10.4 ± 2.0 *
Gender (N ♀/♂)	16/14	18/12	21/9

Demographic variables of the three groups. CAG = Cytosine-Adenosine-Guanine repeat. UHDRS = Unified Huntington's Disease Rating Scale Total Motor Score, TFC = Total Functional Capacity. n.a. = not applicable, n.e. = not examined. * = significant different from the control and premanifest HD group with $p < 0.05$.

Volumetric analysis

Significant differences in overall volumes between the premanifest and control group were apparent in the accumbens nucleus, caudate nucleus, left hippocampus and putamen. In the manifest HD group all volumes were significantly reduced as compared to controls, except for the amygdala. The overall volumes are shown in table 2.

Shape analysis

The shape analyses for the basal ganglia structures accumbens nucleus, caudate nucleus, pallidum and putamen are displayed in figure 2. The remaining structures amygdala, hippocampus and thalamus are shown in figure 3. The displacements shown in the figures are all significant at the 99% significance level, with the colour coding of the amount of displacements in millimeters. All displacements were inwards, representing atrophy. No significant areas of hypertrophy were observed.

For the accumbens nucleus it is apparent that the shape changes were localized at the caudal side, most prominently seen in the manifest stage. In the premanifest stage a displacement is seen in the right accumbens nucleus. The caudate nucleus showed displacements in both the premanifest and manifest HD groups. A generalized displacement is seen across the whole caudate nucleus, most significantly in the body on the medial side. In premanifest HD significant displacement is seen in some areas more towards the tail. The pallidum showed a diffuse pattern of displacement in the manifest HD group, with the dorsal part displaying the most extensive displacements. Displacement is also seen in this

part of the dorsal pallidum in the premanifest HD group. The putamen showed displacement over the entire structure in the manifest stage, small patches were found in the premanifest stage on the medial side of the left putamen.

For the amygdala the shape changes were seen in the manifest stage, specifically on the cranial side. No displacements were seen in the premanifest group. The hippocampus showed patchy displacement areas at the ventral as well as the dorsal part, this displacement being limited to the manifest group only. Finally the thalamus showed some patchy displacements on the ventro-medial and ventro-lateral side of the structure, but no real displacement areas could be found in the premanifest group.

Table 2: Volumes of subcortical nuclei

	Control		Premanifest HD		Manifest HD	
	Mean volume	SD	Mean Volume	SD	Mean Volume	SD
Accumbens Nucleus						
Right	0.444	0.135	0.369 *	0.107	0.356 *	0.184
Left	0.605	0.136	0.544 *	0.112	0.381 **	0.140
Amygdala						
Right	1.344	0.191	1.376	0.312	1.251	0.307
Left	1.216	0.316	1.218	0.381	1.084	0.343
Caudate Nucleus						
Right	3.339	0.504	2.922 *	0.430	2.450 **	0.447
Left	3.207	0.399	2.848 *	0.493	2.283 **	0.394
Hippocampus						
Right	3.855	0.658	3.820	0.664	3.132 **	0.671
Left	3.660	0.570	3.390 *	0.510	3.121 **	0.478
Pallidum						
Right	1.528	0.278	1.443	0.326	1.025 **	0.319
Left	1.648	0.348	1.524	0.331	1.071 **	0.333
Putamen						
Right	4.597	0.692	4.078 *	0.690	3.283 **	0.463
Left	4.664	0.742	4.176 *	0.607	3.255 **	0.511
Thalamus						
Right	7.424	0.605	7.432	0.730	6.795 *	0.806
Left	7.328	0.840	7.260	0.894	6.782 *	0.794

Volumetric analysis of seven structures. Means are the absolute measured values (mm³). Significance is after correction for intracranial volume, gender and age

* significant difference from controls $p < 0.05$

** significant difference from controls $p < 0.001$

Shape analysis of accumbens nucleus, caudate nucleus, pallidum and putamen in premanifest and manifest HD

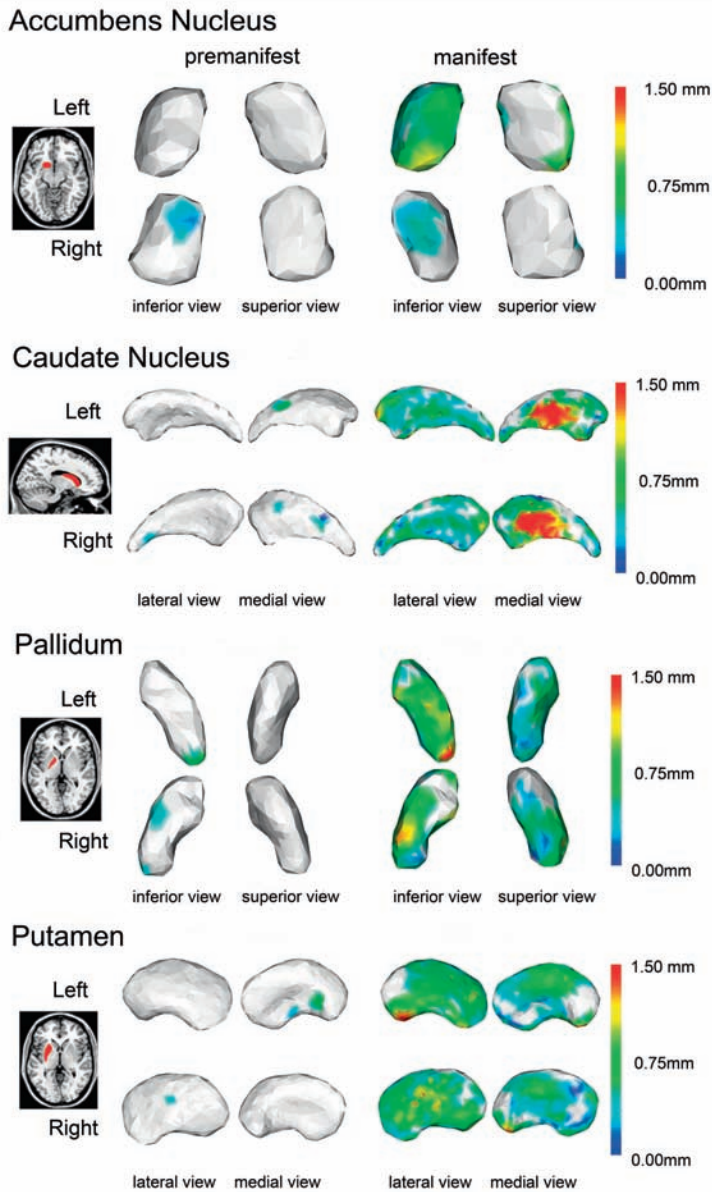
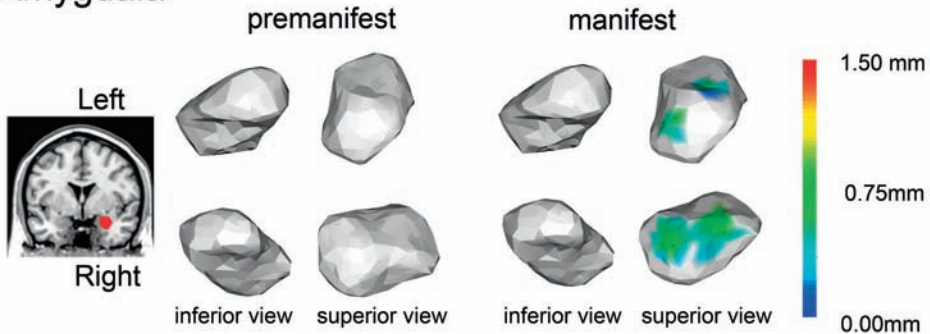


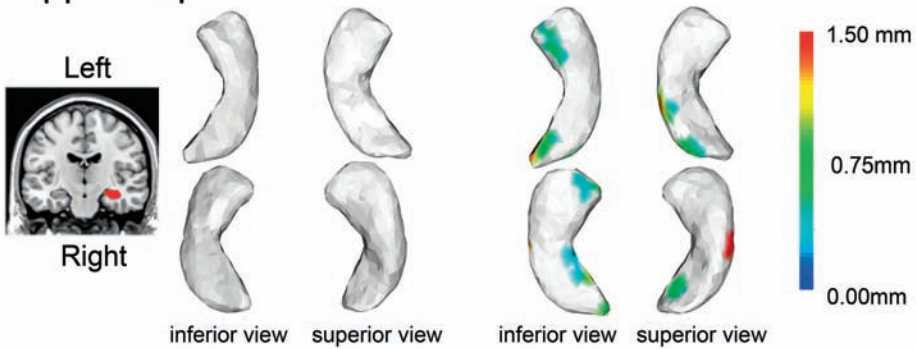
Figure 2: Shape analysis of accumbens nucleus, caudate nucleus, pallidum and putamen. On the left a T1-weighted image with one sided location of the structure analyzed. Group comparison of shape changes between the premanifest and control group on the second and third image. Left and right are separately displayed, and different views are provided. The fourth and fifth images display the control group versus the manifest HD group. The color bar on the right indicates the significant displacement in mm, white/gray indicates no significant displacement, while red indicates a displacement of 1,5 mm or higher

Shape analysis of amygdala, hippocampus and thalamus in premanifest and manifest HD

Amygdala



Hippocampus



Thalamus

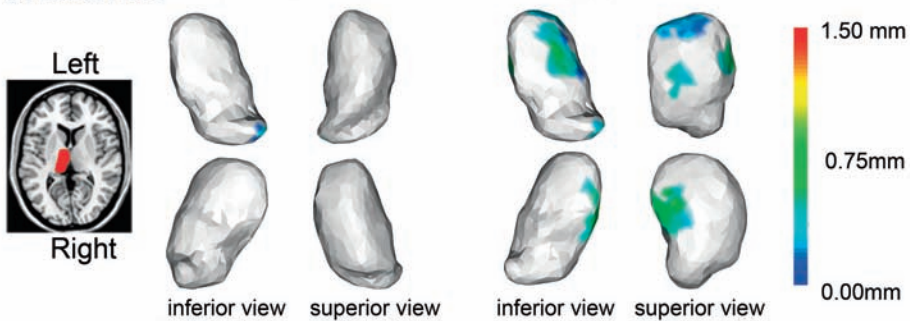


Figure 3: Shape analysis of amygdala, hippocampus and thalamus. On the left a T1-weighted image with one sided location of the structure analysed. Group comparison of shape changes between the premanifest and control group on the second and third image. Left and right are separately displayed, and different views are provided. The fourth and fifth images display the control group versus the manifest HD group. The colour bar on the right indicates the significant displacement in mm, white/gray indicates no significant displacement, while red indicates a displacement of 1,5 mm or higher

Shape analysis of accumbens nucleus, caudate nucleus, pallidum and putamen in the premanifest groups A and B

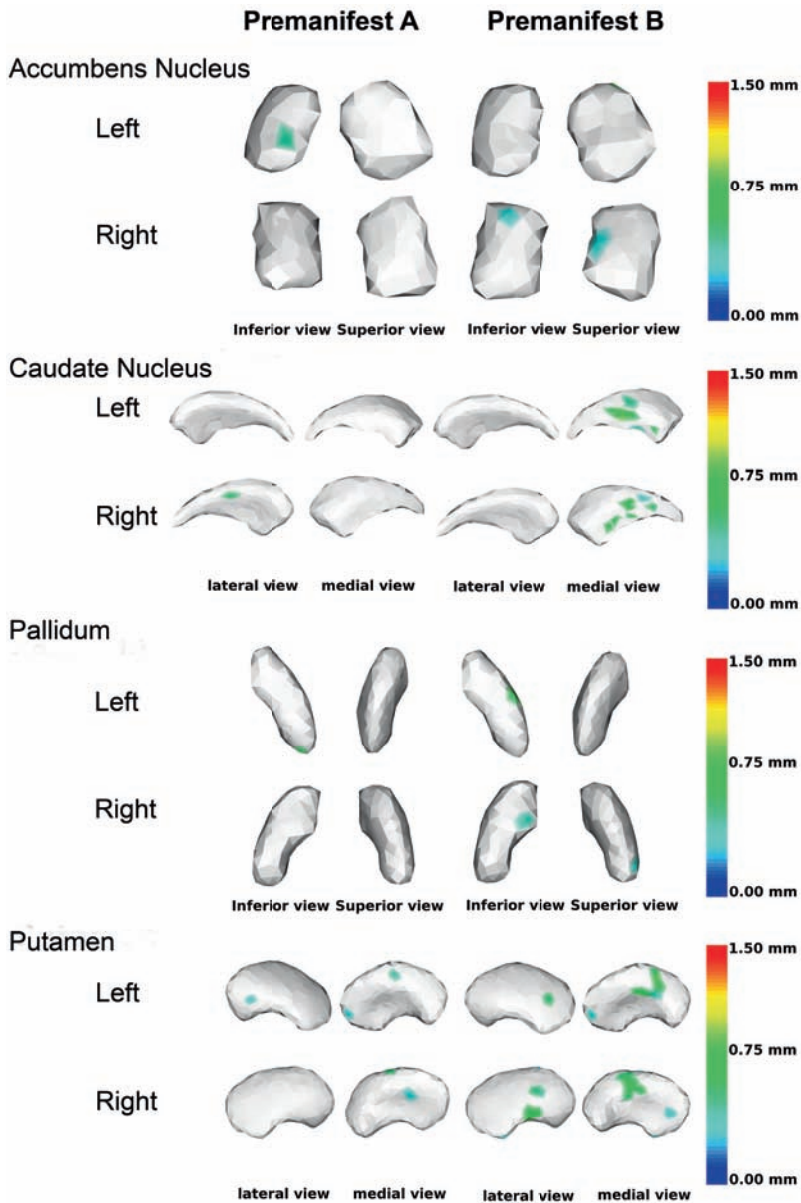


Figure 4: Shape analysis of accumbens nucleus, caudate nucleus, pallidum and putamen in the premanifest groups A and B. Group comparisons of shape changes between the premanifest far from expected onset (A) and close to expected onset (B) versus control group are shown. Left and right are separately displayed, and different views are provided. The colour bar on the right indicates the significant displacement in mm, white/gray indicates no significant displacement, while red indicates a displacement of 1,5 mm or higher

Shape analysis of amygdala, hippocampus and thalamus in the premanifest groups A and B

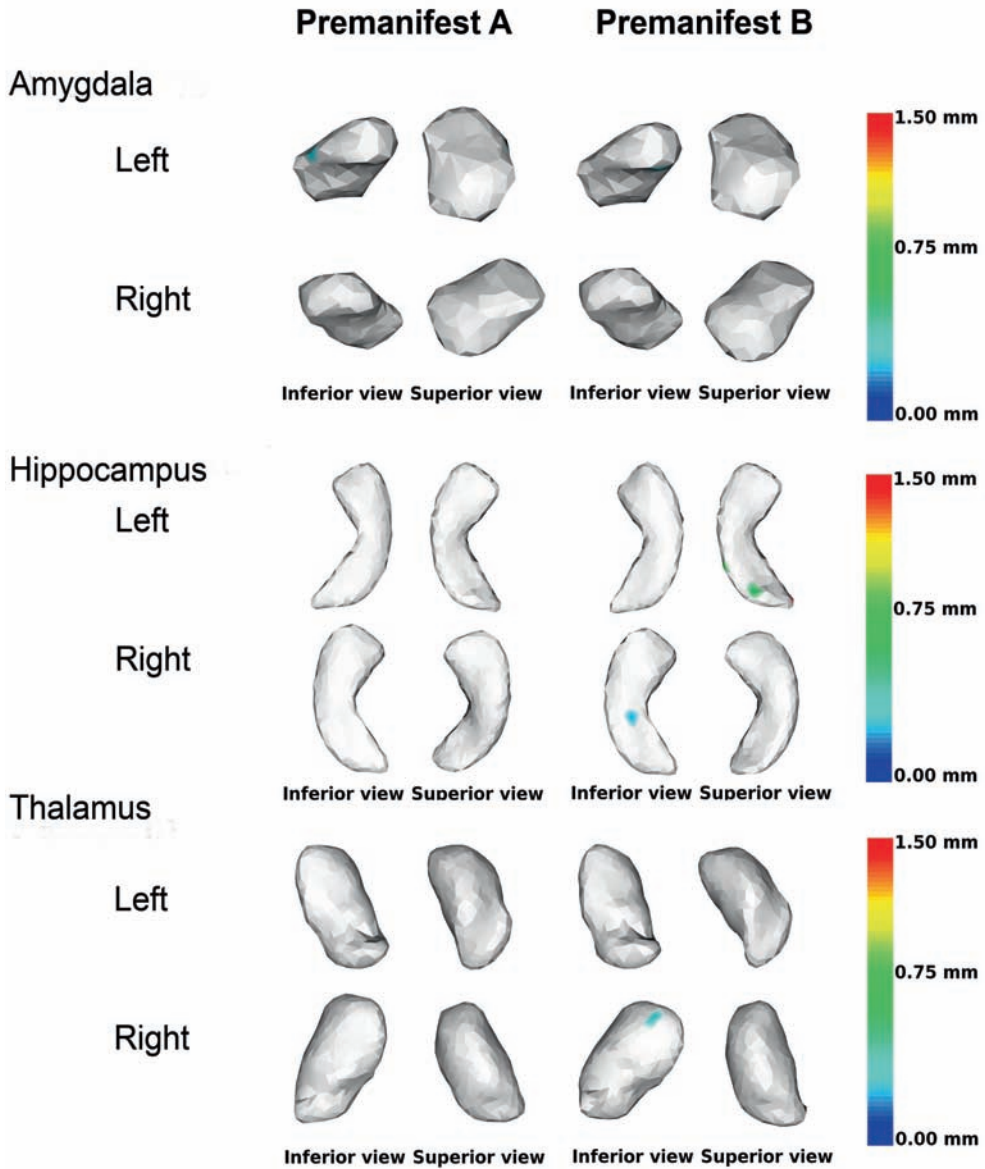


Figure 5: Shape analysis of amygdala, hippocampus and thalamus in the premanifest groups A and B. Group comparisons of shape changes between the premanifest far from expected onset (A) and close to expected onset (B) versus control group are shown. Left and right separately displayed, different views are provided. The color bar on the right indicates the significant displacement in mm, white/gray indicates no significant displacement, while red indicates a displacement of 1,5 mm or higher

The additional analysis within the premanifest group shows significant results in portions of the caudate nucleus, pallidum and putamen for the premanifest B group and hardly any significant results in premanifest A group (figures 4 and 5). In general this seems to point out more pronounced shape changes closer to disease onset.

Discussion

The main focus of this study was to investigate shape changes as a potentially sensitive measure to quantify pathologic changes in subcortical nuclei in HD, and in this way provide us with understanding of the atrophy patterns. The atrophy patterns acquired show localized changes in almost all structures in manifest HD, with a limited result in premanifest HD, most pronounced closer to predicted disease onset. Our analysis provides potential specific target areas for disease tracking measures, although longitudinal confirmation is needed.

Localized in vivo shape analysis is a relatively new analysis technique, not previously implemented in HD research. The potential scope for application of this analysis is evident as several studies demonstrated atrophy of the basal ganglia. Overall volume estimates may not capture the highly localized changes in these subcortical gray matter structures as these may not have a significant impact on overall volume. Shape analysis may bridge this gap. We emphasize that the shape analysis approach can be used in all stages of the disease, whereas microscopic studies can only be performed in the post-mortem stage. Post-mortem neuron counts imply that the parts where the most significant losses of neurons are seen in very advanced stages of HD, are also the areas where the shape or volume change would occur first. The pathologic studies available seem to point towards neuronal changes in specific portions of the caudate nucleus, namely the earliest changes are seen in the medial paraventricular portions of the caudate nucleus and in the tail of the caudate nucleus⁵, which are also the areas seen in our shape analysis. According to Vonsattel *et al.* (1985) the neuropathological changes are seen along the antero-posterior, lateral-medial and ventro-dorsal axis. Also the dorsal part of the putamen, along the dorsal-ventral axis, has been reported to show the most significant neuronal loss^{5,6}, in our study the whole putamen seems affected and no specific conclusions on pattern can be drawn from this cross sectional analysis.

Our findings are in concurrence with the in vivo findings of Kassubek *et al.* (2005), who used a VBM approach describing regional striatal changes corresponding

to the dorso-ventral gradient of neuronal loss described in neuropathological studies²². Furthermore, regarding the thalamus, Kassubek *et al.* (2005) found thalamic subnuclei projecting to prefrontal areas (dorso-medial subnucleus) and connections to the striatum (ventromedian/parafascicular and ventrolateral nuclear complex) to display volume loss²³. In our study the thalamus shows patchy displacements in predominantly ventral-medial and ventral-lateral areas. Although a VBM approach is methodologically very different from our approach, both give indications on local changes, and more importantly, the findings do seem to point to the same general areas.

The volume analysis in our cohort is in accordance with the literature^{1;2;4;24}. Possibly, shape analysis is sensitive in detecting some changes that volumetric analysis could not pick up. The pallidum does show some regions being affected in the premanifest group, yet no significant result in overall volume difference could be detected. It must be noted that there is a decline in volume detectable when the left and right pallidum are combined and the premanifest group is split into two groups according to the predicted years to onset (data not shown). In contrast, in the premanifest group the accumbens nucleus, caudate nucleus and putamen show only minor regional shape changes, alongside their overall volume change, resulting in the conclusion that a more overall volume decrease is observed in these specific structures, rather than any specific regional change only. However, in manifest HD the shape differences provides specific knowledge about the location of the most significant neuron losses, and gives insight into the non-uniform pattern of atrophy of the subcortical gray matter structures. It might be that these specific areas could be targeted for sensitive assessment of pathological change, possibly correlating to disease onset. Perhaps the body of the caudate nucleus is in respect the most promising candidate as this is already demonstrated in the premanifest close to disease onset

As this regional shape analysis approach brings new insights as to where specifically these neurons are lost, it is possible to extend this in vivo knowledge to known anatomical regions within these structures. For example, the hippocampus anatomy is complex with multiple distinct functional substructures²⁵. Neuropathologic reports on specific regions of the hippocampus being involved, such as the CA1 region in the R2/6 HD mouse model²⁶, could be supported by this type of in vivo analysis. This is also true for the thalamus, whose anatomy is known to be subdivided into several substructures. Our analysis shows the medial side to be affected, which could correspond to the mediodorsal part of the thalamus. Interestingly, Heinsen *et al.* (1999) reported that this part of the thalamus

is specifically affected in HD²⁷. This part of the thalamus receives input from the prefrontal cortex and the limbic system and in turn relays them to the prefrontal association cortex. As a result, it plays a crucial role in cognitive functions such as attention, planning, organization, multi-tasking and memory which are known to be impaired in HD²⁸. Haber *et al.* (2009) reviews all cortico-basal ganglia-thalamus circuits, and when correlating our findings to the described pathways one might argue that the regions found in our study correlate to the orbital frontal cortex and the anterior cingulate cortex (ventromedial striatum) and the (pre-) motor cortex (ventral anterior and ventral lateral nuclei) and to circuits between thalamus and basal ganglia in general as the mediodorsal part of the thalamus receives the bulk of the basal ganglia output²⁹.

More specific pathways on striatal-cortical connections are described by Lehericy *et al.* (2004)³⁰. Extending this knowledge Draganski *et al.* (2008) demonstrated in healthy subjects in vivo the coexistence of clearly segregated and also overlapping connections from cortical sites to basal ganglia subregions³¹. They found that the basal ganglia are connected in a rostrocaudal gradient of prefrontal connections in addition to projections to sensorimotor and parietal cortical areas. Using this knowledge we can extract from our own results the most severely affected subregions of the basal ganglia and their associated cortical projections. One example is the severe shape change in the body of the caudate nucleus which is, according to the connections described by Draganski *et al.* (2008), strongly connected to the dorsolateral prefrontal cortex³¹. This seems to be consistent with the above described thalamic connections of the prefrontal cortex which seem to be affected in HD. Another example is the dorsal part of the pallidum which has strong connections to the motor cortex, known to be affected in HD^{1;31;32}. In this way the locally found shape changes in subcortical nuclei can be used to extend knowledge on affected pathways.

However, some caution must be taken not to over interpret these results, as the outer surface of a structure does not necessarily mean that neurons are lost within one small specific subnuclei, as the outer surface cannot give information about remodeling within one large structure or the specific neuronal cell changes, although it does give important clues as such.

A limitation of our study could be the usage of a relatively new software package from FSL for segmentation, which hasn't specifically been validated in HD. Visual inspection, however, did not reveal any significant mismatches. The method applied gives structure segmentation on an individual basis and can therefore be

used to compare groups. In contrast to this limitation clear several reasons exist in favor of using FIRST; first of all, compared to manual segmentation the automated segmentation uses voxel intensity in contrast to the sometimes difficult visual contrast differences, reducing a rater dependent bias. Secondly this automated technique is suitable for implantation on large datasets, whereas manual segmentation is labour intensive. Other techniques such as VBM, although proven to adequately compare groups, is prone to registration artifacts in the deep gray matter and may not be suitable for analysis of the pattern of atrophy in an individual subject^{47,33}.

Another limitation of this study is apparent in applying a statistical paradigm not specifically set for detecting changes in the premanifest group, where changes are relatively small. When less statistical scrutiny would be applied larger regions may show displacement, yet these standards were set before the analysis was performed and did not interfere with achieving the goal of the study, namely finding specific regional shape changes. Another limitation could also be the fact that our premanifest group is quite heterogeneous, in regards to the disease burden which has a substantial range. This disease burden score can be calculated by: $(\text{CAG repeat length} - 35.5) \times \text{Age}$, and correlates well with striatal damage and expected age of onset⁹. This heterogeneity within the premanifest group has been addressed by performing an additional analysis within the premanifest group, showing the relationship of shape changes with disease onset. A final limitation is the cross sectional design, which is unsuited to prove the biomarker quality of localized shape changes and longitudinal follow up should be performed.

In conclusion, shape analysis provides new insights in patterns of atrophy in Huntington's disease. Specific parts of the subcortical gray matter structures are demonstrated to show major shape changes besides an overall volume change. This study assesses these differences in vivo and finds support in known pathologic findings in advanced HD. These localized areas provides not only additional knowledge in localized intrastructural atrophy patterns, but can also potentially serve as specific target areas for disease tracking.

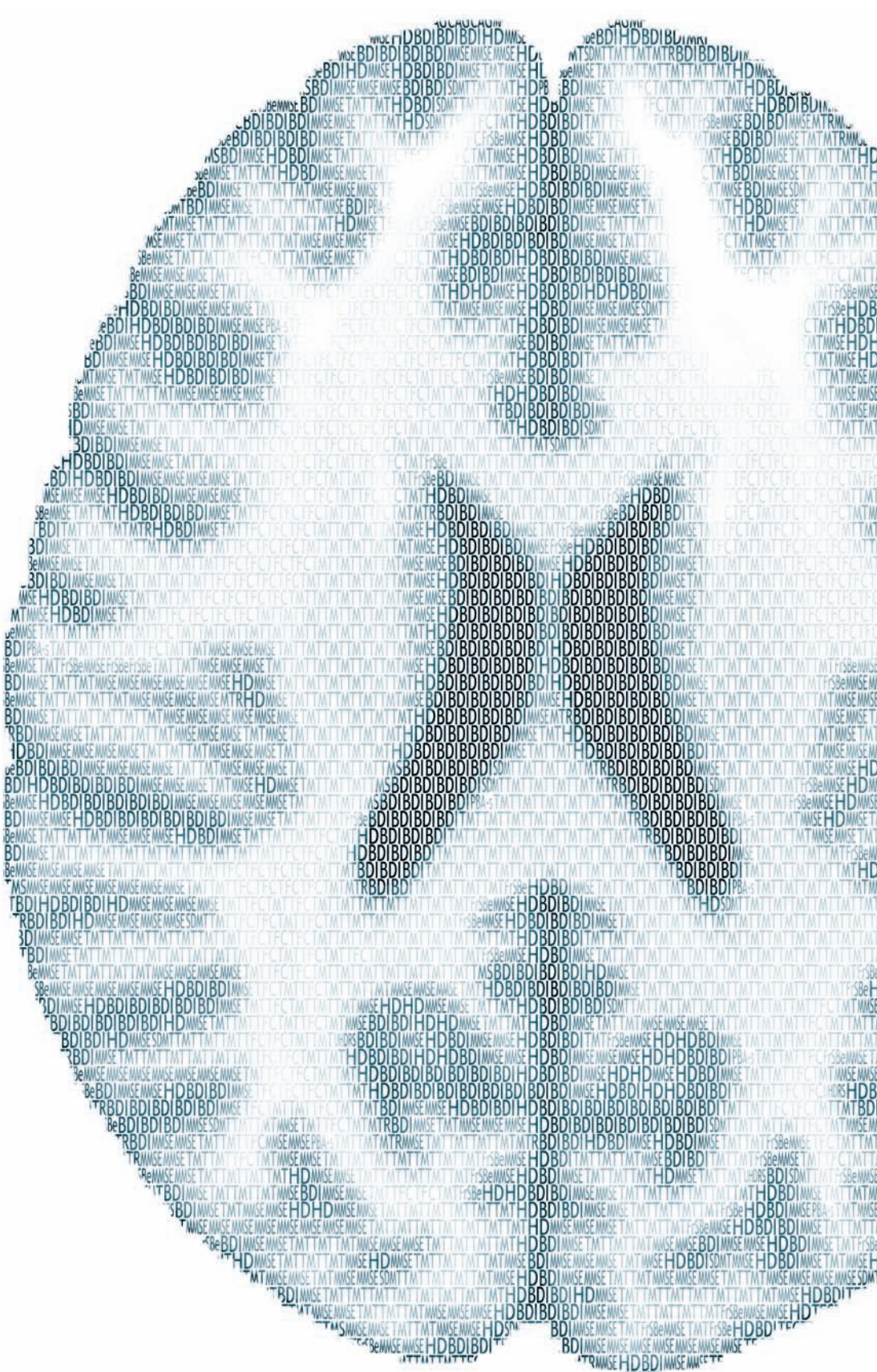
Acknowledgment

The authors wish to thank the TRACK-HD study participants, the “CHDI/High Q Foundation”, a not-for-profit organization dedicated to finding treatments for HD, for providing financial support (www.chdifoundation.org), and all TRACK-HD investigators for their efforts in conducting this study (www.track-hd.net). We would like to thank BioRep for the CAG determinations. We would also like to acknowledge the following individuals personally for their contributions. Caroline Jurgens, Marie-Noelle Witjes-Ane and Ellen ‘t Hart for assistance with coordination and data collection, Gail Owen for coordination of data transfer and Felix Mudoh Tita for data monitoring.

References

1. Tabrizi SJ, Langbehn DR, Leavitt BR, et al. Biological and clinical manifestations of Huntington's disease in the longitudinal TRACK-HD study: cross-sectional analysis of baseline data. *Lancet Neurol*. 2009 Sep;8(9):791-801
2. Paulsen JS, Langbehn DR, Stout JC, et al. Detection of Huntington's disease decades before diagnosis: the Predict-HD study. *J Neurol Neurosurg Psychiatry* 2008;79:874-80
3. Bohanna I, Georgiou-Karistianis N, Hannan AJ, et al. Magnetic resonance imaging as an approach towards identifying neuropathological biomarkers for Huntington's disease. *Brain Res Rev*. 2008 Jun;58(1):209-25
4. Aylward EH. Change in MRI striatal volumes as a biomarker in preclinical Huntington's disease. *Brain Res Bull* 2007;72:152-58
5. Vonsattel JP, Myers RH, Stevens TJ, et al. Neuropathological classification of Huntington's disease. *J Neuropathol Exp Neurol* 1985;44:559-77
6. Roos RA, Pruyt JF, de Vries J, et al. Neuronal distribution in the putamen in Huntington's disease. *J Neurol Neurosurg Psychiatry* 1985;48:422-25
7. Bookstein FL. "Voxel-based morphometry" should not be used with imperfectly registered images. *Neuroimage* 2001;14(6):1454-62
8. Henley SM, Ridgway GR, Scahill RI, et al. Pitfalls in the use of voxel-based morphometry as a biomarker: examples from huntington disease. *AJNR Am J Neuroradiol* 2010;31:711-19
9. Penney JB, Jr., Vonsattel JP, MacDonald ME, et al. CAG repeat number governs the development rate of pathology in Huntington's disease. *Ann Neurol* 1997;41:689-92
10. Langbehn DR, Hayden MR, Paulsen JS. CAG-repeat length and the age of onset in Huntington disease (HD): A review and validation study of statistical approaches. *Am J Med Genet B Neuropsychiatr Genet*. 2010 Mar 5;153B(2):397-408.
11. Langbehn DR, Brinkman RR, Falush D, et al. A new model for prediction of the age of onset and penetrance for Huntington's disease based on CAG length. *Clin Genet* 2004;65:267-77
12. van den Bogaard SJ, Dumas EM, Acharya TP, et al. Early atrophy of pallidum and accumbens nucleus in Huntington's disease. *J Neurol*. 2011 Mar;258(3):412-20
13. Patenaude B, Smith S, Kennedy D, et al. FIRST - FMRIB's integrated registration and segmentation tool. 2007. In Human Brain Mapping Conference.
14. Patenaude B, Smith S, Kennedy D, et al. Improved Surface Models for FIRST. 2008. In Human Brain Mapping Conference.
15. Patenaude B. Bayesian Statistical Models of Shape and Appearance for Subcortical Brain Segmentation. 2007. Thesis. D.Phil.
16. de Jong LW, van der Hiele K, Veer IM, et al. Strongly reduced volumes of putamen and thalamus in Alzheimer's disease: an MRI study. *Brain* 2008;131(Pt 12):3277-85
17. Morey RA, Petty CM, Xu Y, et al. A comparison of automated segmentation and manual tracing for quantifying hippocampal and amygdala volumes. *Neuroimage* 2009;45(3):855-66
18. Morey RA, Selgrade ES, Wagner HR, et al. Scan-rescan reliability of subcortical brain volumes derived from automated segmentation. *Hum Brain Mapp* 2010;31(11):1751-62
19. Ferrarini L, Olofsen H, Palm WM, et al. GAMEs: growing and adaptive meshes for fully automatic shape modeling and analysis. *Med Image Anal* 2007;11:302-14
20. Ferrarini L, Palm WM, Olofsen H, et al. MMSE scores correlate with local ventricular enlargement in the spectrum from cognitively normal to Alzheimer disease. *Neuroimage* 2008;39:1832-38
21. Ferrarini L, Palm WM, Olofsen H, et al. Ventricular shape biomarkers for Alzheimer's disease in clinical MR images. *Magn Reson Med* 2008;59:260-67
22. Kassubek J, Juengling FD, Kioschies T, et al. Topography of cerebral atrophy in early Huntington's disease: a voxel based morphometric MRI study. *J Neurol Neurosurg Psychiatry* 2004;75:213-20
23. Kassubek J, Juengling FD, Ecker D, et al. Thalamic atrophy in Huntington's disease co-varies with

- cognitive performance: a morphometric MRI analysis. *Cereb Cortex* 2005;15:846-53
24. Rosas HD, Koroshetz WJ, Chen YI, et al. Evidence for more widespread cerebral pathology in early HD: an MRI-based morphometric analysis. *Neurology* 2003;60:1615-20
 25. van Strien NM, Cappaert NL, Witter MP. The anatomy of memory: an interactive overview of the parahippocampal-hippocampal network. *Nat Rev Neurosci* 2009;10:272-82
 26. Murphy KP, Carter RJ, Lione LA, et al. Abnormal synaptic plasticity and impaired spatial cognition in mice transgenic for exon 1 of the human Huntington's disease mutation. *J Neurosci* 2000;20:5115-23
 27. Heinsen H, Rub U, Bauer M, et al. Nerve cell loss in the thalamic mediodorsal nucleus in Huntington's disease. *Acta Neuropathol* 1999;97(6):613-22
 28. Lemiere J, Decruyenaere M, Evers-Kiebooms G, et al. Cognitive changes in patients with Huntington's disease (HD) and asymptomatic carriers of the HD mutation—a longitudinal follow-up study. *J Neurol* 2004;251(8):935-42
 29. Haber SN, Calzavara R. The cortico-basal ganglia integrative network: the role of the thalamus. *Brain Res Bull* 2009;78(2-3):69-74
 30. Lehericy S, Ducros M, Van de Moortele PF, et al. Diffusion tensor fiber tracking shows distinct corticostriatal circuits in humans. *Ann Neurol* 2004;55(4):522-29
 31. Draganski B, Kherif F, Klöppel S, et al. Evidence for segregated and integrative connectivity patterns in the human Basal Ganglia. *J Neurosci* 2008;28(28):7143-52
 32. Dumas EM, van den Bogaard SJ, Ruber ME, et al. Early changes in white matter pathways of the sensorimotor cortex in premanifest Huntington's disease. *Hum Brain Mapp.* 2012 Jan;33(1):203-12.
 33. Frisoni GB, Whitwell JL. How fast will it go, doc? New tools for an old question from patients with Alzheimer disease. *Neurology* 2008;70(23):2194-95





CHAPTER 5

MAGNETIZATION TRANSFER IMAGING IN PREMANIFEST AND MANIFEST HUNTINGTON'S DISEASE

S.J.A. VAN DEN BOGAARD¹, E.M. DUMAS¹, J. MILLES²,
R. REILMANN³, J.C. STOUT⁴, D. CRAUFURD⁵, M.A. VAN BUCHEM⁶,
J. VAN DER GROND⁶, R.A.C. ROOS¹

1. DEPARTMENT OF NEUROLOGY, LEIDEN UNIVERSITY MEDICAL CENTER, LEIDEN, THE NETHERLANDS
2. DIVISION OF IMAGE PROCESSING (LKEB), DEPARTMENT OF RADIOLOGY, LEIDEN UNIVERSITY MEDICAL CENTER, LEIDEN, THE NETHERLANDS
3. DEPARTMENT OF NEUROLOGY, UNIVERSITY OF MUNSTER, MUNSTER, GERMANY
4. SCHOOL OF PSYCHOLOGY AND PSYCHIATRY, MONASH UNIVERSITY, VICTORIA, AUSTRALIA
5. UNIVERSITY OF MANCHESTER, MANCHESTER ACADEMIC HEALTH SCIENCES CENTRE AND CENTRAL MANCHESTER UNIVERSITY HOSPITALS NHS FOUNDATION TRUST, MANCHESTER, UK
6. DEPARTMENT OF RADIOLOGY, LEIDEN UNIVERSITY MEDICAL CENTER, LEIDEN, THE NETHERLANDS

Abstract

Background and Purpose

Magnetization Transfer Imaging (MTI) has the potential to detect abnormalities in normal-appearing white and gray matter on conventional MR imaging. Early detection methods and disease progression markers are needed in Huntington's Disease (HD) research. Therefore we investigated MTI parameters and their clinical correlates in premanifest and manifest HD.

Method

From the Leiden TRACK-HD study, 78 participants (28 controls, 25 premanifest HD gene carriers, 25 manifest HD) were included. Brain segmentation of cortical grey matter, white matter, caudate nucleus, putamen, pallidum, thalamus, amygdala and hippocampus was performed using FSL's automated tools FAST and FIRST. Individual Magnetization Transfer Ratio (MTR) values were calculated from these regions and MTR histograms constructed. Regression analysis of MTR measures from all gene carriers with clinical measures was performed.

Results

MTR peak height was reduced in both cortical grey ($p=0.01$) and white matter ($p=0.006$) in manifest HD compared to controls. Also mean MTR was reduced in cortical grey matter ($p=0.01$) and showed a trend in white matter ($p=0.052$). Deep grey matter structures showed a uniform pattern of reduced MTR values ($p<0.05$). No differences between premanifest gene carriers and controls were found. MTR values correlated with disease burden, motor and cognitive impairment.

Conclusion

Throughout the brain disturbances in MTI parameters are apparent in early HD and are homogeneous across white and grey matter. The correlation of MTI with clinical measures indicates the potential to act as a disease monitor in clinical trials. However, our study does not provide evidence for MTI as a marker in premanifest HD.

Introduction

Huntington's disease (HD) is a progressive neurodegenerative genetic brain disorder with clinical features consisting of motor signs, cognitive impairment and psychiatric disturbances. Disease onset is typically during mid-life¹. Since genetic testing became available for this autosomal dominant inheritable disease, it has become possible to identify premanifest gene carriers and in this way ascertain with certainty that they will eventually develop the disease. The disease is caused by a genetic defect on chromosome 4 which results in an expanded polyglutamine in the gene coding for the huntingtin protein². This mutant huntingtin predominantly affects the brain, resulting in malfunction and loss of neurons. Histopathologically, the disease is characterized by cellular loss of grey matter structures, most profoundly that of the medium spiny neurons within the striatum, but also significant white matter volume loss³.

Sensitive and reliable biomarkers are needed for evaluating clinical trials in HD. The challenges in this field lay in the fact that a biomarker should be able to monitor pathophysiological changes not only in the manifest phase, but also in the preceding premanifest stage, when no overt symptoms exist. MRI characterization of brain changes is regarded as a potential source of biomarkers as previous studies have shown that atrophy of the striatum is apparent already a decade or more before symptom onset⁴⁻⁶. Also, abnormalities in white matter^{7,8} and cortical grey matter⁵ have been reported. It is likely that the underlying pathologic processes resulting in brain atrophy occur before or in concurrence with the volumetric changes.

Magnetization Transfer Imaging (MTI) has the potential to quantify the pathologic changes in central nervous system disorders in the normal appearing white and grey matter on conventional MRI sequences^{9,10}. MTI offers a way of examining tissue structure and structural components, normally not resolvable with conventional MRI¹¹. This allows for examination of structural integrity in a different and possibly more sensitive manner than volumetric changes alone. The technique of MTI relies on interaction between protons in free fluid and protons bound to macromolecules. The magnetization saturation and relaxation within macromolecules affect the observable signal. The MTR, representing the percentage of variation in the MR signal between the saturated and unsaturated acquisitions, is an effective and simple MTI measure to use as a clinical application. MTI has been used to characterize many different disorders, including Multiple Sclerosis, Alzheimer's and Parkinson's disease⁹.

This study aims to examine MTR measures in a well defined premanifest and manifest HD population, and to determine associations between MTR and clinical features of HD. By examining MTR in this sample we aim to advance understanding of the timing of pathophysiological changes in HD and we also evaluate the suitability of MTI/MTR as a potential biomarker for HD.

Materials and Methods

Subjects

Of the 90 participants from the Leiden TRACK-HD study, 12 did not receive MTI scanning due to either unexpected claustrophobia or time constraints of the full TRACK-HD protocol, resulting in 78 participants. The cohort consisted of three groups; 28 healthy controls, 25 Premanifest HD gene carriers (PMGC) and 25 manifest HD (MHD). Inclusion criteria for the PMGC consisted of genetically confirmed expanded CAG repeat ≥ 40 , a disease burden score (calculated as: $((\text{CAG repeat length} - 35.5) \times \text{Age})$ of >250 ¹² and absence of motor abnormalities on the Unified Huntington's disease rating scale (UHDRS), defined as a total motor score (TMS) of ≤ 5 . Inclusion criteria for MHD consisted of genetically confirmed CAG repeat ≥ 40 , presence of motor abnormalities on the UHDRS-TMS of >5 . Also a total functional capacity (TFC) score of 7 or higher was required to ensure that the HD group was in the earliest disease stages. Healthy gene negative family members, spouses or partners were recruited as control subjects. Exclusion criteria consisted of significant (neurological) co-morbidity, active major psychiatric disturbance and MRI incompatibility. Full details on recruitment are available from the TRACK-HD baseline paper⁵. Local IRB approval and written informed consent were obtained from all participants.

Imaging sequences

All 78 participants underwent scanning on a 3 Tesla Philips whole body scanner (Philips, Best, The Netherlands) with an 8-channel receive and transmit coil. T1-weighted image volumes were acquired using an ultrafast gradient echo 3D acquisition sequence with the following imaging parameters: TR = 7.7ms, TE = 3.5ms, FA = 8° , FOV = 24cm, matrix size 224x224x164 with sagittal slices to cover the entire brain with a slice thickness of 1.0 mm.

A 3D gradient MTI sequence was subsequently performed with the following parameters: TR = 100 ms, TE = 11 ms, FA = 9° , matrix 224x180x144 mm, voxel size: 1.0x1.0x7.2 mm. Two consecutive imaging sets were acquired, one with and one without a saturation pulse. The imaging parameters are identical to those

described by Jurgens *et al.* (2010)¹³. Total scanning time for T1-weighted and MTI sequences was 12 minutes maximum.

Post-processing

T1-weighted images were segmented using FAST¹⁴ and FIRST^{15;16} from FSL¹⁷. This provided individual brain masks for: total white matter, cortical grey matter, caudate nucleus, putamen, pallidum, thalamus, amygdala, and hippocampus. To correct for possible partial volume effects, an eroded mask of these segmentations was created by removing one voxel in plane for all above named volumes of interest (VOI). All brain masks were then registered to the MTI volumes using the transform obtained from linear registration of the T1-weighted volume with 7 degrees of freedom (FSL FLIRT). MTR is calculated per voxel as $M0-Ms / M0$, whereby Ms is the saturated image and M0 the unsaturated image. The mean MTR per VOI was calculated. Additionally, to represent voxel based MTR variations/variability within each VOI we constructed MTR histograms and calculated MTR peak height using FSL-STATs. Mean MTR and MTR peak height, normalized for the size of the volume of interest, were the primary outcome variables.

Clinical Measures

A total measure of motor dysfunction was obtained with the UHDRS-TMS (range 0-124). Quantification of subtle motor dysfunction by measuring variability of dominant hand finger tapping and tongue protrusion force was achieved with force transducer based quantitative motor assessments^{18;19}. The tapping and tongue measures are expressed as a logarithmic number, higher numbers representing more motor disturbances. TFC score (range: 0-13) and mini-mental state exam (MMSE) for global assessment of cognitive functioning (range: 0-30) were obtained. Cognitive scores included the total scores from the symbol digit modality test (SDMT), Stroop word reading card, trail making test (TMT) A and B and verbal fluency (VF). For the TMT a subtraction of TMT B minus TMT A was used to minimize the potential effects of motor speed on performance. The university of Pennsylvania smell identification test (UPSIT) (Sensonics, Haddon Heights, New Jersey) quantifies smell ability with a 20-item smell test, and is known to correlate to clinical features of neurodegenerative diseases²⁰. An IQ estimate was obtained with the Dutch adult reading test (DART) (a validated translation of the National Adult Reading Test). For assessment of psychiatric disturbances the Beck Depression Inventory II, the Problem Behaviour Assessment, short version, and the Frontal Systems Behavior²¹ were used. Predicted years to disease onset were calculated for PMGC as described in the TRACK-HD baseline paper. For a more detailed description of these clinical assessments see Tabrizi *et al.* (2009)⁵.

Statistics

Statistical analysis was performed using the Statistical Package for Social Sciences (Version 17.0.2, Chicago, USA). An analysis of variance was conducted for all demographic variables. For group comparisons, all MTR values were analysed in a three group analysis of variance with post hoc analysis to determine differences between groups. Hierarchical multiple regression analysis was performed to ascertain the relationship of MTR values with clinical measures. For this analysis only gene carriers (premanifest + manifest) were included as the aim was to examine the relationship to disease progression. MTR values and 14 different clinical assessments were assessed for all regions of interest. In the hierarchical regression age and gender were entered at step 1, thus correcting for the influence of these variables. This was applied for all motor and general assessments, for the specific cognitive tasks (SDMT, Stroop word reading, VF and TMT) IQ was also entered at step 1 as IQ can have a significant impact on cognitive scores.

Results

Demographic variables (table 1) show that there were no differences between the groups in terms of age or CAG repeat length, but that there was a significant difference ($p < 0.05$) between groups for all clinical tests, except for IQ and the FrSBe-scores.

MTR peak height was significantly reduced in the MHD group as compared to either controls or PMGC in the following regions: white matter, grey matter, putamen, pallidum, amygdala, left thalamus (with a trend for the right thalamus) and the right hippocampus. No significant results were found between the control and PMGC. The mean MTR value was significantly lower between MHD and controls in the following regions: grey matter, both caudate nuclei, both thalami and right putamen. All MTR values are shown (table 2) for all regions as examined for each group.

Overall, the MTR histograms showed similar patterns for all study groups in white and cortical grey matter (figure 1) as well as all subcortical grey matter regions separately (figure 2). Whereby, in all histograms the MHD group displayed a lower and broader histogram, as compared to controls and PMGC.

The regression analysis revealed several highly significant correlations between the MTR values and clinical measures (Table 3). The disease burden score was significantly correlated with both cortical grey and white matter MTR peak height

and mean MTR. The deep grey matter structures mainly showed a correlation of MTR peak height to the disease burden except the right caudate nucleus and right putamen. The motor tests also correlated significantly with the MTR values in most regions of interest, predominantly with the UHDRS-TMS and the tapping measure and only minimally with the tongue measure. The cognitive measures showed correlations in the following regions; cortical grey matter, white matter, thalamus, left putamen, right pallidum and left amygdala. The TFC showed a correlation with white matter and the left putamen. The smell identification test was correlated to MTR values in both cortical grey and white matter as in the caudate nucleus, amygdala and thalamus. The MMSE and the measures of behavioural/psychiatric functioning revealed no correlation to any structures and are therefore not displayed in table 3.

Table 1: Group characteristics

	Control Mean (SD)	PMGC Mean (SD)	MHD Mean (SD)	p-value between groups
N	28	25	25	
Age	48.3 (8.0)	43.8 (8.5)	48.4 (10.9)	0.131
CAG larger allele	n.a.	42.72 (2.6)	43.73 (2.8)	0.182
UHDRS TMS	2.3 (2.3)	2.5 (1.5)	22.9 (11.4)	0.000
TFC	12.96 (0.2)	12.56 (0.8)	10.2 (2.1)	0.000
YTO	n.a.	7.06 (1.99)	n.a.	n.a.
IQ	104 (9)	100 (11)	99 (12)	0.260
MMSE	29.1 (1.2)	28.7 (1.5)	27.2 (2.6)	0.001
Tongue Force	3.56 (0.40)	3.97 (0.51)	4.88 (0.65)	0.000
Tapping	11.6 (5.8)	16.7 (8.5)	30.9 (18.2)	0.000
SDMT	50.6 (9.3)	50.7 (10.2)	35.7 (11.10)	0.000
Stroop	98.1 (14.2)	93.0 (13.7)	76.7 (20.6)	0.000
TMT	33.5 (23.5)	43.2 (26.9)	90.3 (73.6)	0.000
Verbal Fluency	26.8 (8.7)	33.3 (14.1)	20.8 (14.5)	0.016
UPSIT	15.89 (2.9)	14.6 (2.5)	12.23 (3.8)	0.000
BDI-II	4.8 (5.9)	7.0 (7.7)	11.1 (10.2)	0.020
PBA-s	6.4 (8.1)	7.6 (8.5)	14.6 (14.7)	0.017
FrSBe	78.1 (19.6)	85.9 (23.8)	87.3 (21.6)	0.259

PMGC= Premanifest HD gene carriers, MHD= manifest Huntington's Disease, CAG= Cytosine-Adenine-Guanine, UHDRS TMS = Unified Huntington's Disease Rating Scale Total Motor Score, TFC = Total Functional Capacity, YTO = Expected years to onset, IQ = Intelligence Quotient based on the Dutch Adult Reading Test, MMSE = Mini Mental State Exam, Tapping = Average speeded tapping for left and right index finger, Tongue = sustained tongue force measure, SDMT = Symbol Digit Modalities test, Stroop = Stroop word reading task, TMT = Trail making test, UPSIT = University of Pennsylvania Smell Identification Test, BDI-II = Becks Depression Inventory 2nd version, PBA-s = Problem Behaviour Assessment-short version, FrSBe = Frontal Systems Behaviour rating scale Self Report, n.a. = not applicable.

Table 2: MTR values for all brain regions

	Control	PMGC	MHD	P-value		
	Mean (SD)	Mean (SD)	Mean (SD)	C - P	C - M	P - M
White matter						
Peak height	1.080 (0.271)	1.118 (0.212)	0.860 (0.234)	0.859	0.006	0.001
Mean MTR	0.389 (0.017)	0.389 (0.015)	0.378 (0.017)	0.986	0.052	0.086
Cortical Grey matter						
Peak height	0.769 (0.121)	0.723 (0.118)	0.610 (0.145)	0.435	0.000	0.010
Mean MTR	0.330 (0.131)	0.326 (0.125)	0.314 (0.174)	0.687	0.001	0.010
Right Caudate						
Peak height	0.804 (0.209)	0.871 (0.198)	0.757 (0.198)	0.486	0.701	0.144
Mean MTR	0.349 (0.029)	0.341 (0.027)	0.325 (0.035)	0.603	0.020	0.199
Left Caudate						
Peak height	0.884 (0.203)	0.949 (0.207)	0.812 (0.231)	0.550	0.474	0.084
Mean MTR	0.367 (0.029)	0.359 (0.021)	0.346 (0.036)	0.586	0.041	0.330
Right Putamen						
Peak height	1.223 (0.388)	1.238 (0.292)	0.976 (0.288)	0.985	0.029	0.023
Mean MTR	0.341 (0.019)	0.333 (0.024)	0.325 (0.023)	0.448	0.034	0.410
Left Putamen						
Peak height	1.316 (0.329)	1.299 (0.241)	1.050 (0.290)	0.977	0.006	0.014
Mean MTR	0.358 (0.018)	0.351 (0.022)	0.356 (0.017)	0.475	0.932	0.711
Right Pallidum						
Peak height	1.449 (0.400)	1.587 (0.296)	1.324 (0.400)	0.404	0.480	0.049
Mean MTR	0.385 (0.022)	0.382 (0.014)	0.385 (0.022)	0.850	0.996	0.816
Left Pallidum						
Peak height	1.563 (0.369)	1.514 (0.285)	1.268 (0.332)	0.868	0.008	0.038
Mean MTR	0.382 (0.027)	0.384 (0.015)	0.394 (0.018)	0.951	0.098	0.197
Right Thalamus						
Peak height	0.995 (0.297)	1.027 (0.215)	0.864 (0.227)	0.896	0.173	0.078
Mean MTR	0.369 (0.028)	0.360 (0.025)	0.340 (0.038)	0.536	0.005	0.093
Left Thalamus						
Peak height	1.055 (0.253)	1.114 (0.241)	0.906 (0.278)	0.711	0.115	0.021
Mean MTR	0.380 (0.035)	0.372 (0.018)	0.355 (0.040)	0.709	0.024	0.168
Right Amygdala						
Peak height	1.299 (0.318)	1.294 (0.228)	1.127 (0.263)	0.998	0.080	0.105
Mean MTR	0.362 (0.020)	0.361 (0.020)	0.355 (0.020)	0.977	0.463	0.607
Left Amygdala						
Peak height	1.462 (0.343)	1.399 (0.231)	1.178 (0.280)	0.733	0.003	0.032
Mean MTR	0.373 (0.028)	0.374 (0.021)	0.368 (0.021)	0.997	0.679	0.648
Right Hippocampus						
Peak height	1.220 (0.334)	1.266 (0.239)	1.081 (0.195)	0.821	0.170	0.054
Mean MTR	0.369 (0.025)	0.363 (0.016)	0.357 (0.021)	0.592	0.122	0.593
Left Hippocampus						
Peak height	0.954 (0.273)	0.965 (0.207)	0.882 (0.230)	0.985	0.555	0.473
Mean MTR	0.390 (0.027)	0.382 (0.018)	0.383 (0.017)	0.400	0.540	0.972

MTR values for white matter, cortical grey matter and subcortical grey matter structures. Peak height represents a normalized for volume peak height. PMGC= Premanifest HD gene carriers, MHD= manifest Huntington's Disease C = controls, P = premanifest HD, M = Manifest HD

Table 3: Regression analysis per region of interest

	Burden	TMS	TFC	Tap	Tongue	SDMT	Stroop	TMT	VF	UPSIT
WM										
Peak height	.204**	.257**	.074*	.168**	.110*	.097*	.060	.089*	.000	.151**
Mean MTR	.114*	.163**	.025	.080	.034	.057	.036	.037	.004	.160**
CGM										
Peak height	.193**	.189**	.061	.111*	.049	.062	.063	.092*	.003	.058*
Mean MTR	.083*	.152**	.110*	.098*	.062	.114*	.125*	.136**	.034	.122*
Right CN										
Peak height	.059	.054	.019	.040	.001	.021	.061	.009	.000	.014
Mean MTR	.076*	.153**	.036	.105*	.008	.050	.052	.034	.003	.101*
Left CN										
Peak height	.083*	.160**	.034	.116*	.104*	.038	.070	.010	.022	.104*
Mean MTR	.047	.111*	.017	.094*	.037	.012	.026	.025	.000	.141*
Right Putamen										
Peak height	.055	.181**	.053	.112*	.044	.067	.067	.038	.001	.061
Mean MTR	.000	.077	.038	.013	.001	.021	.037	.005	.001	.002
Left Putamen										
Peak height	.076*	.209**	.090*	.117*	.060	.054	.077*	.035	.000	.070
Mean MTR	.025	.000	.007	.010	.002	.041	.035	.006	.078*	.008
Right Pallidum										
Peak height	.110*	.175**	.035	.174**	.051	.071	.048	.041	.004	.075
Mean MTR	.001	.017	.046	.003	.001	.001	.006	.019	.033	.010
Left Pallidum										
Peak height	.104*	.164**	.043	.131*	.051	.060	.070	.080*	.000	.045
Mean MTR	.001	.001	.026	.000	.012	.036	.053	.011	.034	.004
Right Amygdala										
Peak height	.145**	.128*	.023	.098*	.016	.037	.034	.020	.002	.116*
Mean MTR	.026	.033	.034	.058	.009	.025	.043	.044	.036	.041
Left Amygdala										
Peak height	.252**	.184**	.060	.216**	.134*	.170**	.116*	.086*	.071	.172**
Mean MTR	.000	.000	.007	.003	.005	.038	.047	.068	.109*	.003
Right HC										
Peak height	.190**	.091*	.002	.075	.002	.073	.026	.010	.001	.061
Mean MTR	.015	.041	.075	.037	.012	.043	.073	.070	.025	.034
Left HC										
Peak height	.095*	.062	.000	.020	.015	.022	.085*	.026	.039	.011
Mean MTR	.003	.006	.002	.013	.001	.015	.027	.006	.010	.008
Right Thalamus										
Peak height	.124*	.099*	.025	.100*	.007	.043	.055	.015	.002	.045
Mean MTR	.162**	.215**	.057	.172**	.033	.072*	.066	.061	.009	.156**
Left Thalamus										
Peak height	.154**	.223**	.065	.167**	.122*	.075	.110*	.030	.032	.122*
Mean MTR	.117*	.156**	.027	.134*	.046	.035	.044	.042	.004	.158**

Regression analysis between 14 clinical and 2 MTI measures in regions of interest. Values stated are R square changes. WM=White Matter, CGM=Cortical Grey Matter, CN=Caudate Nucleus, HC =hippocampus, TMS = Unified Huntington's Disease Rating Scale Total Motor Score, TFC = Total Functional Capacity, Tap= speeded tapping, Tongue = tongue force, SDMT = Symbol Digit Modalities test, Stroop = Stroop word reading task, TMT = Trail making test, VF = verbal fluency, UPSIT = University of Pennsylvania Smell Identification Test, *= $p < 0.05$, **= $p < 0.005$

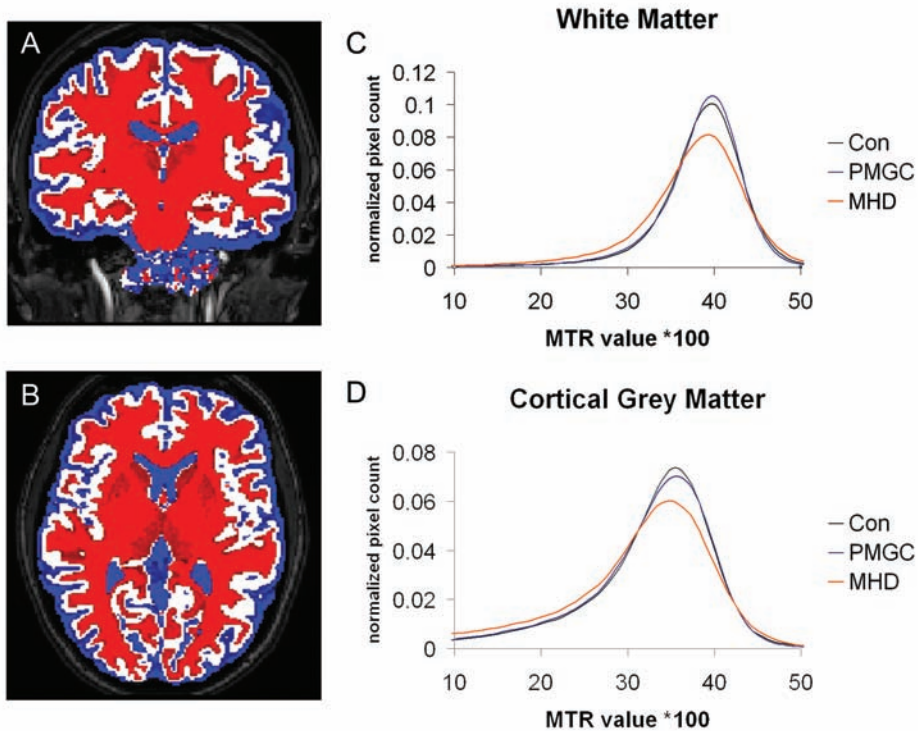


Figure 1: (A & B) example segmentations acquired with FAST software showing white matter (red), grey matter (white) and cerebral spinal fluid (blue). The subcortical grey matter structures were subtracted from these masks. Magnetization Transfer Ratio Histogram for the white matter (C) and cortical grey matter (D), corrected for volume size of the region for 3 groups.

Discussion

MTI applied in HD reveals disturbances throughout the brain in early HD as compared to controls and PMGC. Disease burden, quantitative motor and cognitive measures have a strong correlation to MTR values, leading to the conclusion that MTI can possibly be used to track disease progression. No abnormalities are quantifiable in the premanifest stages of the disease compared to controls, which leads to suggest that MTI, although perhaps a good disease monitor, is not an early marker of the disease.

Currently, conventional structural MRI and Diffusion Tensor Imaging (DTI) are the two most widely applied methods in HD research with respect to the search for a

MRI biomarker covering all disease stages of HD. Only three reports on MTI in HD are available^{13;22;23}. The value derived from MTI is the MTR value per brain voxel and is thought to represent structural integrity. The value quantifies the exchange of magnetization from the non-water components in the region at hand. The most frequently reported outcome measures of MTR are mean MTR and MTR peak height. Mean MTR represents the average MTR value of all voxels in a region of interest, with lower mean MTR corresponding to poorer integrity. MTR peak height reflects the most frequently occurring MTR value in a region of interest when all the MTR values are set out in a MTR histogram. When each MTR value occurs less frequently, the histogram becomes broader, and the maximum peak height decreases. This reduction represents reduced capacity to optimally exchange magnetization over the region of interest, hence representing reduced structural integrity^{24;25}. For example in white matter, myelin is the main component and therefore MTR is thought to relate to myelinisation or myelin integrity. To which cellular structure, whether neurons or glia cells, MTR in gray matter specifically refers is unknown.

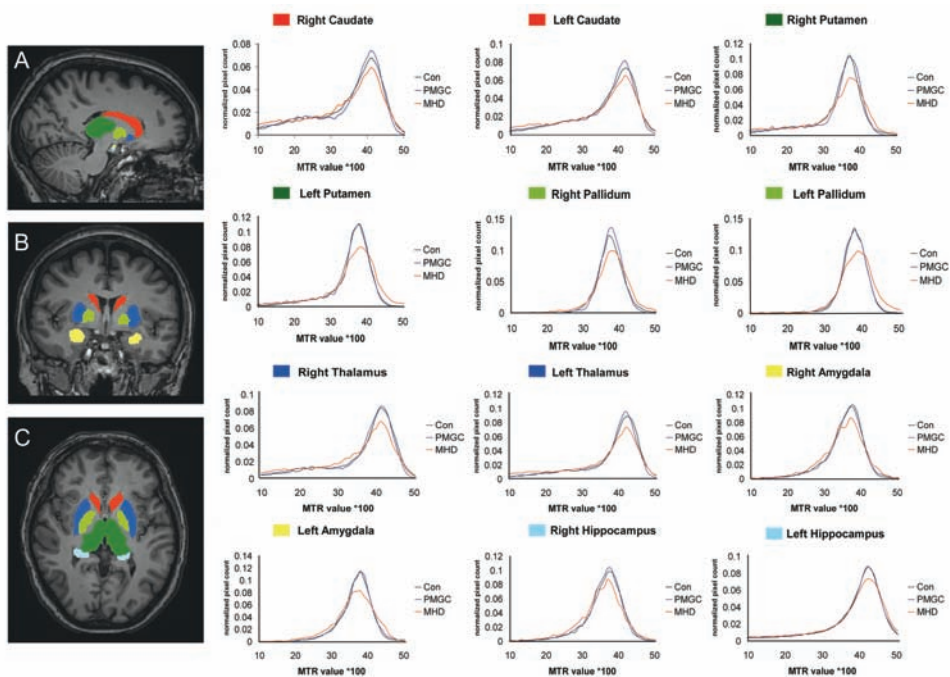


Figure 2: Magnetization Transfer Ratio histogram for 6 deep grey matter structures bilaterally, corrected for volume size of the region for 3 groups. Red = caudate nucleus, dark blue = putamen, light green = pallidum, dark green = thalamus, yellow = amygdala, light blue = hippocampus. Con = controls

In our study it does not solely reflect atrophy, as the differences found in peak height were corrected for size of the volume examined, thereby accounting for atrophy. From histopathological studies we know that medium spiny neurons in HD are most affected, making these the most likely source of the differences.

In the current study, we found that both MTR measures were significantly reduced in the manifest stages of HD in cortical grey matter, deep gray matter structures and white matter. This finding conflicts with the findings by Mascalchi *et al.* (2004), who reported no differences between a group of 21 gene carriers (of which 19 manifest HD) and controls²². The differences could be explained by the fact that Mascalchi *et al.* (2004) applied a different (manual) segmentation technique, used a lower field strength, included a slightly smaller group and did not examine MTR peak height. Mean MTR in our study does show significant results, however not in the white matter. In general we found that the peak height tended to be the more sensitive MTR measure rather than the mean MTR. The study by Jurgens *et al.* (2010) is comparable to our study with the same type of scanner and analysis. We replicate their findings as they also demonstrated a lack of group difference between PMGC and controls¹³. Furthermore, the clinical correlation of the MTI peak height with clinical measures in gene carriers is confirmed in our study, and this knowledge is extended from a premanifest study group to both PMGC and MHD. Ginestroni *et al.* (2010) applied a similar methodology to our study, as both used the FSL tools for segmentation²³. The main difference between these two studies is that we examined an explicitly premanifest and manifest groups separately, instead of a “gene carrier group with a range of clinical severity”. The outcomes of the studies are highly comparable with reduced MTR in subcortical and cortical grey matter. The absence of white matter differences in mean MTR is similar in both reports. However we did find white matter differences with an outcome measure not examined by Ginestroni *et al.* (2010), namely MTR peak height. Finally the correlation of MTR values with clinical measures was similarly reported by both studies.²³.

The finding of reduced MTR measures throughout the brain is remarkably homogeneous. This seems in contrast to the volumetric data available in HD research. Striatal degeneration is the key feature of brain pathology in HD, yet evermore evidence is building up that, although the damage starts in the striatum, HD is truly a whole brain disease, as numerous volumetric studies demonstrate widespread volumetric loss in both gray and white matter²⁶. So the seemingly paradoxical homogeneity is really not that surprising.

The application of MTI and its relationship to clinical severity has been demonstrated in other neurological diseases such as Multiple Sclerosis and Alzheimer disease^{10;27;28;28-31}. Our findings indicate that MTI measures in HD correlate to disease burden, specific motor tasks and cognitive measures in this study population. The finding of correlations of MTI with specific clinical parameters indicates that MTI is a good reflection of the disease status as shown by motor and cognitive measures. Furthermore the disease burden, which encompasses the CAG-repeat length, has been demonstrated to correlate with striatal degeneration and predicted time to disease onset¹², therefore indirectly linking MTI outcomes to such measures.

The lack of significant group differences between PMGC and controls was unexpected. We anticipated differences on the basis of previous reports on white matter integrity loss in premanifest HD using DTI^{7;8;32}. DTI can be used to examine protons in free water and their diffusive properties in more than one way, namely the strength of the directional of diffusivity (FA), the average amount of diffusivity (mean diffusivity), but also the amount of diffusivity in either the radial and axial direction. DTI has the potential for examining and quantifying many features of brain tissue, all captured by the terms structural integrity and/or organization. In white matter DTI is heavily influenced by axonal membranes and myelin sheaths³³. In contrast MTI can be used to examine tissue structure according to the protons bound to macromolecules³⁴. As myelin is the main component of white matter, MTI is thought to mainly represent myelin integrity. Therefore, these techniques characterize fundamentally different aspects of brain tissue, possibly explaining (part of) the differences found between DTI-studies and MTI-studies. The question remains whether DTI or MTI is more sensitive in detecting the pathologic neuronal integrity breakdown. However, answering this question was not the aim of this study.

The potential role for MTI as a biomarker in HD is apparent as there are both significant differences between groups and a clear relationship to clinical measures. However, MTI may be sensitive to a particular (early) disease state and not to all disease stages in HD. Longitudinal follow up is needed to confirm this. The biomarker role for MTI has already been suggested in Alzheimer disease by Ridha *et al.* (2007)³¹ and the reports for using MTI as a biomarker in MS are building³⁵, strengthening the possibility for MTI as a biomarker in neurodegenerative disorders such as HD. TRACK-HD is specifically designed for longitudinal assessment of potential biomarkers, and is therefore the ideal platform to confirm the findings longitudinally.

Limitations of our study lay in the fact that the automated segmentation technique has not specifically been validated for HD. However, we used these only for obtaining the brain regions of interest. Furthermore, we accounted for some possible incorrect segmentation and/or partial volume effects by using an eroded version of the brain masks. A limitation could also be that we have chosen a region of interest (ROI) based analysis as opposed to voxelwise analysis. However as the morphology of the structures at hand change due to the disease, registration issues could be a severe problem, not to mention that the mean MTR can remain constant while intensities do change. Therefore ROI based analysis is potentially more sensitive. Furthermore, we examined voxel based variations within structures, by representing this in histograms of each VOI. Another limitation could be that the exploratory nature of this study accounted for a high number of correlations included, which could lead to false positive results. It seems, however, that MTI measures are fairly stable in every region we examined and provides a rather uniform picture of group differences and clinical correlation outcomes. Finally, a limitation of MTI in general has been the limited reproducibility across centres due to the fact that the MT phenomenon is dependent on many technical parameters and lack of a standardized protocol⁹.

Conclusions

MTI demonstrates that whole brain disturbances are apparent in early HD and furthermore, these structural integrity differences seem to be relatively homogeneous throughout the brain in early HD. The strong correlations to clinical features, especially motor and cognitive measures, suggest that there is potential for this analysis to serve as a disease monitor in future clinical trials. However, MTI does not seem to be an early marker of HD as no disturbances in MTI measures can be detected in the premanifest stages of the disease.

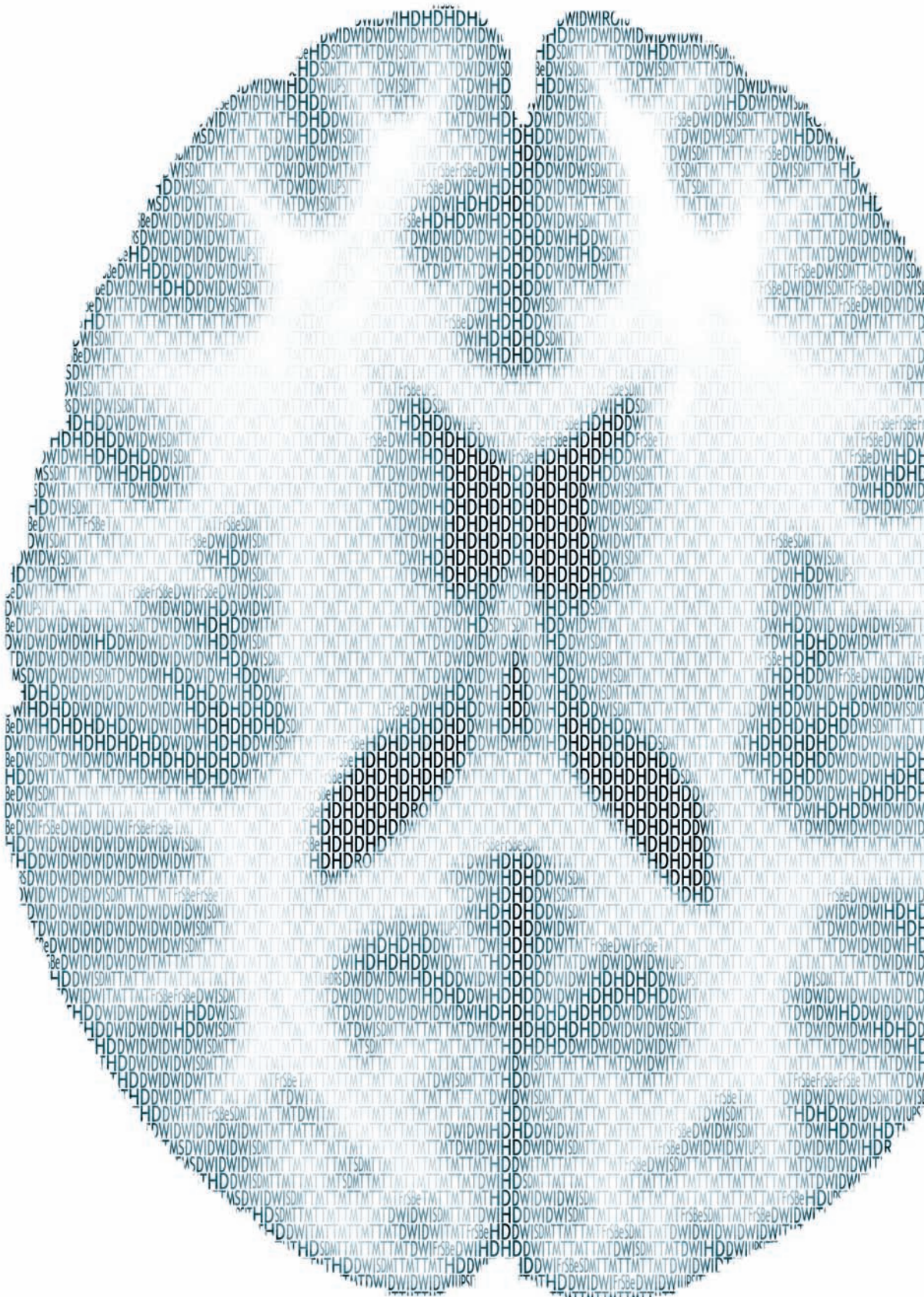
Acknowledgement

We wish to thank the TRACK-HD participants, the “CHDI/High Q Foundation”, a not-for-profit organization dedicated to finding treatments for HD, for providing financial support, and all TRACK-HD investigators for their efforts in conducting this study.

References

1. Novak MJ, Tabrizi SJ. Huntington's disease. *BMJ* 2010;340:c3109
2. A novel gene containing a trinucleotide repeat that is expanded and unstable on Huntington's disease chromosomes. The Huntington's Disease Collaborative Research Group. *Cell* 1993;72(6):971-83
3. de la Monte SM, Vonsattel JP, Richardson EP, Jr. Morphometric demonstration of atrophic changes in the cerebral cortex, white matter, and neostriatum in Huntington's disease. *J Neuropathol Exp Neurol* 1988;47:516-25
4. Paulsen JS, Langbehn DR, Stout JC, et al. Detection of Huntington's disease decades before diagnosis: the Predict-HD study. *J Neurol Neurosurg Psychiatry* 2008;79:874-80
5. Tabrizi SJ, Langbehn DR, Leavitt BR, et al. Biological and clinical manifestations of Huntington's disease in the longitudinal TRACK-HD study: cross-sectional analysis of baseline data. *Lancet Neurol*. 2009 Sep;8(9):791-801.
6. van den Bogaard SJ, Dumas EM, Acharya TP, et al. Early atrophy of pallidum and accumbens nucleus in Huntington's disease. *J Neurol*. 2011 Mar;258(3):412-20.
7. Rosas HD, Tuch DS, Hevelone ND, et al. Diffusion tensor imaging in presymptomatic and early Huntington's disease: Selective white matter pathology and its relationship to clinical measures. *Mov Disord* 2006;21:1317-25
8. Dumas EM, van den Bogaard SJ, Ruber ME, et al. Early changes in white matter pathways of the sensorimotor cortex in premanifest Huntington's disease. *Hum Brain Mapp*. 2012 Jan;33(1):203-12
9. Filippi M, Rocca MA. Magnetization transfer magnetic resonance imaging of the brain, spinal cord, and optic nerve. *Neurotherapeutics* 2007;4(3):401-13
10. Dehmeshki J, Chard DT, Leary SM, et al. The normal appearing grey matter in primary progressive multiple sclerosis: a magnetisation transfer imaging study. *J Neurol* 2003;250(1):67-74
11. McGowan JC. The physical basis of magnetization transfer imaging. *Neurology* 1999;53(5 Suppl 3):S3-S7
12. Penney JB, Jr., Vonsattel JP, MacDonald ME, et al. CAG repeat number governs the development rate of pathology in Huntington's disease. *Ann Neurol* 1997;41(5):689-92
13. Jurgens CK, Bos R, Luyendijk J, et al. Magnetization transfer imaging in 'premanifest' Huntington's disease. *J Neurol* 2010;257(3):426-32
14. Zhang Y, Brady M, Smith S. Segmentation of brain MR images through a hidden Markov random field model and the expectation-maximization algorithm. *IEEE Trans Med Imaging* 2001;20:45-57
15. Patenaude B, Smith S, Kennedy D, et al. FIRST - FMRIB's integrated registration and segmentation tool. 2007. In *Human Brain Mapping Conference*
16. Patenaude B. Bayesian Statistical Models of Shape and Appearance for Subcortical Brain Segmentation. 2007. Thesis. D.Phil, available from www.fmrib.ox.ac.uk
17. Smith SM, Jenkinson M, Woolrich MW, et al. Advances in functional and structural MR image analysis and implementation as FSL. *Neuroimage* 2004;23 Suppl 1:S208-S219
18. Bechtel N, Scahill RI, Rosas HD, et al. Tapping linked to function and structure in premanifest and symptomatic Huntington disease. *Neurology* 2010;75:2150-60
19. Reilmann R, Bohlen S, Klopstock T, et al. Tongue force analysis assesses motor phenotype in premanifest and symptomatic Huntington's disease. *Mov Disord* 2010;25:2195-202
20. McKinnon J, Evidente V, Driver-Dunckley E, et al. Olfaction in the elderly: a cross-sectional analysis comparing Parkinson's disease with controls and other disorders. *Int J Neurosci* 2010;120(1):36-39
21. Grace J, Stout JC, Malloy PF. Assessing frontal lobe behavioral syndromes with the frontal lobe personality scale. *Assessment* 1999;6:269-84
22. Mascalchi M, Lolli F, Della NR, et al. Huntington disease: volumetric, diffusion-weighted, and magnetization transfer MR imaging of brain. *Radiology* 2004;232:867-73

23. Ginestroni A, Battaglini M, Diciotti S, et al. Magnetization Transfer MR Imaging Demonstrates Degeneration of the Subcortical and Cortical Gray Matter in Huntington Disease. *AJNR Am J Neuroradiol*. 2010 Nov;31(10):1807-12.
24. Filippi M, Rocca MA, Comi G. The use of quantitative magnetic-resonance-based techniques to monitor the evolution of multiple sclerosis. *Lancet Neurol* 2003;2:337-46
25. Jurgens CK, Bos R, Luyendijk J, et al. Magnetization transfer imaging in 'premanifest' Huntington's disease. *J Neurol* 2010;257(3):426-32
26. Rosas HD, Koroshetz WJ, Chen YI, et al. Evidence for more widespread cerebral pathology in early HD: an MRI-based morphometric analysis. *Neurology* 2003;60:1615-20
27. van Buchem MA, Grossman RI, Armstrong C, et al. Correlation of volumetric magnetization transfer imaging with clinical data in MS. *Neurology* 1998;50(6):1609-17
28. Khaleeli Z, Sastre-Garriga J, Ciccarelli O, et al. Magnetisation transfer ratio in the normal appearing white matter predicts progression of disability over 1 year in early primary progressive multiple sclerosis. *J Neurol Neurosurg Psychiatry* 2007;78(10):1076-82
29. Ge Y, Grossman RI, Udupa JK, et al. Magnetization transfer ratio histogram analysis of gray matter in relapsing-remitting multiple sclerosis. *AJNR Am J Neuroradiol* 2001;22(3):470-75
30. Hayton T, Furby J, Smith KJ, et al. Grey matter magnetization transfer ratio independently correlates with neurological deficit in secondary progressive multiple sclerosis. *J Neurol* 2009;256(3):427-35
31. Ridha BH, Tozer DJ, Symms MR, et al. Quantitative magnetization transfer imaging in Alzheimer disease. *Radiology* 2007;244(3):832-37
32. Magnotta VA, Kim J, Kosciak T, et al. Diffusion Tensor Imaging in Preclinical Huntington's Disease. *Brain Imaging and Behavior* 2009;3:77-84
33. Beaulieu C. The basis of anisotropic water diffusion in the nervous system - a technical review. *NMR Biomed* 2002;15(7-8):435-55
34. Laule C, Vavasour IM, Kolind SH, et al. Magnetic resonance imaging of myelin. *Neurotherapeutics* 2007;4(3):460-84
35. Filippi M, Agosta F. Magnetic resonance techniques to quantify tissue damage, tissue repair, and functional cortical reorganization in multiple sclerosis. *Prog Brain Res* 2009;175:465-82





CHAPTER 6

EARLY CHANGES IN WHITE MATTER PATHWAYS OF THE SENSORIMOTOR CORTEX IN PREMANIFEST HUNTINGTON'S DISEASE

EVE M. DUMAS¹, SIMON J.A. VAN DEN BOGAARD¹, MARGOT E. RUBER¹,
RALF REILMANN², JULIE C. STOUT^{3,4}, DAVID CRAUFURD⁵,
STEPHEN L. HICKS⁶, CHRIS KENNARD⁶,
SARAH J. TABRIZI⁷, MARK A. VAN BUCHEM⁸,
JEROEN VAN DER GROND⁸, AND RAYMUND A.C. ROOS¹

1. DEPARTMENT OF NEUROLOGY, LEIDEN UNIVERSITY MEDICAL CENTRE, LEIDEN, THE NETHERLANDS

2. DEPARTMENT OF NEUROLOGY, UNIVERSITY OF MUNSTER, MUNSTER, GERMANY

3. SCHOOL OF PSYCHOLOGY, PSYCHIATRY AND PSYCHOLOGICAL MEDICINE, MONASH UNIVERSITY,
CLAYTON CAMPUS, VIC, AUSTRALIA

4. DEPARTMENT OF PSYCHOLOGICAL AND BRAIN SCIENCES, INDIANA UNIVERSITY, BLOOMINGTON, INDIANA, USA

5. GENETIC MEDICINE, UNIVERSITY OF MANCHESTER, MANCHESTER ACADEMIC HEALTH SCIENCES CENTRE,
MANCHESTER, UNITED KINGDOM

6. CENTRAL MANCHESTER UNIVERSITY HOSPITALS NHS FOUNDATION TRUST, ST. MARY'S HOSPITAL, MANCHESTER,
UNITED KINGDOM

7. DEPARTMENT OF CLINICAL NEUROLOGY, UNIVERSITY OF OXFORD, UNITED KINGDOM, UCL INSTITUTE OF
NEUROLOGY, UNIVERSITY COLLEGE LONDON, QUEEN SQUARE, LONDON, UNITED KINGDOM

8. DEPARTMENT OF RADIOLOGY, LEIDEN UNIVERSITY MEDICAL CENTRE, LEIDEN, THE NETHERLANDS

Abstract

Objectives

To investigate the function-structure relationship of white matter within different stages of Huntington's disease using diffusion tensor imaging (DTI).

Experimental design

From the TRACK-HD study, an early stage HD group and a pre-manifest gene carrier group (PMGC) were age-matched to two healthy control groups; all underwent 3T MRI scanning of the brain. Region of interest (ROI) segmentation of the corpus callosum, caudate nucleus, thalamus, prefrontal cortex and sensorimotor cortex was applied, and the apparent fiber pathways of these regions were analyzed. Functional measures of motor, oculomotor, cognition, and behavior were correlated to DTI measures.

Principle observations

In PMGC versus controls, higher apparent diffusion coefficient (ADC) was seen in white matter pathways of the sensorimotor cortex ($p < 0.01$) and in the ROI of corpus callosum ($p < 0.017$). In early HD, fiber tract analysis showed higher ADC in pathways of the corpus callosum, thalamus, sensorimotor and pre-frontal region ($p < 0.01$). ROI analysis showed higher diffusivity in the corpus callosum and caudate nucleus ($p < 0.017$). Motor, oculomotor, cognition, and probability of onset within 2 and 5 years, correlated well with ADC measures of the corpus callosum ($p < 0.01 - p < 0.005$), sensorimotor ($p < 0.01 - p < 0.005$) and prefrontal region ($p < 0.01$).

Conclusions

Disturbances in the white matter connections of the sensorimotor cortex can be demonstrated not only in manifest HD but also in pre-manifest gene carriers. Connectivity measures are well related to clinical functioning. DTI measures can be regarded as a potential biomarker for HD, due to their ability to objectify changes in brain structures and their role within brain networks.

Introduction

Huntington's disease (HD) is a neurodegenerative genetic disorder characterized by a progressive deterioration of motor control, cognitive functioning, and mood and behavioral functioning. The presence of an abnormal expansion of CAG repeats in the *HTT* gene, on chromosome four is responsible for the disease. The effect of the HD gene is seen in the brain as progressive cerebral atrophy of the basal ganglia and cortex¹⁻⁴. It has been shown that the onset of atrophy may already be present in gene carriers up to 10 years prior to disease manifestation^{4,5}. On the contrary, less is known about white matter changes in HD. Some reports demonstrate global atrophy of the white matter in manifest HD^{6,7}, whereas others show regional differences only^{8,9}. A global volume reduction of white matter was seen only in one study of premanifest gene carriers¹⁰. The specific impact of HD on specific white matter pathways, and the clinical relevance of these changes, remains unclear.

The development and clinical application of magnetic resonance diffusion tensor imaging (DTI) has increased knowledge of grey and white matter structure in a variety of neurodegenerative diseases¹¹. In patients with HD, a few studies have applied DTI to characterize changes in the macrostructure and microstructure of the basal ganglia. Lower fractional anisotropy (FA) values were found for premanifest gene carriers in the putamen, caudate nucleus¹² and thalamus³. On the contrary, Rosas *et al.* (2006) found higher FA in the putamen and pallidum¹⁴. In healthy subjects, FA values of grey matter structures are generally below 0.15. In white matter, values tend to be much higher ranging from 0.2 up to 1¹⁵. In general, the higher the FA value the more directional the organization of the tissue is regarded to be - as seen in white matter fiber tracts. For this reason FA is generally accepted as an indication of tissue integrity.

In white matter, lower FA and increased apparent diffusion coefficient (ADC) values have been found in the internal capsule and corpus callosum in premanifest and manifest HD compared with healthy control subjects^{13,14}. In several of neurodegenerative disorders, such as Alzheimer's and Parkinson's Disease, ADC values have been found to higher, indicating that degeneration negatively affects the brain tissue structure¹⁶⁻¹⁸. Higher ADC values indicate that the microstructure of the tissue allows a faster movement of water molecules. These higher values were also found in manifest HD¹⁹⁻²². To find white matter differences that are related to the earliest changes in HD, specific white matter fiber tracts that are related to HD symptomatology should preferably be investigated. A reduction in cognitive, motor,

oculomotor performance is present up to a decade before clinical manifestation of HD^{5,23,24}, therefore, it can be hypothesized that the fibers associated with these function may also be affected in the premanifest phase. The direct nature of this relationship is unknown, and therefore, the aim of the present study is, first, to investigate early FA and ADC changes in white matter fiber bundles running to and from brain areas known to be affected by HD (e.g. caudate nucleus) or those related to the clinical characteristics of HD (e.g. sensorimotor cortex or prefrontal cortex). Second, to investigate to which extent changes in brain tissue structure and integrity in white matter fibers are related to clinical functioning.

Method

Participants

As part of the Track-HD study 90 participants were included at the Leiden University Medical Centre study site (for details see Tabrizi *et al.*, 2009⁴). Diffusion tensor magnetic resonance imaging was added to the standard MRI protocol. DTI was not performed because of claustrophobia in 10 participants, and another nine were excluded from analysis due to movement artifacts. Of the remaining 71 subjects, 16 subjects had early HD, 27 were premanifest gene carriers and 28 were healthy control subjects. Inclusion criteria for premanifest HD gene carriers were a CAG repeat ≥ 40 with a total motor score on the Unified Huntington's Disease Rating Scale 1999 (UHDRS) ≤ 5 . Inclusion criteria for the early manifest HD patients were a CAG repeat ≥ 40 , with a UHDRS motor score > 5 and a total functional capacity (TFC) score ≥ 7 . Healthy gene negative family members or partners were recruited as control subjects. Because the early HD group is inherently older than the premanifest group, the control group was split into two separate groups of each 14 subjects to achieve age-matching. The younger healthy control subjects were age matched to the premanifest gene carriers (control group A). The older healthy controls subjects were age-matched to the manifest group (control group B). None of the participants suffered from a neurological disorder, a major psychiatric diagnosis, or had a history of severe head injury. The study was approved by the Medical Ethical Committee of the Leiden University Medical Centre. All participants gave informed consent.

DTI acquisition

MRI acquisition was performed on a 3 Tesla whole body scanner (Philips Achieva, Healthcare, Best, the Netherlands) with an eight channel SENSE head coil. T1-weighted image volumes were acquired using a 3D MPRAGE acquisition sequence with the following imaging parameters: TR = 7.7 ms, TE = 3.5 ms,

FOV = 24 cm, matrix size 224x224, number of slices = 164, slice thickness = 1.00 mm, slice gap = 0. A volumetric T2-weighted image (VISTA) was acquired with the same parameters for field of view, acquisition matrix, and slice thickness as the T1-weighted images, with TE = 250 ms and TR = 2500 ms. A single-shot echo-planar DTI sequence was applied with 32 measurement directions and the following scan parameters: TR = 10004 ms, TE = 56 ms, FOV = 220 x 220 x 128 with an acquisition matrix of 112 x 110, 2.00 mm slice thickness, transversal slice orientation, slice gap = 0, flip angle = 90°, single reconstruction voxel dimensions were 1.96 x 1.96 x 2.00 mm, number of slices = 64, B factor = 1000, halfscan factor = 0.61. Parallel imaging (SENSE) was used with a reduction factor of 2, NSA = 1 and fat suppression was applied. DTI acquisition time was 6.55 minutes.

Regions of interest segmentation

A priori, the caudate nuclei, thalami, and the corpus callosum were determined as regions of interest (ROI). A semiautomatic segmentation and analysis procedure was used as part of the software program FibreTrak (release 2.5.3, Philips Medical Systems, Best, the Netherlands). The caudate nucleus and thalamus were segmented separately on each side, but considered as one ROI during data analysis. On the DTI scans, special caution was taken to prevent inclusion of any non grey matter voxels, as both the caudate nucleus and thalamus are laterally bordered by the internal capsule. All analyses and segmentations were performed blinded to group status. For more detailed information on segmentations see the supplementary material.

Fiber tract analysis

Fiber analysis of fibers running through the following five structures was performed: the corpus callosum (Figure 1A), sensorimotor cortex (Figure 1B), caudate nucleus (Figure 1C), superior prefrontal cortex (Figure 1D) and thalamus (Figure 1E). To analyze fibers running through the corpus callosum, caudate nucleus and thalamus, the previously segmented ROIs were used. Additional segmentations for ROIs of the superior prefrontal cortex and sensorimotor cortex were performed. The superior prefrontal region was segmented on the basis of Brodmann areas 9 and 10. The sensorimotor cortex on Brodmann areas 1, 2, 3 and 4¹². To calculate the average ADC and FA of the five white matter pathways FibreTrak was used (release 2.5.3, Philips Medical Systems, Best, The Netherlands). The software applies fiber assignment by continuous tracking²⁵. The following standard parameters were implemented: minimum FA value 0.10, maximum angle change 27°, minimum fiber length 10 mm. For more detailed information on the application of the fiber tracking software see the supplementary material.

Clinical Assessments

From the extensive assessment battery in the TRACK-HD study, specific tasks were chosen that gave a representation of functioning in each symptom domain. Furthermore, these were tasks that had been proved to provide sensitive outcome measures for group comparisons, even in the premanifest stages⁴: index finger speeded tapping and sustained tongue force measures (motor), anti-saccade latency and error rate (oculomotor), symbol digit modalities test, the Stroop word reading test, trail making task part B, and a visual working memory task – the spot the change task (cognition); Beck's depression inventory 2nd version (BDI-II) and the frontal systems behavior inventory which yields three subscores of disinhibition, executive functioning and apathy (psychiatry). CAG repeat length and probability of onset within 5 years and Burden of pathology $((\text{CAG} - 35.5) \times \text{age})^{26}$ were also added to the analysis. For the complete set of clinical assessments and variables see Tabrizi *et al.* (2009)⁴.

Statistics

Statistical analyses were performed with the Statistical Package for Social Sciences (SPSS for Windows; version 17.0.2, SPSS inc, Chicago, IL). Distributions and assumptions were checked. Independent student's t-tests and Chi-square tests were applied where appropriate in the analysis of group differences based on descriptive data; age, CAG, Dutch adult reading test (IQ), TFC and UHDRS. To test for differences in FA and ADC in the three ROIs and the five white matter fiber bundles between premanifest or manifest gene carriers and their corresponding control groups, analyses were performed using independent student's t-tests. Correction for multiple comparisons was applied to each analysis. Each analysis of ADC in the basal ganglia ROIs, the FA in the basal ganglia ROIs, the FA of the fiber pathways, and the ADC of the fiber pathways was regarded as a separate analyses. Therefore a Bonferroni correction was applied to each analysis. For the ADC and FA ROI analysis this lead to $0.05/3 = 0.017$, and for the ADC and FA fiber pathways analysis this lead this to $0.05/5 = 0.01$. The number of voxels in each seed ROI was compared between groups. Partial Pearson correlations analysis was performed to explore and test for possible associations between measures of white matter fiber pathway integrity and clinical measures. Age and gender were added into this analysis as covariates. The number of voxels in a ROI were also correlated to the clinical variables in order to examine the possibility that grey matter volume explains any possible correlations. The ADC and FA values of the white matter fiber pathways were correlated to each other to examine other explanations for possible results.

Results

Premanifest

No differences in age, gender, IQ, TFC, and UHDRS motor score between the premanifest gene carriers and their controls were present (Table I). The ADC and FA values of the ROIs and fiber pathways are shown in Table I. Premanifest gene carriers showed increased ADC values in the corpus callosum compared with controls. A significant increase in ADC of the white matter fibers of the sensorimotor cortex was also found between premanifest gene carriers and controls. No differences in ADC were found in the regions of the caudate nucleus and thalamus. No difference in FA was found in any of the three regions between the two groups. Also, no FA or ADC differences were found in any of the fiber pathways between the two groups. The number of voxels in the caudate nucleus ROI of premanifest group is significantly lower than the number in the control group ROI.

Early HD

The demographic data of the early HD and control group B showed no differences in age, gender or IQ. TFC and UHDRS differed significantly (Table II). In the corpus callosum and the caudate nucleus, the ADC values were larger in early HD when compared with controls. Between the two groups, no difference in FA was found in any of the ROIs. ADC values were significantly increased in fibers from all regions, except for the caudate nucleus fibers. FA was decreased in fibers running to and from the prefrontal cortex in early HD patients. No difference in FA was found in fibers passing through the corpus callosum, caudate nucleus, thalamus and sensorimotor cortex. The number of voxels of the caudate nucleus as well as in the corpus callosum was significantly lower in the patient group than in the control group (Table II).

Clinical correlations

The correlation analysis between the ADC of the fiber bundles with genetics, probability of onset within five years, burden of pathology, motor, oculomotor, cognition and behavior in all participants are shown in Table III.

Tapping was moderately associated with the diffusivity (ADC) of bundles through the corpus callosum, thalamus, sensorimotor cortex and prefrontal cortex. For the tongue force, similar but weaker associations were found. Latency of anti-saccades and the percentage of antisaccade errors in the oculomotor task were found to correlate with increased diffusivity of the corpus callosum, sensorimotor cortex and prefrontal cortex fibers. All cognitive measures were moderately to strongly associated with the ADC of fibers through the corpus callosum, sensorimotor cortex

and to a lesser extent the prefrontal cortex. In premanifest gene carriers, probability of expected onset within 5 years and burden of pathology showed a high positive correlation with the diffusivity of the corpus callosum fibers and with those of the sensorimotor cortex, whereby a loss of integrity related to a higher probability of onset within five years and higher burden of pathology. No association in any cognitive domain with fibers of the thalamus was found. CAG repeat length and behavioral measures did not show association with the ADC of any of the fiber bundles studied. No measures showed association with the fibers of the caudate nucleus. FA of the corpus callosum and sensorimotor cortex fibers negatively correlated with the latency ($r = -0.52$, $p < 0.001$) and percentage of errors ($r = -.038$, $p = 0.001$) in the anti-saccade oculomotor task. FA did not demonstrate any significant correlation with genetics, motor, cognition, and behavior.

The results from a correlational analysis between number of voxels in a seed region and clinical variables showed five significant moderate correlations. Only one of these also showed a significant correlation in the analysis of ADC values with clinical variables. This was the correlation between the caudate nucleus and TMT task performance ($r = -0.36$, $p < 0.01$). Directly correlating the ADC and FA values of the white matter pathways with each other revealed a number of significant correlations which is shown in table IV in the supplementary material. The direct correlation of ADC and FA of the same fiber bundle shows that the ADC and FA of the sensorimotor cortex and prefrontal white matter pathways are correlated.

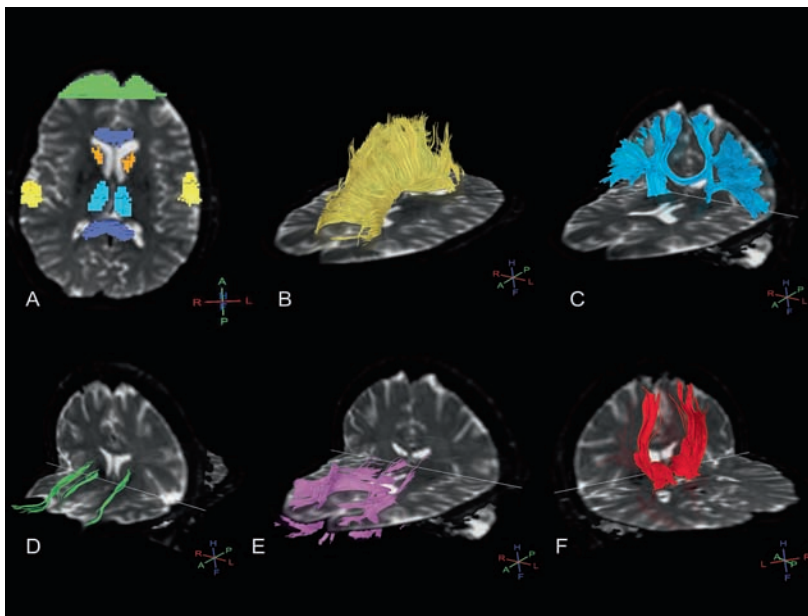


Figure 1. Typical example of ROIs (A) and subsequent white matter fiber pathways in a premanifest gene carrier of the corpus callosum (B), sensorimotor cortex (C), caudate nucleus (D), prefrontal cortex (E) and thalamus (F). 3D crosses depict orientation, whereby H = head, F = feet, A = anterior, P = posterior, R = right, L = left.

Table 1. Group demographics, ADC and FA values, and number of seed voxels per region of interest for the premanifest gene carriers and their controls.

	Control group A n: 14, male: 7		Premanifest gene carriers n: 27, male: 16		
	Mean (SD)	range	Mean (SD)	range	
Age (yrs)	46 (7,5)	35 - 58	43 (8,3)	26 - 61	
CAG	- (-)	-	43 (2,5)	39 - 50	
IQ	105,6 (11,3)	88 - 130	101,3 (11,3)	76 - 118	
TFC	13 (0)	13 - 13	12,6 (0,8)	10 - 13	
UHDRS	1,9 (1,8)	0 - 6	2,4 (1,4)	0 - 4	
ADC ROI	# voxels ± SD	mean ± SD	# voxels ± SD	mean ± SD	<i>p</i>
Corpus Callosum	1884 ± 378	0.78 ± 0.028	1767 ± 319	0.81 ± 0.033*	0.014
Caudate Nucleus	58 ± 13	0.73 ± 0.071	47 ± 11***	0.76 ± 0.053	0.160
Thalamus	2700 ± 843	0.73 ± 0.023	2601 ± 657	0.73 ± 0.023	0.994
FA ROI					
Corpus Callosum	1884 ± 378	0.76 ± 0.019	1767 ± 319	0.75 ± 0.021	0.461
Caudate Nucleus	58 ± 13	0.17 ± 0.015	47 ± 11***	0.18 ± 0.023	0.058
Thalamus	2700 ± 843	0.34 ± 0.025	2601 ± 657	0.33 ± 0.022	0.368
ADC Fiber pathway	# voxels ± SD	mean ± SD	# voxels ± SD	mean ± SD	
Corpus Callosum	1884 ± 378	0.89 ± 0.049	1767 ± 319	0.91 ± 0.054	0.206
Caudate Nucleus	58 ± 13	0.98 ± 0.116	47 ± 11***	0.94 ± 0.075	0.166
Thalamus	2700 ± 843	0.87 ± 0.055	2601 ± 657	0.89 ± 0.071	0.476
Motor cortex	595 ± 86	0.78 ± 0.017	580 ± 71	0.80 ± 0.029**	0.009
Prefrontal cortex	1136 ± 183	0.88 ± 0.044	1117 ± 322	0.89 ± 0.037	0.631
FA Fiber pathway					
Corpus Callosum	1884 ± 378	0.49 ± 0.015	1767 ± 319	0.49 ± 0.016	0.785
Caudate Nucleus	58 ± 13	0.36 ± 0.017	47 ± 11***	0.35 ± 0.031	0.683
Thalamus	2700 ± 843	0.42 ± 0.018	2601 ± 657	0.41 ± 0.021	0.515
Motor cortex	595 ± 86	0.40 ± 0.017	580 ± 71	0.39 ± 0.020	0.190
Prefrontal cortex	1136 ± 183	0.41 ± 0.018	1117 ± 322	0.40 ± 0.021	0.120

SD: standard deviation, CAG: CAG repeat length, IQ: estimate of premorbid intelligence quotient. TFC: Total Functional Capacity score. UHDRS: Unified Huntington's Disease Rating Scale total motor score. ROI: Region of interest analysis. ADC: Apparent Diffusion Coefficient in $\mu\text{m}^2/\text{ms}$, FA: Fractional Anisotropy (no unit), Fiber pathway: fiber pathways analysis between the listed region and the rest of the brain. * $p < 0.017$, ** $p < 0.01$ (adjusted for multiple comparisons). # voxels: mean number of voxels in the listed seed region. ***Number of voxels differs significantly from healthy controls

Table 2. Group demographics, ADC and FA values, and number of seed voxels per region of interest for the early HD patients and their controls.

	Control group B n: 14, male: 7		Early HD n: 16, male: 12		<i>p</i>
	Mean (SD)	range	Mean (SD)	range	
Age (yrs)	51.4 (7.9)	42 - 65	48.2 (10)	31 - 63	
CAG	- (-)	-	43 (1.6)	41 - 46	
IQ	102.6 (6.6)	88 - 115	99.6 (12)	72 - 118	
TFC	12.9 (0.3)	12 - 13	10.6 [§] (2)	7 - 13	
UHDRS	3.1 (2.8)	0 - 7	18.3 [§] (10.4)	6 - 45	
ADC ROI	# voxels ± SD	mean ± SD	# voxels ± SD	mean ± SD	<i>p</i>
Corpus Callosum	1934 ± 312	0.80 ± 0.031	1445 ± 371***	0.85 ± 0.040*	0.000
Caudate Nucleus	57 ± 12	0.74 ± 0.048	40 ± 7***	0.83 ± 0.069*	0.001
Thalamus	2480 ± 531	0.74 ± 0.032	3102 ± 1062	0.74 ± 0.034	0.863
FA ROI					
Corpus Callosum	1934 ± 312	0.75 ± 0.012	1445 ± 371***	0.73 ± 0.033	0.046
Caudate Nucleus	57 ± 12	0.17 ± 0.018	40 ± 7***	0.19 ± 0.019	0.072
Thalamus	2480 ± 531	0.33 ± 0.021	3102 ± 1062	0.32 ± 0.034	0.95
ADC Fiber pathway	# voxels ± SD	mean ± SD	# voxels ± SD	mean ± SD	
Corpus Callosum	1934 ± 312	0.89 ± 0.051	1445 ± 371***	0.95 ± 0.067**	0.008
Caudate Nucleus	57 ± 12	0.88 ± 0.107	40 ± 7***	0.97 ± 0.079	0.023
Thalamus	2480 ± 531	0.85 ± 0.080	3102 ± 1062	0.93 ± 0.063**	0.007
Motor cortex	589 ± 117	0.79 ± 0.023	593 ± 110	0.82 ± 0.027**	0.001
Prefrontal cortex	1118 ± 239	0.88 ± 0.023	1202 ± 274	0.95 ± 0.056**	0.000
FA Fiber pathway					
Corpus Callosum	1934 ± 312	0.48 ± 0.013	1445 ± 371***	0.47 ± 0.017	0.027
Caudate Nucleus	57 ± 12	0.35 ± 0.027	40 ± 7***	0.35 ± 0.021	0.592
Thalamus	2480 ± 531	0.41 ± 0.016	3102 ± 1062	0.41 ± 0.024	0.644
Motor cortex	589 ± 117	0.38 ± 0.019	593 ± 110	0.37 ± 0.024	0.059
Prefrontal cortex	1118 ± 239	0.39 ± 0.016	1202 ± 274	0.38 ± 0.014**	0.006

SD: standard deviation, CAG: CAG repeat length, IQ: estimate of premorbid intelligence quotient. TFC: Total Functional Capacity score. UHDRS: Unified Huntington's Disease Rating Scale total motor score.

[§]Significant difference from control group, *p* < 0.01. ROI: Region of interest analysis. ADC: Apparent Diffusion Coefficient in $\mu\text{m}^2/\text{ms}$, FA: Fractional Anisotropy (no unit), Fiber pathway: fiber pathways analysis between the listed region and the rest of the brain. **p* < 0.017, ***p* < 0.01 (adjusted for multiple comparisons). # voxels: mean number of voxels in the listed seed region. ***Number of voxels differs significantly from healthy controls.

Table 3. Standardized correlation coefficients matrix for ADC of white matter fiber bundles and clinical measures in all participants.

	Motor			Cognitive					Behavior			
	Tapping	Tongue	SDMT	SWR	TMT B	SPOT	BDI-II	FrSBe Dis-inhib	FrSBe Exec dysf	FrSBe apathy		
Corpus Callosum	0.38**	0.27	-0.32*	-0.39**	0.36**	-0.39**	0.11	0.01	0.09	0.10		
Caudate Nucleus	0.13	0.23	-0.08	-0.04	0.13	-0.19	-0.05	0.05	-0.02	-0.01		
Thalamus	0.41**	0.33*	-0.27	-0.28	0.26	-0.30	0.02	0.03	0.09	0.07		
Motor cortex	0.46**	0.32*	-0.46**	-0.52**	0.55**	-0.33*	0.15	-0.02	0.11	0.17		
Prefrontal cortex	0.33*	0.28	-0.28	-0.34*	0.25	-0.28	0.15	-0.02	-0.06	0.04		
	Genetics	Probability of onset	Burden of Pathology					Oculomotor				
	CAG	Gene carrier only	within 5 years (preHD only)	(CAG-35.5) x age	Latency of anti-saccades	Error % of anti-saccades						
Corpus Callosum	0.36		0.61**	0.51**	-0.32*	-0.39**						
Caudate Nucleus	0.09		0.42	0.27	-0.08	-0.04						
Thalamus	0.10		0.06	0.19	-0.27	-0.28						
Motor cortex	0.32		0.58**	0.52**	-0.46**	-0.52**						
Prefrontal cortex	0.09		0.41*	0.37	-0.28	-0.34*						

Tapping = Average speeded tapping intertap variability for left and right index finger, Tongue = sustained tongue force measure, SDMT = Symbol Digit Modalities test, SWR = Stroop word reading task, TMT B = Trail making test part B, SPOT = Visual array comparison task for visual short-term memory capacity, BDI-II = Beck's Depression Inventory 2nd version, FrSBe = Frontal Systems Behaviour rating scale Self Report, disinhibition, executive dysfunction and apathy subscores, CAG = CAG repeat length (in gene carriers only), Expected years to onset correlations are only for premanifest gene carriers. All correlations are controlled for the effects of age and gender. * $p < 0.01$ ** $p < 0.005$

Discussion

The main finding of this study is that in premanifest gene carriers, the white matter pathway of the sensorimotor cortex is impaired. Furthermore, our data show that in the early manifest phase of the disease impairment is more widespread and present in the white matter pathways of the sensorimotor cortex, corpus callosum, thalamus, and prefrontal cortex. Finally, a relationship is seen between the changes in white matter pathways and functionality in the domains of motor, oculomotor and cognition. Moreover this study confirms findings of regional differences in the corpus callosum of premanifest and the caudate nuclei and corpus callosum of early HD^{14,27}.

In the premanifest phase of the disease, our study demonstrated a reduction of integrity of only the sensorimotor cortex fibers pathway, therefore this suggests that this pathway may be one of the first to be affected by HD. This is supported by the positive relationship between a higher probability of onset within 5 years, and a higher burden of pathology, with the loss of integrity of the sensorimotor cortex fibers. This premanifest cohort is 'free' of motor symptoms, and therefore these findings in a truly 'premotor' premanifest group further support the idea that these white matter changes are among the first to occur. This study is the first to demonstrate this change across the whole pathway; however, other studies examining this area do provide support for this finding. The findings of the voxel-by-voxel white matter analysis of Reading *et al.* (2005)¹² found differences in a cluster of voxels coinciding with the primary motor cortex (Brodmann area 4). Atrophy of the sensorimotor cortex was demonstrated as the only cortical region to be affected in premanifest gene carriers far from predicted onset⁴. Furthermore differences have been reported in functions that utilize this area in premanifest gene carriers, such as measures of motor function^{5,28}. The other important finding of our study in premanifest gene carriers is the differences in diffusivity in the corpus callosum, thereby replicating previous findings by Rosas *et al.* (2006,2009)^{14,27}. However we add that these differences are not seen in the white matter projections specifically going to and from the corpus callosum. Therefore, when looking beyond the main structure it can be suggested that the loss of integrity of the main structure is apparent, but not spread over its entire network, as is the case in manifest HD.

In the early manifest phase of HD, our data show that the diffusivity of the fiber pathways of the thalamus, corpus callosum, sensorimotor, and prefrontal cortex was higher in HD than in healthy controls. This suggests a disintegration of these structures. Of the five white matter pathways examined in HD all were found to be

affected except the pathways of the caudate nuclei. The absence of affected white matter from the caudate nucleus should be interpreted with some caution. It may suggest that the magnitude of integrity loss may not be the same for a structure as for its fibers at a given stage of the disease. However the variance of these measurements is larger than that of the other fibers pathways. The remaining results, such as that of reduced integrity of the prefrontal cortex fibers, find support in the regional differences demonstrated by Rosas *et al.* (2006)¹⁴. Our results show changes in ADC and almost no changes in FA. This suggests that of these two closely related measures, ADC is more sensitive in demonstrating changes across large pathways in HD. The results of the regional analysis showed higher diffusivity in the caudate nucleus and corpus callosum in HD than in healthy controls. This was not the case in the thalamus, whereby similar diffusion properties were seen in both HD and controls. Our findings concur with previous cross-sectional and longitudinal findings of a widespread effect of HD on white matter^{14;20;22;29}. The finding that a region was not affected, but its fibers were, demonstrates the need to embrace the full potential of DTI measures for HD, as this shows that despite a structure not showing integrity differences, the fibers that are needed for this structure to communicate with the brain may well be affected. In the case of the thalamus this is especially relevant to the clinical expression of the disease as this structure is vital to a large number of functional processes.

The previously discussed outcomes demonstrate that almost all fiber pathways that we examined are affected in early manifest HD and that one specific pathway is also affected in premanifest gene carriers. In exploring the clinical implications of these findings we see strong relationships between both motor, oculomotor and cognitive measures, and diffusivity measures of the pathways of the corpus callosum, thalamus, sensorimotor and prefrontal cortex. Although one cognitive measure does correlate to the prefrontal cortex fiber the cognitive measures are most strongly related to the sensorimotor cortex fibers. This finding can be explained with two complementary hypotheses. First, as seen in the premanifest group, the fibers of the sensorimotor cortex are the first to show decreased integrity. This suggests that these are the most severely affected fibers in the earliest (premanifest) stages of HD; therefore, it is not surprising that the clinical measures of decline relate to these fibers. Second, HD effects both cognition and motor function, and all cognitive tests require a motor response. A consequent finding in cognitive HD literature is that cognitive tests sensitive to psychomotor speed are the most sensitive tasks. A great deal of voluntary motor functioning is initiated in the sensorimotor cortex. Because of this we were not entirely surprised that cognitive tests relate strongly to the fibers of the sensorimotor cortex. The tasks chosen for analysis were those that provide meaningful outcomes for all

study groups, and did not show ceiling or floor effects. Therefore, we can conclude that fibers associated with higher order cognitive and motor coordination are affected in a manner that is congruent to clinical manifestations and that for this reason, DTI measures can be applied to characterize the structure-function relationship of white matter. This conclusion is supported in other studies of white and grey matter and clinical measures^{6,30}. In another study of eye movements and fiber tracking, similar results were found as ours, especially finding a relationship between eye movements and fiber FA³¹. We did not show a relationship between CAG repeat length or behavioral processes and changes in white matter integrity. The CAG repeat length is not dependent on disease progression or white matter pathways and this stable quality may, in part, explain this finding. A possible explanation for the absence of a relationship between behavioral measures and diffusivity may be the complex pathophysiological and psychological process underlying these behavioral changes that may not be primarily dependent on white matter. Alternatively, the use of medication may be a factor in the level of symptoms reported (full details of medication use are outlined in Tabrizi *et al.* (2009)⁴ leading to an underestimation of neuropsychiatric problem behavior. However, a recent study has shown that behavioral changes in premanifest HD remain stable³², thereby reinforcing the idea that degenerative processes are not at the root of these neuropsychiatric differences. Therefore we conclude that behavioral changes may not be directly reflected by white matter changes.

This study examined and demonstrated differences in white matter pathways of five HD relevant regions, this restriction is a limitation of the study. Differences were found in the number of seed voxels in the caudate nucleus in premanifest gene carriers and in the caudate nucleus and corpus callosum in manifest HD. On the contrary, differences were not seen in the number of voxels in the thalamus, sensorimotor region, or prefrontal regions in the patient group. These reductions do seem to reflect expected atrophy, but do not follow the pattern of differences found in ADC. Therefore these differences do not seem to explain the differences in diffusivity. The results from a correlation analysis between number of voxels in a seed region and clinical variables reveal only five significant moderate correlations. This is in contrast to the analysis of relationship between average ADC and the clinical variables whereby 25 moderate to high correlations were significant. Furthermore only one of these five was the same as one of the 25 clinical correlations. These results suggest the volume of the seed region does not explain the observed original correlations. With this possibility excluded, it can be stated with more certainty that the relationships observed reflect the underlying changes in structure of the white matter pathways. Furthermore, direct correlation of the ADC and FA of the white matter pathways also supports this conclusion.

It can be seen that only significant relationships between the ADC and FA of the same pathways were apparent for pathways that showed (nearly) significant group differences. Overall, the results call for further examination of white matter pathways. The findings warrant confirmation with longitudinal follow-up.

In conclusion, we demonstrated that the sensorimotor cortex fibers are affected already in the premanifest phase of HD and therefore may be a good target for following progression of the disease. Our data show that impairment is seen in corpus callosum, nuclei and fiber projections of HD relevant brain regions in both premanifest and early manifest HD. These impairments relate to proven correlates of clinical dysfunction. Overall, the findings of this study confirm the feasibility and use of DTI measures in HD research, whereby we show that ADC is a good measure in characterizing the impaired function-structure relationship present in HD.

Acknowledgments

The authors wish to thank the TRACK-HD study participants, the “CHDI/High Q Foundation”, a not-for-profit organization dedicated to finding treatments for HD, for providing financial support (www.chdifoundation.org), and all TRACK-HD investigators for their efforts in conducting this study (www.track-hd.net). We would like to thank BioRep for the CAG determinations. We would also like to acknowledge the following individuals personally for their contributions. Caroline Jurgens, Marie-Noelle Witjes-Ane and Ellen 't Hart for assistance with coordination and data collection, Gail Owen for coordination of data transfer, Mike Sharman for his comments and input and Felix Mudoh Tita for data monitoring.

References

1. Roos RA, Bots GT, Hermans J. Quantitative analysis of morphological features in Huntington's disease. *Acta Neurol Scand* 1986;73:131-35
2. Aylward EH, Li Q, Stine OC, et al. Longitudinal change in basal ganglia volume in patients with Huntington's disease. *Neurology* 1997;48:394-99
3. Rosas HD, Liu AK, Hersch S, et al. Regional and progressive thinning of the cortical ribbon in Huntington's disease. *Neurology* 2002;58:695-701
4. Tabrizi SJ, Langbehn DR, Leavitt BR, et al. Biological and clinical manifestations of Huntington's disease in the longitudinal TRACK-HD study: cross-sectional analysis of baseline data. *Lancet Neurol* 2009;8:791-801
5. Paulsen JS, Langbehn DR, Stout JC, et al. Detection of Huntington's disease decades before diagnosis: the Predict-HD study. *J Neurol Neurosurg Psychiatry* 2008;79:874-80
6. Beglinger LJ, Nopoulos PC, Jorge RE, et al. White matter volume and cognitive dysfunction in early Huntington's disease. *Cogn Behav Neurol* 2005;18:102-07
7. Fennema-Notestine C, Archibald SL, Jacobson MW, et al. In vivo evidence of cerebellar atrophy and cerebral white matter loss in Huntington disease. *Neurology* 2004;63:989-95
8. Aylward EH, Anderson NB, Bylsma FW, et al. Frontal lobe volume in patients with Huntington's disease. *Neurology* 1998;50:252-58
9. Jech R, Klempir J, Vymazal J, et al. Variation of selective gray and white matter atrophy in Huntington's disease. *Mov Disord* 2007;22:1783-89
10. Paulsen JS, Hayden M, Stout JC, et al. Preparing for preventive clinical trials: the Predict-HD study. *Arch Neurol* 2006;63:883-90
11. Nucifora PG, Verma R, Lee SK, et al. Diffusion-tensor MR imaging and tractography: exploring brain microstructure and connectivity. *Radiology* 2007;245:367-84
12. Reading SA, Yassa MA, Bakker A, et al. Regional white matter change in pre-symptomatic Huntington's disease: a diffusion tensor imaging study. *Psychiatry Res* 2005;140:55-62
13. Magnotta VA, Kim J, Kosciak T, et al. Diffusion Tensor Imaging in Preclinical Huntington's Disease. *Brain Imaging and Behavior* 2009;3:77-84
14. Rosas HD, Tuch DS, Hevelone ND, et al. Diffusion tensor imaging in presymptomatic and early Huntington's disease: Selective white matter pathology and its relationship to clinical measures. *Mov Disord* 2006;21:1317-25
15. Mori S, van Zijl PC. Fiber tracking: principles and strategies - a technical review. *NMR Biomed* 2002;15:468-80
16. Stebbins GT, Murphy CM. Diffusion tensor imaging in Alzheimer's disease and mild cognitive impairment. *Behav Neurol* 2009;21:39-49
17. Rizzo G, Martinelli P, Manners D, et al. Diffusion-weighted brain imaging study of patients with clinical diagnosis of corticobasal degeneration, progressive supranuclear palsy and Parkinson's disease. *Brain* 2008;131:2690-700
18. Zhang K, Yu C, Zhang Y, et al. Voxel-based analysis of diffusion tensor indices in the brain in patients with Parkinson's disease. *Eur J Radiol*. 2011 Feb;77(2):269-73.
19. Mascalchi M, Lolli F, Della NR, et al. Huntington disease: volumetric, diffusion-weighted, and magnetization transfer MR imaging of brain. *Radiology* 2004;232:867-73
20. Vandenberghe W, Demaerel P, Dom R, et al. Diffusion-weighted versus volumetric imaging of the striatum in early symptomatic Huntington disease. *Journal of Neurology* 2009;256:109-14
21. Sritharan A, Egan G, Johnston L, et al. A longitudinal diffusion tensor imaging study in symptomatic Huntington's disease. *J Neurol Neurosurg Psychiatry*. 2010 Mar;81(3):257-62.
22. Douaud G, Behrens TE, Poupon C, et al. In vivo evidence for the selective subcortical degeneration in Huntington's disease. *Neuroimage* 2009;46:958-66
23. Stout JC, Weaver M, Solomon AC, et al. Are cognitive changes progressive in prediagnostic HD? *Cogn Behav Neurol* 2007;20:212-18

24. Lasker AG, Zee DS. Ocular motor abnormalities in Huntington's disease. *Vision Res* 1997;37(24):3639-45
25. Mori S, Crain BJ, Chacko VP, et al. Three-dimensional tracking of axonal projections in the brain by magnetic resonance imaging. *Ann Neurol* 1999;45:265-69
26. Penney JB, Vonsattel JP, MacDonald ME, et al. CAG repeat number governs the development rate of pathology in Huntington's disease. *Annals of Neurology* 1997;41:689-92
27. Rosas HD, Lee SY, Bender A, et al. Altered white matter microstructure in the corpus callosum in Huntington's disease: Implications for cortical "disconnection". *Neuroimage*. 2010 Feb 15;49(4):2995-3004.
28. Solomon AC, Stout JC, Weaver M, et al. Ten-year rate of longitudinal change in neurocognitive and motor function in prediagnosis Huntington disease. *Mov Disord* 2008;23:1830-36
29. Weaver KE, Richards TL, Liang O, et al. Longitudinal diffusion tensor imaging in Huntington's Disease. *Exp Neurol* 2009;216:525-29
30. Wolf RC, Vasic N, Schonfeldt-Lecuona C, et al. Cortical dysfunction in patients with Huntington's disease during working memory performance. *Hum Brain Mapp*. 2009 Jan;30(1):327-39.
31. Kloppel S, Draganski B, Golding CV, et al. White matter connections reflect changes in voluntary-guided saccades in pre-symptomatic Huntington's disease. *Brain* 2008;131:196-204
32. van Duijn E, Kingma EM, Timman R, et al. Cross-sectional study on prevalences of psychiatric disorders in mutation carriers of Huntington's disease compared with mutation-negative first-degree relatives. *J Clin Psychiatry* 2008;69:1804-10

Supplementary Material

Supplementary Methods

Segmentation

Based on the anatomical co-registration images, the ROIs were segmented in native space for each individual. This was done by two experienced radiographers, blinded to patient group. Two types of ROIs were defined. Basal ganglia ROIs for analysis, and seed-ROIs as starting point for fiber tracking. The basal ganglia ROIs were segmented as follows. For the caudate nucleus all voxels clearly bounded by the lateral ventricle and the anterior limb of the internal capsule were selected. The putamen segmentation included all voxels within the structure bounded on the medial side by the globus pallidus and the anterior limb of the internal capsule, and on the lateral side by the capsula extrema. The thalamus segmentation was performed by allocating all voxels to the ROI that medially bordered the third ventricle, were superiorly bordered by the lateral ventricle, and were laterally bordered by the internal capsule. The seed ROIs were cortically based, and because these areas were not as clearly anatomically bounded as the other structures, Brodmann areas were used to define the segmentation. Reading *et al.* (2005) defined areas of the cortex in their analysis of presymptomatic HD by means of these Brodmann areas¹. The superior prefrontal region was segmented on areas 9 (frontal portion) and 10. Brodmann area 10 is medially bound by the superior rostral sulcus, and dorsally by the inferior frontal sulcus and the frontomarginal sulcus. Area 9 bordered inferiorly by area 10 and dorsally by the superior frontal sulcus. After all ROIs were drawn, the radiographers switched scans and carefully checked the segmentations for potential miss-segmentation. After all scans had been segmented a random 20% were selected for verification by a neurologist specialized in neuro-imaging. Any segmentation voxels that were felt to be outside of the targeted anatomy were discussed until a consensus was formed and these few voxels were changed accordingly.

Analysis

We applied the software supplied by the manufacturer by transferring the raw DTI data and the anatomic co-registration images to an off-line manufacturer provided console. In doing so the data were loaded into the Philips Research Image-processing Development Environment (PRIDE) (Philips Medical Systems). Then the diffusion tensor and derived measures, including ADC and FA, were calculated using the Philips PRIDE Fiber Tracking tool (version 2.5.3). This allows fiber tracking based on the Fiber Assignment by Continuous Tracking (FACT) algorithm². The algorithm values for restricting fiber tracking were kept at default

Supplementary Results

Table 4. Cross tabulation of correlation coefficients of the FA and ADC of the white matter fiber pathways with each other.

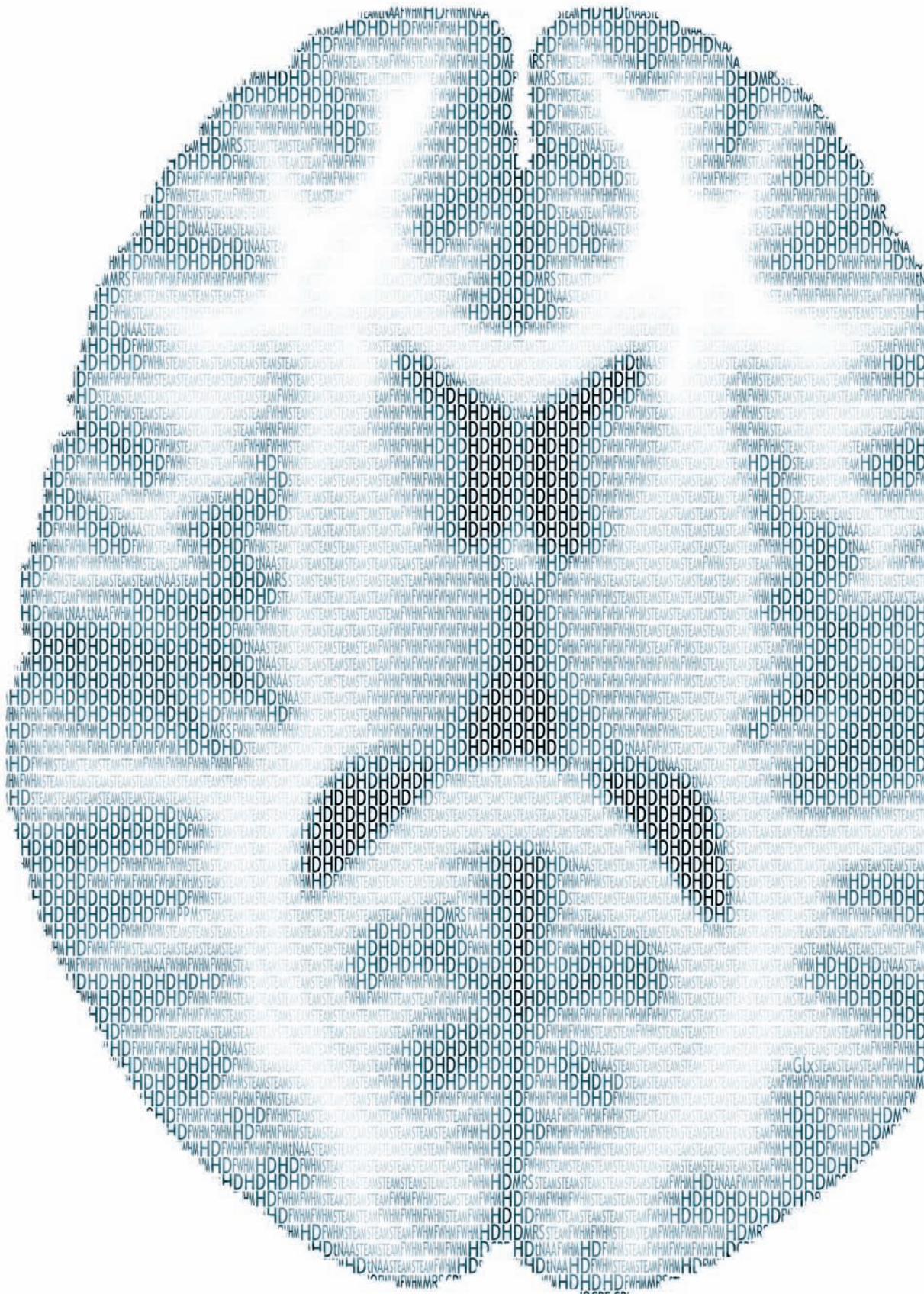
		Corpus Callosum		Caudate Nucleus		Thalamus		Motor cortex		Prefrontal cortex	
		ADC	FA	ADC	FA	ADC	FA	ADC	FA	ADC	FA
Corpus Callosum	ADC	-	-.123	.482	-.262	.705	.069	.644	-.312	.572	-.432
	FA		-	.002	.136	-.065	.472	-.439	.581	-.272	.516
Caudate Nucleus	ADC			-	.028	.594	.153	.185	.091	.206	-.077
	FA				-	-.116	.404	-.052	.190	-.352	.046
Thalamus	ADC					-	.034	.476	-.145	.353	-.183
	FA						-	-.021	.290	-.050	.126
Motor cortex	ADC							-	-.604	.548	-.530
	FA								-	-.492	.473
Prefrontal cortex	ADC									-	-.483
	FA										-

ADC: Apparent Diffusion Coefficient, FA: Fractional Anisotropy. **Bold** = significant correlation

and were: minimum FA value of 0.10, maximum angle change: 27°, and a minimum fiber length of 10mm. This same method and software has been applied in a number of disorders of both brain and muscle, such as developmental CNS anomalies³, corticospinal tract stroke⁴, lateral patellar dislocation⁵ and Lissencephaly⁶.

References

1. Reading SA, Yassa MA, Bakker A, et al. Regional white matter change in pre-symptomatic Huntington's disease: a diffusion tensor imaging study. *Psychiatry Res* 2005;140:55-62
2. Mori S, Crain BJ, Chacko VP, et al. Three-dimensional tracking of axonal projections in the brain by magnetic resonance imaging. *Ann Neurol* 1999;45(2):265-69
3. Lee SK, Kim DI, Kim J, et al. Diffusion-tensor MR imaging and fiber tractography: a new method of describing aberrant fiber connections in developmental CNS anomalies. *Radiographics* 2005;25:53-65
4. Lee JS, Han MK, Kim SH, et al. Fiber tracking by diffusion tensor imaging in corticospinal tract stroke: Topographical correlation with clinical symptoms. *Neuroimage* 2005;26:771-76
5. Kan JH, Heemskerk AM, Ding Z, et al. DTI-based muscle fiber tracking of the quadriceps mechanism in lateral patellar dislocation. *J Magn Reson Imaging* 2009;29:663-70
6. Rollins, N., Reyes, T., Chia, J., 2005. Diffusion tensor imaging in lissencephaly. *AJNR Am.J.Neuroradiol.* 26, 1583-1586.



Abstract

Background

Huntington's Disease (HD) is a genetic disorder affecting the brain. Atrophy of deep grey matter structures has been reported and it is likely that underlying pathologic processes occur before or in concurrence with volumetric changes. Measurement of metabolite concentrations in these brain structures has the potential to provide insight into pathological processes. We aim to gain understanding of metabolite changes with respect to the disease stage and pathophysiological changes.

Methods

We studied five brain regions using magnetic resonance spectroscopy (MRS) using a 7-Tesla MRI scanner. Localized proton spectra were acquired to obtain five metabolite concentrations. MRS was performed in the caudate nucleus, putamen, thalamus, hypothalamus and frontal lobe in 44 control subjects, premanifest gene carriers and manifest HD.

Results

In the caudate nucleus HD patients display lower NAA ($p=0.009$) and lower creatine concentration ($p=0.001$) as compared to controls. In the putamen, manifest HD patients show lower NAA ($p=0.024$), lower creatine concentration ($p=0.027$) and lower glutamate ($p=0.013$). Although absolute values of NAA, creatine and glutamate were lower, no significant differences to controls were found in the premanifest gene carriers.

Conclusion

The lower concentrations of NAA and creatine in the caudate nucleus and putamen of early manifest HD suggest deficits in neuronal integrity and energy metabolism. The changes in glutamate could support the excitotoxicity theory. These findings not only give insight in neuropathological changes in HD, but also indicate that MRS can possibly be applied in future clinical trials to evaluate medication targeted at specific metabolic processes.

Introduction

Huntington's Disease (HD) is a neurodegenerative autosomal dominant disorder. The causative gene mutation is located on the short arm of chromosome 4 and consists of an expanded Cytosine-Adenine-Guanine (CAG)-repeat within the *Htt*-gene. This expansion results in the synthesis of an abnormal huntingtin protein that causes neuronal damage, brain atrophy, ultimately leading to functional disturbances of motor, cognition and behavior.

HD research has revealed widespread changes throughout the brain¹. Controversy remains as to which structures are affected at different disease stages. Atrophy of the striatum is regarded as the hallmark of the pathologic findings in HD². MRI studies demonstrate that the caudate nucleus and putamen begin to show atrophy up to a decade before clinical manifestations occur³. Structures such as the thalamus, hypothalamus, the frontal lobe, white matter and cortical grey matter have all been implicated to some degree at this pre-manifest stage, although findings differ^{1,4-6}.

The pathophysiological mechanism leading to neuronal damage remains unclear. Currently the two most accepted hypotheses describe impaired energy metabolism and the excitotoxicity of neurons^{7,8}. Both hypotheses can potentially be explored by means of non-invasive in vivo measurements of metabolites such as creatine and glutamate, using localized magnetic resonance spectroscopy (MRS). However, previous studies measuring the changes in the metabolite levels related to the damaging processes in HD have reported conflicting results. In one study a lower level of N-acetylaspartate (NAA) was confirmed post-mortem in the putamen and cortex in manifest HD⁹. In vivo altered levels of NAA, creatine, choline and glutamate have been reported in both premanifest and manifest HD in several brain structures, such as the striatum and thalamus using MRS¹⁰⁻¹⁶. However, in contrast, other studies using localized MRS did not detect changes in these metabolite levels in either manifest or premanifest HD¹⁷⁻¹⁹.

One of the factors that might explain discrepancies between previous studies is the relatively poor spatial and/or spectral resolution of localized spectra. Improvement in MRS methodology in terms of spectral resolution in combination with small voxel size and total scanning time can be achieved using a high field MRI scanner^{20,21}. This allows metabolite quantification in small, well defined anatomical structures, such as the caudate nucleus and putamen.

The major aims of the present study were to assess metabolite differences between manifest HD patients or premanifest HD gene carriers and controls, and to assess the association between these metabolite differences and clinical measures of disease severity in order to obtain a greater understanding of the pathophysiological changes in HD with respect to the disease stage. The hypotheses were as follows; as the neuronal integrity and the energy metabolism would be compromised, we expected the NAA and creatine to be lower in premanifest and manifest HD, especially in the striatum. Possible changes in glutamate could be expected based on the excitotoxicity theory, with higher levels in both premanifest and manifest HD.

Materials and Methods

Subjects

Participants were recruited from the outpatient neurology clinic of the Leiden University Medical Center. Inclusion criteria for the early manifest HD consisted of genetic confirmation with a CAG repeat ≥ 39 , and the presence of motor disturbances as measured by the Unified Huntington's Disease Rating Scale '99 (UHDRS) defined as a total motor score (TMS) > 5 and a Total Functional Capacity (TFC) ≥ 7 . All participants received a diagnostic confidence rating of 4, representing "motor abnormalities that are unequivocal signs of HD (>99% confidence)". Inclusion criteria for the premanifest HD participants consisted of genetic confirmation with a CAG repeat ≥ 39 , and the absence of motor disturbances on the UHDRS defined as a TMS ≤ 5 . Healthy gene negative family members or partner/spouses were recruited as control subjects in an effort to reduce influences of environmental factors. Exclusion criteria for all participants consisted of significant (neurological) comorbidity, a major psychiatric diagnosis, history of severe head injury or incompatibility for MRI. In total 44 subjects were recruited to undergo MRS in one or more regions of interest (ROI). Time constraints and HD related issues (such as patient motion) accounted for not all participants completing the MRS protocol in all five of the ROI's. The study was approved by the local Medical Ethical Committee of the Leiden University Medical Center. All participants provided written informed consent.

Clinical measures

Clinical evaluation for all subjects consisted of the UHDRS motor scale (score 0-124) and TFC, a global scale of impairment in daily life activities, score 0 -13. Furthermore, a short cognitive battery was administered, consisting of the Mini Mental State Exam (MMSE), Stroop test word reading card (Stoop-II), the Symbol

Digit Modality Test (SDMT), Trail making Test part B (TMT-B), the Wechsler Memory Scale (MQ) and premorbid IQ estimation using the Dutch Adult Reading Test (DART)²². Behavioural disturbances were evaluated with the Beck Depression Inventory 2nd version (BDI-II)²³ and the Problem Behaviour Assessment short version (PBA-s). Predicted years to onset were calculated from current age and CAG repeat length using the formula by Langbehn *et al.*(2004)²⁴.

MRI/MRS acquisition:

MRI and MRS were performed on a Philips 7-Tesla Achieva whole body scanner (Philips Healthcare, Best, The Netherlands) with a NOVA Medical quadrature transmit coil and 16 channel receive coil array. For accurate planning, a high resolution, three-dimensional T1-weighted GRE scan was acquired (TR/TE = 11/5.4 ms, voxel size 0.44 x 0.44 x 0.84 mm, total scan time 1:46). Localized proton spectra were acquired using a stimulated echo acquisition mode (STEAM) sequence. The voxel was placed within the region of interest with the maximum volume containing only tissue from the intended structure, minimizing the contribution from surrounding tissue, and also partial volume effects. Regions of interest consisted of the caudate nucleus, putamen, thalamus, hypothalamus and the prefrontal white and cortical grey matter. For the prefrontal voxel, positioning included approximately 50% white and 50% cortical grey matter. Only for the hypothalamus voxel was some cerebral spinal fluid (CSF) necessarily present since the voxel was placed bilaterally. For each voxel in each ROI a water reference signal was acquired for adequate quantification. The following scan parameters were used for the STEAM spectra: TR/TE/TM = 2000/19/25 ms, BW 4 kHz, 2048 complex data points and 128 signal averages, giving a data acquisition time of approximately 5 minutes per spectrum. The chemical shift artifact was minimal (<1 mm), which is shown in figure 1. Water suppression was performed using a frequency-selective RF pulse and gradient spoiling, six saturation bands were additionally applied to suppress signal from surrounding tissue. All scans included a reference scan without water suppression for quantification. When an MRS scan failed (for example due to motion) it was standard protocol to try the same ROI again: however, this did, in some cases, result in insufficient time for the full protocol to be completed since the time for each patient in the magnet was strictly limited to one hour.

MRS post-processing

MRS data were analyzed with LCModel^{25,26}, using the unsuppressed water as an internal reference to calculate the concentrations of metabolites. Concentrations of choline, creatine, glutamine+glutamate (Glx), total NAA

(N-acetylaspartateglutamate + NAA), myo-inositol and lactate were calculated for analysis.

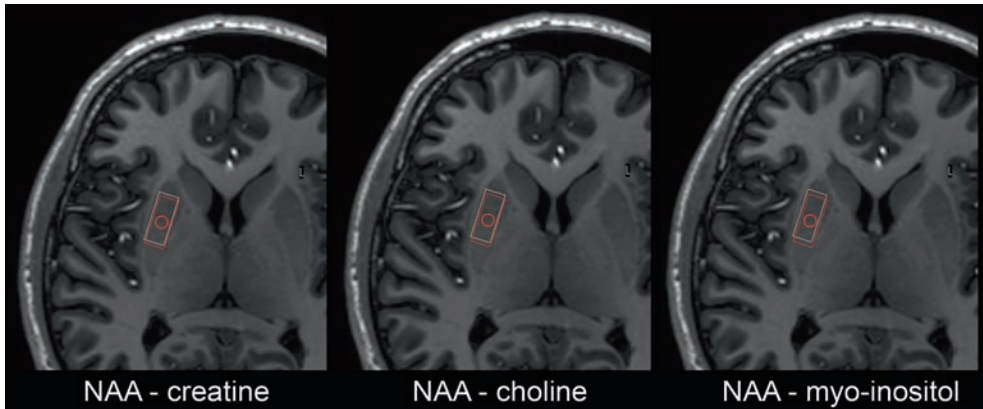


Figure 1. Example of chemical shifts at 7-Tesla using STEAM provided for an actual planning. Red box = NAA, white box = metabolite as stated below each figure. Only a minimal chemical shift exists. The chemical shift of water is almost zero, as the separate water file is planned according to the NAA-voxel. NAA= N-acetylaspartate

Stringent quality control was enforced to exclude data with high estimated errors. A signal to noise ratio of ≤ 3 and very high values of residual errors in the LCmodel fitting were applied as initial spectral exclusion criteria. Furthermore, the LCModel fit for metabolites were required to have a Cramér-Rao Lower Bound (CRLB) of 20% or less. This was required for all metabolites within a single spectrum, with the exception of lactate. For lactate CRLB above 100% were excluded from further analysis. If lactate was not quantified with CRLB $< 100\%$ in at least 50% of analyzed spectra, the analysis of lactate was deemed not detectable; this method was first presented by Tkac *et al.* (2009)²⁰. In total 30 spectra were included in the analysis for the hypothalamus, 36 of the thalamus, 28 of the caudate nucleus, 27 of the putamen and 32 subjects of the prefrontal region.

Statistics

Statistical analyses were performed using SPSS for Windows (SPSS version 17.0, SPSS inc, Chicago, IL). All clinical variables were assessed between groups with a one-way analysis of variance (ANOVA), with post-hoc testing. To compare all metabolites in the five brain regions between the manifest and premanifest HD group versus the control group, an ANOVA with planned comparisons was performed. The nature of this study is exploratory, and therefore in order to prevent inflation of type II errors and avoid important results going unreported, no correction for multiple testing was performed, as is accepted practice in such types

of study²⁷. To examine the relationship between metabolic concentrations and clinical measures in gene carriers (manifest and premanifest HD), partial Pearson correlation analysis corrected for age was performed.

Results

Demographics

No differences in age, education level or IQ were present between the manifest HD and control group, or between the premanifest HD and control group. No significant difference exists in CAG repeat length between the premanifest and the manifest HD group. For all other clinical assessments variables we refer to the results in table 1.

Voxel planning

Typical examples of localized proton spectra for the five examined regions, along with metabolite identification, are shown in figure 2. The voxel location is shown on the left side, for clarity the voxel is only shown in one orientation. Actual planning of the voxel required oblique planning in all three dimensions. Figure 3 provides a typical example spectrum and fit from the LCmodel.

Voxel sizes were individually set, based upon the different sizes of structures in different individuals, although the voxel size was never below 1.0 ml. With these sizes it was possible in all cases to include only the intended (grey matter) structure, without contamination of other (white matter) structures, the exception being the prefrontal region. The voxel size ranged from 1.0 ml in the caudate nucleus for a manifest HD participant to a maximum of 3.4 ml for the putamen of a participant in the control group.

Metabolite analysis

The concentrations of the six metabolites (NAA, creatine, choline, glutamate, lactate and myo-inositol) in the five brain regions are shown in table 2 for the three groups. In the caudate nucleus the manifest HD group demonstrated significantly lower NAA ($F = 8.12$, $p = 0.009$) and lower creatine concentration ($F = 13.60$, $p = 0.001$) compared to control subjects. In the putamen, manifest HD showed

Table 1: Demographic variables and scores on clinical assessments for the three groups.

	<i>Control</i> n: 18 (♂:9 ♀:9)		<i>Premanifest</i> n: 14 (♂:6 ♀:8)		<i>Manifest</i> n:12 (♂:5 ♀:7)	
	Mean	SD	Mean	SD	Mean	SD
Age	47.7	7.4	42.9	11.0	48.6	7.0
Years of education	15.9	3.2	14.3	3.3	15.3	2.7
IQ	106.7	7.8	102.2	12.5	102.3	9.5
CAG	20.3 ^c	2.9	43.1	3.4	43.7	2.3
Disease burden	n.a.	n.a.	306.4	87.0	385.4 ^e	72.5
Predicted YTO	n.a.	n.a.	10.4	8.2	n.a.	n.a.
UHDRS TMS	2.0	2.4	2.6	1.3	20.9 ^a	14.1
UHDRS TFC	12.9	0.2	12.6	0.6	11.3 ^a	1.9
PBA-s	5.9	1.4	5.0	1.3	13.2 ^a	3.8
BDI-II	3.9	4.6	5.2	5.5	6.4	6.1
MMSE	29.5	0.7	28.5	1.7	28.3 ^b	1.6
SDMT	59.2	8.9	48.5	10.8	37.3 ^d	6.7
TMT-B	46.7	15.1	67.8	27.8	101.4 ^a	51.2
Stroop II	104.0	15.4	95.1	19.4	79.3 ^b	19.9
MQ	127.3	11.5	115.5	23.2	99.7 ^b	13.2

SD = Standard Deviation. CAG = CAG repeat length of larger allele. Predicted YTO = predicted years to onset. UHDRS TMS = Unified Huntington's Disease Rating Scale Total Motor Score, PBA-s = Problem Behaviour Assessment short version, TFC = Total Functional Capacity, BDI-II = Beck Depression Inventory 2nd version, MMSE = Mini Mental State Exam, TMT = Trail Making Test part B, SDMT = Symbol Digit Modality Test, MQ = Memory Quotient, Stroop II = Stroop word reading card, n.a.=not applicable. a = significant differences between early HD compared to both premanifest and controls. b = significant differences between early HD and controls. c=significant differences between control and both premanifest and manifest HD. d=significant differences between all three groups. e=significant difference between premanifest and manifest HD

significantly lower NAA ($F = 5.81$, $p = 0.024$), lower creatine concentration ($F = 5.58$, $p = 0.027$) and glutamate/glutamine ($F = 7.21$, $p = 0.013$) compared to controls. No significant differences were found in the hypothalamus, thalamus or prefrontal region. Comparison of the premanifest gene carrier group and the control group did not show any significant differences in any of the regions. However, the absolute values of NAA, creatine and glutamate were lower in the caudate nucleus and putamen in the premanifest gene carrier group, but did not reach significance.

Table 2: Metabolite concentrations from five brain regions in HD

	Control			Premanifest			Manifest		
	N	Mean	SD	N	Mean	SD	N	Mean	SD
Hypothalamus	11			10			9		
Creatine		10.7	2.1		9.4	2.0		9.3	1.7
Choline		3.7	0.7		3.4	0.6		3.3	0.8
NAA		12.1	1.9		11.9	1.5		11.3	2.1
Glx		12.5	3.0		12.0	4.0		11.0	4.8
Myo-inositol		13.4	4.8		12.7	3.1		13.3	2.8
Lactate		1.5	1.0		1.1	1.1		1.0	1.4
Thalamus	14			13			9		
Creatine		12.7	3.5		12.8	3.6		12.1	1.6
Choline		3.1	0.8		3.0	0.7		3.1	0.4
NAA		17.8	6.0		15.8	2.6		15.9	1.6
Glu/Gln		14.8	5.1		15.1	3.4		12.8	3.4
Myo-inositol		8.5	4.1		7.3	2.6		9.5	4.4
Lactate		1.1	1.0		0.5	0.7		1.8	0.9
Caudate nucleus	12			11			5		
Creatine		12.5	1.7		11.7	2.2		8.9*	1.2
Choline		3.1	0.7		2.8	0.5		2.6	0.6
NAA		12.1	2.3		10.8	2.0		9.0**	1.1
Glx		15.4	5.2		13.3	5.7		10.8	1.6
Myo-inositol		6.2	1.4		7.1	2.0		7.9	2.0
Lactate		1.2	0.9		1.5	0.9		0.5	0.8
Putamen	13			9			5		
Creatine		13.6	2.3		12.1	2.2		10.9*	0.9
Choline		3.4	0.8		3.1	0.5		3.0	0.4
NAA		14.8	1.6		14.4	1.7		12.8*	0.9
Glx		16.3	3.4		14.2	3.4		11.4*	3.8
Myo-inositol		7.3	2.1		6.5	3.1		10.5	4.0
Lactate		0.8	0.6		1.0	1.3		0.3	0.4
Prefrontal	13			9			10		
Creatine		9.1	2.4		9.2	1.6		9.9	2.1
Choline		2.3	0.5		2.4	0.4		2.3	0.5
NAA		11.7	2.4		11.6	1.5		11.9	3.0
Glx		11.3	2.8		9.8	2.2		13.3	4.0
Myo-inositol		9.5	2.4		8.8	1.9		11.9	4.9
Lactate		1.2	1.1		1.5	1.5		0.8	0.9

Concentrations of metabolites in the three groups. Since the water concentration and the T1 and T2 relaxation times of the individual metabolites in the specific voxels of interest are unknown at the field strength of 7 Tesla, data are expressed as relative values to the water peak in arbitrary units (AU). NAA = N-acetylaspartate, Glx = glutamate + glutamine, * $p < 0.05$, ** $p < 0.005$

Relationship to clinical measures

The association of metabolite levels with clinical measures is shown in table 3. TFC was associated with creatine levels in caudate nucleus and putamen and with NAA in the putamen, showing decreased metabolite levels corresponding to poorer clinical scores. The NAA concentration in the putamen was associated with higher scores on the UHDRS TMS, indicating lower NAA to correspond to more motor disturbances. Lower glutamate/glutamine related to poorer scores on the cognitive tests SDMT and TMT. Finally, a higher PBA score, indicating more behavioural disturbances, corresponded to lower creatine in the caudate nucleus.

Table 3: Relationship of the clinical measures with metabolite concentration in the caudate nucleus and putamen

		Caudate nucleus		Putamen		
		Creatine	NAA	Creatine	NAA	Glx
Disease burden	R	-0.266	-0.473	0.168	0.284	-0.400
	p	0.339	0.075	0.584	0.347	0.157
UHDRS TMS	R	-0.280	-0.228	-0.324	-0.415	-0.255
	p	0.157	0.253	0.106	0.035*	0.200
PBA-s	R	-0.545	-0.207	-0.063	0.064	0.052
	p	0.003*	0.300	0.758	0.754	0.797
TFC	R	0.409	0.106	0.440	0.556	0.095
	p	0.034*	0.598	0.025*	0.003*	0.636
BDI-II	R	-0.256	-0.022	0.005	0.206	0.152
	p	0.197	0.914	0.983	0.323	0.457
MMSE	R	-0.196	-0.106	-0.070	-0.108	-0.223
	p	0.328	0.598	0.735	0.601	0.265
TMT-B	R	0.310	0.270	0.185	0.049	0.438
	p	0.115	0.173	0.366	0.813	0.022*
SDMT	R	0.171	0.133	0.239	0.125	0.555
	p	0.404	0.518	0.250	0.552	0.003*
MQ	R	0.151	0.078	-0.049	-0.013	0.326
	p	0.451	0.700	0.811	0.951	0.097
Stroop II	R	-0.196	-0.106	-0.070	-0.108	-0.223
	p	0.328	0.598	0.735	0.601	0.265

Correlation analysis of metabolite concentration with clinical measures. UHDRS TMS = Unified Huntington's Disease Rating Scale Total Motor Score, PBA-s = Problem Behaviour Assessment short version, TFC = Total Functional Capacity, BDI-II = Beck Depression Inventory 2nd version, MMSE = Mini Mental State Exam, TMT = Trail Making Test part B, SDMT = Symbol Digit Modality Test, MQ = Memory Quotient, Stroop II = Stroop word reading card, R = partial r correlation coefficient. * $p < 0.05$

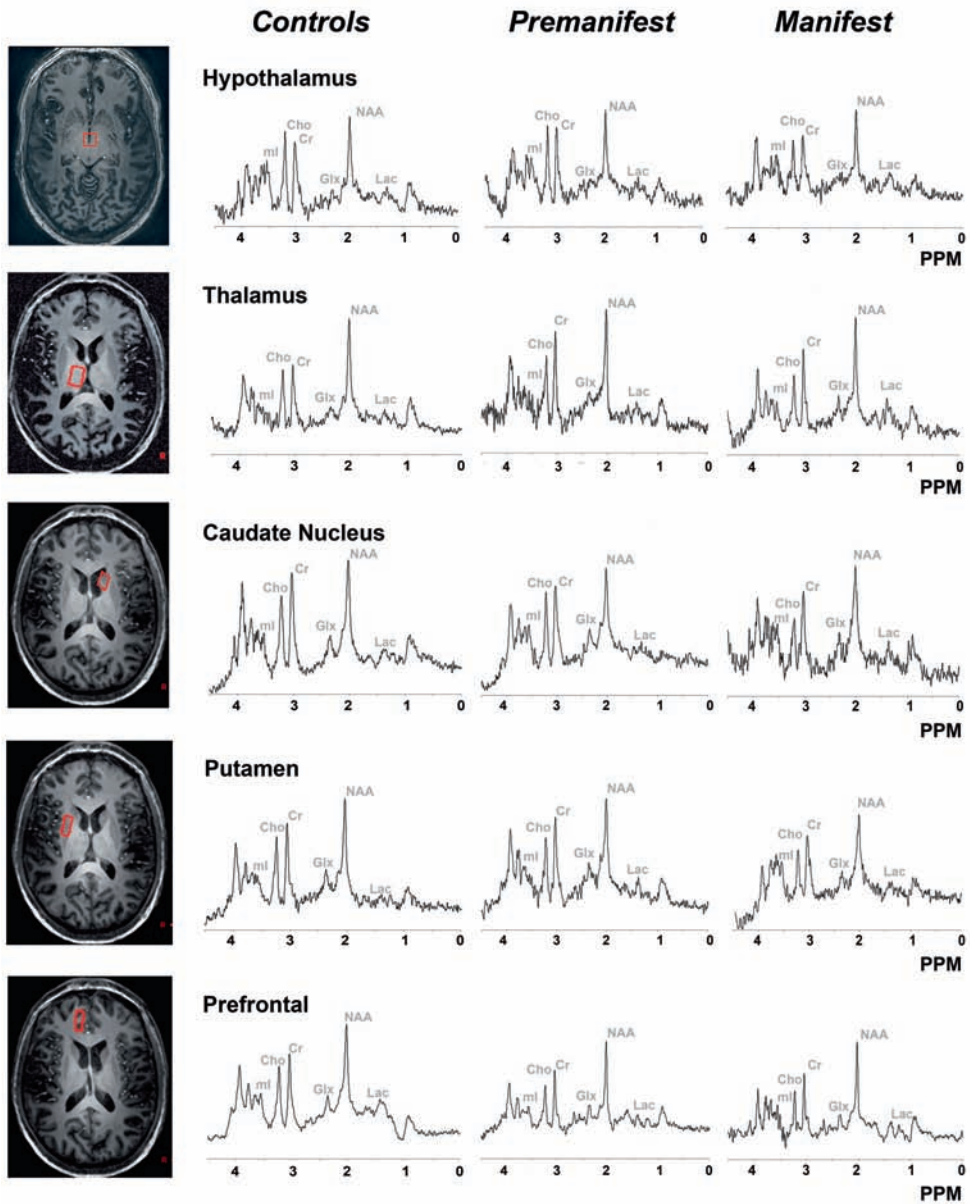


Figure 2: Localized proton MR spectra from different regions of the brain. On the left side the voxel is displayed in the transverse direction, a typical spectrum of that structure is shown on the right side for the three groups. Five different regions are displayed: hypothalamus, thalamus, caudate nucleus, putamen, prefrontal region. Cho=choline, Cr=creatine, NAA=N-acetylaspartate, ml=myo-inositol, Glx=glutamate+glutamine, Lac=lactate, PPM=parts per million. A Gaussian filter of 4 Hz was applied.

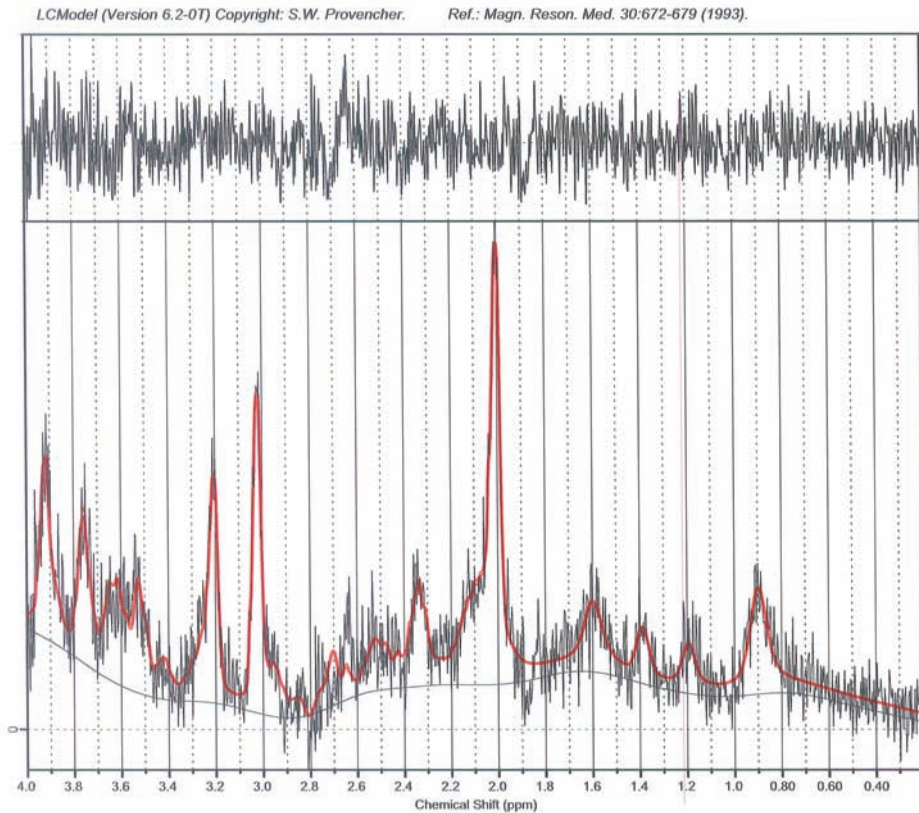


Figure 3: LCModel output example. The black line is the raw spectrum, the red line is the fit by LCModel. PPM = parts per million

Discussion

The major findings of this study are lower concentrations of creatine and NAA in the caudate nucleus and the putamen, and a reduction of glutamate in the putamen in manifest HD. A relationship between differences in these metabolic levels and clinical measures of disease severity, especially global functioning, was demonstrated. No statistically significant differences in any metabolite concentration were observed when the premanifest group was compared to controls, although the absolute lower values could indicate a subtle decline.

As creatine is considered an important marker for brain energy metabolism²⁸, the finding of lower creatine levels suggests impaired energy metabolism in manifest HD. In the healthy population, the concentration of creatine in the brain is considered to be fairly stable, however, specific pathology has been shown to influence creatine concentrations²⁸. The finding of lower creatine in putamen and

caudate nucleus is supported by findings of Sanchez *et al.* (1999), who observed a reduction of both creatine and NAA in the striatum¹⁰. Reynolds *et al.* (2005) went on to propose creatine as a possible biomarker, when they demonstrated lower levels in the caudate nucleus in premanifest HD¹⁸. Contrary to our findings, Reynolds *et al.* (2005) did not report altered creatine levels in the putamen. Results from the TRACK-HD study reported by Sturrock *et al.* (2010) show similar lower values of creatine in the putamen as our study²⁹. Jenkins *et al.* (1998) found additional evidence for impaired energy metabolism as displayed by elevated lactate levels in HD within the occipital cortex^{11;12}. However, our study did not show elevated lactate in any of the examined structures. This finding can possibly be explained by the fact that Jenkins *et al.* (1993) used a more severely affected HD population with a lower mean TFC score of 7.3¹¹. Moreover, the region analyzed by Jenkins *et al.* (1993, 1998)^{11;12} did not consist of the basal ganglia, but of the occipital cortex, which is a very metabolically active area of the cortex and is also severely atrophied in HD³⁰. Although, these studies are not completely comparable on the basis of methodology and results, they do all point towards the importance of assessment of metabolic changes and specifically the energy metabolism markers such as creatine.

NAA is a marker for the integrity of neurons and axons²⁸ and lower NAA levels suggest a decrease in neuronal integrity. As atrophy of numerous brain structures is apparent in manifest HD, it is likely that neurons are affected and decrease in NAA may occur. This hypothesis was previously confirmed within the striatum^{10;11;17}. Again the recent report from Sturrock *et al.* (2010) is similar to our findings of lower NAA in the putamen²⁹. Our study confirms the finding of decreased NAA in the striatum (caudate nucleus plus putamen), and more importantly, our data show that neuronal damage may be present in both the caudate nucleus and putamen separately. The ability to acquire spectra from relatively small voxels is an important advantage of higher magnetic fields in localized MR spectroscopy.

Glutamate is of interest in light of the excitotoxicity theory which states that an overstimulation of neurons causes cell damage and eventually cell death. In neurons this can occur either due to increased levels of glutamate (and/or its precursor glutamine) or due to an increase in sensitivity of the glutamate receptors, both resulting in the same effect^{7;8}. Taylor *et al.* (1994, 1996) described increased levels of glutamate, supporting this theory^{14;15}. However, the glutamate levels in these studies were expressed as a ratio to creatine, and could also be influenced by changes of the creatine level. Our study demonstrates reduced glutamate levels in the putamen. An explanation may be that the number of viable neurons is decreased to an extent where glutamate is lowered along with the neuron count.

Also, the sensitivity of glutamate receptors could be altered, resulting in altered levels of glutamate. However, without further investigation these propositions are highly speculative.

In the premanifest HD group no changes in any of the examined metabolites levels could be demonstrated. This was an unexpected finding, as previous studies have reported structural abnormalities, e.g. atrophy, at this stage^{1,31,32} and some reports exist of lowered levels of metabolites in premanifest HD gene carriers^{10,18}. Sanchez-Pernaute *et al.* (1999) did report lower NAA and lower creatine in the striatum in 4 premanifest gene carriers; however the article already stated that there were soft motor signs present in two out of four in this group¹⁰. Reynolds *et al.* (2005) reported on lower values of creatine and NAA, yet he concluded that there was no pathognomonic profile in metabolite changes, but stated that there was great heterogeneity in this respect¹⁸. Nonetheless, we did hypothesize that premanifest HD would show altered levels of metabolites as atrophy (which is already present more than a decade before disease onset^{3,30-32} is logically the result of underlying processes. We must therefore conclude that either we cannot (yet) measure these changes or the processes involved are more complex than simple linear correlation between metabolite levels and disease severity. For instance the excitotoxicity theory can possibly be a process measured by increased (damaging effects) or decreased (loss of healthy neurons) levels of glutamate depending on the individual disease stage. When performing group analysis, these measurements can become diluted. Individual assessment of longitudinal changes could shed more light on these changes. An explanation as to why no significant differences in our premanifest population were found, may be that our premanifest group was too heterogeneous in terms of proximity to disease onset. When taking into consideration the 'disease burden score', a proven correlate of striatal damage and thereby proximity to onset³³, a range of 121.5 to 450.5 exists within our premanifest HD sample. This large range suggests a great deal of variability in striatal damage and therefore of possible metabolite differences. Even so, despite this large range in disease burden score, a decline in absolute values of NAA and creatine was observed in the premanifest group, although this did not reach statistical significance. A second explanation could be our very stringent inclusion criteria. Only premanifest participants were included when there was no evidence of motor symptoms, as quantified by an UHDRS motor score of 5 or less, whereas other studies may have allowed participation of premanifest gene carriers with a higher degree of clinical abnormalities.

Our data show that metabolite levels are associated with clinical measures of disease severity. This finding highlights the feasibility of MRS in clinical trials, whereby metabolite levels could be target outcome measures. Endeavours using creatine as a treatment for HD with MRS as a monitoring tool have demonstrated the feasibility of this method³⁴.

This study shows the clinical application of high field 7-Tesla MRI. The spectral resolution in combination with small voxel size and total scanning time is a clear improvement in MRS methodology^{21;35}. This allows the examination of metabolites in small, well defined anatomical structures, such as the caudate nucleus and putamen for HD, and can be used in the examination of many other disorders where spectral and spatial resolution is of great importance.

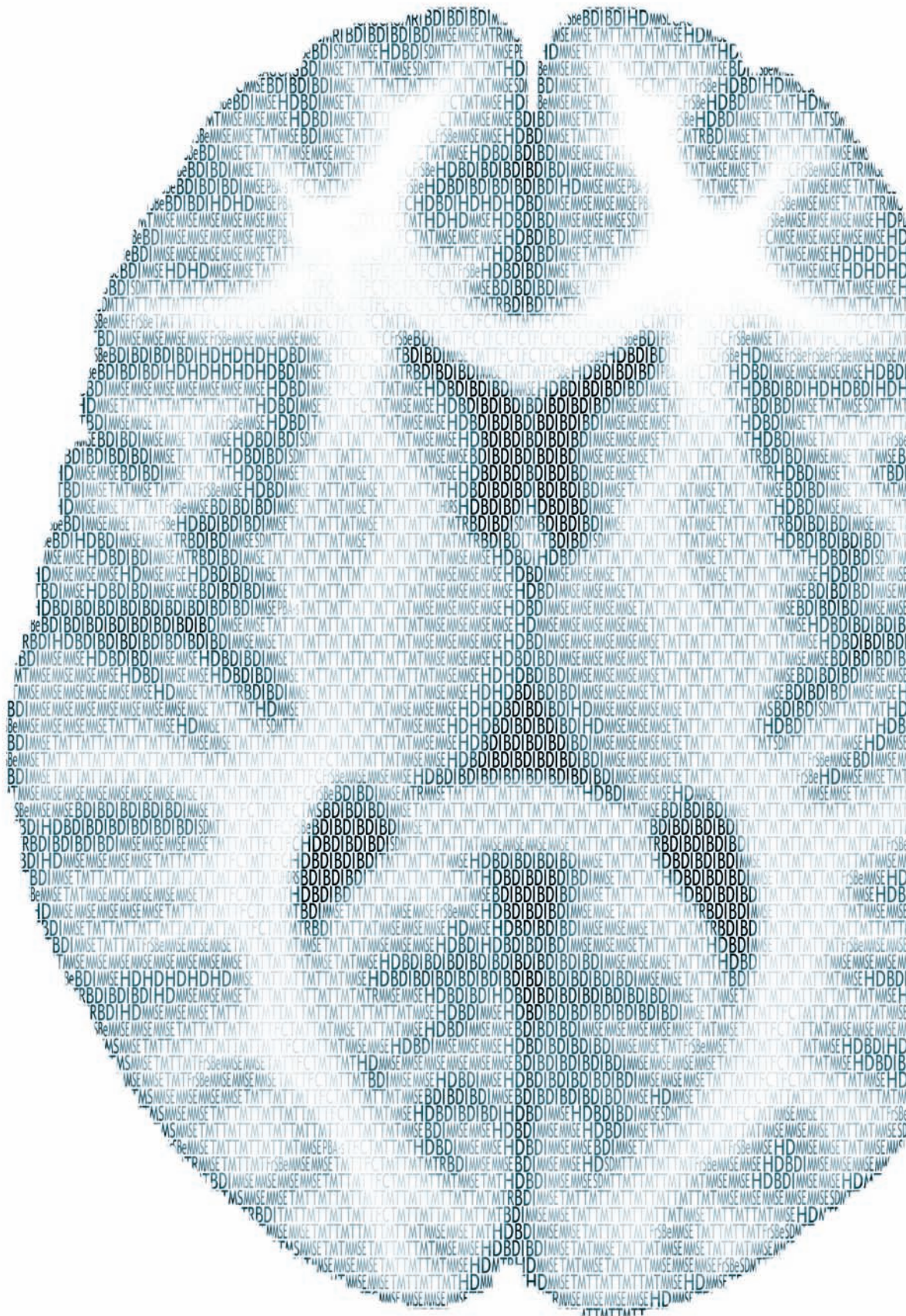
A limitation of our study was the fact that the premanifest group was not uniformly distributed according to expected disease onset, which may have lead to a relatively large spread of the metabolite concentrations. A more homogeneous group close to onset could possibly reveal more significant results already in the premanifest stage of the disease. Also the small number of participants included in the manifest groups could be seen as a limitation. However, despite the small amount of participants the results were still significant. Furthermore, the hypothalamus region (bilaterally) included some CSF in the voxel, especially in the manifest HD group, as a result of atrophy, which could account for less reliable measurements. This was not a problem for any of the other regions. Finally, the frontal region consisted of approximately 50 % of both grey and white matter, which could lead to false negative findings if grey or white matter would be unequally affected.

In conclusion, in manifest HD, lower NAA and creatine were found in the caudate nucleus and putamen, supporting the theory of impaired energy metabolism as part of the pathophysiology of Huntington's disease. Glutamate levels were lowered in the putamen, however to which extent this finding supports the excitotoxicity theory remains unclear. The relationship with clinical measures of function makes MRS a potential disease monitor and could also possibly be used to evaluate therapeutics targeted at metabolic processes in HD.

References

1. Bohanna I, Georgiou-Karistianis N, Hannan AJ, et al. Magnetic resonance imaging as an approach towards identifying neuropathological biomarkers for Huntington's disease. *Brain Res Rev* 2008;
2. Roos RAC. Neuropathology of Huntington's chorea. Vinken, P. J., Bruyn, G. W, and Klawans, H. L. *Handbook of Clinical Neurology; Extrapyramidal Disorders*. 5. 1986. Elsevier Science Publishers.
3. Aylward EH, Sparks BF, Field KM, et al. Onset and rate of striatal atrophy in preclinical Huntington disease. *Neurology* 2004;63:66-72
4. Aylward EH, Anderson NB, Bylsma FW, et al. Frontal lobe volume in patients with Huntington's disease. *Neurology* 1998;50:252-58
5. Politis M, Pavese N, Tai YF, et al. Hypothalamic involvement in Huntington's disease: an in vivo PET study. *Brain* 2008;131:2860-69
6. Aziz NA, Pijl H, Frolich M, et al. Increased hypothalamic-pituitary-adrenal axis activity in Huntington's disease. *J Clin Endocrinol Metab* 2009;94:1223-28
7. Roze E, Saudou F, Caboche J. Pathophysiology of Huntington's disease: from huntingtin functions to potential treatments. *Curr Opin Neurol* 2008;21:497-503
8. Estrada Sanchez AM, Mejia-Toiber J, Massieu L. Excitotoxic neuronal death and the pathogenesis of Huntington's disease. *Arch Med Res* 2008;39:265-76
9. Dunlop DS, Mc Hale DM, Lajtha A. Decreased brain N-acetylaspartate in Huntington's disease. *Brain Res* 1992;580:44-48
10. Sanchez-Pernaute R, Garcia-Segura JM, del Barrio AA, et al. Clinical correlation of striatal 1H MRS changes in Huntington's disease. *Neurology* 1999;53:806-12
11. Jenkins BG, Koroshetz WJ, Beal MF, et al. Evidence for impairment of energy metabolism in vivo in Huntington's disease using localized 1H NMR spectroscopy. *Neurology* 1993;43:2689-95
12. Jenkins BG, Rosas HD, Chen YC, et al. 1H NMR spectroscopy studies of Huntington's disease: correlations with CAG repeat numbers. *Neurology* 1998;50:1357-65
13. Ruocco HH, Lopes-Cendes I, Li LM, et al. Evidence of thalamic dysfunction in Huntington disease by proton magnetic resonance spectroscopy. *Mov Disord* 2007;22:2052-56
14. Taylor-Robinson SD, Weeks RA, Sargentoni J, et al. Evidence for glutamate excitotoxicity in Huntington's disease with proton magnetic resonance spectroscopy. *Lancet* 1994;343:1170
15. Taylor-Robinson SD, Weeks RA, Bryant DJ, et al. Proton magnetic resonance spectroscopy in Huntington's disease: evidence in favour of the glutamate excitotoxic theory. *Mov Disord* 1996;11:167-73
16. Gomez-Anson B, Alegret M, Munoz E, et al. Decreased frontal choline and neuropsychological performance in preclinical Huntington disease. *Neurology* 2007;68:906-10
17. Clarke CE, Lowry M, Quarrell OWJ. No change in striatal glutamate in Huntington's disease measured by proton magnetic resonance spectroscopy. *Parkinsonism and Related Disorders* 1998; 4(3) 123-127
18. Reynolds NC, Jr., Prost RW, Mark LP. Heterogeneity in 1H-MRS profiles of presymptomatic and early manifest Huntington's disease. *Brain Res* 2005;1031:82-89
19. van Oostrom JC, Sijens PE, Roos RA, et al. 1H magnetic resonance spectroscopy in preclinical Huntington disease. *Brain Res* 2007;1168:67-71
20. Tkac I, Oz G, Adriany G, et al. In vivo 1H NMR spectroscopy of the human brain at high magnetic fields: metabolite quantification at 4T vs. 7T. *Magn Reson Med* 2009;62:868-79
21. Mekle R, Mlynarik V, Gambarota G, et al. MR spectroscopy of the human brain with enhanced signal intensity at ultrashort echo times on a clinical platform at 3T and 7T. *Magn Reson Med* 2009;61:1279-85
22. Schmand B, Bakker D, Saan R, et al. [The Dutch Reading Test for Adults: a measure of premorbid intelligence level]. *Tijdschr Gerontol Geriatr* 1991;22:15-19
23. Beck AT, Steer RA, Brown GK. BDI-II, Beck depression inventory: manual. 1996.

24. Langbehn DR, Brinkman RR, Falush D, et al. A new model for prediction of the age of onset and penetrance for Huntington's disease based on CAG length. *Clin Genet* 2004;65:267-77
25. Provencher SW. Estimation of metabolite concentrations from localized in vivo proton NMR spectra. *Magn Reson Med* 1993;30:672-79
26. Provencher SW. Automatic quantitation of localized in vivo ¹H spectra with LCModel. *NMR Biomed* 2001;14:260-64
27. Perneger TV. What's wrong with Bonferroni adjustments. *BMJ* 1998;316:1236-38
28. Gujar SK, Maheshwari S, Bjorkman-Burtscher I, et al. Magnetic resonance spectroscopy. *J Neuroophthalmol* 2005;25:217-26
29. Sturrock A, Laule C, Decolongon J, et al. Magnetic resonance spectroscopy biomarkers in premanifest and early Huntington disease. *Neurology* 2010;75(19):1702-10
30. Tabrizi SJ, Langbehn DR, Leavitt BR, et al. Biological and clinical manifestations of Huntington's disease in the longitudinal TRACK-HD study: cross-sectional analysis of baseline data. *Lancet Neurol*. 2009 Sep;8(9):791-801
31. van den Bogaard SJ, Dumas EM, Acharya TP, et al. Early atrophy of pallidum and accumbens nucleus in Huntington's disease. *J Neurol*. 2011 Mar;258(3):412-20.
32. Paulsen JS, Langbehn DR, Stout JC, et al. Detection of Huntington's disease decades before diagnosis: The Predict HD study. *J Neurol Neurosurg Psychiatry*. 2008 Aug;79(8):874-80
33. Penney JB, Jr., Vonsattel JP, MacDonald ME, et al. CAG repeat number governs the development rate of pathology in Huntington's disease. *Ann Neurol* 1997;41:689-92
34. Tabrizi SJ, Blamire AM, Manners DN, et al. Creatine therapy for Huntington's disease: clinical and MRS findings in a 1-year pilot study. *Neurology* 2003;61:141-42
35. Tkac I, Oz G, Adriany G, et al. In vivo ¹H NMR spectroscopy of the human brain at high magnetic fields: metabolite quantification at 4T vs. 7T. *Magn Reson Med* 2009;62:868-79



Abstract

Background and Purpose

Magnetization transfer imaging (MTI) is a quantitative MRI technique which has recently demonstrated structural integrity differences between controls and Huntington's disease (HD) patients. Potentially MTI can be used as a biomarker for monitoring disease progression. To establish the value of MTI as a biomarker, we aimed to examine the change of these measures during the course of HD.

Method

From the Leiden TRACK-HD study 25 controls, 21 premanifest gene carriers and 21 manifest HD patients, participated at baseline and during a 2 year follow up visit. Brain segmentation of cortical grey matter, white matter, caudate nucleus, putamen, pallidum, thalamus, amygdala, and hippocampus was performed using FSL's automated tools FAST and FIRST. Individual MTR values were calculated from these regions and MTR histograms constructed.

Results

In the premanifest HD group stage "far from disease onset" a significant *increase* in MTR peak height of the putamen was observed over time. During the manifest HD stage neither the mean MTR nor the MTR peak height showed a significant change during a 2 year follow up.

Conclusion

MTI derived measures are not suitable for disease monitoring in Huntington's disease over a 2 year period as there is no decrease in structural integrity detected in any of the manifest HD groups longitudinally. The finding of increased putaminal MTR peak height in the premanifest "far from disease onset" group could relate to a pre-degenerative process, compensatory mechanisms or aberrant development, but should be interpreted with caution until future studies confirm this finding.

Introduction

Magnetization transfer imaging (MTI) is a MRI technique which has been developed to perform structural imaging in a different, possibly more sensitive way, as it has demonstrated abnormalities in the normal appearing grey and white matter on conventional MRI in MS research^{1,2}. The technique of MTI is based on the exchange of two pools of protons: one bound to macromolecular structures and one bound to free water molecules³. MTI has first and foremost been applied in patients with MS, however many other diseases have been studied using MTI, such as Alzheimer's disease⁴, Parkinson's disease⁵ and Huntington's disease (HD)^{6,7}.

Previous MRI studies in HD mainly focused on the search for a biomarker for monitoring disease progression. In this field lays a great opportunity to study the potential of MTI at very early stages of neurodegeneration. The genetic defect which is responsible for HD is located on the short arm of chromosome 4 and has an autosomal dominant inheritance pattern with full penetrance⁸. Therefore when the gene defect has been established in an individual, this inevitably leads to a certain clinical diagnosis at some point in their life. Mean disease onset is approximately 35-40 years of age with a wide range partly depended on the length of the abnormal CAG-repeat⁹. The ability to establish the gene defect well before any symptoms are present, gives an unique opportunity to study asymptomatic gene carriers, commonly referred to as "premanifest gene carriers"(PMGC). In previous structural MRI studies significant brain disturbances in terms of striatal atrophy^{10,11}, white matter disturbances^{12,13}, cortical thickness reductions¹⁴ and whole brain volume reduction^{10,15} have been described. These studies all used either conventional MRI or DTI. Some of these measures are well established, however no golden standard for disease monitoring by MRI is currently present. In essence, what technique and what region are most suitable as a biomarker? Possible problems in HD are non-linear and non-uniformly affected brain regions. The need for further research into a robust and sensitive MRI measure to monitor disease onset and progression is still evident.

Previous work in HD using MTI consists of four reports, all cross-sectional in design^{6,7,16,17}. The main outcome measures used were mean Magnetization Transfer Ratio (MTR) and MTR peak height and are thought to represent structural integrity¹⁷⁻¹⁹. Mean MTR represents the average MTR value of all voxels in a region of interest, with a lower mean MTR corresponding to loss of tissue integrity. MTR peak height reflects the most frequently occurring MTR value in a region of interest when all the MTR values are set out in a MTR histogram, again with

lower peak height being associated with loss of structural integrity. Results from these previous studies show reduced structural integrity in manifest HD patients (MHD) compared to healthy controls or PMGC in multiple regions, namely the white matter, cortical grey matter, caudate nucleus, putamen, pallidum, thalamus and amygdala. The results are suggestive of the potential of MTI as a biomarker^{6,7}. However no longitudinal reports are available.

TRACK-HD is specifically designed to determine the most valuable measures to monitor disease progression²⁰. This study allows following both PMGC as MHD over several years. To determine the true value of any potential (MRI) biomarker, longitudinal confirmation is crucial. Therefore we aim to examine whether MTI measures change over a 2 year period during the progressive course of HD. Secondly, if any longitudinal change in a group is present, we sought to determine the correlation to clinical measures of disease progression.

Methods

Subjects

Participants were recruited from the Leiden site of the TRACK-HD study. From the baseline cohort (n=90) in 2008 a total of 78 participants could be included. This cohort consisted of three groups; 28 healthy controls, 25 PMGC and 25 MHD. Inclusion criteria for the PMGC consisted of genetically confirmed expanded CAG repeat ≥ 40 , a disease burden score (calculated as: $((\text{CAG repeat length} - 35.5) \times \text{Age})$ of >250 ²¹ and absence of motor abnormalities on the UHDRS, defined as a TMS of ≤ 5 . Inclusion criteria for MHD consisted of genetically confirmed CAG repeat ≥ 40 , presence of motor abnormalities on the UHDRS-TMS of >5 . Also a TFC of 7 or higher was required to ensure that the MHD group was in the early disease stage. Subdivision of the premanifest group was made on the basis of their expected years to onset, calculated by the formula from Langbehn *et al.* (2004)⁹. This results in a premanifest HD group “far from expected disease onset” (PreHD-A) and premanifest HD group “close to expected disease onset” (PreHD-B). Subdivision of the manifest group was made by their staging according to the Shoulson and Fahn Scale, based on the TFC score, resulting in a manifest HD group stage 1 (HD 1) and manifest group stage 2 (HD 2). HD 1 describes a group of manifest HD in the earliest stage after disease onset, with only minor symptoms. HD 2 is the next stage in the disease with increased symptoms and impact on daily activities, but these patients are still considered “early manifest”. Healthy gene negative family members, spouses or partners were recruited as control subjects. Exclusion criteria consisted of significant (neurological) co-

morbidity, active major psychiatric disturbance and MRI incompatibility. Full details on recruitment are available in the TRACK-HD baseline paper¹⁰. Local IRB approval and written informed consent were obtained from all participants.

The same cohort was scanned 24 months later within a 6 week window of their follow up date. Of the 78 participants, 67 participants were available for follow up scanning in 2010 with the MTI-protocol included. Reasons for unavailability included too advanced disease stage, time restraints on the full TRACK-HD scanning protocol and unspecified reasons of withdrawal.

Imaging sequences

At both time points exactly the same study protocol was enforced. The scanning protocol described in our cross-sectional report⁶ was performed in an identical manner two years after the baseline visit. In short all participants underwent scanning on a 3 Tesla Philips whole body scanner (Philips, Best, The Netherlands) with an 8-channel receive and transmit coil. 3D T1-weighted sequences (TR = 7.7ms, TE= 3.5ms, FA= 8°, matrix size 224x224x164 mm, voxel size 1.0x1.0x1.0mm, acquisition time ~9min) and 3D gradient MTI sequences (TR = 100 ms, TE = 11 ms, FA = 9°, matrix 224x180x144 mm, voxel size 1.0x1.0x7.2 mm, acquisition time ~3min) were acquired. For the MTI sequences two consecutive imaging sets were acquired, one with and one without a saturation pulse. A sinc pulse of 25 ms with a maximal B1 of 10 uT and 2 sidelobes on an off-resonance frequency of 1100 Hz was applied. Total scanning time for T1-w and MTI sequences was maximally 12 minutes.

Post-processing

The post-processing pipeline was identical to that described previously in the cross sectional result paper⁶. T1-weighted images were segmented using FAST²² and FIRST²³ from FMRIB's Software Library (Oxford, United Kingdom)²⁴. This provided individual brain masks for: total white matter, cortical grey matter, caudate nucleus, putamen, pallidum, thalamus, amygdala, hippocampus and whole brain. To correct for possible partial volume effects, an eroded mask of these segmentations was created by removing one voxel in plane for all above named VOI's. All brain masks were then registered to the MTI volumes using the transform obtained from linear registration of the T1-w volume with 7 degrees of freedom (FSL-FLIRT). MTR was calculated per voxel as $M0 - Ms / M0$, whereby Ms is the saturated image and M0 the unsaturated image. The mean MTR per VOI was calculated. Additionally, to represent the variations of voxel based MTR within each VOI we constructed MTR histograms. The MTR peak height was normalized for the size of the volume

of interest. MTR peak height and mean MTR were the primary outcome variables. For correction of the (largely unknown) influence of age on MTI values, the MTR parameters were calibrated to the control values, assuming no changes in the control subjects. This entailed scaling the individual premanifest and manifests values according to the mean MTR parameter difference between baseline and follow up of the control group, which could either be an increase or a decrease over time. In the supplementary materials (table 3) actual values of the control group on both time points are available.

To compare the biomarker potential of MTI to volumetric analysis, volumes were calculated for all subcortical regions, white matter volume and whole brain volume using the FSL tools of FIRST²³ and SIENAX²⁵. The volume calculation and a correction for intracranial volume was performed as described previously¹¹.

Clinical Measures

A total measure of motor dysfunction was obtained with the UHDRS-TMS (range 0-124). TFC score (range: 0-13) and MMSE for global assessment of cognitive functioning (range: 0-30) were obtained. Cognitive scores included the total scores from the SDMT and the Stroop word reading card. For assessment of psychiatric disturbances the PBA-s was used. For a more detailed description of these clinical assessments see Tabrizi *et al.* (2009)¹⁰.

Statistics

To examine the longitudinal change in clinical, MTI and volumetric values (corrected for intracranial volumes) per group, paired T-testing per group was used. Alpha was set to 0.05 to be significant. Secondly, to account for multiple testing (15 regions) a Bonferroni correction was applied, resulting in an alpha < 0.0033 for the strongest findings. For correlation analysis between significant longitudinal findings, a Pearson correlation was applied to the difference between the 2 time points of the clinical and MTI values.

Results

Group characteristics and clinical measures on both the baseline visit as the follow up visit are shown in table 1. A significant longitudinal increase in motor disturbances is evident in PreHD-B, HD 1 and HD 2. Global functioning as measured by the TFC significantly decreases in 2 years in the HD 2 group as does the cognitive measure of Stroop word reading.

Table 1: Group characteristics for controls, premanifest HD groups A +B and Manifest HD groups 1 and 2.

		Controls	PreHD-A	PreHD-B	Manifest 1	Manifest 2
N		25	10	11	9	12
Age	baseline	48.3 (7.6)	45.5 (5.2)	42.9 (11.2)	47.7 (11.8)	50.9 (9.4)
CAG	baseline	n.a.	41.3 (1.3)	44.0 (3.1)	43.8 (3.5)	43.2 (1.9)
YTO	baseline	n.a.	13.8 (3.8)	8.4 (1.6)	n.a.	n.a.
TMS	baseline	2.4 (2.4)	2.3 (1.7)	3.0 (1.1)	16.9 (8.8)	26.2 (11.7)
	follow up	1.7 (1.4)	6.0 (6.9)	6.3 (2.5) *	23.0 (9.0) *	37.8 (14.3) *
TFC	baseline	12.9 (0.2)	12.7 (0.7)	12.6 (0.9)	12.0 (1.0)	8.6 (1.2)
	follow up	12.8 ()	12.5 (0.9)	12.4 (1.2)	11.2 (2.0)	6.0 (3.3) *
MMSE	baseline	29.2 (1.2)	29.0 (1.2)	28.4 (1.9)	29.0 (0.9)	26.5 (3.1)
	follow up	29.1 (1.2)	29.3 (0.8)	28.6 (1.7)	28.7 (1.1)	27.0 (3.9)
SDMT	baseline	50.1 (9.6)	52.7 (7.4)	46.9 (12.0)	42.0 (8.1)	31.2 (11.1)
	follow up	51.5 (10.8)	52.7 (9.5)	48.3 (9.9)	39.6 (10.7)	27.9 (13.3)
Stroop	baseline	99.8 (13.4)	97.1 (10.5)	86.9 (16.3)	88.4 (13.6)	69.4 (21.5)
	follow up	102.7 (16.9)	92.5 (7.5)	83.4 (19.3)	89.8 (18.9)	55.6 (22.6) *
PBA-s	baseline	6.4 (8.4)	6.7 (8.7)	7.4 (7.1)	11.7 (11.7)	14.0 (11.8)
	follow up	6.6 (9.0)	6.1 (11.9)	7.8 (9.70)	9.7 (11.7)	22.6 (16.3)

Values are Mean (SD). PreHD-A = premanifest HD far from expected disease onset, PreHD-B premanifest HD close to expected disease onset, CAG = CAG-repeat length, YTO = expected years to disease onset, TMS = total motor score, TFC = total functional capacity, MMSE = mini mental state exam, SDMT = symbol digit modality test, Stroop = stroop word reading test, PBA = problem behaviour assessment - short version.* = $p < 0.005$ significant longitudinal change

All MTI-values for 15 VOI's are displayed in the supplementary material table 1 for the premanifest HD groups and in supplementary material table 2 for the Manifest HD groups. In PreHD-A five subcortical grey matter regions show an *increase* in MTI parameters, namely the mean MTR of the right caudate nucleus ($p=0.049$), the MTR peak height of the right putamen($p=0.003$), MTR peak height of the left pallidum ($p=0.032$), mean MTR of the right thalamus ($p=0.047$) and MTR peak height of the right amygdala ($p=0.050$). However, after Bonferroni correction, the only statistically significant variation was the MTR peak height of the right putamen. In the PreHD-B group the cortical grey matter shows a longitudinal reduction in mean MTR ($p=0.020$) and the left hippocampus an increase in MTR histogram peak height ($p=0.037$). For the HD 1 group the right amygdala mean MTR decreases ($p=0.036$) in the 2 year follow up period. Only the left amygdala

mean MTR shows a reduction ($p=0.022$) in the HD 2 group. None of the results in the PreHD-B, HD 1 or HD 2 group are statistically significant after correction for multiple comparisons.

The statistical analysis procedure was also applied to a 3 group division instead of the 5 group division, encompassing the total premanifest group (PreHD A + B) and the total manifest group (HD 1 + 2) and the control group. This was performed in order to increase the power of the study, however in essence no additional information can be gathered from this analysis. The supplementary material contains exact details of the findings. The results also display subcortical MTR parameter increases in the premanifest group and a decrease in MTR parameters of the amygdala in the manifest HD group. The subdivision of groups is therefore more informative as it gives more exact disease stage related changes.

Correlation analysis of the significant longitudinal findings (without correction for multiple comparison) in MTI values with clinical measures resulted in two significant findings, namely in the PreHD-B group the MTR peak height of the left hippocampus correlated to TFC reduction ($R = -.622$, $p= 0.043$) and in the HD 2 group the reduction of mean MTR correlated to the reduction in SDMT performance ($R = -.667$, $p= 0.018$). Both findings did not survive Bonferroni correction for multiple comparisons.

All volumetric values are shown in the supplementary materials table 3. Significant volumetric decline of several VOI's was seen in premanifest (caudate nucleus and putamen) and manifest groups (caudate nucleus, putamen, thalamus, white matter and whole brain).

Discussion

The main finding of this study is the fact that MTI parameters do not change over a two year follow up period in manifest HD. The expected decline in structural integrity in this group could not be detected with MTI. However an interesting finding in the premanifest “far from expected disease onset” was made, namely an increase in MTR value in the putamen, which possibly can be interpreted as a form of aberrant development or compensatory mechanism. There is no relationship of changing MTR parameters to increasing clinical symptoms in any of the groups. Clinical progression was evident in premanifest close to disease onset group and the manifest HD groups.

Previous cross-sectional observations with MTI in HD showed promising results for both mean MTR as MTR histogram peak height for these measures to serve as a disease monitoring biomarker^{6,7,17}. Mean MTR was found to be lower in several brain regions in manifest HD⁶ or in a combined cohort of premanifest and manifest HD⁷ compared to controls. Also MTR peak height in several regions was found to be lower in manifest HD⁶ and, although there was no group difference, the MTR peak height related to subtle motor abnormalities and higher CAG repeat length in a premanifest HD cohort¹⁷. To date no longitudinal MTI studies in HD were available. In fact there is relatively little longitudinal research of MTI values available at all. Only in multiple sclerosis, optic neuritis and systemic lupus erythematosus reports are available, suggesting a good potential for MTI to examine both grey and white matter as lesion evolution²⁶⁻²⁹. In normal aging Ge et al. (2008) described, via a histogram analysis, reduction of MTR values after the age of 40 and significant group differences after the age of 50 years³⁰. The groups in our study span exactly this age range. We therefore calibrated our MTR values of the HD groups to the control values.

The goal of this study was to examine the potential of MTI to detect loss of structural integrity in HD to ultimately serve as an outcome measure in future therapeutic trials, as is the overall main goal of the TRACK-HD study¹⁰. This current study and the recently published 24-month analysis of the main TRACK-HD study demonstrate that volumetric MRI measures are sensitive for detecting change over a 2 year period³¹. In our MTI study no statistically strong changes were seen in any of the regions. Three regions did show longitudinal reduction, namely the cortical grey matter in PreHD-B and the amygdala in HD 1 and 2, however these findings did not survive correction for multiple comparison, thus should be interpreted with extreme caution. These regions are shown to be affected at these disease

stages^{10;11}, however other regions such as the caudate nucleus or putamen or pallidum are known to be more severely affected in terms of atrophy. Noteworthy is the fact that MTR histogram peak height was normalised for volume and mean MTR is non-dependent on atrophy; only the number of voxels from which this mean is calculated could have an influence. The measures used are therefore relatively non-influenced by atrophy. We must conclude from our study, based on the group comparisons of MTI-parameters, group comparisons of volumes and the lack of correlation of MTI to clinical measures, that MTI is inferior to volumetric measures to serve as a biomarker to detect longitudinal change in a 2 year follow up. It is noteworthy to mention that clinical trials from a practical point of view will not last longer than two years, hence a longer follow up period may be of interest scientifically, but the impact on biomarker research in HD will be limited.

The interesting finding in this study in PreHD-A is that an increase in MTI values was observed. This pattern was seen in 5 subcortical grey matter structures, with the finding of increased MTR histogram peak height in the putamen, one of the most heavily involved structures in HD, surviving the stringent correction for multiple comparisons. The explanation of this increase could be sought in an earlier postulated theory by Paulsen et al. They gave two possible explanations when their group detected increased cortical volume in premanifest HD. These explanations consist of either a predegenerative process, such as swelling of tissue, or alternatively it may be a reflection of aberrant brain development or maturation³².

Furthermore, evidence from fMRI studies point towards another possible explanation. Two reports exist on increased activation in premanifest HD, which is thought to represent cortical recruitment as compensatory strategies, this was specifically true for premanifest HD far from expected onset and not in the close to onset group^{33;34}. In our view any of these proposed explanations could be true, however we should be extremely cautious not to overly interpret the findings as the correction for multiple comparisons reduced the number and strength of the findings. This finding could however lead to broader examination of MTI and other MRI measures in the premanifest far from disease onset group as this potentially can lead to better understanding of the neuropathology in HD.

Limitations of our study lay in the fact that not all participants were retained for the follow up period. However, those lost to follow up were evenly divided over the groups; hence we do not believe this ultimately influenced our results. Furthermore the group sizes were relatively small, possibly suggesting the study could be

underpowered, however combining the groups did not result in any additional findings. On the other hand aggregated groups could be too heterogeneous to yield additional significant findings.

Conclusion

We believe MTI derived measures are not suitable for disease monitoring in HD as there is no significant decrease in structural integrity in any of the groups over two years and there is no significant relation to clinical measures. The finding of increased MTI measures in the premanifest far from disease onset group could relate to a pre-degenerative process, compensatory mechanisms or aberrant development, but should be interpreted with caution until confirmation of these findings in future studies is made.

Acknowledgement

We wish to thank Mr. B. Mertens from the Department of Medical Statistics for his input in the statistical analysis and Rachael Scahill for her input in the volumetric analysis. We wish to thank all TRACK-HD participants, and the “CHDI/High Q Foundation”, a not-for-profit organization dedicated to finding treatments for HD, for providing financial support, and all TRACK-HD investigators for their efforts in conducting this study.

References

1. Dehmeshki J, Chard DT, Leary SM, et al. The normal appearing grey matter in primary progressive multiple sclerosis: a magnetisation transfer imaging study. *J Neurol* 2003;250(1):67-74
2. Filippi M, Rocca MA. Magnetization transfer magnetic resonance imaging of the brain, spinal cord, and optic nerve. *Neurotherapeutics* 2007;4(3):401-13
3. McGowan JC. The physical basis of magnetization transfer imaging. *Neurology* 1999;53(5 Suppl 3):S3-S7
4. Ridha BH, Tozer DJ, Symms MR, et al. Quantitative magnetization transfer imaging in Alzheimer disease. *Radiology* 2007;244(3):832-37
5. Eckert T, Sailer M, Kaufmann J, et al. Differentiation of idiopathic Parkinson's disease, multiple system atrophy, progressive supranuclear palsy, and healthy controls using magnetization transfer imaging. *Neuroimage* 2004;21(1):229-35
6. van den Bogaard SJ, Dumas EM, Milles J, et al. Magnetization Transfer Imaging in Premanifest and Manifest Huntington Disease. *AJNR Am J Neuroradiol* 2012 Jan[Epub ahead of print]
7. Ginestroni A, Battaglini M, Diciotti S, et al. Magnetization Transfer MR Imaging Demonstrates Degeneration of the Subcortical and Cortical Gray Matter in Huntington Disease. *AJNR Am J Neuroradiol* 2010;31:1807-12
8. A novel gene containing a trinucleotide repeat that is expanded and unstable on Huntington's disease chromosomes. The Huntington's Disease Collaborative Research Group. *Cell* 1993;72(6):971-83
9. Langbehn DR, Brinkman RR, Falush D, et al. A new model for prediction of the age of onset and penetrance for Huntington's disease based on CAG length. *Clin Genet* 2004;65:267-77
10. Tabrizi SJ, Langbehn DR, Leavitt BR, et al. Biological and clinical manifestations of Huntington's disease in the longitudinal TRACK-HD study: cross-sectional analysis of baseline data. *Lancet Neurol* 2009;8:791-801
11. van den Bogaard SJ, Dumas EM, Acharya TP, et al. Early atrophy of pallidum and accumbens nucleus in Huntington's disease. *J Neurol* 2011;258:412-20
12. Dumas EM, van den Bogaard SJ, Ruber ME, et al. Early changes in white matter pathways of the sensorimotor cortex in premanifest Huntington's disease. *Hum Brain Mapp* 2012;33(1):203-12
13. Rosas HD, Tuch DS, Hevelone ND, et al. Diffusion tensor imaging in presymptomatic and early Huntington's disease: Selective white matter pathology and its relationship to clinical measures. *Mov Disord* 2006;21:1317-25
14. Rosas HD, Hevelone ND, Zaleta AK, et al. Regional cortical thinning in preclinical Huntington disease and its relationship to cognition. *Neurology* 2005;65:745-47
15. Henley SM, Frost C, Macmanus DG, et al. Increased rate of whole-brain atrophy over 6 months in early Huntington disease. *Neurology* 2006;67:694-96
16. Mascalchi M, Lolli F, Della NR, et al. Huntington disease: volumetric, diffusion-weighted, and magnetization transfer MR imaging of brain. *Radiology* 2004;232:867-73
17. Jurgens CK, Bos R, Luyendijk J, et al. Magnetization transfer imaging in 'premanifest' Huntington's disease. *J Neurol* 2010;257(3):426-32
18. van Waesberghe JH, Kamphorst W, De Groot CJ, et al. Axonal loss in multiple sclerosis lesions: magnetic resonance imaging insights into substrates of disability. *Ann Neurol* 1999;46(5):747-54
19. Filippi M, Rocca MA, Comi G. The use of quantitative magnetic-resonance-based techniques to monitor the evolution of multiple sclerosis. *The Lancet Neurology* 2003;2:337-46
20. Tabrizi SJ, Scahill RI, Durr A, et al. Biological and clinical changes in premanifest and early stage Huntington's disease in the TRACK-HD study: the 12-month longitudinal analysis. *Lancet Neurol* 2011;10:31-42
21. Penney JB, Jr., Vonsattel JP, MacDonald ME, et al. CAG repeat number governs the development rate of pathology in Huntington's disease. *Ann Neurol* 1997;41(5):689-92

22. Zhang Y, Brady M, Smith S. Segmentation of brain MR images through a hidden Markov random field model and the expectation-maximization algorithm. *IEEE Trans Med Imaging* 2001;20:45-57
23. Patenaude B, Smith SM, Kennedy DN, et al. A Bayesian model of shape and appearance for subcortical brain segmentation. *Neuroimage* 2011;56:907-22
24. Smith SM, Jenkinson M, Woolrich MW, et al. Advances in functional and structural MR image analysis and implementation as FSL. *Neuroimage* 2004;23 Suppl 1:S208-S219
25. Smith SM, Zhang Y, Jenkinson M, et al. Accurate, robust, and automated longitudinal and cross-sectional brain change analysis. *Neuroimage* 2002;17:479-89
26. Melzi L, Rocca MA, Marzoli SB, et al. A longitudinal conventional and magnetization transfer magnetic resonance imaging study of optic neuritis. *Mult Scler* 2007;13(2):265-68
27. Mesaros S, Rocca M, Sormani M, et al. Bimonthly assessment of magnetization transfer magnetic resonance imaging parameters in multiple sclerosis: a 14-month, multicentre, follow-up study. *Mult Scler* 2010;16(3):325-31
28. Filippi M, Inglese M, Rovaris M, et al. Magnetization transfer imaging to monitor the evolution of MS: a 1-year follow-up study. *Neurology* 2000;55(7):940-46
29. Emmer BJ, Steens SC, Steup-Beekman GM, et al. Detection of change in CNS involvement in neuropsychiatric SLE: a magnetization transfer study. *J Magn Reson Imaging* 2006;24(4):812-16
30. Ge Y, Grossman RI, Babb JS, et al. Age-related total gray matter and white matter changes in normal adult brain. Part II: quantitative magnetization transfer ratio histogram analysis. *AJNR Am J Neuroradiol* 2002;23(8):1334-41
31. Tabrizi SJ, Reilmann R, Roos RA, et al. Potential endpoints for clinical trials in premanifest and early Huntington's disease in the TRACK-HD study: analysis of 24 month observational data. *Lancet Neurol* 2012;11:42-53
32. Paulsen JS, Magnotta VA, Mikos AE, et al. Brain structure in preclinical Huntington's disease. *Biol Psychiatry* 2006;59:57-63
33. Zimbelman JL, Paulsen JS, Mikos A, et al. fMRI detection of early neural dysfunction in preclinical Huntington's disease. *J Int Neuropsychol Soc* 2007;13:758-69
34. Paulsen JS, Zimbelman JL, Hinton SC, et al. fMRI biomarker of early neuronal dysfunction in presymptomatic Huntington's Disease. *AJNR Am J Neuroradiol* 2004;25:1715-21

Supplementary Material

Results

Control values

The control values displayed a significant change over time in three regions, as shown in table 4. In the left thalamus and the left caudate nucleus a significant decrease in mean MTR was seen and in the right putamen a significant increase in mean MTR was observed. To ensure that our most significant longitudinal finding, namely MTR peak height of the right putamen, was not affected by the potential influence of calibration, we also examined the difference over time of this value without calibration to controls. As expected, the MTR peak height from the right putamen in the premanifest far from onset group also displayed a very significant ($p=0.005$) increase over the 2 year follow up.

Premanifest versus manifest in three group division

When the two premanifest and two manifest groups were combined there were six noteworthy increases: the MTR peak height of the right putamen ($p=0.010$), the MTR peak height of the left pallidum ($p=0.001$), MTR peak height of cortical grey matter ($p=0.024$), mean MTR of the left amygdala ($p=0.024$) and mean MTR of the right thalamus ($p=0.048$). Furthermore a decrease is seen in mean MTR of the left caudate nucleus ($p=0.030$) and in the manifest HD group the left and right amygdale show a decrease in mean MTR (left amygdale $p=0.042$, right amygdale $p=0.025$). However, when the Bonferroni correction for multiple testing was applied, only the increase in MTR peak height of the left pallidum remains statistically significant.

Table 1: MTI derived values in 14 different regions on both baseline and follow up visit for the premanifest HD A and premanifest HD B group.

	Premanifest A					Premanifest B				
	Baseline		Follow up		ρ	Baseline		Follow up		ρ
	Mean	SD	Mean	SD		Mean	SD	Mean	SD	
White matter										
Peak height	1.144	0.161	1.176	0.223	0.567	1.092	0.258	1.188	0.134	0.172
Mean MTR	0.387	0.013	0.389	0.010	0.249	0.388	0.017	0.388	0.010	0.903
Cortical grey matter										
Peak height	0.752	0.107	0.796	0.109	0.091	0.685	0.136	0.727	0.111	0.152
Mean MTR	0.326	0.014	0.329	0.013	0.079	0.325	0.012	0.319	0.013	0.020
Caudate Right										
Peak height	0.852	0.133	0.910	0.184	0.320	0.849	0.182	0.838	0.169	0.804
Mean MTR	0.339	0.018	0.346	0.020	0.049	0.333	0.031	0.340	0.025	0.353
Caudate Left										
Peak height	0.974	0.245	1.046	0.085	0.367	0.964	0.199	1.013	0.146	0.480
Mean MTR	0.357	0.021	0.351	0.016	0.308	0.359	0.024	0.346	0.022	0.062
Putamen Right										
Peak height	1.132	0.235	1.375	0.206	0.003	1.338	0.354	1.409	0.241	0.396
Mean MTR	0.329	0.015	0.335	0.012	0.160	0.330	0.031	0.334	0.021	0.312
Putamen Left										
Peak height	1.291	0.199	1.340	0.181	0.614	1.298	0.314	1.433	0.295	0.091
Mean MTR	0.352	0.013	0.356	0.015	0.119	0.353	0.031	0.356	0.024	0.494
Pallidum Right										
Peak height	1.569	0.333	1.740	0.272	0.112	1.617	0.318	1.701	0.285	0.400
Mean MTR	0.381	0.006	0.382	0.007	0.740	0.382	0.021	0.387	0.013	0.300
Pallidum Left										
Peak height	1.471	0.285	1.721	0.218	0.032	1.528	0.310	1.709	0.223	0.086
Mean MTR	0.386	0.010	0.386	0.009	0.958	0.383	0.019	0.392	0.013	0.094
Thalamus Right										
Peak height	1.013	0.139	1.083	0.159	0.142	1.003	0.204	0.999	0.167	0.946
Mean MTR	0.359	0.015	0.367	0.018	0.047	0.352	0.028	0.359	0.021	0.398
Thalamus left										
Peak height	1.166	0.279	1.197	0.098	0.717	1.116	0.222	1.196	0.167	0.332
Mean MTR	0.372	0.018	0.380	0.014	0.090	0.371	0.020	0.375	0.020	0.467
Amygdala Right										
Peak height	1.297	0.116	1.405	0.191	0.050	1.259	0.327	1.279	0.240	0.837
Mean MTR	0.357	0.017	0.358	0.011	0.817	0.364	0.027	0.351	0.019	0.164
Amygdala Left										
Peak height	1.530	0.190	1.613	0.212	0.236	1.304	0.231	1.486	0.325	0.064
Mean MTR	0.374	0.016	0.370	0.015	0.506	0.377	0.026	0.364	0.018	0.200
Hippocampus Right										
Peak height	1.346	0.219	1.298	0.224	0.586	1.164	0.266	1.198	0.288	0.637
Mean MTR	0.360	0.015	0.363	0.009	0.635	0.365	0.021	0.355	0.017	0.124
Hippocampus Left										
Peak height	1.010	0.195	1.059	0.170	0.558	0.888	0.188	1.088	0.197	0.037
Mean MTR	0.381	0.022	0.387	0.018	0.347	0.380	0.018	0.373	0.013	0.317
Whole brain										
Peak height	0.923	0.123	0.963	0.141	0.198	0.864	0.181	0.936	0.094	0.118
Mean MTR	0.352	0.013	0.355	0.011	0.110	0.353	0.013	0.350	0.010	0.297

MTR = Magnetization Transfer Ratio. **Bold** =significant finding at $p \leq 0.05$

Table 2: MTI derived values in 14 different regions on both baseline and follow up visit for the manifest HD 1 and manifest HD 2 group.

	Manifest 1					Manifest 2				
	Baseline		Follow up		<i>p</i>	Baseline		Follow up		<i>p</i>
	Mean	SD	Mean	SD		Mean	SD	Mean	SD	
White matter										
Peak height	0.747	0.274	0.824	0.243	0.388	0.866	0.263	0.916	0.245	0.560
Mean MTR	0.372	0.025	0.384	0.013	0.121	0.380	0.016	0.379	0.014	0.713
Cortical grey matter										
Peak height	0.589	0.174	0.587	0.137	0.961	0.602	0.127	0.632	0.097	0.239
Mean MTR	0.319	0.014	0.316	0.015	0.264	0.311	0.017	0.311	0.013	0.928
Caudate Right										
Peak height	0.726	0.234	0.704	0.182	0.762	0.777	0.204	0.703	0.200	0.371
Mean MTR	0.331	0.034	0.344	0.039	0.321	0.323	0.034	0.339	0.032	0.123
Caudate Left										
Peak height	0.784	0.240	0.798	0.156	0.852	0.833	0.244	0.898	0.236	0.311
Mean MTR	0.339	0.045	0.338	0.045	0.930	0.346	0.039	0.346	0.037	0.999
Putamen Right										
Peak height	0.877	0.326	1.018	0.287	0.152	0.961	0.282	1.082	0.334	0.221
Mean MTR	0.330	0.029	0.338	0.024	0.276	0.329	0.018	0.323	0.029	0.455
Putamen Left										
Peak height	0.941	0.332	1.037	0.178	0.415	1.029	0.295	1.177	0.275	0.106
Mean MTR	0.346	0.026	0.352	0.031	0.720	0.360	0.015	0.353	0.033	0.348
Pallidum Right										
Peak height	1.178	0.466	1.325	0.359	0.203	1.307	0.409	1.356	0.394	0.714
Mean MTR	0.396	0.039	0.389	0.018	0.565	0.384	0.021	0.394	0.019	0.146
Pallidum Left										
Peak height	1.138	0.366	1.240	0.211	0.321	1.237	0.364	1.370	0.282	0.268
Mean MTR	0.376	0.047	0.396	0.026	0.237	0.399	0.012	0.392	0.023	0.308
Thalamus Right										
Peak height	0.825	0.297	0.826	0.208	0.988	0.874	0.234	0.838	0.205	0.667
Mean MTR	0.349	0.035	0.360	0.038	0.396	0.335	0.042	0.358	0.028	0.079
Thalamus left										
Peak height	0.884	0.311	0.901	0.183	0.856	0.933	0.285	0.993	0.280	0.477
Mean MTR	0.346	0.054	0.367	0.045	0.230	0.354	0.044	0.373	0.038	0.214
Amygdala Right										
Peak height	1.076	0.366	1.100	0.336	0.875	1.131	0.277	1.080	0.325	0.536
Mean MTR	0.361	0.019	0.333	0.029	0.036	0.351	0.024	0.349	0.017	0.686
Amygdala Left										
Peak height	1.128	0.344	1.298	0.388	0.102	1.198	0.265	1.121	0.228	0.434
Mean MTR	0.377	0.042	0.345	0.036	0.157	0.369	0.020	0.354	0.015	0.022
Hippocampus Right										
Peak height	0.974	0.264	0.976	0.233	0.994	1.097	0.235	0.948	0.249	0.131
Mean MTR	0.372	0.036	0.344	0.022	0.073	0.354	0.027	0.359	0.018	0.576
Hippocampus Left										
Peak height	0.717	0.226	0.798	0.181	0.142	0.957	0.256	1.062	0.232	0.350
Mean MTR	0.394	0.045	0.364	0.029	0.150	0.389	0.017	0.379	0.020	0.284
Whole brain										
Peak height	0.661	0.217	0.696	0.184	0.579	0.719	0.174	0.762	0.153	0.428
Mean MTR	0.343	0.016	0.347	0.014	0.098	0.342	0.016	0.343	0.012	0.728

MTR = Magnetization Transfer Ratio. Bold =significant finding at $p \leq 0.05$

Table 3: Volumetric analysis of 14 brain regions in premanifest and manifest HD

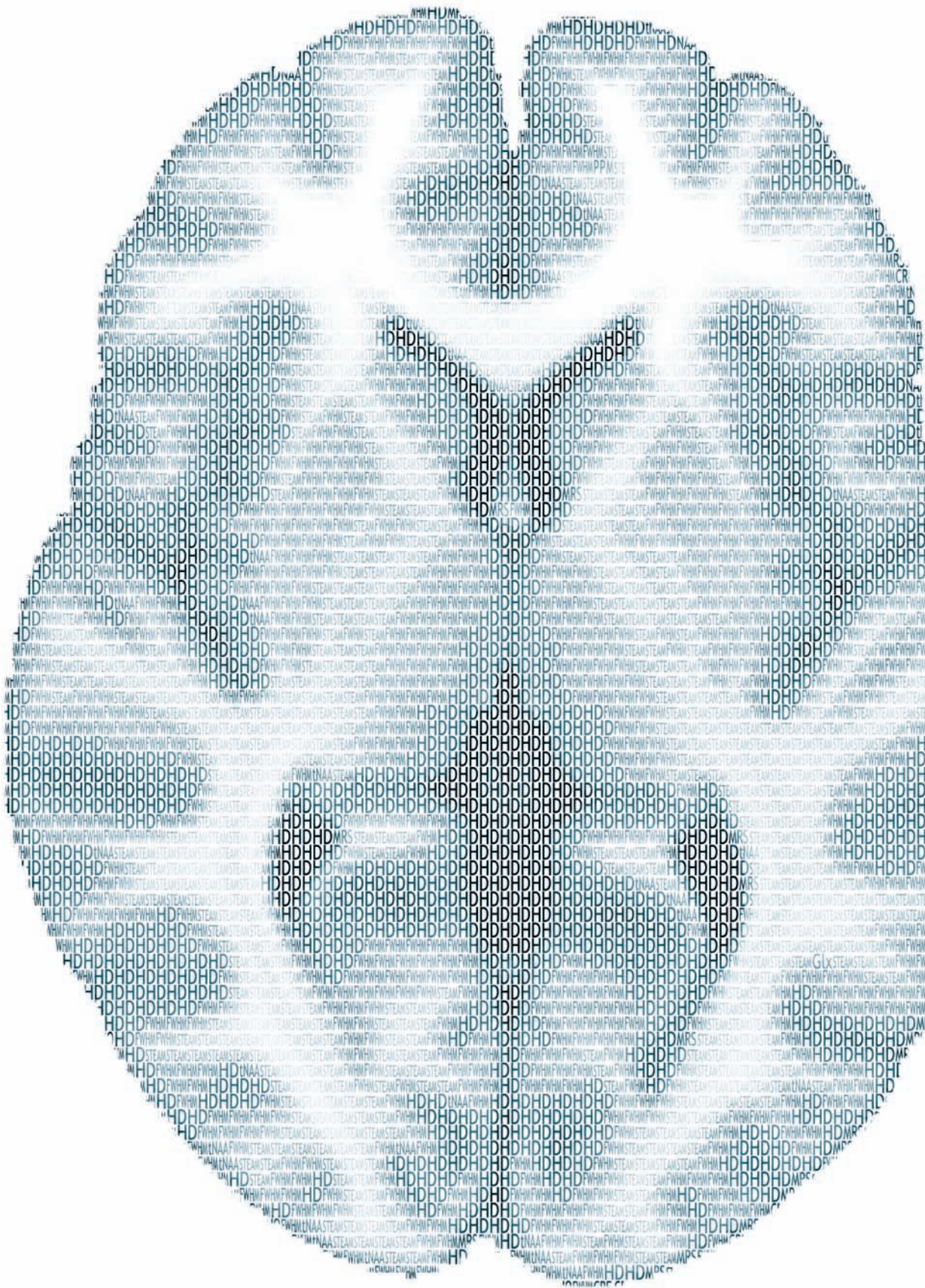
	Premanifest A				Premanifest B						
	Baseline		Follow up		Baseline		Follow up				
	Mean	SD	Mean	SD	Mean	SD	Mean	SD			
									<i>p</i>		
Caudate	Right	3.907	0.428	3.705	0.482	0.004	3.897	0.339	3.739	0.353	0.001
	Left	3.797	0.395	3.651	0.406	0.001	3.713	0.359	3.576	0.376	0.002
Putamen	Right	4.832	0.619	4.680	0.603	0.009	4.582	0.497	4.397	0.525	0.001
	Left	4.916	0.502	4.748	0.544	0.006	4.681	0.556	4.483	0.586	0.002
Pallidum	Right	2.056	0.173	2.089	0.207	0.555	2.009	0.155	1.952	0.142	0.067
	Left	1.931	0.205	1.890	0.226	0.199	1.995	0.134	1.925	0.175	0.081
Thalamus	Right	8.155	0.545	8.122	0.468	0.566	7.718	0.637	7.595	0.741	0.044
	Left	8.492	0.595	8.452	0.554	0.474	7.833	0.659	7.777	0.722	0.382
Amygdala	Right	1.689	0.242	1.672	0.222	0.821	1.799	0.268	1.793	0.306	0.891
	Left	1.772	0.266	1.752	0.259	0.578	1.711	0.229	1.733	0.234	0.626
Hippocampus	Right	5.519	0.385	5.411	0.431	0.033	5.204	0.470	5.252	0.619	0.497
	Left	5.315	0.358	5.392	0.319	0.034	4.925	0.750	4.962	0.853	0.552
White matter		673.9	36.2	667.2	34.0	0.028	647.2	46.2	637.0	44.4	0.014
Whole brain		1486.4	38.7	1477.3	33.2	0.208	1445.7	72.9	1429.0	73.4	0.036
	Manifest 1				Manifest 2						
	Baseline		Follow up		Baseline		Follow up				
	Mean	SD	Mean	SD	Mean	SD	Mean	SD	<i>p</i>		
Caudate	Right	3.290	0.530	3.165	0.621	0.046	3.302	0.495	3.223	0.624	0.219
	Left	3.178	0.478	3.002	0.481	0.019	3.094	0.472	2.916	0.515	0.001
Putamen	Right	4.002	0.603	3.839	0.602	0.009	3.518	0.325	3.296	0.392	0.012
	Left	4.176	0.548	3.962	0.593	0.004	3.455	0.479	3.285	0.437	0.003
Pallidum	Right	1.834	0.086	1.790	0.058	0.029	1.845	0.248	1.751	0.226	0.014
	Left	1.866	0.207	1.793	0.201	0.117	1.769	0.288	1.679	0.324	0.141
Thalamus	Right	7.603	0.703	7.427	0.661	0.003	7.285	0.593	7.207	0.435	0.352
	Left	7.745	0.729	7.567	0.728	0.001	7.358	0.897	7.176	0.892	0.018
Amygdala	Right	1.643	0.258	1.732	0.194	0.257	1.623	0.149	1.633	0.279	0.918
	Left	1.654	0.311	1.676	0.357	0.707	1.638	0.106	1.594	0.115	0.295
Hippocampus	Right	5.127	0.511	5.063	0.374	0.354	4.961	0.579	4.807	0.578	0.018
	Left	5.096	0.591	5.033	0.556	0.557	4.542	0.440	4.446	0.550	0.233
White matter		632.9	52.9	619.4	53.9	0.001	633.8	35.8	616.1	34.8	0.009
Whole brain		1396.6	95.3	1371.9	93.8	0.001	1383.1	77.8	1350.6	81.4	0.001

Volumes (mm³) of 14 VOI's on both baseline and follow up. **Bold** = significant finding after Bonferroni correction (*p*<0.0033)

Table 4: control values of MTR parameters

Control group (n = 25)			Mean	SD	
White matter	MTR peak height	Baseline	1.109	0.220	
		Follow up	1.125	0.231	
	Mean MTR	Baseline	0.391	0.012	
		Follow up	0.394	0.012	
Cortical grey matter	MTR peak height	Baseline	0.769	0.119	
		Follow up	0.735	0.132	
	Mean MTR	Baseline	0.329	0.013	
		Follow up	0.330	0.014	
Caudate nucleus	right	MTR peak height	Baseline	0.799	0.192
			Follow up	0.830	0.224
		Mean MTR	Baseline	0.349	0.026
			Follow up	0.343	0.025
	left	MTR peak height	Baseline	0.892	0.188
			Follow up	0.831	0.198
		Mean MTR	Baseline	0.369	0.018
			Follow up	0.354	0.018
Putamen	right	MTR peak height	Baseline	1.257	0.372
			Follow up	1.240	0.271
		Mean MTR	Baseline	0.340	0.019
			Follow up	0.351	0.017
	left	MTR peak height	Baseline	1.337	0.268
			Follow up	1.266	0.265
		Mean MTR	Baseline	0.360	0.015
			Follow up	0.357	0.016
Pallidum	right	MTR peak height	Baseline	1.494	0.343
			Follow up	1.435	0.230
		Mean MTR	Baseline	0.382	0.015
			Follow up	0.388	0.014
	left	MTR peak height	Baseline	1.601	0.301
			Follow up	1.490	0.268
		Mean MTR	Baseline	0.386	0.014
			Follow up	0.388	0.014
Thalamus	right	MTR peak height	Baseline	0.988	0.261
			Follow up	0.936	0.236
		Mean MTR	Baseline	0.369	0.021
			Follow up	0.350	0.021
	left	MTR peak height	Baseline	1.067	0.226
			Follow up	1.003	0.251
		Mean MTR	Baseline	0.383	0.020
			Follow up	0.368	0.016
Amygdala	right	MTR peak height	Baseline	1.329	0.295
			Follow up	1.287	0.289
		Mean MTR	Baseline	0.360	0.020
			Follow up	0.363	0.025
	left	MTR peak height	Baseline	1.475	0.307
			Follow up	1.328	0.369
		Mean MTR	Baseline	0.370	0.021
			Follow up	0.370	0.026
Hippocampus	right	MTR peak height	Baseline	1.240	0.309
			Follow up	1.194	0.273
		Mean MTR	Baseline	0.366	0.019
			Follow up	0.371	0.020
	left	MTR peak height	Baseline	0.981	0.247
			Follow up	0.929	0.222
		Mean MTR	Baseline	0.386	0.015
			Follow up	0.391	0.017
Whole brain	MTR peak height	Baseline	0.917	0.152	
		Follow up	0.906	0.156	
	Mean MTR	Baseline	0.356	0.011	
		Follow up	0.359	0.012	

MTR = Magnetization Transfer Ratio. **Bold** = significant finding after bonferroni correction ($p < 0.0033$)



CHAPTER 9

FROM PREMANIFEST TO MANIFEST HUNTINGTON'S DISEASE: A TWO YEAR FOLLOW UP STUDY WITH MAGNETIC RESONANCE SPECTROSCOPY AT 7 TESLA

SIMON J.A. VAN DEN BOGAARD¹, EVE M. DUMAS¹, WOUTER M. TEEUWISSE²,
HERMIEN E. KAN², ANDREW WEBB², MARK A. VAN BUCHEM³,
RAYMUND A.C. ROOS¹, JEROEN VAN DER GROND³

1. DEPARTMENT OF NEUROLOGY, LEIDEN UNIVERSITY MEDICAL CENTRE, LEIDEN, THE NETHERLANDS

2. C.J. GORTER CENTRE FOR HIGH FIELD MRI, LEIDEN UNIVERSITY MEDICAL CENTRE, LEIDEN, THE NETHERLANDS

3. DEPARTMENT OF RADIOLOGY, LEIDEN UNIVERSITY MEDICAL CENTRE, LEIDEN, THE NETHERLANDS

SUBMITTED

Abstract

Background

Previous cross-sectional magnetic resonance spectroscopy (MRS) studies in Huntington's disease (HD) have demonstrated differences in metabolite concentrations compared to controls in several regions of interest, especially the putamen and caudate nucleus. It has been suggested that metabolite changes could be used as biomarker in future therapeutic trials. The aim of the present study was to assess metabolite changes in both premanifest and early HD over a two year follow up period using MRS at 7 Tesla.

Methods

In 13 HD gene carriers (10 premanifest and 3 manifest HD) proton MRS was performed at baseline and after 24 months. At follow up, four of the premanifest HD gene carriers had progressed into manifest HD, as assessed by clinical measures. 7T MR proton spectroscopy was performed in three regions of interest; the caudate nucleus, putamen and prefrontal cortex. Six metabolites were quantified for each region at each time point. Statistical analysis was performed using paired t-tests.

Results

In the caudate nucleus a decrease in creatine ($p=0.032$) and myo-inositol ($p=0.006$) concentrations was observed. A significant decrease in the putamen was seen in the total N-acetylaspartate (tNAA) ($p=0.022$) and choline concentrations ($p=0.007$). Premanifest HD converters showed higher rates of tNAA decrease in the putamen ($p<0.003$) than non-converting premanifest HD.

Conclusion

Over a period of 2 years we have demonstrated metabolite changes in the caudate nucleus and putamen of HD gene carriers around disease onset. This demonstrates the potential of MRS for providing a biomarker of disease progression and for evaluating future therapeutic interventions.

Introduction

Huntington's disease (HD) is a devastating neurological disorder causing widespread neuronal damage throughout the brain¹⁻³. Atrophy of the striatum is regarded as the hallmark of the pathologic findings in HD⁴ and is consistently reported as the earliest brain structure affected, well before clinical symptoms arise^{1-3,5}. Almost all other brain regions show structural changes at later stages of the disease, which can be examined in vivo with MRI² and post-mortem⁴.

The pathophysiological mechanism leading to neuronal damage still remains unclear. The genetic defect is located at chromosome 4 in the Htt-gene, leading to a mutant huntingtin protein⁶. Several pathophysiological hypotheses have been postulated. First, direct toxic effects of the aggregated and misfolded huntingtin protein could lead to neuronal damage. Second, transcriptional dysregulation of multiple genes is reported with associated functions in neurotransmitter receptors, enzymes and proteins involved in neuron structure, stress responses and axonal transport. Furthermore, there is evidence for impaired energy metabolism due to mitochondrial disturbances and disrupted dynamic intracellular processes, such as trafficking of intracellular vesicles and synaptic disruptions. Finally, the excitotoxicity hypothesis has gained a lot of support, which describes an increased sensitivity to neurotransmitter mediated stimulation, causing overstimulation and cell death⁷⁻⁹. Magnetic resonance spectroscopy (MRS) can be used in HD research either to explore pathophysiological mechanisms of the disease and/or in the search for a HD biomarker. Both objectives are closely linked as a robust biomarker should have a basis in the pathologic mechanisms of the disease. In HD, there is a need for objective biomarkers both for disease monitoring purposes and for evaluation of future therapeutic compounds. Novel compounds targeting specific pathogenic pathways, such as disturbed energy metabolism and those related to excitotoxicity theory, can potentially be monitored by means of MRS.

Previous studies have consistently demonstrated reduced N-acetylaspartate (NAA) and creatine levels in the caudate nucleus and/or putamen in manifest HD¹⁰⁻¹². Whether these reductions in metabolite concentrations start in the premanifest phase of the disease or at a later disease stage remains a matter of debate. Lower concentrations of NAA and creatine in premanifest HD have been demonstrated¹², although not all studies agree on this finding^{10,13}. In addition to NAA and creatine, changes in choline¹⁴, glutamate^{11,15}, lactate¹⁶ and myo-inositol¹⁰ concentration in HD have been reported. Choline was found to be reduced in the frontal lobe and was related to cognitive deficits¹⁴. Glutamate levels have been reported to be either increased¹⁵ or decreased¹¹ in the striatum in manifest HD. This discrepancy could possibly be explained by the use of a glutamate-to-creatine ratio in one

publication¹⁵, against a glutamate concentration calculation using water as a concentration standard in the other¹¹. Increased lactate in the occipital cortex and basal ganglia has been reported, suggestive of impaired energy metabolism¹⁶. Finally, a myo-inositol increase in the putamen has recently been reported in a large cohort from the TRACK-HD study¹⁰.

All of the above described studies have been cross-sectional in design. In terms of identifying potential biomarkers, following changes in metabolite concentrations in longitudinal studies is imperative. Our study population consists of predominantly premanifest HD participants, which show a high conversion rate, meaning progression from the premanifest to manifest HD. This specific study group is of particular interest given the fact that if any potential therapeutic compound should prove effective, it is in this premanifest stage of the disease, when neuronal loss is still limited, that one would start with interventions. Therefore, the aims of our study were to assess metabolite changes in both premanifest and early HD over a two year follow up period and how potential changes relate to clinical outcome measures. The current study consists of the follow up data of previously reported 7T MRS results in manifest and premanifest HD¹¹.

Materials and methods

Subjects

Recruitment of participants was performed as described previously¹¹. In short, participants were recruited from the outpatient neurology clinic of the Leiden University Medical Centre. The presence of a positive genetic test with a CAG repeat ≥ 39 and the absence of significant comorbidity were mandatory inclusion criteria for both participant groups. The premanifest HD group was defined by the absence of motor disturbances on the Unified Huntington's Disease Rating Scale '99 (UHDRS), with a total motor score (TMS) < 5 . Early manifest HD was defined as a TMS of ≥ 5 , a Total Functional Capacity (TFC) ≥ 7 and a diagnostic confidence level of 4 on the UHDRS. In total thirteen gene carriers were available for a follow up scan after two years. The study was approved by the local Medical Ethical Committee of the Leiden University Medical Centre. All participants provided written informed consent.

Clinical measures

At both time points the same set of clinical measures was performed. This included the UHDRS motor scale (score 0-124) and the TFC, a global scale of

impairment in daily life activities, score 0-13. In addition, a short cognitive battery was administered, consisting of the Mini Mental State Exam (MMSE), Stroop word reading card (Stroop), the Symbol Digit Modality Test (SDMT) and the Trail Making Test part B (TMT-B). Behavioural disturbances were evaluated with the Beck Depression Inventory 2nd version (BDI-II) and the Problem Behaviour Assessment short version (PBA-s). Predicted years to onset were calculated from current age and CAG repeat length using the formula by Langbehn *et al.*(2004)¹⁷.

MR data acquisition:

The MR protocol performed at the baseline time point has been described previously: it consisted of a T1-weighted MRI and an MRS sequence performed on a Philips 7 Tesla Achieva whole body scanner (Philips Healthcare, Best, The Netherlands) with a NOVA Medical quadrature transmit coil and 16 channel receive coil array. A three-dimensional, high resolution, T1-weighted gradient echo (GRE) scan was acquired (TR/TE = 11/5.4 ms, voxel size 0.44 x 0.44 x 0.84 mm, total scan time 1:46 mins) for accurate planning. Localized proton spectra were acquired using a stimulated echo acquisition mode (STEAM) sequence with the following scan parameters: TR/TE/TM = 2000/19/25 ms, BW 4 kHz, 2048 complex data points and 128 signal averages. Water suppression was performed using a frequency-selective RF pulse and gradient spoiling, six saturation bands were additionally applied to suppress signal from surrounding tissue. All scans included a reference scan without water suppression for quantification. The voxel was placed within the region of interest with the maximum volume containing only tissue from the intended structure, minimizing the contribution from surrounding tissue, and also partial volume effects. Regions of interest consisted of the caudate nucleus, putamen, and the prefrontal white and cortical grey matter. For the prefrontal voxel, positioning included approximately 50% white and 50% cortical grey matter.

In the follow up studies minor changes were made to improve the signal to noise ratio (SNR), without changing the basic imaging and spectroscopy sequences which remained identical; volume-selective rather than global power optimization was implemented¹⁸, the first- and second-order shims were adjusted using a B0 map¹⁹ rather than a pencil-beam shimming routine, and water suppression was achieved using variable-power RF pulses with optimized relaxation delays (VAPOR)^{20;21} rather than frequency selective excitation and spoiling.

MRS post-processing

MRS data were analyzed with LCModel^{22,23} according to the procedure described previously¹¹. The unsuppressed water was used as an internal reference to calculate the concentrations of the metabolites of interest: choline, creatine, glutamine + glutamate (Glx), total NAA (N-acetylaspartateglutamate + NAA), myo-inositol and lactate. Data processing was identical for both time points, with a Cramer-Rao Lower Bound (CRLB) of 20% or less as calculated by LCmodel required for all spectra as inclusion criteria for all metabolites with the exception of lactate for which we followed the guidelines of Tkac *et al.* (2009)²⁴. For lactate CRLB above 100% were excluded from further analysis. If lactate was not quantified with a CRLB <100% in at least 50% of analyzed spectra, the analysis of lactate was not performed. For inclusion in the statistical analysis the participant had to have spectra of sufficient quality at both time points. After this quality check, longitudinal data of 9 participants was included for the caudate nucleus, 7 data sets for the putamen and 9 for the prefrontal cortex.

Statistics

All statistical analysis was performed with SPSS for Windows (version 17.0, SPSS Inc, Chicago, IL, USA). Paired t-tests were applied to assess differences between the baseline visit and follow up for clinical variables as well as for metabolite concentrations. The differences in clinical measures and metabolite concentrations between the two time points were calculated. Pearson's correlation was used to explore the relationship between changes in metabolite concentrations and clinical measures. This correlation analysis was only performed for those metabolites that demonstrated statistically significant longitudinal change. Finally, paired t-tests were used to examine two separate subgroups; premanifest gene carriers that progressed to manifest HD as opposed to those premanifest HD participants that did not undergo this conversion. Again this procedure was only performed for those metabolites demonstrating significant longitudinal changes.

Results

Demographics and clinical measures

The gene carrier group consisted of 10 premanifest and three early manifest participants. During the two year follow up period four premanifest participants converted to manifest HD as defined by their UHDRS TMS. At baseline the mean age of the group was 43.5 years with a standard deviation (SD) of 10.6 years and the mean CAG-repeat length was 44.0 (SD 3.2). The group consisted of 5 males and 8 females. The premanifest HD group was mean 7.8 years (SD 4.3) to

predicted years to onset. The clinical characteristics at baseline visit and follow up are shown in Table 1. Over the 24 month period a significant decrease in the BDI-II and Stroop performance was observed.

Table 1: Clinical measures at baseline and follow up of 13 gene carriers

		Mean	SD	t	p-value
TMS	Baseline	4.69	5.60	-1.639	0.127
	Follow up	7.31	6.59		
TFC	Baseline	12.38	0.65	0.322	0.753
	Follow up	12.31	1.03		
PBA-s	Baseline	10.92	13.10	1.194	0.256
	Follow up	8.31	10.40		
BDI-II	Baseline	7.85	6.54	2.386	0.034
	Follow up	5.62	4.23		
TMT-B	Baseline	74.62	30.00	-0.978	0.347
	Follow up	85.69	50.65		
SDMT	Baseline	45.54	9.66	-0.892	0.390
	Follow up	46.54	10.08		
Stroop	Baseline	91.23	17.27	3.014	0.011
	Follow up	84.31	18.89		
MMSE	Baseline	28.77	1.54	-0.433	0.673
	Follow up	28.85	1.68		
Total gene carriers			N = 13		
Total premanifest at baseline (includes 4 converters during follow-up)			N = 10		
Total manifest at baseline			N = 3		

TMS = total motor score, TFC = total functional capacity, PBA-s= problem behaviour assessment short version, BDI-II: beck's depression inventory, second version, TMT-B= trail making test, part B, SDMT=symbol digit modality test, MMSE=mini mental state exam, SD = standard deviation, n = number of participants

Metabolite analysis

All metabolite concentrations at both baseline and follow up are shown in Table 2. In the caudate nucleus a decrease in creatine ($p=0.032$) and myo-inositol ($p=0.006$) concentrations was observed. In addition, in the putamen significant decreases in total N-acetylaspartate ($p=0.022$) and choline concentration ($p=0.007$) were observed. No metabolite concentration differences were found in the prefrontal region. Figure 1 shows typical examples of spectra from the follow up visit.

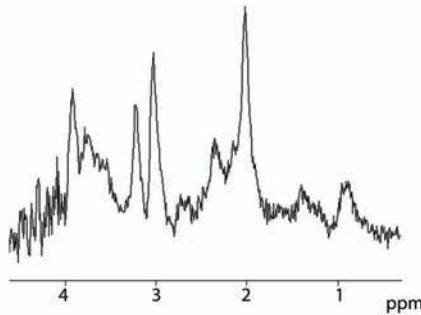
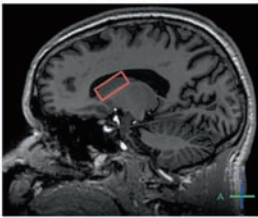
Relationship to clinical measures

Table 3 shows the association between cognitive changes over time and (significant) metabolite changes in the putamen and caudate nucleus. A decrease in depressive symptoms as measured by the BDI-II was related to a decrease in myo-inositol ($p=0.020$). Furthermore a decrease in cognitive performance as measured by the Stroop test was correlated to choline concentration decrease in the putamen ($p=0.048$).

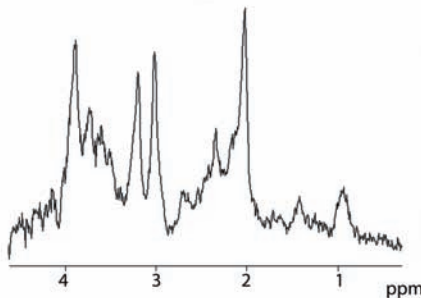
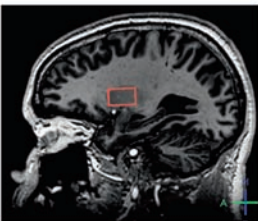
Conversion from premanifest to manifest HD

The premanifest HD group that converted to manifest HD showed longitudinal changes in concentrations in both caudate nucleus and putamen for three metabolites, namely myo-inositol ($p=0.019$), choline ($p=0.025$) and NAA ($p=0.003$), as shown in table 4. The premanifest non-converter group showed a significant longitudinal change in creatine in the caudate nucleus ($p=0.040$).

Caudate nucleus



Putamen



Prefrontal cortex

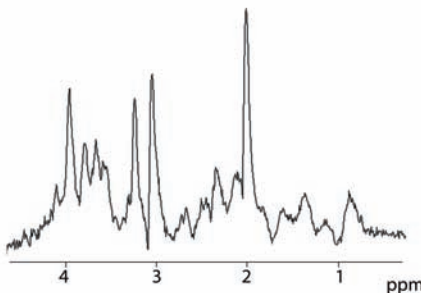
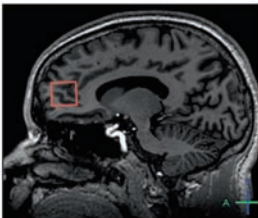


Figure 1: Typical example spectra and LCModel fit from 3 regions of interest in Huntington's disease gene carriers from the follow up visit of 3 premanifest participants. On the left the actual voxel in the sagittal plane. Actual planning was performed in 3 directions. ppm=part per million

Table 2: Metabolite concentrations at baseline and follow up in 3 regions of interest in Huntington's disease gene carriers

Caudate nucleus (N=9, 7 PGMC (incl. 2 converters), 2 MHD)					
		Mean	SD	t	p
Creatine	Baseline	11.18	2.84	2.588	0.032
	Follow up	9.14	1.19		
Choline	Baseline	2.83	0.60	0.473	0.649
	Follow up	2.76	0.48		
Lactate	Baseline	1.08	0.98	0.018	0.986
	Follow up	1.07	0.74		
Myo- inositol	Baseline	7.34	1.88	3.705	0.006
	Follow up	4.85	1.48		
tNAA	Baseline	10.05	2.19	0.501	0.630
	Follow up	9.76	1.53		
Glx	Baseline	12.11	4.09	0.824	0.434
	Follow up	11.18	2.85		
Putamen (N=7, 6 PGMC (incl. 3 converters), 1 MHD)					
		Mean	SD	t	p
Creatine	Baseline	12.14	2.61	1.631	0.154
	Follow up	10.23	1.68		
Choline	Baseline	3.31	0.33	3.986	0.007
	Follow up	2.67	0.32		
Lactate	Baseline	1.13	1.48	1.005	0.354
	Follow up	0.46	0.46		
Myo- inositol	Baseline	7.40	5.00	1.011	0.351
	Follow up	5.05	1.78		
tNAA	Baseline	14.78	1.19	3.062	0.022
	Follow up	11.83	2.05		
Glx	Baseline	13.29	3.13	0.387	0.712
	Follow up	12.73	2.41		
Frontal (N=9, 7 PGMC (incl. 4 converters), 2 MHD)					
		Mean	SD	t	p
Creatine	Baseline	8.73	1.58	-0.092	0.929
	Follow up	8.76	1.35		
Choline	Baseline	2.30	0.66	-0.173	0.867
	Follow up	2.34	0.51		
Lactate	Baseline	1.23	0.81	1.231	0.253
	Follow up	0.77	0.69		
Myo- inositol	Baseline	10.13	4.49	1.742	0.120
	Follow up	7.54	1.69		
tNAA	Baseline	11.98	2.29	1.067	0.317
	Follow up	11.27	1.75		
Glx	Baseline	10.52	3.48	-0.005	0.996
	Follow up	10.53	1.71		

PMGC = premanifest gene carriers, MHD = manifest HD, tNAA=total N-acetylaspartate, Glx = Glutamate and Glutamine

Table 3: Correlation analysis between metabolite concentrations and clinical measures in Huntington's disease gene carriers

		TMS	TFC	PBA-S	BDI-II	TMT-B	SDMT	Stroop	MMSE
Caudate Nucleus									
Creatine	R	-.562	-.027	.255	.056	-.320	-.091	-.135	-.297
	<i>p</i>	0.116	0.944	0.507	0.887	0.400	0.817	0.730	0.437
Myo-Inositol	R	-.228	-.507	-.560	-.749	.329	.464	.404	.274
	<i>p</i>	0.555	0.164	0.117	0.020	0.387	0.208	0.281	0.476
Putamen									
Choline	R	.248	-.195	-.355	-.474	-.031	.236	.759	-.143
	<i>p</i>	0.593	0.675	0.435	0.282	0.948	0.611	0.048	0.760
tNAA	R	.721	-.489	-.413	-.678	.030	.613	.324	.087
	<i>p</i>	0.067	0.265	0.358	0.094	0.949	0.143	0.478	0.853

TMS = total motor score, TFC = Total Functional Capacity, PBA-s= problem behaviour assessment short version, BDI-II: becks depression inventory, second version, TMT-B= trail making test, part B, SDMT= symbol digit modality test, MMSE=mini mental state exam, tNAA=total N-acetylaspartate

Table 4: Metabolite concentrations in the conversion from premanifest to manifest HD versus non-conversion

		Baseline		Follow up		<i>p</i> -value	
Caudate nucleus		N	Mean	SD	Mean	SD	
Creatine	non converters	5	11.31	2.23	9.28	1.62	0.040
	converters	2	14.11	2.03	9.23	0.52	0.137
Myo-inositol	non converters	5	6.83	1.69	4.98	1.89	0.108
	converters	2	8.01	1.81	4.56	1.66	0.019
Putamen							
Choline	non converters	3	3.19	0.28	2.86	0.19	0.353
	converters	3	3.57	0.22	2.67	0.11	0.025
tNAA	non converters	3	14.05	1.13	13.79	1.01	0.457
	converters	3	15.83	0.26	10.81	0.42	0.003

SD = standard deviation, tNAA=total N-acetylaspartate

Discussion

The main findings of this study show that over a period of two years, significant metabolite changes were observed in the progression of HD. More specifically, these changes occurred in a predominantly premanifest gene carrier group in which four participants converted from premanifest to manifest HD. The premanifest HD participants who converted to manifest HD seem to show a more rapid decline in NAA in the putamen than those who did not convert.

This longitudinal study expands the knowledge on metabolite changes in HD by demonstrating changes in creatine concentration in the caudate nucleus and total NAA concentration in the putamen. This reduction occurs in a mixed premanifest and early manifest HD group (peri-manifest). In participants converting from premanifest to manifest HD, higher rates of decrease were particularly observed in the total NAA of the putamen. In our previous cross-sectional study, NAA and creatine were significantly decreased in both the putamen and caudate nucleus in manifest HD, but not in the premanifest group¹¹. However, it was suggested that this decrease in concentration might already be visible in the premanifest group, but due to large intersubject variations in metabolite concentrations in combination with a small sample size, this finding did not reach statistical significance. The results of other cross-sectional results are in line with our longitudinal study^{10;12}; one study reported decreases in NAA and creatine concentrations in the putamen in premanifest HD¹², whereas in another study lower total NAA and creatine in the putamen in manifest HD as well as a non-significant decrease in these metabolites in premanifest HD were reported¹⁰. In contrast to these findings, one study reported no altered metabolite concentration in premanifest HD¹³, however relative metabolite concentrations as opposed to absolute ones referenced to water were used. In this respect, the use of metabolite ratio's should be approached with caution, since in HD it has been demonstrated, cross-sectionally¹⁰⁻¹² and longitudinally, that both NAA and creatine concentrations change. Summing all the data, it seems that creatine in the caudate nucleus and especially NAA in the putamen are metabolites that show great potential for use as a biomarker.

Our study demonstrated a decrease in choline in the putamen over the two year follow up. One other study also reported decreased choline concentrations in the frontal region in premanifest HD¹⁴. A possible explanation for a reduced choline concentration in the frontal lobe is that membrane turnover slows down prior to neuronal death¹⁴.

Myo-inositol concentration in the caudate nucleus was found to decrease over time in our study population. Abnormalities in myo-inositol concentrations have only been found by one other study reporting an increase rather than a decrease¹⁰. However, this increase in myo-inositol concentration was found only in the manifest stage of the disease as compared to controls with a cross-sectional design. It might be that the changes in the concentration of myo-inositol are non-linear and dependent on disease stage. It is possible that myo-inositol initially decreases in premanifest stages before increasing in manifest HD. However, this hypothesis must be investigated in larger longitudinal trials including multiple disease stages such as the TRACK-HD study^{3,10}.

Two changes in clinical measures were found to relate with lower metabolite concentrations. First, the decrease in depressive symptoms as measured by the BDI-II was significantly related to myo-inositol concentration decreases in the caudate nucleus. However, it must be noted that the clinical impact of this decrease in depressive symptoms is relatively small. The higher baseline BDI-II score could be explained by the fact that, before disease onset, anxiety to receive an imminent and expected diagnosis adds to psychological stress²⁵. Reduced symptom awareness after disease onset may explain the lower scores during follow up²⁶. Still, the relationship of BDI-II scores with myo-inositol, which is thought to be a glial marker, is not straightforward and these two changes could occur in parallel and be unrelated. The second relationship between changes in clinical measures and changes in metabolite concentrations is the simultaneous reduction in choline and Stroop performance. A similar neuropsychological disturbance relating to frontal choline concentrations has previously been reported¹⁴. As choline could possibly represent a pathogenic process related to neuronal loss or dysfunction in the putamen, the relationship to decline in executive functioning as measured by the Stroop seems plausible.

A limitation to our study is the relatively small sample size, which could obscure subtle changes. However, even with the relative small numbers statistically significant results are obtained for different metabolites in various regions of the brain, emphasizing the robustness of these findings and suggesting the high potential of MRS as a biomarker in HD. The sample size for the analysis of specifically premanifest converters is even smaller, hence findings should be treated with caution. However, again the differences observed between the premanifest group that converted to manifest HD versus the non-converter group are in line with other cross-sectional results and as expected, all metabolites show a higher rate of decrease in the progressive premanifest group.

In conclusion, we have demonstrated several metabolite changes in the putamen and caudate nucleus close to disease onset in HD over a two year period. This demonstrates the potential of MRS for providing a biomarker of disease progression and could be useful in evaluating future therapeutic interventions. Specifically the NAA in the putamen seems the best candidate biomarker.

References

1. van den Bogaard SJ, Dumas EM, Acharya TP, et al. Early atrophy of pallidum and accumbens nucleus in Huntington's disease. *J Neurol*. 2011 Mar;258(3):412-20.
2. van den Bogaard S, Dumas E, van der Grond J, et al. MRI biomarkers in Huntington's disease. *Front Biosci (Elite Ed)* 2012;4:1910-25
3. Tabrizi SJ, Langbehn DR, Leavitt BR, et al. Biological and clinical manifestations of Huntington's disease in the longitudinal TRACK-HD study: cross-sectional analysis of baseline data. *Lancet Neurol*. 2009 Sep;8(9):791-801.
4. Vonsattel JP, Keller C, Cortes Ramirez EP. Huntington's disease - neuropathology. *Handb Clin Neurol* 2011;100:83-100
5. Paulsen JS, Langbehn DR, Stout JC, et al. Detection of Huntington's disease decades before diagnosis: the Predict-HD study. *J Neurol Neurosurg Psychiatry* 2008;79:874-80
6. A novel gene containing a trinucleotide repeat that is expanded and unstable on Huntington's disease chromosomes. The Huntington's Disease Collaborative Research Group. *Cell* 1993;72(6):971-83
7. Roze E, Saudou F, Caboche J. Pathophysiology of Huntington's disease: from huntingtin functions to potential treatments. *Curr Opin Neurol* 2008;21:497-503
8. Ross CA, Tabrizi SJ. Huntington's disease: from molecular pathogenesis to clinical treatment. *Lancet Neurol* 2011;10(1):83-98
9. Sturrock A, Leavitt BR. The clinical and genetic features of Huntington disease. *J Geriatr Psychiatry Neurol* 2010;23:243-59
10. Sturrock A, Laule C, Decolongon J, et al. Magnetic resonance spectroscopy biomarkers in premanifest and early Huntington disease. *Neurology* 2010;75(19):1702-10
11. van den Bogaard SJ, Dumas EM, Teeuwisse WM, et al. Exploratory 7-Tesla magnetic resonance spectroscopy in Huntington's disease provides in vivo evidence for impaired energy metabolism. *J Neurol* 2011;258:2230-39
12. Sanchez-Pernaute R, Garcia-Segura JM, del Barrio AA, et al. Clinical correlation of striatal 1H MRS changes in Huntington's disease. *Neurology* 1999;53:806-12
13. van Oostrom JC, Sijens PE, Roos RA, et al. 1H magnetic resonance spectroscopy in preclinical Huntington disease. *Brain Res* 2007;1168:67-71
14. Gomez-Anson B, Alegret M, Munoz E, et al. Decreased frontal choline and neuropsychological performance in preclinical Huntington disease. *Neurology* 2007;68:906-10
15. Taylor-Robinson SD, Weeks RA, Bryant DJ, et al. Proton magnetic resonance spectroscopy in Huntington's disease: evidence in favour of the glutamate excitotoxic theory. *Mov Disord* 1996;11:167-73
16. Jenkins BG, Koroshetz WJ, Beal MF, et al. Evidence for impairment of energy metabolism in vivo in Huntington's disease using localized 1H NMR spectroscopy. *Neurology* 1993;43:2689-95
17. Langbehn DR, Brinkman RR, Falush D, et al. A new model for prediction of the age of onset and penetrance for Huntington's disease based on CAG length. *Clin Genet* 2004;65:267-77
18. Versluis MJ, Kan HE, van Buchem MA, et al. Improved signal to noise in proton spectroscopy of the human calf muscle at 7 T using localized B1 calibration. *Magn Reson Med* 2010;63(1):207-11
19. Schar M, Kozerke S, Fischer SE, et al. Cardiac SSFP imaging at 3 Tesla. *Magn Reson Med* 2004;51(4):799-806
20. Tkac I, Gruetter R. Methodology of H NMR Spectroscopy of the Human Brain at Very High Magnetic Fields. *Appl Magn Reson* 2005;29(1):139-57
21. Tkac I, Starcuk Z, Choi IY, et al. In vivo 1H NMR spectroscopy of rat brain at 1 ms echo time. *Magn Reson Med* 1999;41(4):649-56
22. Provencher SW. Estimation of metabolite concentrations from localized in vivo proton NMR spectra. *Magn Reson Med* 1993;30:672-79

23. Provencher SW. Automatic quantitation of localized in vivo ¹H spectra with LCModel. *NMR Biomed* 2001;14:260-64
24. Tkac I, Oz G, Adriany G, et al. In vivo ¹H NMR spectroscopy of the human brain at high magnetic fields: metabolite quantification at 4T vs. 7T. *Magn Reson Med* 2009;62:868-79
25. Timman R, Roos R, Maat-Kievit A, et al. Adverse effects of predictive testing for Huntington disease underestimated: long-term effects 7-10 years after the test. *Health Psychol* 2004;23(2):189-97
26. Duff K, Paulsen JS, Beglinger LJ, et al. "Frontal" behaviors before the diagnosis of Huntington's disease and their relationship to markers of disease progression: evidence of early lack of awareness. *J Neuropsychiatry Clin Neurosci* 2010;22(2):196-207



CHAPTER 10

DISCUSSION, CONCLUDING REMARKS AND FUTURE PERSPECTIVES

The aim of this thesis was to find potential MRI biomarkers for Huntington's disease (HD). A hypothetical model of disease processes, MRI abnormalities and clinical signs is shown in Figure 1. These hypothetical s-shaped curves are commonly used to illustrate pathological change, whereby the pathophysiological processes starts relatively slowly, subsequently shows a faster increase at a certain point in the pathologic cascade, and slows down towards the end. This model has been used in other neurodegenerative diseases such as Alzheimer's disease¹ and we now applied this model to HD. MRI abnormalities in HD emerge more than a decade before symptom onset^{2,3}. However, the line depicting MRI abnormalities is an oversimplification in this model as many different techniques are used with different sensitivity. In this thesis volumetric MRI, magnetization transfer imaging (MTI), diffusion tensor imaging (DTI) and magnetic resonance spectroscopy (MRS) were investigated in different disease stages of HD.

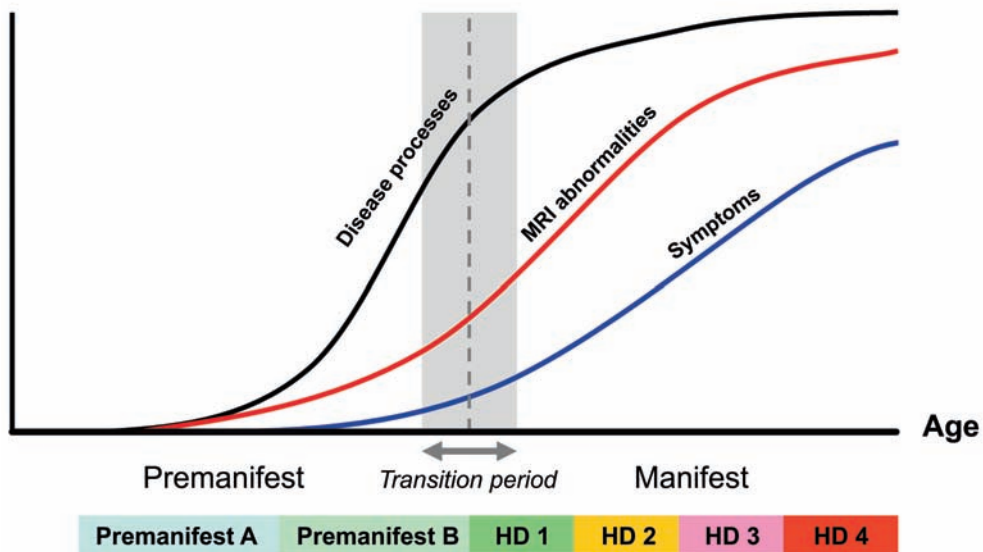


Figure 1: Hypothetical Huntington's disease model. Premanifest A = premanifest gene carriers far from expected disease onset, Premanifest B = premanifest gene carriers close to expected disease onset, HD 1 = Huntington's disease stage 1, HD 2 = Huntington's disease stage 2, HD 3 = Huntington's disease stage 3, HD 4 = Huntington's disease stage 4

MRI parameter changes per disease stage

Volumetric analysis of subcortical grey matter structures in HD have shown striatal volume decreases in premanifest and manifest stages of HD^{2,4}. The volumetric

study in this thesis extended this knowledge to six other subcortical grey matter structures and demonstrated more widespread involvement of the brain and in particular the basal ganglia (Chapter 3). Furthermore, an assessment was developed regarding the rate of atrophy of subcortical structures in respect to whole brain atrophy, to determine the relative speed of volume loss. This provided insight into patterns and rate of atrophy. Besides the caudate nucleus and putamen, the pallidum and accumbens nucleus also demonstrated strong volume reductions in the premanifest stage of the disease. All structures at some point showed atrophy, however, when compared to whole brain atrophy the amygdala and brainstem were relatively spared in the early stage of manifest disease. Hippocampus atrophy only exceeded the whole brain atrophy rate at later disease stages.

To further enhance our knowledge about volume changes we applied a surface based technique, whereby localized loss of volume can be detected (Chapter 4). This technique visualizes 3D boundary displacements of specific regions in subcortical structures⁵. With this application we showed that specifically the corpus of the caudate nucleus is affected. The putamen, on the other hand, shows more uniformly distributed displacements. These regions of displacements have specific cortical projections and therefore, for striatal and all other subcortical structures, we can extrapolate these findings to functional cortical regions and clinical symptoms.

Structural integrity of brain regions was assessed using MTI (Chapter 5). This technique quantifies structural brain disturbances dissimilar to conventional volumetric MRI. When neuronal loss is present, it can be assumed that structural integrity of those regions is reduced, hence MTI parameters could potentially be a sensitive biomarker. This analysis provided the insight that in the manifest stage loss of structural integrity is present. In premanifest HD, although atrophy is present at this stage, no structural integrity loss was detected using MTI. MTI performed longitudinally did not show any significant reduced structural integrity in a 2 year follow up in either premanifest or manifest HD (Chapter 8). This greatly diminished the potential of MTI as a biomarker. Despite this disappointing result, an unexpected finding was made when the premanifest group far from disease onset exhibited increased MTR peak height in the putamen (Chapter 8). A novel finding which could lead to a new insight in compensatory mechanisms in neurodegenerative processes in HD. However confirmation of this novel finding is needed.

When neuronal degradation is present, it is not unlikely that also their axons will be affected. The structural integrity of white matter pathways is therefore of interest, providing new targets for sensitive MRI measures. DTI can be used to visualize white matter pathways and quantify integrity parameters of these fiber bundles. DTI analysis showed multiple white matter pathways being affected in manifest HD, but also specifically showed that the white matter projecting from the sensorimotor cortex was affected in premanifest HD (Chapter 6).

Tapping into more dynamic cell processes as well as structural integrity, MRS provided evidence that both energy metabolism and cellular integrity are impaired in manifest HD (Chapter 7). Moreover, longitudinal analysis of metabolite changes revealed that these changes occur in the transition phase from premanifest to manifest HD (Chapter 9).

Clinical features

The genetic defect is present from the embryonic stage⁶, but when does the pathophysiological cascade of events start and lead to neuronal loss and subsequently functional loss, manifesting in clinical signs? And what period must be considered premanifest HD? In this thesis premanifest is best described as *pre-motor* manifest as the clinical inclusion criteria only describes the motor score from the UHDRS, which is a practical tool with good interrater reliability⁷. For the interpretation of all HD research, it is good to bear in mind that we label a person premanifest only by agreement about cut-off points in this clinical scale, mainly describing motor features. Cognitive or psychiatric impairments are harder to objectify. Cognition, for instance, is influenced by factors such as education. The psychiatric disturbances are difficult to link directly to HD pathology. This is especially relevant during the premanifest stage when the predictive genetic test alone causes significant stress⁸.

Relating MRI disturbances to clinical measures is important but not an easy feat. It is difficult to select the appropriate participant group. If we want to encompass the whole course of HD, including the transition period, only one group, namely gene carriers (both premanifest and manifest HD), should be examined. However, the downside to this approach is that it assumes, during the total disease course, a more or less linear relationship between clinical measures of disease and MRI parameters. This is probably not the case. Performing correlations per disease stage group could help to overcome this problem. The advantage is that possible linearity problems would be less evident within these more homogeneous groups.

However the disadvantage of this approach is that the cut-off points are rigid, but the scales on which these cut off points are based can be quite variable. The second reason why relating MRI parameters to clinical measures is not straightforward is that it is hard to prove a *causal* relationship between these MRI disturbances and the observed symptoms. Conclusions based on correlations can also reflect an epiphenomenon. For example, a high UHDRS motor score can be observed in manifest HD at the same time as a reduced hippocampus volume. Correlation analysis could be significant, however hippocampal volume may not be responsible for motor score. Thus, the correlation between these two simultaneously occurring changes does not reflect causality. In this example, it is more plausible that motor disturbances occur as a result of structural changes in the motor performance networks such as volume reduction of the basal ganglia or reductions in integrity of motor cortex projections. The hippocampus is not part of the motor performance networks and its volumetric decline may result in other symptoms than motor disturbances. Thus, one should always be wary of epiphenomological results when interpreting relationships of clinical disturbances to MRI changes.

Despite the above-described difficulties in relating MRI measures to clinical measures, in recent literature the existence of a relationship seems hardly disputed. In this thesis volumetric measures were correlated to main features of the UHDRS, namely total motor score and TFC (Chapter 3). Volume reductions of the accumbens nucleus, putamen and pallidum were most strongly related to the motor disturbances in manifest HD, and surprisingly, there was no relationship of the caudate nucleus to this clinical measure. The putamen and hippocampus were related to global functioning measured by the TFC, however TFC is only applicable in the manifest stages of the disease. The putamen is the most important structure for both measures.

MTI abnormalities have a correlation to clinical measures (Chapter 5). However, there were no significant longitudinal changes in MTI parameters where clinical deterioration was evident (Chapter 8). Further assessment of structural integrity using DTI, showed a relationship with motor and oculomotor measures to integrity loss of white matter fiber bundles of the sensorimotor cortex, prefrontal cortex, thalamus and corpus callosum. Interestingly, again no relationship was found between disturbances of the fiber bundles from the caudate nucleus and clinical measures of disease. Cognitive decline was related to white matter pathway disturbances in the corpus callosum, sensorimotor cortex and prefrontal cortex white matter pathways (Chapter 6).

Using MRS a relationship of the neuronal marker NAA in the putamen was

found with UHDRS total motor score and TFC (Chapter 7). This is in line with the volumetric correlations described above. Furthermore, the caudate nucleus NAA concentration did not relate to UHDRS total motor score, again similarly to the volumetric correlations. The NAA reductions in the caudate nucleus did relate to psychiatric disturbances and TFC. Glutamate, a neurotransmitter possibly implicated in the pathophysiological pathway of excitotoxicity, showed a correlation to cognitive decline. Changes in metabolites from premanifest to manifest HD progression showed only modest correlations to changes in clinical features (Chapter 9); however, this particular analysis was performed in a predominantly premanifest HD group where clinical features are only subtle.

Considering all these correlations a pattern emerges; clinical motor measures are related to disruptions of multiple parts of motor networks, such as putamen and white matter pathways, but not to the caudate nucleus. However, the caudate nucleus is involved in global and specific cognitive functions and psychiatric disturbances. This highlights the fact that examining the individual parts of the striatum is necessary. Conversely, we should not think of any structure alone as being responsible for a single task or clinical feature. All these functions are integrated in complex networks. These correlations only tell us something about the relative contribution of each of these structures to such networks at a certain point in time.

Conclusion

Different MRI techniques have different sensitivities for detecting pathogenic changes in HD. From this thesis the temporal relationship of the examined techniques in different disease stages can be extrapolated. These temporal relationships are displayed in figure 2. Volumetric changes, especially of the caudate nucleus and putamen, show early and rapid volume reductions. Longitudinal evaluation of volumetric MRI is available from the main TRACK-HD paper⁹. DTI displays early disturbances of white matter pathways of the sensorimotor cortex. The longitudinal evaluation is not discussed in this thesis, and is thus depicted as a dotted line. However, evidence from other cross-sectional^{10;11} and longitudinal¹² reports, suggestive of the high potential of DTI as a biomarker, are incorporated into this hypothetical curve. MRS parameters change close to disease onset, especially in the transition period. MTI parameters are significantly reduced in manifest HD, however the rate of change is relatively slow and is thus depicted below the clinical symptoms line. Note that the MTI line in premanifest far from expected disease onset is modestly below the x-axis, depicting the possible

increased MTR peak height of the putamen. For all techniques, this thesis only examined premanifest and early HD stages (HD 1 and 2) and thus the lines are dotted beyond this point. This hypothetical model is the interpretation of all the combined research in this thesis. It is not presented as proven fact, but rather provides a framework for future research into the MRI parameter changes in premanifest and early HD.

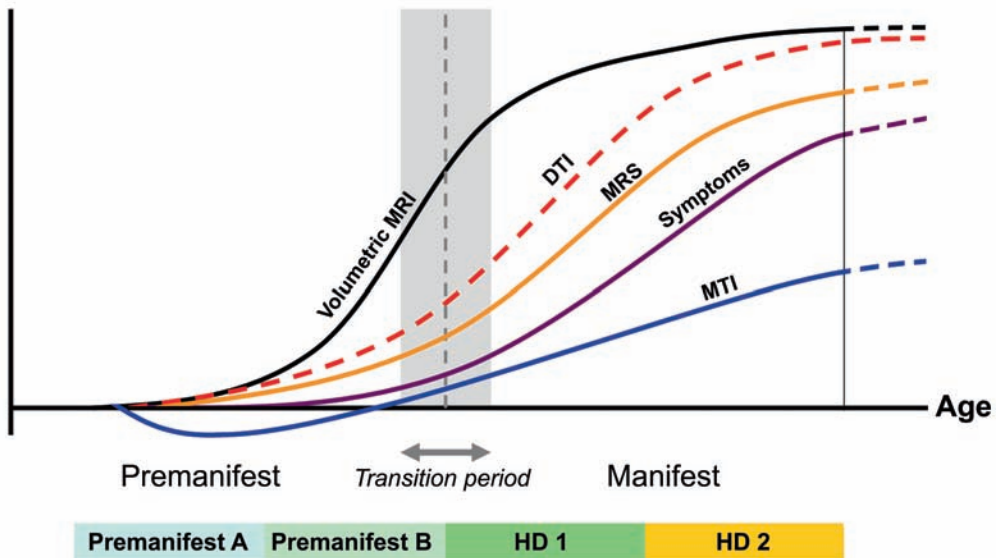


Figure 2: temporal relationships of volumetric MRI, DTI, MTI and MRS. Premanifest A = premanifest gene carriers far from expected disease onset, Premanifest B = premanifest gene carriers close to expected disease onset, HD 1 = Huntington's disease stage 1, HD 2 = Huntington's disease stage 2. DTI = diffusion tensor imaging, MRS = magnetic resonance spectroscopy, MTI = magnetization transfer imaging

Choosing the correct biomarker for evaluating therapeutic effects is dependent on the disease stage and therapeutic compound. To evaluate the premanifest stages of the disease, volumetric MRI of putamen, caudate nucleus, accumbens nucleus and pallidum and DTI of the white matter pathway of the sensorimotor cortex are most suitable. When the transition period is the desired timeframe for evaluation, MRS can also be useful, especially if the compound in question has a direct potential influence on pathogenic pathways which in turn have an impact on specific metabolites such as creatine or NAA. In early manifest HD volumetric MRI, DTI and MRS would be appropriate. With regards to volumetric biomarkers, the most appropriate structures may be different than in premanifest HD as subcortical gray matter structures show a differential atrophy pattern as the disease progresses.

Future perspectives

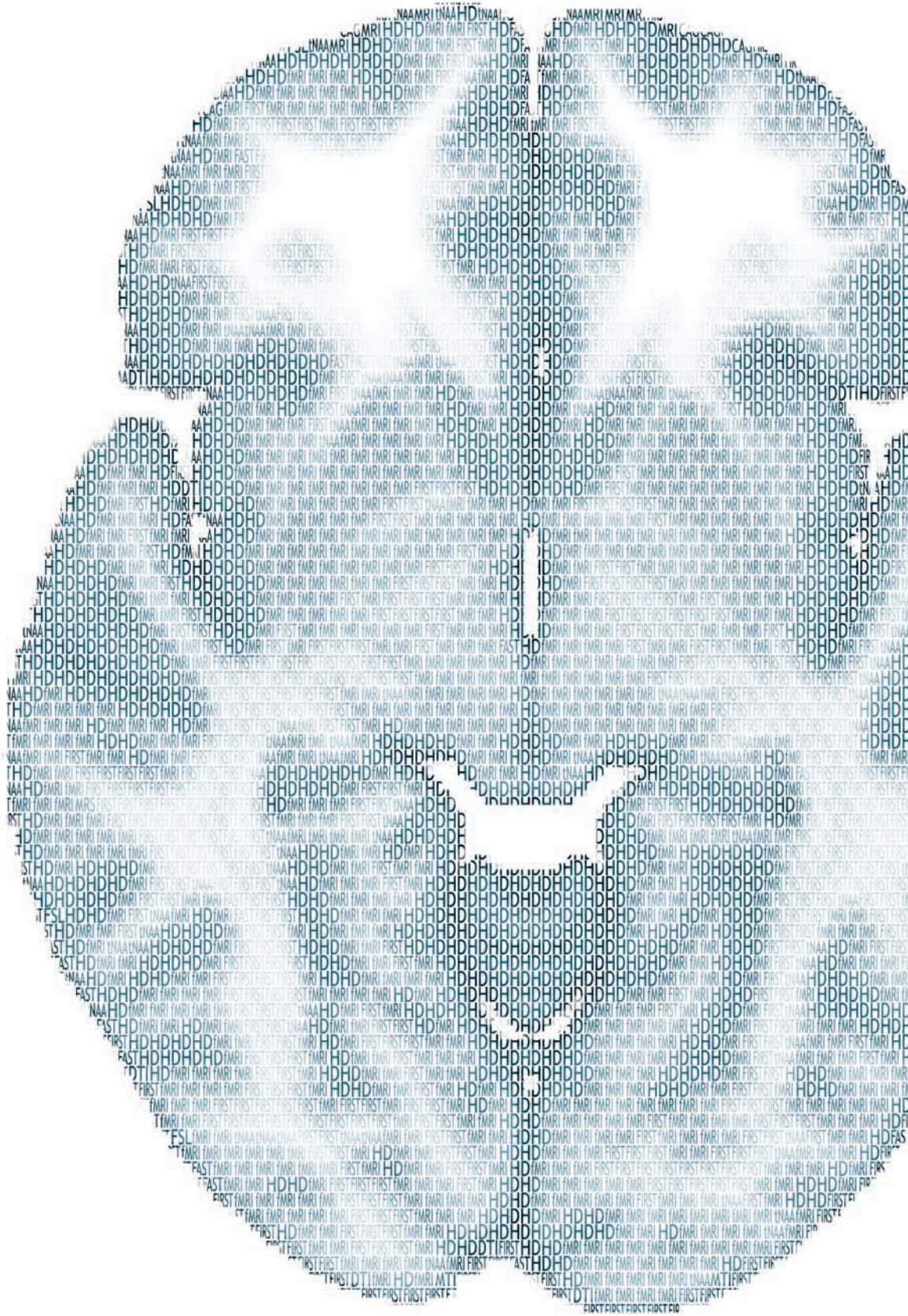
The future for MRI biomarkers for HD must continue in the direction of multimodal imaging. In this thesis individual MRI parameters were evaluated for their value as biomarkers. At a group level several measures were shown to be valuable; however, overlap in these measures between disease stages still exists. Thus, further improvement of the sensitivity of these MRI biomarkers is desired to accurately distinguish between disease groups. At an individual level it remains difficult to evaluate disease progression as the heterogenic clinical profile of HD is not captured by a single MRI parameter. Composite MRI-based biomarkers, based on a combination of markers with proven sensitivity for HD pathology, could be beneficial for biomarker research and have clinical applications. A composite MRI biomarker has the potential to distinguish between disease groups more accurately than a single biomarker and in this way improve the evaluation of therapeutic compounds. It is not unlikely that a new compound could have an effect on one MRI parameter, but not on another. For example, when a neuroprotective agent would have a positive influence on functional MRI, but not on volumetric MRI, a possibly valuable effect of such a compound could be missed. Furthermore, it could lead to an improved understanding of the structural-functional relationship during the disease course. On an individual level it could lead to a better prediction of disease onset than genetic models currently allow. The first reports on multimodal imaging are now emerging in both HD^{13,14} and Alzheimer's disease¹⁵, showing the potential of this approach. These reports also show that a multimodal approach does not have to be limited to MRI parameters, but can also incorporate other imaging techniques such as positron emission tomography (PET).

Taking the multimodal imaging approach a step further, it is even worth considering constructing a model summing or averaging all these variables into a so-called 'HD-quotient' of MRI parameters. However the sensitivity and utility of such a quotient is highly speculative. Large longitudinal multicentre trials, such as TRACK-HD² and PREDICT-HD¹⁶ are ideal platforms to apply multimodal image sequences. The challenge lies in combining all current and future data generated by these studies.

As a final remark, it must be noted that eventually a clinical endpoint is always needed to confirm a therapeutic effect. However, in the absence of appropriate clinical endpoints, the use of surrogate endpoints in the form of MRI parameters is invaluable to HD research.

References

1. Jack CR, Jr., Knopman DS, Jagust WJ, et al. Hypothetical model of dynamic biomarkers of the Alzheimer's pathological cascade. *Lancet Neurol* 2010;9:119-28
2. Tabrizi SJ, Langbehn DR, Leavitt BR, et al. Biological and clinical manifestations of Huntington's disease in the longitudinal TRACK-HD study: cross-sectional analysis of baseline data. *Lancet Neurol*. 2009 Sep;8(9):791-801.
3. Paulsen JS, Nopoulos PC, Aylward E, et al. Striatal and white matter predictors of estimated diagnosis for Huntington disease. *Brain Res Bull* 2010;82(3-4):201-07
4. Aylward EH, Sparks BF, Field KM, et al. Onset and rate of striatal atrophy in preclinical Huntington disease. *Neurology* 2004;63:66-72
5. Ferrarini L, Olofsen H, Palm WM, et al. GAMEs: growing and adaptive meshes for fully automatic shape modeling and analysis. *Med Image Anal* 2007;11:302-14
6. Sermon K, Goossens V, Seneca S, et al. Preimplantation diagnosis for Huntington's disease (HD): clinical application and analysis of the HD expansion in affected embryos. *Prenat Diagn* 1998;18(13):1427-36
7. Unified Huntington's Disease Rating Scale: reliability and consistency. Huntington Study Group. *Mov Disord* 1996;11:136-42
8. Timman R, Roos R, Maat-Kievit A, et al. Adverse effects of predictive testing for Huntington disease underestimated: long-term effects 7-10 years after the test. *Health Psychol* 2004;23(2):189-97
9. Tabrizi SJ, Reilmann R, Roos RA, et al. Potential endpoints for clinical trials in premanifest and early Huntington's disease in the TRACK-HD study: analysis of 24 month observational data. *Lancet Neurol*. 2012 Jan;11(1):42-53.
10. Magnotta VA, Kim J, Kosciak T, et al. Diffusion tensor imaging in preclinical Huntington's disease. *Brain Imaging and Behavior* 2009;3:77-84
11. Rosas HD, Tuch DS, Hevelone ND, et al. Diffusion tensor imaging in presymptomatic and early Huntington's disease: Selective white matter pathology and its relationship to clinical measures. *Mov Disord* 2006;21:1317-25
12. Weaver KE, Richards TL, Liang O, et al. Longitudinal diffusion tensor imaging in Huntington's Disease. *Exp Neurol* 2009;216(2):525-29
13. Blockx I, Van CN, Verhoye M, et al. Genotype specific age related changes in a transgenic rat model of Huntington's disease. *Neuroimage* 2011;58(4):1006-16
14. Politis M, Pavese N, Tai YF, et al. Microglial activation in regions related to cognitive function predicts disease onset in Huntington's disease: a multimodal imaging study. *Hum Brain Mapp* 2011;32(2):258-70
15. Zarei M, Patenaude B, Damoiseaux J, et al. Combining shape and connectivity analysis: an MRI study of thalamic degeneration in Alzheimer's disease. *Neuroimage* 2010;49(1):1-8
16. Paulsen JS, Hayden M, Stout JC, et al. Preparing for preventive clinical trials: the Predict-HD study. *Arch Neurol* 2006;63:883-90



The aim of this thesis was to find potential MRI biomarkers for Huntington's disease (HD). Therefore, after an overview of the current literature on MRI biomarkers (**Chapter 2**) volumetric MRI, magnetization transfer imaging (MTI), diffusion tensor imaging (DTI) and magnetic resonance spectroscopy (MRS) were applied in patients in different disease stages of HD.

Volumetric analysis of subcortical grey matter structures demonstrated widespread involvement of the brain in general and the basal ganglia in particular. The rate of atrophy of subcortical structures as compared to whole brain atrophy was used to determine the relative speed of volume loss. Our data demonstrated that besides the caudate nucleus and putamen, also the pallidum and accumbens nucleus demonstrate strong volume reductions in the premanifest stage of the disease. Furthermore, we observed that all structures at some point show atrophy, but when compared to whole brain atrophy, the amygdala and brainstem are relatively spared in the early stage of manifest disease. Hippocampus atrophy only exceeds the whole brain atrophy rate at later disease stages. Volumetric measures were correlated to main features of the Unified Huntington's disease Rating Scale (UHDRS), namely total motor score (TMS) and total functional capacity (TFC). Volume reductions of the accumbens nucleus, putamen and pallidum are most strongly related to the motor disturbances in manifest HD, and surprisingly, the impact of the caudate nucleus is minimal. The putamen and hippocampus are related to global functioning measured by TFC; however, TFC is only applicable in manifest stages of the disease. The putamen is for both measures the most important structure (**Chapter 3**).

Using a technique that visualizes 3D displacements of boundaries of subcortical structures (shape analysis), we showed that many subcortical regions are not uniformly reduced in volume, but show localized volume loss. In premanifest HD small areas of displacement in putamen, pallidum, accumbens and caudate nucleus were shown. Analysis of shape in manifest HD showed widespread shape differences, most prominently in the caudal part of the accumbens nucleus, body of the caudate nucleus, putamen and dorsal part of the pallidum. These specific regions all have their specific cortical projections and therefore we can use these findings and extrapolate them to functional cortical regions and clinical symptoms (**Chapter 4**).

Assessment of structural integrity of brain regions was subsequently performed using MTI. This technique, based on the exchange of magnetization between a pool of protons bound to macromolecular structures and a pool of free water

protons, allows for quantifying structural brain changes in a sensitive way. This analysis demonstrated that in the manifest but not premanifest stages loss of structural integrity is present (**Chapter 5**). MTI performed longitudinally did not show any significant reduced structural integrity in a 2-year follow up period, lowering the potential of MTI as a biomarker. Despite this disappointing result, an unexpected finding was that the premanifest group who was far from disease onset, exhibited increased MTR peak height in the putamen. A novel finding which could lead to new insight in compensatory mechanisms in neurodegenerative processes in HD. However these findings should be confirmed first. (**Chapter 8**)

Diffusion Tensor Imaging can be used to visualize white matter pathways and quantify integrity of these fiber bundles. DTI showed multiple white matter pathways being affected in manifest HD, but also specifically showed that the white matter projecting on the sensorimotor cortex was affected in premanifest HD. DTI disturbances showed a relationship of motor and oculomotor measures to white matter fibre bundles of the sensorimotor cortex, prefrontal cortex, thalamus and corpus callosum. Cognitive decline was related to disturbances in the corpus callosum, sensorimotor cortex and prefrontal cortex white matter pathways (**Chapter 6**).

Magnetic Resonance Spectroscopy (MRS) provided evidence that both creatine and N-acetylaspartate (NAA) concentrations are reduced in manifest HD in caudate nucleus and putamen. NAA in the putamen was found to correlate to UHDRS and TFC (Chapter 7). Moreover longitudinal analysis of metabolite changes revealed that multiple metabolite concentrations changes occur around the time of disease onset, such as NAA, creatine, choline and myo-inositol decreases. Among these NAA seems the most promising candidate for a biomarker (**Chapter 9**).

Final concluding remarks and future perspectives are portrayed (**Chapter 10**). Choosing the optimal biomarker for evaluating therapeutic effects is dependent on the disease stage and therapeutic compound. To evaluate the premanifest stages of the disease volumetric MRI and DTI are most suitable. When the transition period is the desired timeframe for evaluation, also MRS can be very useful, especially if the compound in question has a direct potential influence on certain pathogenic pathways which in turn have an impact on specific metabolites. Future research should focus on combining multiple imaging techniques; “multimodal imaging”. A composite MRI biomarker has the potential to distinguish between disease groups more accurately than a single biomarker and in this way improve the evaluation of therapeutic compounds.



CHAPTER 12

NEDERLANDSE SAMENVATTING

In dit manuscript was het doel gesteld om potentiële MRI biomarkers te vinden voor de ziekte van Huntington. Na een overzicht van alle huidige literatuur over MRI biomarkers (**hoofdstuk 2**), worden achtereenvolgens de technieken van conventionele (volumetrische) MRI, magnetization transfer imaging (MTI), diffusion tensor imaging (DTI) en magnetic resonance spectroscopy (MRS) toegepast in verschillende stadia van de ziekte van Huntington.

Volume analyse van subcorticale grijze stof structuren liet zien dat de gehele hersenen zijn aangedaan, maar in het bijzonder de basale ganglia. De relatieve hoeveelheid volumeverlies per structuur werd bepaald aan de hand van een ratio van volumeverlies ten opzichte van volumeverlies van het gehele brein. Naast de bekende atrofie van de nucleus caudatus en putamen werd ook gevonden dat de nucleus accumbens en het pallidum sterk volumeverlies tonen in de premanifeste fase van de ziekte. Verder werd het duidelijk dat alle onderzochte structuren op een gegeven moment in de ziekte enig volumeverlies tonen, maar wanneer we dit relateren aan het volumeverlies van het gehele brein, bleek dat de amygdala en de hersenstam relatief gespaard werden in de vroege manifeste fase. Hippocampus atrofie overtrof de snelheid van atrofie van het gehele brein pas in latere ziektestadia. Volume metingen werden gecorreleerd aan de hoofdonderdelen van de 'unified Huntington's disease rating scale' (UHDRS); namelijk de totale motor score (TMS) en de totale functionele capaciteit (TFC). Volume veranderingen van de nucleus accumbens, het putamen en het pallidum bleken het sterkst gerelateerd aan de motoriek afwijkingen bij de ziekte van Huntington, en de invloed van de nucleus caudatus was minimaal. Volume veranderingen van het putamen en de hippocampus waren gerelateerd aan het globale functioneren zoals gemeten met de TFC, echter, TFC is alleen van toepassing in de manifeste fase van de ziekte. Het volume van het putamen had de meeste invloed op de uitkomst van zowel TMS als TFC (**hoofdstuk 3**).

Door gebruik te maken van een techniek die 3D verplaatsingen van de oppervlakte van subcorticale grijze stof structuren visualiseert ('shape' analyse), konden we aantonen dat veel van deze structuren niet uniform aangedaan zijn, maar juist een meer gelokaliseerd volumeverlies tonen. Kleine gebieden van oppervlakteverplaatsingen werden gezien in het putamen, pallidum, nucleus accumbens en nucleus caudatus in premanifeste gendragers. In manifeste Huntington werden meer wijdverspreide gebieden gezien in alle structuren, maar het meest opvallend in het caudale gedeelte van de nucleus accumbens, het corpus van de nucleus caudatus, het putamen en het dorsale gedeelte van het pallidum. Deze specifieke regio's hebben hun eigen specifieke verbindingen

naar de cortex en daaruit afgeleid kunnen we deze bevindingen extrapoleren naar functionele corticale regio's en klinische symptomen **(hoofdstuk 4)**.

De structurele integriteit van verschillende hersenstructuren werd geanalyseerd door gebruik te maken van MTI. Deze techniek is gebaseerd op de uitwisseling van magnetisatie van protonen. Deze uitwisseling vindt plaats tussen protonen gebonden aan macromoleculen en protonen gebonden aan water. Deze techniek is mogelijk zeer sensitief voor het detecteren en kwantificeren van hersenveranderingen. De analyse toonde aan dat in de manifeste fase van de ziekte de structurele integriteit van het brein duidelijk verminderd is, maar dat dit nog niet aanwezig is in de premanifeste fase **(hoofdstuk 5)**. Een longitudinale analyse van deze methode liet geen afname van de structurele integriteit zien in een periode van 2 jaar. Dit verlaagt het biomarker potentieel van deze methode aanzienlijk. Ondanks dit tegenvallende resultaat, was er een onverwachte bevinding, namelijk een verhoogde MTR piekhoogte in het putamen in de premanifeste Huntington groep die ver van het verwachte ziektebegin was. Dit is een nieuwe bevinding die mogelijk kan leiden tot nieuwe inzichten in compensatiemechanismen in neurodegeneratieve processen bij de ziekte van Huntington. Echter deze nieuwe bevindingen moeten eerst bevestigd worden door verder onderzoek **(hoofdstuk 8)**.

DTI kan worden gebruikt voor het visualiseren van witte stof banen en het kwantificeren van de integriteit van deze axonbundels. In manifeste HD liet DTI zien dat multi-pele witte stof banen aangedaan zijn in deze fase van de ziekte, in premanifeste Huntington waren specifiek de witte stof banen aangedaan die naar de sensorimotorcortex gaan. De integriteitsveranderingen in witte stof banen van de sensorimotor cortex, de prefrontale cortex, de thalamus en het corpus callosum lieten een relatie zien met (oog)motoriek afwijkingen. Cognitieve achteruitgang was gerelateerd aan afwijkingen in de witte stof banen naar de sensorimotor cortex, de prefrontale cortex en het corpus callosum **(hoofdstuk 6)**.

Gebruik makend van de techniek MRS werd aangetoond dat zowel creatine als N-acetylaspartate (NAA) concentraties verlaagd waren in de nucleus caudatus en het putamen. NAA concentratie in het putamen was gerelateerd aan de UHDRS motor score en de TFC **(hoofdstuk 7)**. Een longitudinale analyse van metaboliëten liet zien dat meerdere metaboliëten veranderen rondom de tijd van ziektebegin. Deze metaboliëten betroffen NAA, creatine, choline and myo-inositol. Van deze metaboliëten liet vooral NAA het grootste potentieel als een biomarker zien **(hoofdstuk 9)**.

Conclusies en toekomstige perspectieven worden besproken (**hoofdstuk 10**): De keuze voor de optimale MRI biomarker is afhankelijk van het te onderzoeken ziektestadium en het type medicament. Voor het evalueren van de premanifeste fase is volumetrische MRI analyse en DTI het meest geschikt. Wanneer ook de overgangsfase naar manifeste Huntington de gewenste tijdsperiode is, is ook MRS zeer bijdragend, zeker als het potentiële medicament invloed uitoefent op bepaalde pathogene processen die te maken hebben met specifieke metabolieten. Toekomstig onderzoek zou zich moeten richten op het combineren van meerdere beeldvormingstechnieken, het zogenoemde 'multimodal imaging'. Een geïntegreerde MRI biomarker heeft het potentieel om verschillende ziektestadia beter te onderscheiden dan een enkele biomarker en kan op deze manier het evalueren van toekomstige therapieën verbeteren.

Publication list

Tapping linked to function and structure in premanifest and symptomatic Huntington disease.

Bechtel N, Scahill RI, Rosas HD, Acharya T, **van den Bogaard SJ**, Jauffret C, Say MJ, Sturrock A, Johnson H, Onorato CE, Salat DH, Durr A, Leavitt BR, Roos RA, Landwehrmeyer GB, Langbehn DR, Stout JC, Tabrizi SJ, Reilmann R.
Neurology. 2010 Dec 14;75(24):2150-60.

Early atrophy of pallidum and accumbens nucleus in Huntington's disease.

van den Bogaard SJ, Dumas EM, Acharya TP, Johnson H, Langbehn DR, Scahill RI, Tabrizi SJ, van Buchem MA, van der Grond J, Roos RA; TRACK-HD Investigator Group.
J Neurol. 2011 Mar;258(3):412-20.

Shape analysis of subcortical nuclei in Huntington's disease, global versus local atrophy - results from the TRACK-HD study.

van den Bogaard SJ, Dumas EM, Ferrarini L, Milles J, van Buchem MA, van der Grond J, Roos RA.
J Neurol Sci. 2011 Aug 15;307(1-2):60-8.

Exploratory 7-Tesla magnetic resonance spectroscopy in Huntington's disease provides in vivo evidence for impaired energy metabolism.

van den Bogaard SJ, Dumas EM, Teeuwisse WM, Kan HE, Webb A, Roos RA, van der Grond J.
J Neurol. 2011 Dec;258(12):2230-9.

Early changes in white matter pathways of the sensorimotor cortex in premanifest Huntington's disease.

Dumas EM, **van den Bogaard SJ**, Ruber ME, Reilmann R, Stout JC, Craufurd D, Hicks SL, Kennard C, Tabrizi SJ, van Buchem MA, van der Grond J, Roos RA.
Hum Brain Mapp. 2012 Jan;33(1):203-12.

MRI biomarkers in Huntington's disease.

van den Bogaard SJ, Dumas EM, van der Grond J, van Buchem MA, Roos RA.
Front Biosci (Elite Ed). 2012 Jan 1;4:1910-25.

Magnetization Transfer Imaging in Premanifest and Manifest Huntington Disease.

van den Bogaard SJ, Dumas EM, Milles J, Reilmann R, Stout JC, Craufurd D, van Buchem MA, van der Grond J, Roos RA.

AJNR Am J Neuroradiol. 2012 Jan 12. 33(5):884-89

Deficient sustained attention to response task and P300 characteristics in early Huntington's disease.

Hart EP, Dumas EM, Reijntjes RH, van der Hiele K, van den Bogaard SJ, Middelkoop HA, Roos RA, van Dijk JG.

J Neurol. 2012 Jun;259(6):1191-98.

Elevated brain iron is independent from atrophy in Huntington's Disease.

Dumas EM, Versluis MJ, van den Bogaard SJ, van Osch MJ, Hart EP, van Roon-Mom WM, van Buchem MA, Webb AG, van der Grond J, Roos RA.

Neuroimage. 2012 Jul 2;61(3):558-64

The structural correlates of functional deficits in early huntington's disease.

Delmaire C, Dumas EM, Sharman MA, van den Bogaard SJ, Valabregue R, Jauffret C, Justo D, Reilmann R, Stout JC, Craufurd D, Tabrizi SJ, Roos RA, Durr A, Lehericy S.

Hum Brain Mapp. 2012 Mar 22. [Epub ahead of print]

Magnetization Transfer Imaging in premanifest and manifest Huntington's disease: a 2 year follow up

van den Bogaard SJ, Dumas EM, Hart EP, Milles J, Reilmann R, Stout JC, Craufurd D, Tabrizi SJ, van Buchem MA, van der Grond J, Roos RA

AJNR Am J Neuroradiol. 2012, in press

A review of cognition in Huntington's Disease

Dumas EM, van den Bogaard SJ, Middelkoop HA, Roos RA

Front Biosci 2012, in press

As part of the investigator group:

Treatment and outcomes of acute basilar artery occlusion in the Basilar Artery International Cooperation Study (BASICS): a prospective registry study.

Schonewille WJ, Wijman CA, Michel P, Rueckert CM, Weimar C, Mattle HP, Engelter ST, Tanne D, Muir KW, Molina CA, Thijs V, Audebert H, Pfefferkorn T, Szabo K, Lindsberg PJ, de Freitas G, Kappelle LJ, Algra A; **BASICS study group**. *Lancet Neurol.* 2009 Aug;8(8):724-30.

Biological and clinical manifestations of Huntington's disease in the longitudinal TRACK-HD study: cross-sectional analysis of baseline data.

Tabrizi SJ, Langbehn DR, Leavitt BR, Roos RA, Durr A, Craufurd D, Kennard C, Hicks SL, Fox NC, Scahill RI, Borowsky B, Tobin AJ, Rosas HD, Johnson H, Reilmann R, Landwehrmeyer B, Stout JC; **TRACK-HD investigators**. *Lancet Neurol.* 2009 Sep;8(9):791-801.

Visuomotor integration deficits precede clinical onset in Huntington's disease.

Say MJ, Jones R, Scahill RI, Dumas EM, Coleman A, Santos RC, Justo D, Campbell JC, Queller S, Shores EA, Tabrizi SJ, Stout JC; **TRACK-HD Investigators**. *Neuropsychologia.* 2011 Jan;49(2):264-70.

Biological and clinical changes in premanifest and early stage Huntington's disease in the TRACK-HD study: the 12-month longitudinal analysis.

Tabrizi SJ, Scahill RI, Durr A, Roos RA, Leavitt BR, Jones R, Landwehrmeyer GB, Fox NC, Johnson H, Hicks SL, Kennard C, Craufurd D, Frost C, Langbehn DR, Reilmann R, Stout JC; **TRACK-HD Investigators**. *Lancet Neurol.* 2011 Jan;10(1):31-42.

Clinical impairment in premanifest and early Huntington's disease is associated with regionally specific atrophy.

Scahill RI, Hobbs NZ, Say MJ, Bechtel N, Henley SM, Hyare H, Langbehn DR, Jones R, Leavitt BR, Roos RA, Durr A, Johnson H, LeHéricy S, Craufurd D, Kennard C, Hicks SL, Stout JC, Reilmann R, Tabrizi SJ; **the TRACK-HD investigators**. *Hum Brain Mapp.* 2011 Nov 18. [Epub ahead of print]

Potential endpoints for clinical trials in premanifest and early Huntington's disease in the TRACK-HD study: analysis of 24 month observational data.

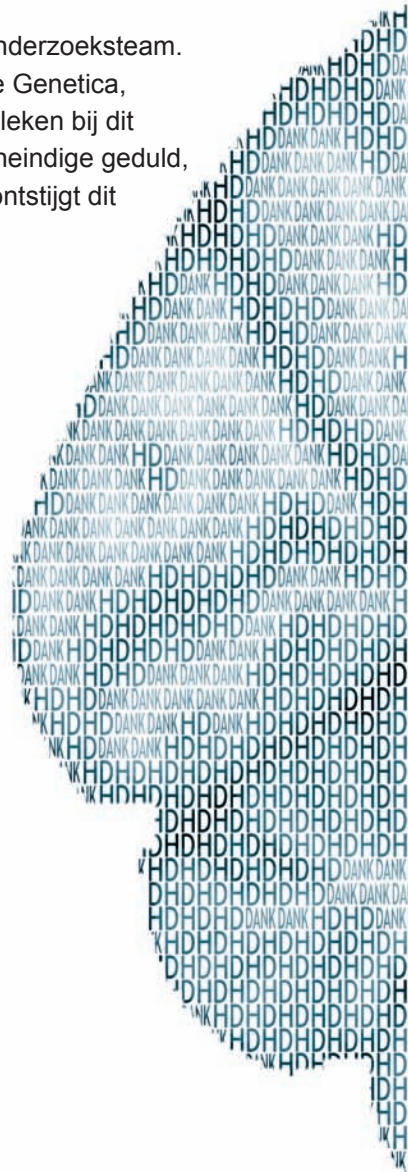
Tabrizi SJ, Reilmann R, Roos RA, Durr A, Leavitt B, Owen G, Jones R, Johnson H, Craufurd D, Hicks SL, Kennard C, Landwehrmeyer B, Stout JC, Borowsky B, Scahill RI, Frost C, Langbehn DR; **TRACK-HD investigators.**

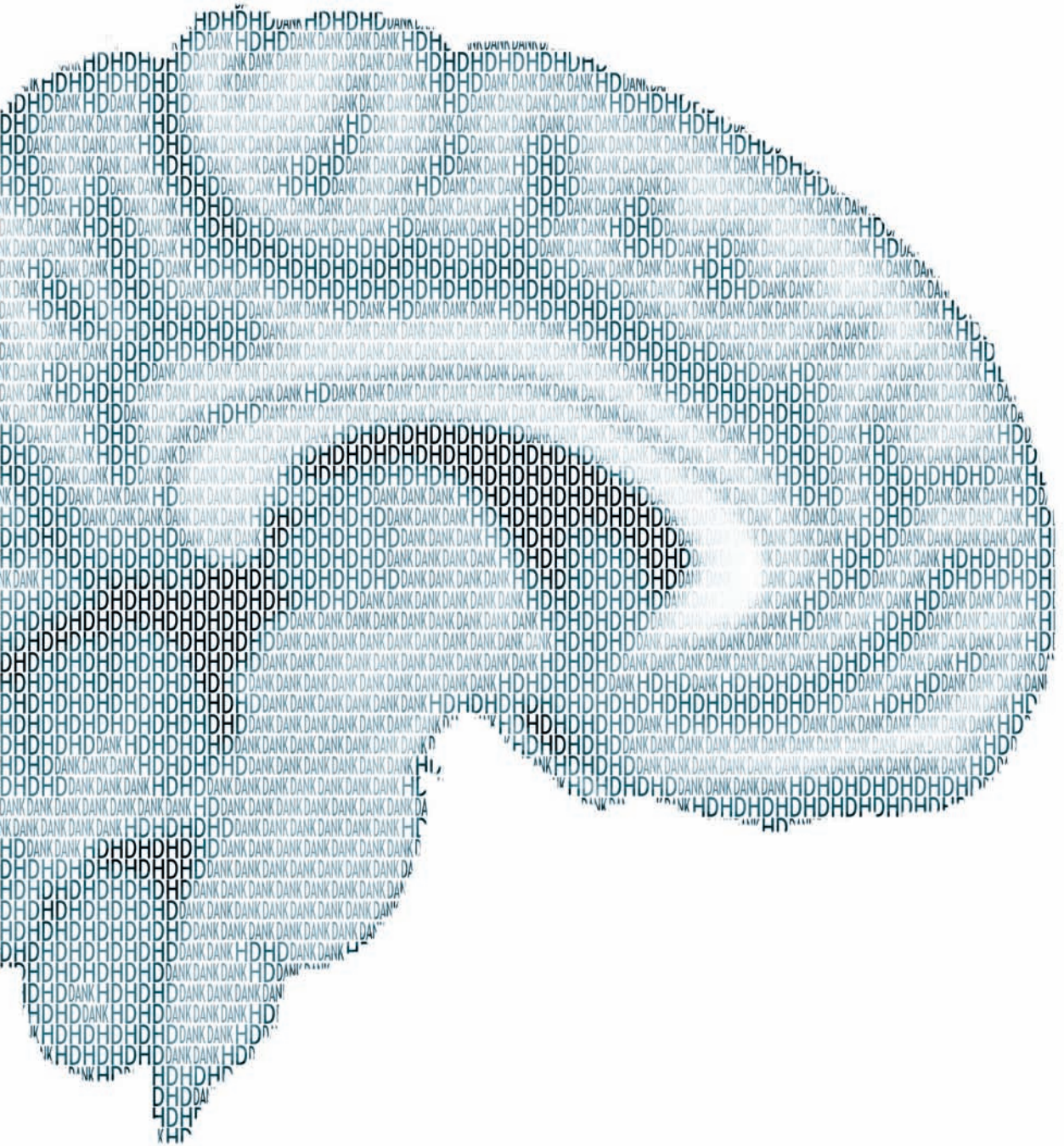
Lancet Neurol. 2012 Jan;11(1):42-53.

Dankwoord

De totstandkoming van dit proefschrift was niet mogelijk geweest zonder de hulp van vele mensen. Als eerste wil ik alle onderzoeksdeelnemers bedanken van zowel het TRACK-HD onderzoek als het 7 Tesla MRI project. Verder wil ik alle medewerkers wereldwijd van het TRACK-HD project bedanken voor al hun inzet. Ook veel dank gaat uit naar de sponsor van het project, de CHDI foundation, voor het mogelijk maken en de financiële ondersteuning van dit project.

Verder veel dank voor alle mensen van het Leiden Huntington onderzoeksteam. De medewerkers van de afdelingen Humane Genetica, Klinische Genetica, Neurologie, Neuropsychologie en Radiologie zijn onmisbaar gebleken bij dit onderzoek. Mijn dank voor de wetenschappelijke bijdrage, het oneindige geduld, maar bovenal de liefdevolle ondersteuning van mijn vrouw Eve ontstijgt dit dankwoord.





Curriculum Vitae

Simon Johannes Adrianus van den Bogaard werd geboren op 4 december 1979 in Woerden. Vanaf 1992 zat hij op het VWO aan het Minkema College te Woerden waar hij in 1998 zijn diploma behaalde.

In 1998 begon hij de studie Geneeskunde aan de Universiteit van Utrecht, waar hij een jaar later zijn propedeuse behaalde. Tijdens de studie was hij actief als student-docent voor eerstejaars geneeskundestudenten in het vak neuro-anatomie. Als onderdeel van het doctoraal examen volgde hij in 2003 een wetenschapsstage met als onderwerp “Stenting the Major Aorta-Pulmonary Collateral Arteries (MAPCA's) in patients with Ventricle Septum Defect and Pulmonary Atresia” in het Wilhelmina Kinderziekenhuis te Utrecht. Het doctoraalexamen geneeskunde behaalde hij in 2003.

Zijn coschappen rondde hij na twee jaar succesvol af met een aandachtsstage in de neurologie in het St. Antonius Ziekenhuis in Nieuwegein. Het artsexamen behaalde hij in 2005, waarna hij aansluitend ging werken in het St. Antonius ziekenhuis te Nieuwegein als arts-assistent neurologie niet in opleiding (ANIOS). Tijdens deze periode volgde hij een stage bij het Stroke Team van het Hermann Memorial Hospital te Houston, USA. Dit werd gecombineerd met onderzoek naar basilaris thrombose. Gedurende de studie geneeskunde en als ANIOS was Simon een fervent volleyballer, waarbij hij naast het zelf spelen ook plezier beleefde aan het lesgeven aan jeugdteams en zitting nam in de commissies jeugd en technisch beleid.

In 2007 is Simon in het LUMC begonnen aan een gecombineerd promotie- en opleidingstraject tot neuroloog. Als arts verbonden aan het TRACK-HD project verrichtte hij onderzoek naar de ziekte van Huntington. Tevens was hij verbonden aan de dubbelblinde placebo-gecontroleerde gerandomiseerde studie naar de effectiviteit van Dimebon bij de ziekte van Huntington. Daarnaast was hij actief binnen het European Huntington's Disease Network (EHDN). Naast de opleiding en promotie is hij bestuurslid van de Vereniging van Arts Assistenten Neurologie (VAAN) waarbinnen hij deeltneemt aan de commissies Landelijke Vereniging voor Medisch Specialisten in Opleiding (LVAG), etalage stages en de Commissie Wetenschappelijk Onderzoek Nederland (CWON). De beoogde einddatum van de opleiding tot neuroloog is in juli 2014.